

Novel Heat Recovery Systems for Building Applications

Mardiana Idayu Ahmad

BTech, MEnv

**Thesis submitted to the University of Nottingham for the degree of Doctor of
Philosophy**

February 2011

Contents

Abstract.....	i
Acknowledgements.....	iii
List of Figures.....	iv
List of Tables.....	xii
Nomenclature.....	xiv
Published Papers.....	xix

Chapter 1 Introduction

1.1 Background.....	1
1.2 Problem statements.....	3
1.3 Research objectives.....	6
1.4 Research methodology.....	7
1.5 Thesis structure.....	7

Chapter 2 Literature review

2.1 Introduction.....	10
2.2 Building and energy consumption.....	11
2.2.1 Primary sources of energy consumption in buildings.....	14
2.2.1.1 Building space heating and cooling/air-conditioning.....	14
2.2.1.2 Ventilation.....	15
2.2.2 Strategies to overcome energy consumption problems in buildings ...	16
2.2.2.1 Regulatory and policy.....	16
2.2.2.2 Awards as energy conservation instruments.....	19

2.2.2.3	Adoption of energy-efficient technologies.....	21
2.3	Heat recovery: An approach of energy-efficient technology for building applications.....	23
2.3.1	Definition and concept of heat recovery.....	24
2.3.2	Types of heat recovery for building applications.....	28
2.3.2.1	Fixed-plate.....	29
2.3.2.2	Heat pipe.....	34
2.3.2.3	Rotary wheel.....	39
2.3.2.4	Run-around.....	42
2.3.3	Heat recovery in integrated energy-efficient system for building application.....	45
2.3.3.1	Heat recovery in mechanical ventilation system.....	45
2.3.3.2	Heat recovery assisted passive ventilation.....	49
2.3.3.3	Heat recovery assisted-cooling or air conditioning.....	51
2.3.3.4	Heat recovery combined with dehumidification system.....	55
2.3.3.5	Heat recovery coupled with photovoltaic/solar panel.....	58
2.4	Summary.....	61

Chapter 3 Review on Theoretical Studies of Heat Recovery System

3.1	Introduction.....	64
3.2	Physical parameters.....	64
3.2.1	Size.....	64
3.2.2	Structure and material.....	68
3.2.2.1	Metal type.....	69

3.2.2.2	Polycarbonate.....	70
3.2.2.3	Fibre.....	71
3.2.2.4	Wick structure.....	72
3.2.2.5	Corrugated structure.....	73
3.2.2.6	Membrane based.....	74
3.2.3	Configuration/Flow arrangement.....	75
3.3	Heat/mass transfer.....	77
3.4	Flow inside a duct.....	82
3.4.1	Velocity boundary layer.....	82
3.4.2	Friction factor and pressure drop.....	83
3.4.3	Flow inside the ducts of various cross sections.....	84
3.5	Performance parameters.....	84
3.5.1	Efficiency/Effectiveness.....	84
3.5.1.1	Sensible heat recovery.....	85
3.5.1.2	Enthalpy recovery/Total recovery.....	86
3.5.1.3	The Effectiveness-NTU method.....	87
3.5.1.4	Global efficiency.....	90
3.5.2	Effect of airflows.....	92
3.5.3	Effects of temperature.....	95
3.5.4	Effects of humidity.....	96
3.5.5	Pressure drop.....	97
3.5.6	Electrical consumption.....	98
3.6	Energy calculation.....	99
3.7	Summary.....	102

Chapter 4 Performance Investigation of an Individual Heat Recovery Unit

4.1	Introduction.....	105
4.2	Description of the heat recovery core.....	105
4.3	Experimental set up.....	107
4.4	Experimental procedure and instrumentation.....	109
4.4.1	Data acquisition.....	110
4.4.2	Temperature measurement.....	111
4.4.3	Airflow measurement.....	112
4.4.4	Pressure measurement.....	114
4.5	Performance Calculation Model.....	115
4.5.1	Efficiency.....	115
4.5.2	Recovered/Transferred energy.....	116
4.6	Test results and performance analysis.....	116
4.6.1	Temperature data.....	116
4.6.2	Heat recovery efficiency.....	117
4.6.2.1	Effects of airflow rates.....	118
4.6.2.2	Effects of supply air inlet temperature.....	119
4.6.3	Recovered/Transferred energy.....	119
4.6.4	Pressure drop.....	121
4.7	Summary.....	123

Chapter 5 Integrated Heat Recovery System Associated with Wind-catcher and Evaporative Cooling

5.1	Introduction.....	125
5.2	System description.....	126

5.2.1	Wind-catcher unit.....	126
5.2.2	Heat recovery unit.....	128
5.2.3	Evaporative cooling unit.....	129
5.2.4	Capital cost of the system.....	131
5.3	Experimental installation.....	131
5.4	Measurement procedures.....	141
5.4.1	Temperature measurements.....	143
5.4.2	Relative humidity measurements.....	146
5.5	System performance calculations model.....	147
5.6	Results and discussion.....	149
5.6.1	Heat recovery performance.....	150
5.6.1.1	Heat recovery efficiency.....	152
5.6.1.2	The sensible transferred energy (heat).....	153
5.6.1.3	Pressure drop.....	154
5.6.2	Cooling performance.....	155
5.6.2.1	Temperature profiles.....	157
5.6.2.2	Relative humidity profiles.....	158
5.6.2.3	Cooling capacity.....	160
5.6.2.4	Water consumption rate.....	162
5.6.2.5	Cooling efficiency.....	163
5.6.3	Coefficient of performance.....	164
5.6.4	System performance.....	164
5.7	Summary.....	167

Chapter 6 Development and Performance Investigation of Novel Building

Integrated Heat recovery (BIHR) System

6.1	Introduction.....	169
6.2	System design features and construction.....	170
6.3	Laboratory investigation of BIHR prototype panel.....	177
6.3.1	Analysis and results.....	181
6.4	Case study I: Full-scale measurements of BIHR panel on a real building in Asford, Kent (Forstal Farm House).....	184
6.4.1	Description of the building.....	184
6.4.2	Installation of BIHR system on the building.....	186
6.4.3	Measurements.....	191
6.4.4	System performance.....	193
6.4.5	Comparison with prototype panel.....	196
6.4.6	Experiments on PV power fan of BIHR system.....	197
6.4.6.1	Material and methods.....	198
6.4.6.2	Analysis of the PV performance.....	201
6.5	Case study II: Full-scale measurements of BIHR panel on a real building in Hastings, Sussex.....	203
6.5.1	Testing description.....	204
6.5.2	Results and discussion.....	207
6.5.2.1	Efficiency and performance.....	207
6.5.2.2	Comparison with prototype and case study I.....	208
6.6	An improved BIHR system employing corrugated channels with four airstreams.....	209
6.6.1	Development of improved BIHR system.....	211

6.6.2	Performance of improved BIHR system.....	213
6.6.2.1	Effects of airflow on performance.....	215
6.6.2.2	Effects of temperature.....	216
6.6.3	Comparison with BIHR two airstreams.....	217
6.7	Economic and environment analysis of BIHR system.....	219
6.7.1	Economic analysis of BIHR prototype with two airstreams and improved BIHR' corrugated channels with four airstreams.....	222
6.7.2	Economic analysis of BIHR system in case study I.....	224
6.8	Performance investigation of BIHR system with fibre wick structure for cooling and dehumidification.....	226
6.8.1	System description.....	227
6.8.1.1	Fibre wick structure.....	228
6.8.1.2	Capital cost.....	230
6.8.2	Case 1: BIHR-fibre wick cooling system.....	231
6.8.2.1	Working principle and theoretical psychrometric analysis....	232
6.8.2.2	Experimental set up.....	235
6.8.2.3	Experimental procedure.....	238
6.8.2.4	Performance analysis and discussion.....	239
6.8.3	Case II: BIHR-fibre wick desiccant dehumidification system.....	244
6.8.3.1	Theory and development.....	247
6.8.3.2	Principles and features of the liquid-desiccant dehumidification.....	250
6.8.3.3	Performance index.....	252
6.8.3.4	Laboratory tests.....	253
6.8.3.5	Results and discussion.....	257

6.9 Summary.....264

Chapter 7 Conclusion and recommendation for future work

7.1 Introduction.....273

7.2 Main conclusions.....273

7.2.1 Literature review.....273

7.2.2 Review on theoretical studies of heat recovery system.....274

7.2.3 Performance investigation of an individual heat recovery unit.....277

7.2.4 Integrated heat recovery system associated with wind-catcher and evaporative cooling.....278

7.2.5 Development and performance investigation of novel building integrated heat recovery (BIHR) system.....279

7.3 Summary of contributions and novel features.....282

7.4 Future work.....283

Reference

Appendix

Abstract

The work presented in this thesis will explore the development of novel heat recovery systems coupled with low carbon technologies, and its integration to become one device with multifunction (building integrated heat recovery/cooling/air dehumidifier). In the first part of this thesis, an experimental performance of an individual heat recovery unit using Micro Heat and Mass Cycle Core (MHM3C) made of fibre papers with cross flow arrangement has been carried out. The unit was tested in an environmental control chamber to investigate the effects of various parameters on the performance of heat/energy recovery unit. The results showed that as the airflow rate and temperature change increase, the efficiency decreases whilst recovered energy increases. Integrating heat recovery system in energy-efficient system represents significant progress for building applications. As part of the research, the integration of heat recovery using a cross-flow fixed-plate with wind-catcher and cellulose fibre papers of evaporative cooling units have allowed part of the energy to be recovered with the efficiency of heat recovery unit ranged from 50 to 70%, cooling efficiency ranged from 31 to 54%.

In another case, the integration of heat recovery system with building part so-called building integrated heat recovery (BIHR) was explored using polycarbonate plate with counter-flow arrangement. It introduces a new approach to MVHR system, an established technology that uses a modified insulation panel, linking the inside and outside of a building, to recover heat while extracting waste air and supplying fresh air. In this configuration it is not only acts a heat recovery, but also as a contribution to building thermal insulation. From the experiments conducted, it was found that through an energy balance on the structure, the efficiency of BIHR prototype was found to be 50 to 61.1% depending on the airflow rate. This efficiency increases to the highest value of 83.3% in a full-scale measurement on a real building in Ashford, Kent as the area of heat transfer surface increases. The increasing of heat surface area again proved a better performance in terms of efficiency as the results on another full-scale measurement on a real house in Hastings, Sussex showed to be 86.2 to 91.7%. With the aiming to have a high performance system, a new improvement design of BIHR' corrugated polycarbonate channels with four airstreams has significant advantages over the previous prototype BIHR with two airstreams. The recovered heat is increased by more than 50%.

With the issue of thermal comfort in hot region area and problems with conventional air conditioning system, a study of BIHR system with fibre wick structure for different hot (summer) air conditions using different working fluids was carried out. For the first case, water was used to give a direct evaporative cooling effect which is suitable to evaluate the system performance under hot and dry climatic conditions and the second case, potassium formate (HCOOK) solution was used as liquid desiccant for dehumidification under hot and humid climate conditions. By supplying the water over the fibre wick structure, with a constant airflow rate of $0.0157\text{m}^3/\text{s}$, the efficiency increased with increasing intake air temperature. The efficiency ranged from 20 to 42.4% corresponding to the minimum and maximum of intake air temperature of 25°C and 38.2°C , respectively. With the variation of airflow rate, the efficiency of the system was found to be 53.2 to 60%. In second case, the HCOOK solution with concentration of 68.6% has been selected as the desiccant and for a defined airflow rate of $0.0157\text{m}^3/\text{s}$, heat recovery efficiency of about 54%, a lower desiccant temperature of 20°C , with higher intake air temperature and relative humidity produces a better dehumidification performance with a good moisture absorption capacity. Therefore, this system is expected to be used efficiently in hot and humid regions.

The research is novel in the following ways:

- The development of multifunction device in one system; building integrated, heat recovery, cooling, desiccant dehumidification.
- The design and development of BIHR is an advanced technology of building thermal insulation and heat recovery. The novel BIHR-fibre wick cooling/dehumidification system has the potential to compete with conventional air conditioning systems under conditions involving high temperature and high moisture load.

Acknowledgements

Firstly, I would like to express my sincere gratitude to my supervisor, Professor Saffa Riffat, Head of Institute of Sustainable Energy, University of Nottingham for his commitment, wide knowledge, his understanding, enthusiasm, encouragement and continued inspiration throughout. Thanks must also goes to Dr Mark Gillott as my second supervisor.

For providing the encouragement and assistance in the laboratory and full-scale experiments, I would like to thank Dr Mark Worall and Rick Richard. I am also grateful to all technicians in the department especially to Mr Dave Oliver for the unlimited help in the laboratory. I particularly wish to thank Mrs. Zeny Amante-Roberts and other staffs of the Department of Architecture and Built Environment for various forms of assistances during the period of my studies.

I wish to express my appreciation to my organisation, School of Industrial Technology, Universiti Science of Malaysia (USM) for the study fellowship and partial supports for living expenses during my study. I am also very grateful to The Ministry of Higher Education, Malaysia (MOHE) for the study scholarship and living allowance in UK. Without these financial supports, this PhD research would not have been undertaken.

Finally, special warmest thanks to my mother for her prayers, advices and supports throughout my life and studies. Thanks also to all my family members, lab-mates and friends especially to Daniel, Liang, and Feng.

Nottingham, UK, February 2011

Mardiana Idayu Ahmad

List of Figures

Chapter 1

Figure 1.1 Link between building and energy and the needs for heat recovery system

Chapter 2

Figure 2.1 World energy consumption from International Energy Agency (Source: Perez-Lombard et al. 2008)

Figure 2.2 Evolution of Malaysia energy policy with crude oil price (Manan et al. 2010)

Figure 2.3 Heat recovery system

Figure 2.4 Structure (1) and air energy-flow (2) schematic diagram of ERV (Source: Zhou et al. 2007)

Figure 2.5 Fixed-plate heat recovery

Figure 2.6 Z-flow fixed plate utilized a porous membrane as the heat and moisture transfer surface (Source: Nasif et al. 2010)

Figure 2.7 (a) The core of a typical MEE. (b) Physical model (Source: Min and Su 2010)

Figure 2.8 Layout of the experimental facility (Source: Fernandez-Seara et al. 2010)

Figure 2.9 Heat pipe

Figure 2.10 Heat pipe recovery in air conditioning system (Source: El-Baky and Mohamed 2007)

Figure 2.11 Heat pipe in HVAC system for tropical climates (Source: Yau 2007)

Figure 2.12 Heat recovery system using heat pipe solution in drying cycle (Source: Lin et al. 2005)

Figure 2.13 Rotary wheel recovery

Figure 2.14 Schematic representation of the rotary wheel (Dallaire et al. 2010)

Figure 2.15 Run-around system

Figure 2.16 Schematic diagram of a run-around heat recovery (Source: Vali et al. 2009)

Figure 2.17 Mechanical ventilation heat pump system with four types of ventilation heat recovery (Source: Nguyen et al. 2005)

Figure 2.18 MVHR heat pump system (Source: Riffat and Gillott 2002)

Figure 2.19 Schematic diagram of the naturally-ventilated room with heat pipe recovery unit (Source: Riffat and Gan 1998)

Figure 2.20 Schematic of the heat recovery concept (Source: Hviid and Svendsen 2010)

Figure 2.21 Schematic diagram of the window-type air conditioner with heat recovery facility (Source: Liu et al. 2007)

Figure 2.22 Heat and mass recovery system in air conditioning (Nasif et al. 2010)

Figure 2.23 Schematic of a run-around heat recovery system in air conditioning (Source: Mahmud et al. 2010).

Figure 2.24 Schematic of air dehumidification system combined with membrane-based total heat recovery (Source: Liang et al. 2010)

Figure 2.25 Schematic of the rotary desiccant wheel for dehumidification and enthalpy recovery (Source: Zhang and Niu 2002)

Figure 2.26 Schematic a rotary wheel heat recovery with rotary desiccant wheel in a dehumidification system (Source: Liu et al. 2007)

Figure 2.27 BiPV with heat recovery energy payback periods (Source: Crawford et al. 2006)

Figure 2.28 Schematic diagram of a condenser heat recovery with a hybrid photovoltaic/thermal (Source: Sukamongkol et al. 2010)

Chapter 3

Figure 3.1 Types of heat exchangers (Source: Soylemez 2000)

Figure 3.2 Effect of heat transfer area on effectiveness (Source: Soylemez 2000)

Figure 3.3 Effect of heat transfer area on net energy savings (Source: Soylemez 2000)

Figure 3.4 Temperature efficiency η as a function of heat exchanger length for two profile types (Source: Manz and Huber 2000)

Figure 3.5 Effect of changing heat exchanger face area on annual energy saving in Kuala Lumpur (air face velocity indicated on top of each point) (Source: Nasif et al. 2010)

Figure 3.6 Segment of an extruded aluminium profile used as a combined duct and heat exchanger (Source: Manz and Huber 2000)

Figure 3.7 Horizontal cross-section of the exchanger (Source: Kragh et al. 2007)

Figure 3.8 Schematic of the wick geometry in the evaporator of heat pipe (Source: Hwang et al. 2007)

Figure 3.9 A schematic representation corrugated structure channel (Source: Islamoglu 2003)

Figure 3.10 Flow arrangements

Figure 3.11 Schematic of a quasi-counter flow parallel-plates total heat exchanger (Source: Zhang 2010)

Figure 3.12 Heat transfer mechanism in fixed-plate

Figure 3.13 Psychrometric chart (Source: www.truetex.com)

Figure 3.14 Effects of total number of heat transfer units on the effectiveness (Source: Niu and Zhang 2001)

Figure 3.15 The tested system (Source: Roulet et al. 2001)

Figure 3.16 Heat recovery efficiency of plain fin unit (Source Shao et al. 1998)

Figure 3.17 Experimental sensible, latent and total effectiveness for 60gsm paper heat exchanger (Source: Nasif et al. 2010)

Figure 3.18 Comparison of measured heat transfer with the literature (source: Hviid and Svendsen 2010)

Figure 3.19 Pressure drop against velocity (Source: Shao et al. 1998)

Figure 3.20 Main and unintentional air flows in a system consisting of a ventilation unit, room and outdoor space (Source: Manz et al. 2001)

Figure 3.21 Effect of fresh air temperature and return air mass flow on effectiveness, ϵ (Source: El-Baky and Mohamed 2007)

Figure 3.22 Effect of fresh air temperature and mass ratio on ΔT_O and ΔT_R (Source: El-Baky and Mohamed 2007)

Figure 3.23 Effects of relative humidity of supply air on effectiveness with supply in temperature (35°C) (Source: Niu and Zhang 2001)

Figure 3.24 Reduction of pressure loss coefficient with increasing air velocity (Source: Shao et al. 1998)

Figure 3.25 Pressure drop measurements (Source: Nasif et al. 2010)

Figure 3.26 Effect of lifetime on net energy savings (Source: Soylemez 2000)

Chapter 4

Figure 4.1 MHM3C core

Figure 4.2 Laboratory experimental rig

Figure 4.3 Schematic view of experimental set up

Figure 4.4 Centrifugal fan

Figure 4.5 DataTaker

Figure 4.6 Data-logging equipments

Figure 4.7 Positions of thermocouples in the experimental rig

Figure 4.8 Airflow through heat recovery core

Figure 4.9 Hot wire anemometer

Figure 4.10 Measuring points for circular duct

Figure 4.11 Variation of the efficiency of the cross-flow heat recovery with air velocity

Figure 4.12 Variation of sensible energy recovered with air velocity

Figure 4.13 Impact of temperature change to the sensible energy recovered

Figure 4.14 Pressure drop between the supply air stream to the heat recovery unit and the ambient

Figure 4.15 Pressure loss coefficient in the duct

Figure 4.16 Pressure drop in the duct against velocity

Chapter 5

Figure 5.1 A square Monodraught™ wind-catcher

Figure 5.2 Operational principle of ventilation mode of wind-catcher in this system

Figure 5.3 Cross-flow fixed-plates

Figure 5.4 Working process of the PEC indirect evaporative cooling unit

Figure 5.5 The schematic diagram of experimental chamber

Figure 5.6 The total dimension of experimental chamber

Figure 5.7 Test room

Figure 5.8 A square Monodraught™ wind-catcher was installed and positioned centrally above the cubic test room

Figure 5.9 The diagram of duct

Figure 5.10 Cross-flow fixed plate Heat recovery was mounted centrally in the ceiling level

Figure 5.11 : Supply stream where indirect evaporative cooling unit was installed

- Figure 5.12 A damper system fitted with the ceiling
- Figure 5.13 Schematic diagram of the system with the PEC indirect evaporative cooling experimental set up
- Figure 5.14 Evaporative cooling experimental set up
- Figure 5.15 Wind tunnel with blower fan
- Figure 5.16 Heaters used to generate warm air
- Figure 5.17 Position of airflow measurements in the ducts
- Figure 5.18 Data acquisition equipment
- Figure 5.19 Schematic of the set up for temperature measurements
- Figure 5.20 Picture of thermocouples position across the system
- Figure 5.21 The position of relative humidity measurement
- Figure 5.22 Temperature change across the heat recovery unit
- Figure 5.23 Efficiency against air velocity
- Figure 5.24 Sensible transferred heat vs airflow rate
- Figure 5.25 Impact of temperature change to the sensible heat transferred for cold and warm air intake conditions
- Figure 5.26 Pressure drop versus air velocity
- Figure 5.27 Temperature vs time
- Figure 5.28 Outlet air temperature vs supply air temperature
- Figure 5.29 Variation of relative humidity difference with temperature change of the evaporative cooling system
- Figure 5.30 Timely variation of supply and outlet air relative humidity across the indirect evaporative cooling unit
- Figure 5.31 Variation of cooling capacity at different air velocity
- Figure 5.32 Cooling capacity variation with supply temperature
- Figure 5.33 Effect of supply air and outlet air temperatures on water consumption rate
- Figure 5.34 Water consumption rate versus temperature change between supply air and outlet air temperatures
- Figure 5.35 Cooling efficiency vs air velocity
- Figure 5.36 Variation of temperature change of heat recovery unit and indirect evaporative cooler
- Figure 5.37 System capacity vs volume airflow rate

Chapter 6

Figure 6.1 Schematic sectional view of building integrated heat recovery panel

Figure 6.2 The wedge layer of insulation material

Figure 6.3 Schematic sectional view along the line A-A

Figure 6.4 The internal channel of insulating panel

Figure 6.5: Experimental rigs for testing structural insulated heat recovery panel performance

Figure 6.6 The heat exchanger (core) is made of polycarbonate and insulated with insulation material

Figure 6.7 Schematic of the set up for temperature measurements

Figure 6.8 BIHR prototype's efficiency

Figure 6.9 Recovered heat of BIHR prototype

Figure 6.10 Pressure drop through the duct of BIHR prototype system

Figure 6.11 Building studied located at Forstal Farm, Kent, UK

Figure 6.12 Wall structure

Figure 6.13 Dimensional information of the building studied

Figure 6.14 Picture of installation

Figure 6.15 Schematic diagram of the set up

Figure 6.16 Heat transfer membrane

Figure 6.17 Network of ducts

Figure 6.18 Gutter and eaves

Figure 6.19 Measurements location

Figure 6.20 Schematic of the set up for temperature measurements

Figure 6.21 Case study I BIHR efficiency

Figure 6.22 Recovered heat against airflow rate

Figure 6.23 Pressure difference at the BIHR intake and exhaust streams

Figure 6.24 Comparison of temperature change between prototype and case study I

Figure 6.25 The enhancement of recovered heat

Figure 6.26 The PV system equipments

Figure 6.27 The schematic diagram of PV powered fan for BIHR system

Figure 6.28 PV system output

Figure 6.29 Electric power from the PV system

Figure 6.30 House in Sussex, UK

Figure 6.31 The installation of BIHR in case study II

Figure 6.32 Ducting system

Figure 6.33 The fresh air was drawn from under the eaves and the stale air was expelled under the roof to the gutter

Figure 6.34 Relationship between efficiency and the airflow rate

Figure 6.35 Comparison efficiency of prototype, case study I and case study II

Figure 6.36 New improved BIHR panel

Figure 6.37 Diagram of corrugated polycarbonate

Figure 6.38 Schematic diagram of the design

Figure 6.39 Diagram of new improved system

Figure 6.40 Effects of airflow on the performance of improved BIHR' system

Figure 6.41 Recovered heat against airflow rate

Figure 6.42 Temperature against recovered heat

Figure 6.43 Comparison of efficiency between BIHR with two airstreams and new BIHR' corrugated channels with four airstreams

Figure 6.44 Comparison of temperature change between BIHR with two airstreams and new BIHR' corrugated channels with four airstreams

Figure 6.45 Comparison of total heat transfer rate for various air velocities between BIHR with two airstreams and new BIHR' corrugated channels with four airstreams

Figure 6.46 Inlet channel of BIHR panel

Figure 6.47 Cross sectional view of the internal channel

Figure 6.48 Direct evaporative cooling model

Figure 6.49 Air convection in the internal channel

Figure 6.50 The novel combined system of BIHR-fibre wick cooling

Figure 6.51 Schematic diagram of experiment set up

Figure 6.52 Inlet channels consists of fibre wick structure wetted by absorbing water

Figure 6.53 Schematic diagram of temperature and RH measurement points

Figure 6.54 Water was supplied to fibre wick structure

Figure 6.55 Variation of water consumption rate with intake air temperature

Figure 6.56 Effect of relative humidity on the water consumption rate

Figure 6.57 Variation of BIHR-fibre wick cooling efficiency with respect to intake air temperature

Figure 6.58 Variation of BIHR-fibre wick cooling efficiency corresponds to air velocity

Figure 6.59 BIHR-fibre wick desiccant dehumidification system

Figure 6.60 Laboratory set up of the present system

Figure 6.62 Variation of supply air to room temperature with intake air temperature

Figure 6.63 Effect of air intake temperature on the performance

Figure 6.64 Moisture absorption capacity against intake air temperature

Figure 6.65 Variation of relative humidity

Figure 6.66 Moisture removal rate against RH in

Figure 6.67 Fibre wick dehumidification performance under constant intake air temperature

Chapter 7

Figure 7.1 Integrated BIHR-PVT concept

Figure 7.2 Schematic of integrated BIHR-PVT system mounted on roof

Figure 7.3 Cut sectional front view of BIHR-PVT integrated system

Figure 7.4 Schematic diagram of BIHR-PVT on roof integrated system with fans installed

Figure 7.6 BIHR-PVT could be used for power supply or drive a heat pump unit

List of Tables

Chapter 2

Table 2.1 Buildings energy consumption (Source: Perez-Lombard et al. 2008)

Table 2.2 Heat/energy recovery types, efficiency and advantages

Chapter 3

Table 3.1 Porosities, pores size and membrane thickness (Source: Liu 2008)

Table 3.2 Performance comparison of different types of ERV (Source: Zhang and Jiang 1999)

Table 3.3 Effect of temperature on flow loss and pressure loss of heat pipe recovery (Source: Shao and Riffat 1997)

Table 3.4 Results of SNES (Source: Roulet et al. 2001)

Chapter 4

Table 4.1 Temperature measurements data

Table 4.2 Efficiency calculation results

Chapter 5

Table 5.1 Results of cold air

Table 5.2 Results of warm air

Table 5.3 Sensible transferred energy (heat)

Table 5.4 Airflow experimental results

Table 5.5 Temperature and relative humidity results

Table 5.6 Testing data

Table 5.7 Water consumption rate of the system

Table 5.8 The results of coefficient of performance

Table 5.9 The temperature values of the system

Table 5.10 Performance results

Chapter 6

Table 6.1 Experiments data of prototype

Table 6.2 The data of case study I (Kent)

Table 6.3 The specifications of PV power fan system component

Table 6.4 Case study II experiments data (Hastings)

Table 6.5 Comparison study data of prototype, case study I and case study II

Table 6.6 Data of the airflow and temperature measurements

Table 6.7 Calculation data from the experiment

Table 6.8 Capital and running cost for BIHR prototype with two airstreams and improved BIHR' corrugated channels with four airstreams

Table 6.9 Capital and running cost for BIHR system in case I

Table 6.10 Experimental data

Table 6.11 Results for instantaneous intake air temperature values

Table 6.12 Results of the BIHR fibre wick cooling test

Table 6.13 Results of BIHR fibre wick desiccant dehumidification experiments

Table 6.14 Moisture absorption capacity calculation results

Table 6.15 Results of the relative humidity experiments

Table 6.16 Results of humidity ratio

Nomenclature

A

A = surface area of heat transfer, m^2

A_f = net free flow area, m^2 ,

B

BIHR = Building integrated heat recovery

BIHR' = Building integrated heat recovery with corrugated airstreams

C

C_{pE} = specific heat of exhaust air stream, $kJ/kg.K$

C_{pS} = specific heat of supply air stream, $kJ/kg.K$

C_E = capacity rate of exhaust air stream, W/K

C_S = capacity rate of supply air stream, W/K

C = capacity rate ratio/heat capacity rate W/K

C_E = present price of the energy

C_A = area dependent first cost of the heat/energy recovery core

C_{pa} = specific heat of air, $kJ/kg.K$

D

D = diameter of the duct, m

D_h = effective diameter of flow channel/hydraulic diameter, m

d_{ia} = humidity ratio of intake air, g/kg dry air

d_{sa} = humidity ratio of supply air to room, g/kg dry air

d_{eq} = humidity of the air which is in vapour pressure equilibrium with the desiccant solution, g/kg dry air

E

ETA = electro-thermal amplification

F

f = friction factor

H

HCOOK = Potassium formate

H = enthalpy of air, kg/kg

$H_{s\ out}$ = enthalpy of supply air before the heat/energy recovery core, kg/kg

$H_{s\ in}$ = enthalpy of supply air after the heat/energy recovery core, kg/kg

$H_{e\ in}$ = enthalpy of supply air after the heat/energy recovery core, kg/kg

h_{cold} = convection coefficient between cold airflow and heat transfer surface,
W/m²K

h_{hot} = convection coefficient between hot airflow and heat transfer surface, W/m²K

h_{fg} = enthalpy of evaporation, kJ/kg

h = specific enthalpy of moist air, kJ/kg dry air

L

L = Duct length, m

Le = Lewis number

M

MHM3C = Heat and Mass Cell Cycle Core

MVHR = Mechanical ventilation heat recovery

M_a = Mass flow rate of air, kg/s

M_E = mass flow rate of exhaust air stream, kg/s

M_r = mass flow rate of return air to heat/energy recovery, kg/s

M_e = mass flow rate of exhaust air out, kg/s

M_S = mass flow rate of supply air stream, kg/s

M_s = mass flow rate of supply air to room, kg/s

M_i = mass flow rate of intake air in, kg/s

m_f = fouling factor, m²K/W

N

Nu = Nusselt number

P

P_f = Fan power/electric used by the fan to blow air in ductwork, W

- Pr = Prandtl number
- P_1 = ratio of total life cycle cost of the heat/energy recovery system to the first year's saving
- P_2 = ratio of total life cycle cost of the heat/energy recovery system to its initial cost
- P_{el} = Electrical power, W
- p = heat transfer perimeter, m

Q

- Q = Volume airflow rate, m^3/s or l/s
- $Q_{h,0}$ = heating load of mechanical ventilation with no heat/energy recovery, W
- Q_h = heating load of mechanical ventilation with heat/energy recovery, W
- q_{HR} = transferred/recovered heat, W
- q_c = cooling capacity, W

R

- R = thermal resistance of heat/energy recovery core, m^2K/W
- Re = Reynold number

S

- SNES = specific net energy saving
- Sh = Sherwood correlation
- s = thickness of the heat transfer surface, m

T

- T_i = temperature of intake air in, $^{\circ}C$
- T_r = temperature of return air to heat/energy recovery, $^{\circ}C$
- T_e = temperature of exhaust air out, $^{\circ}C$
- T_s = temperature of supply air to room, $^{\circ}C$
- $T_{surface}$ = surface temperature, $^{\circ}C$
- T_f = fluid temperature, $^{\circ}C$
- $T_{s out}$ = temperature of supply air before the heat/energy recovery core, $^{\circ}C$
- $T_{s in}$ = temperature of supply air after the heat/energy recovery core, $^{\circ}C$
- $T_{e in}$ = temperature of exhaust air before the heat/energy recovery core, $^{\circ}C$

- T_R = indoor air temperature
 $\overline{T_e}$ = average ambient temperature of timescale Δt
 T_{op} = operating time of air handling unit per day, h/day.

U

- U = heat transfer coefficient, W/m^2K

V

- V = air velocity, m/s

Greek symbols

- ΔP = pressure drop/pressure difference, Pa
 ΔT_{max} = maximum temperature differential in the heat/energy recovery system
 Δt = annual operation time of the heat/energy recovery in seconds
 Δt = period of time, h/day
 ν = kinematic viscosity of the fluid, m^2/s .
 ρ = air density, kg/m^3
 ω = air humidity ratio, kg/kg
 α_E = surface convection heat transfer coefficient from exhaust air to heat/energy recovery core. W/m^2K
 α_S = surface convection heat transfer coefficient from supply air to heat/energy recovery core. W/m^2K
 α_D = thermal diffusivity, m^2/s
 λ = thermal conductivity of heat exchange material, W/m^2K ,
 λ_f = thermal conductivity of the fluid, W/mK
 ε_f = fan efficiency
 ε_S = sensible effectiveness/temperature efficiency, %
 ε_L = latent effectiveness/moisture transfer efficiency, %
 ε_T = total effectiveness/enthalpy transfer efficiency, %
 ε_{HR} = Heat/energy recovery efficiency, %

$\omega_{s \text{ out}}$ = moisture/humidity ratio of supply air before the heat/energy recovery core,
kg/kg

$\omega_{s \text{ in}}$ = moisture/humidity ratio of supply air after the heat/energy recovery core,
kg/kg

$\omega_{e \text{ in}}$ = moisture/humidity ratio of exhaust air before the heat/energy recovery core,
kg/kg

Published Papers

The following articles have been published by the author during the preparation of this thesis:

1. **A. Mardiana-Idayu**, S. B. Riffat, M. Worall and M. Gillott, Experimental investigation of air-to-air plate heat recovery performance with wind-catcher ventilation system, SET8th, Aachen, Germany, (2009).
2. **A. Mardiana-Idayu**, S.B. Riffat, A novel integrated heat recovery system for building ventilation, SET9th, Shanghai, China, (2010).
3. **A. Mardiana-Idayu**, S.B. Riffat, Performance investigation of novel building integrated heat recovery system with fibre wick structure for cooling/dehumidification, SET10th, Istanbul (2011). (submitted)
4. **A. Mardiana-Idayu**, S.B. Riffat, An experimental study on the performance of enthalpy heat recovery system for building applications, Energy and Buildings (under review).
5. **A. Mardiana-Idayu**, S.B. Riffat, Development and performance investigation of building integrated heat recovery system, Journal of Low Carbon Technologies (under review).
6. **A. Mardiana-Idayu**, S.B. Riffat, A review on heat recovery systems for building applications, Renewable and Sustainable Energy Journal (under review).

CHAPTER 1

Introduction

1.1 Background

“Energy and persistence conquer all things”

Benjamin Franklin

Buildings are the most significant energy-consuming economic sector right from the construction phase to the operation and maintenance stage. Energy use is a central issue as enormous energy is used in the construction of buildings. There are several different uses of energy in buildings. The major uses are for lighting, heating, cooling, power delivery to equipment and appliances and domestic hot water owing to global energy crisis. The amount that each contributes to the total energy use varies according to the climate, type of building, and time of year. Literatures have proven that space heating, ventilating and/or air conditioning (HVAC) system takes a large proportion of the total building energy consumption on a national level in most of the countries worldwide. In areas where very mild winters occur, cooling load will be greater than heating load in terms of the total energy use. In some types of buildings in certain climatic zones, the air conditioning might be greater than either the heating or cooling loads. On the other hand, industrial and commercial buildings are very similar in terms of energy use except that many industries use large quantities of energy for specialized processed. Thus, it is difficult to generalize about energy use by type of building because there are so many variables that determine the energy use in a particular location.

As stated by Perez-Lombard et al. (2008) building energy consumption has increased as a result of economic growth, expansion of building sectors and spread of heating, ventilation and air conditioning (HVAC) system. As buildings have a long life of several decades or even centuries, all decisions made at the design stage have long-term effects on the energy balance and the environment. Apart from that, the following four goals are set by ASHRAE in the Advanced Energy Design Guide for buildings, for achieving energy savings in a new construction:

- Reducing internal and external loads
- Matching the capacity of the HVAC and other systems to the reduced loads (because oversized systems cost more and do not operate at their optimum efficiency)
- Using higher efficiency equipment that will use less energy to meet any given load
- Integration of low carbon systems to increase energy savings potential

1.2 Problem statement

All life on earth depends in some way on energy and it has a tremendous influence on human lives. In the context of built environment, literatures have proven that buildings are responsible for about 40% of national energy demand in EU (Ekins and Lees 2008), 47% in UK (DTI 2005), 46.7% in China (Wang et al. 2010), increasing at a rate of 4.2% and 1.9% per annum in Spain and North America respectively, 20 to 40% in developed countries (Perez-Lombard et al. 2008) and predicted to increase by 34% in the next 20 years (IEA 2004). This increasing trend of energy consumption in buildings is contributed in large proportion by building space heating/cooling and ventilation. In order to overcome energy consumption and at the

same time to promote energy conservation in buildings, most countries in the world have shown their commitments by setting up new building standards, policies, regulations, recognition and technologies. For example, in the EU, the Energy Performance of Building Directive (EPBD) being adopted in December 2002 where in this policy all new buildings must be nearly zero energy buildings by 2018 and Member States shall set intermediate targets for 2018. On the other hand, Building Regulations under UK Government is a standard for design and construction which apply to most new buildings and many alterations to existing buildings in UK. Revisions Part L (conservation of fuel and power) also came into effect in October 2010 stating that *“reasonable provision shall be made for the conservation of fuel and power in buildings by limiting heat gains and losses through thermal elements and other parts of the building fabric; and from pipes, ducts and vessels used for space heating, space cooling and hot water services”*. When the proposed energy efficiency standards in Part L are strengthened, there is likely to be a tendency to more airtight buildings. This approach encourages the building design to adopt energy-efficient building materials and technologies and at same time to ensure adequate means of ventilation are provided.

However the existing technologies in terms of conventional heating, ventilation and air conditioning (HVAC) are designed without taking into account the energy-efficient consideration has led to large wasteful amount of energy loss. In addition to this, the energy consumption of the conventional HVAC systems produce a large emission of CO₂ and could possibly cause indoor air pollution and leading to Sick Building Syndrome (SBS) that affect health and comfort of building occupants. Thus, in order to maintain good and healthy indoor environment, provide a habitable

and comfortable place for human occupation as well as conserve the energy, energy-efficient technologies should be adopted in building services such as evaporative cooling, desiccant dehumidification, photovoltaic and passive ventilation and building integrated design. Therefore, the challenge is then to develop an energy-efficient system which can make a big contribution to CO₂ emission reduction, to fulfil the building code requirements and energy conservation either as an alternative to the conventional systems or as an incorporating system to the existing technologies. One of the significant ways for this purpose is by the installation or usage of heat or energy recovery device which is known as one of the main energy-efficient systems that will decrease the power demands of building heating, air conditioning and ventilation loads as illustrated in Figure 1.2.

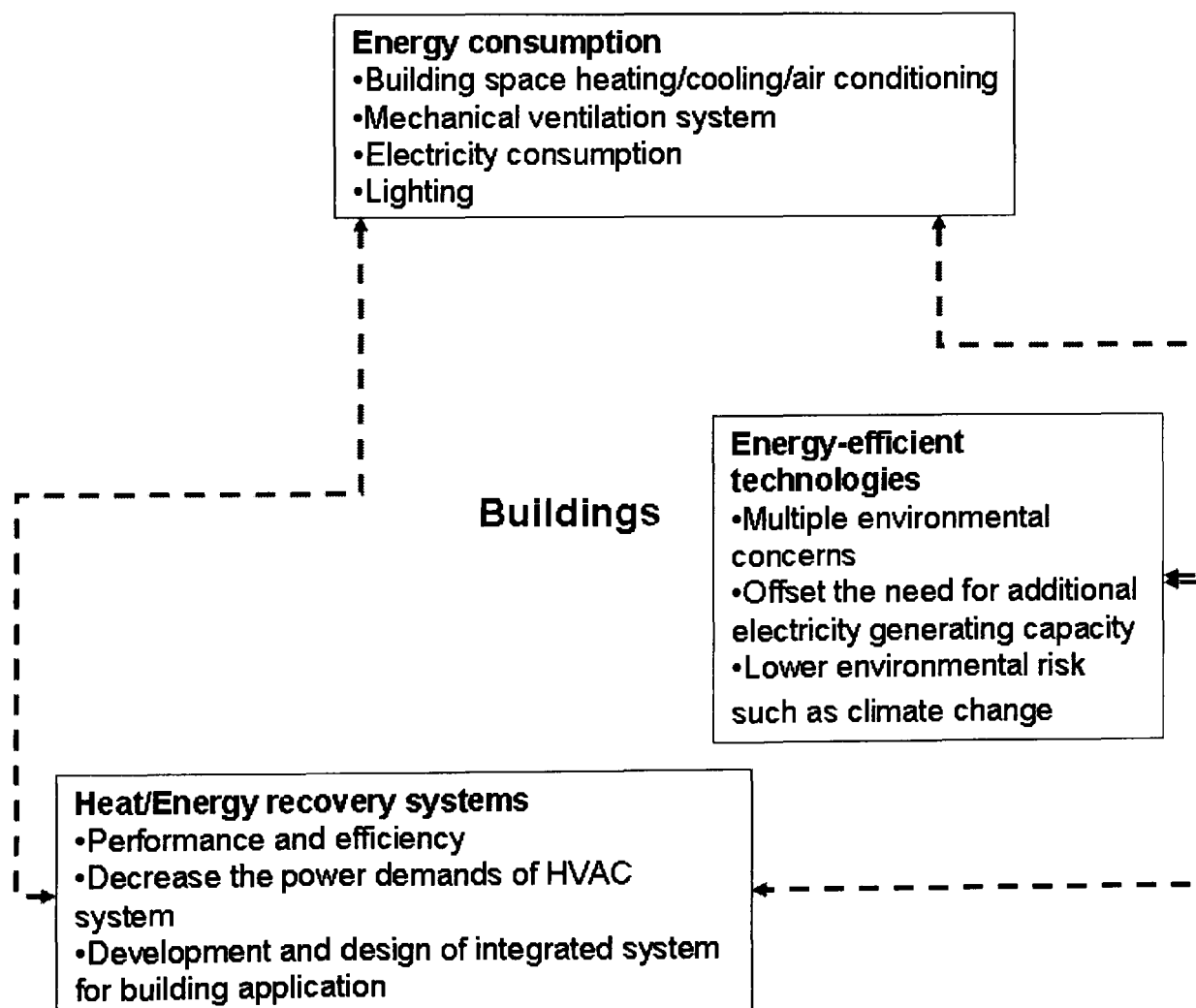


Figure 1.1 Link between building and energy and the needs for heat recovery system

Heat recovery systems have a dense of works in the literatures. Many theoretical and experimental works in literatures have been conducted for individual systems as well as the integration of the systems with mechanical ventilation, natural ventilation, air conditioning and dehumidification technologies. However, little research has been done on the integration or combination of heat recovery with low carbon technologies such as evaporative cooling, photovoltaic panel and desiccant dehumidification. In addition, better knowledge of building integrated heat recovery system is still fundamental and no practical work has been done for integration of heat recovery with low carbon technologies to become one device with multifunction in one system to be used in buildings. Thus, the work presented in this thesis will explore the development of novel heat recovery systems coupled with low carbon technologies, and its integration to become one device with multifunction (building integrated heat recovery/cooling/air dehumidifier) in order to achieve integrated energy-efficient system for building applications.

1.3 Research objectives

This research project generally aimed to achieve a substantial improvement in the understanding of the heat recovery for building applications on an existent load of knowledge in the field. The objectives of the research are:

- To assess heat recovery performance parameters based on theoretical background study and investigate the performance of some heat recovery devices.

- To integrate the heat recovery system with low carbon technologies such as wind-catcher and evaporative cooling and investigate its performance in order to develop energy-efficient system for building applications.
- To develop and evaluate the performance of a building integrated heat recovery (BIHR) system utilizing polycarbonate heat transfer surface under laboratory condition.
- To investigate and collect quality experimental data using full-scale measurements of building integrated heat recovery (BIHR) performance on existing buildings in UK.
- To build and assess the performance of a building integrated heat recovery (BIHR) system with fibre wick structure in order to develop an adaptable system for cooling and dehumidification under laboratory condition.

1.4 Research Methodology

The study of heat recovery system for building applications is based on the investigation of the following topics:

- Theoretical and parametric background study based on physical basis of heat recovery system.
- Experimental investigations under laboratory conditions to determine efficiency, effects of temperatures, recovered heat and effects of velocity on heat recovery performance.

- Development and experimental performance evaluation of integrated heat recovery system associated with wind-catcher technology and evaporative cooling.
- Laboratory and full-scale measurements on real buildings in UK of building integrated heat recovery (BIHR) system.
- Construction and performance assessment of building integrated heat recovery (BIHR) with fibre wick structure for cooling and dehumidification.

1.5 Thesis structure

The research has been carried out in different stages and covered a number of tasks. This thesis comprises eight chapters. Chapter 1 discusses the general introduction of the thesis. It presents the proposed area of research, research objectives, research methodology and concludes with the thesis structure.

Chapter 2 describes an in-depth discussion on the literature review of energy consumption and its relation with buildings, primary sources of energy consumption in buildings, strategies to overcome in terms of regulatory, awards and the adoption of energy-efficient technologies. The major part of this chapter outlines the different types of heat recovery as an approach of energy-efficient technology for building applications. It also reviews the development of the heat recovery system in integrated or combined with other technologies such as mechanical and passive ventilation, air conditioning, dehumidification and photovoltaic panel.

Chapter 3 presents the review on theoretical studies of heat recovery system based on existing literatures. Chapter 4 describes the experimental investigation of an

individual heat recovery unit in order to understand the various performance parameters. This chapter presents experimental procedure and instrumentation used to measure heat recovery performance. This chapter also covers theoretical calculations, test results and performance analysis. The procedures outlined in this chapter were the basis for all heat recovery performance experiments in this thesis.

Chapter 5 concentrates on the design and experimental study of an integrated heat recovery system for building applications associated with wind-catcher technology and evaporative cooling in a large scale model. It presents the details of each component, working principle of the system, the experimental techniques adopted and the results gained.

Chapter 6 introduces a development of the design of a novel building integrated heat recovery (BIHR) system. The chapter discusses system design features and construction, operation of the design and experimental investigation under laboratory condition for prototype investigation. Besides, the performance investigations of BIHR system on real buildings in UK are also discussed in this chapter which involving two case studies in Ashford, Kent and Hastings, Sussex. It shows the details of test building, description of building integrated heat recovery system, experimental work and results. This chapter also presents integrated heat recovery with fans driven by photovoltaic panels which covers the methodology of the test, experimental set-up and concludes with a discussion of the results. The new improvement design of BIHR corrugated channels with four airstreams has also been developed and described. The economic and environmental analysis is also presented in this chapter. The development of BIHR with fibre wick structure is also explored which involving two

difference cases. Two different cases are presented where the case I discusses the BIHR-fibre wick structure for cooling system while case II involves the development of design for desiccant dehumidification purpose. Each case study covers the development and experimentation as well as performance analyses based on experimental results.

Finally, in Chapter 7 a summary of the research findings which consists main conclusions of each chapter, contributions and novel features of the research are drawn. It also presents future work related to the novel heat recovery systems for building applications investigated in this thesis.

CHAPTER 2

Literature Review

2.1 Introduction

Literature review is essential to have an insight into existing knowledge leading to the understanding of the previous works and researches carried out concerning the area keeping in mind the latest state of development. In the process a collection of research materials such as books, journal articles, reports, internet documents and so on were utilized. This chapter presents the literatures of the basic understanding of building and energy consumption, primary sources of energy consumption in buildings, strategies to overcome with approaching to regulatory, awards and energy-efficient technologies. Throughout, the need for an integrated approach to energy-efficient design will be stressed. The main part of this chapter consists of a thorough review of heat recovery systems as an approach of energy-efficient design in order to conserve the energy in buildings and their development in integrated or combined with other technologies for building applications by previous researchers are explored.

2.2 Building and energy consumption

Energy is essential to economic and social development and improved quality of life. Much of the world's energy, however, is currently produced and consumed in ways that could not be sustained and significantly higher than the environmentally friendly renewable energy source. According to The International Energy Agency, during the last two decades (1984 to 2004) primary energy has grown by 49% and CO₂ emission by 43% with an average annual increase of 2% and 1.8% respectively

as shown in Figure 2.1 by Perez-Lombard et al. (2008). He also reported that the energy use by nations with emerging economies (South East Asia, Middle East, South America and Africa) will grow at an average annual rate of 3.2% and will exceed by 2020 that for the developed countries (North America, Western Europe, Japan, Australia and New Zealand) at an average growing rate of 1.1. On the other hand, in the Ninth Malaysia Plan, the energy demand is estimated to increase at the rate of 6.3 annually (National Energy Balance (2008) to sustain the nation's economic growth (Manan et al. 2010). A recent World Energy Council (WEC) study found that without any change in our current practice, the world energy demand in 2020 would be 50 to 80% higher than 1990 levels (Omer 2008).

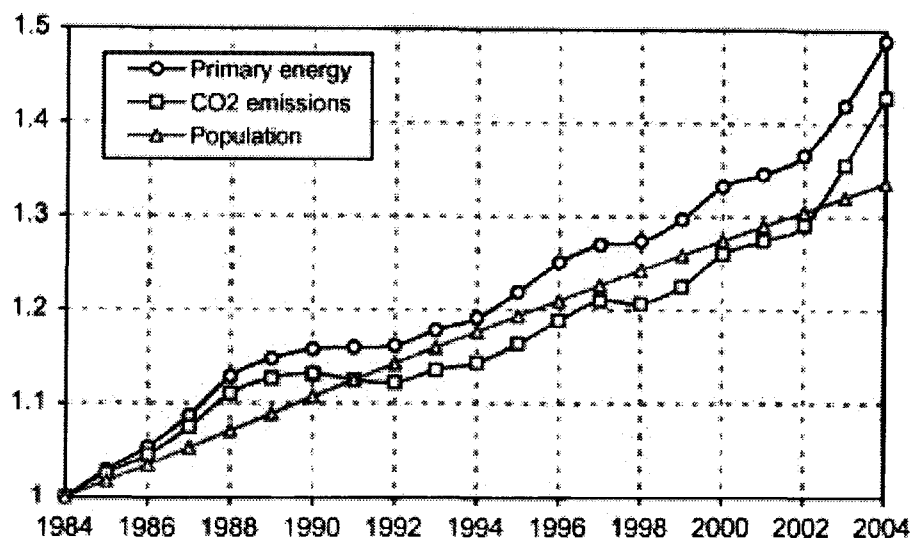


Figure 2.1 World energy consumption in percentage ratio from International Energy Agency (Source: Perez-Lombard et al. 2008)

Buildings are a fundamental part of a country's culture and heritage and much more than a thermal envelope that transmits or conserves energy or a locus for indoor energy consumption. Thus, it is interesting first to review very briefly how building and energy are related to each other. Literatures have proven that people spend 90% of their time live and works in buildings. Furthermore, growth in population, together with the enhancement of building services and comfort levels, buildings have

contribute to major of world energy consumption. Energy in buildings can be categorized into two types:

- Energy for the maintenance/servicing of a building during its useful life.
- Energy capital that goes into production of a building (embodied energy) using various building materials.

Energy is used by the building services installed within buildings to create a comfortable, safe, healthy and productive environment. To achieve this, the following systems are commonly used:

- Space heating/cooling/air conditioning
- Mechanical ventilation
- Domestic hot water heating
- Lighting

Recent reports by the Inter-governmental Panel on Climate Change (IPCC) have raised public awareness of energy use and the environmental implications and generated a lot of interest in having a better understanding of the energy use characteristics in buildings (IPCC 2007). Energy consumption in buildings can be described in terms of primary energy or delivered energy. Primary energy is that which is found within the fossil fuels in the ground. Delivered energy is that which is delivered to the building. Buildings are responsible for about 40% of EU energy demand (Ekins and Lees 2008). Whilst in the UK, buildings are responsible for 47% of national energy consumption (DTI 2005). On the other hand, in China, building stocks accounted for about 24.1% in 1996 of total national energy use, rising to 27.5% in 2001 and were predicted to increase about 35% in 2020 (Yao and Li 2005). In

addition, Wang et al. (2010) reported that the buildings in China increased for 46.7% of the total energy consumption of the country.

Table 2.1 shows the weight of buildings energy consumption of several countries reported by EIA in 2004 and analyzed by Perez-Lombard et al. (2008). From the table, it can be seen that in the UK building energy consumption has increased at a rate of 0.5% per annum and is responsible for 47% of national energy consumption. In addition, by analysing current trends, the EIA forecasted the future trends in building energy consumption which would grow by 34% in the next 20 years.

Table 2.1 Buildings energy consumption (Source: Perez-Lombard et al. 2008)

Final energy consumption (%)	Commercial	Residential	Total
USA	18	22	40
UK	11	28	39
EU	11	26	37
World	7	16	24

On the other hand, the buildings in China account for 46.7% of the total energy consumption of the country (Wang 2010). On the other hand, energy consumption of buildings in developed countries comprises 20 to 40% of total energy use and is above industry and transport figures in EU and USA (Perez-Lombard et al. (2008).

2.2.1 Primary sources of energy consumption in buildings

2.2.1.1 Building space heating and cooling/air-conditioning

Parts of the major energy consumption in buildings are the heating and cooling system. They are indoor climate controls that regulate humidity and temperature to provide thermal comfort. Space heating is the most important building energy user in cold countries, whereas air conditioning is a major contributor to peak electricity demand in hot climate countries or during summer. Energy consumption of building space heating and air conditioning will continue to take a large proportion of the total building energy consumption (Gong et al. 2008) with economic prosperity. This fact was then supported by Liu et al. (2010) by stating that the heating or cooling of an enclosed space to maintain thermal comfort is a highly energy intensive process accounting for as much as 60 to 70% of total energy. In the UK, energy used for space heating was about 50% of the service sector energy consumption in 2004 (IEA 2008). On the other hand, air conditioning and heating contributes for 65% of the total building energy consumption of the building in China (Wu 2003). Kwok and Rajkovich (2010) reported that the building sector accounted almost 39% of the total primary energy requirements (PER) in the United States of which almost 35% was used for heating, ventilation and air conditioning (HVAC). By and large, HVAC consumption in developed countries accounts for half the energy use in buildings and one fifth of the total national energy use. These heating, cooling loads and air conditioning are having an impact on CO₂ emissions, as well as on security of energy supply (IEA 2007).

2.2.1.2 Ventilation

Ventilation is generally defined as a supply of outside air into the building's interior allowing air motion and replacement of stale exhaust air by fresh outside air. According to ASHRAE Standard 62 and the ASHRAE Handbook, ventilation air is the air used for providing acceptable indoor air quality. Ventilation air is necessary to dilute odours and limit the concentrations of carbon dioxide and airborne pollutants. Thus, the primary aims of ventilation are to improving the qualities of air and maintain human comfort. Lack of ventilation has been claimed to cause Sick Building Syndrome (SBS) a combination of ailments (a syndrome) associated with an individual's place of work or residential (Wargocki et al. 2000). In addition, Khan et al. (2008) stated that less ventilation can cause excessive humidity, condensation, overheating and a build-up odours, smokes and pollutants.

Thus, to fulfil the needs of good indoor air quality and thermal comfort for occupants large energy load is imposed on buildings and this is the reason for HVAC in the context of mechanical ventilation system becomes a major contribution of energy consumption in buildings. Ventilation though essential for maintaining acceptable indoor air quality, is always accompanied by energy loss since outdoor air must be cooled or heated to bring it to the space condition (Nguyen et al. 2005). In Europe, with the consolidation of the demand for thermal comfort and indoor air quality, the energy demand for heating from ventilation air tends to reach about 60% to 70% of the total annual energy demand for the building (Besant 2000). Of this 30 to 50% is related to ventilation (Khan et al. 2008). Since the envelope of building equipped with HVAC system is becoming tighter, the energy consumption resulted by the ventilation can be much higher than that caused by the heat transfer through the

building shell (Juodis 2006; Lazzarin and Gasparella 1998). In modern building, the ventilation losses may become more than 50% of total thermal loss (Routlet et al. 2001).

2.2.2 Strategies to overcome energy consumption problems in buildings

In general, there are three key instruments to overcome energy consumption and at the same time to promote energy conservation in built environment including residential, non-domestic, office and commercial namely policy or regulation, awards or recognition and technologies. Thus, government sectors, scientists, researchers, engineers, architects and other built environment professionals are trying very extremely to enforce policies, find advanced technologies, renewable energies and useful strategies to reduce carbon emission and conserve energy.

2.2.2.1 Regulatory and policy

In recognition of the need to save energy, conservation of fuel and power is included within the building regulations which are enforceable by law. In the past the regulations have concentrated on reducing the space heating energy use of buildings. The now include lighting, ventilation and air-conditioning with an expected tightening of standards in future years. For instance, in order to achieve energy conservation, help alleviate global warming and improve local environmental sustainability, the Hong Kong Government has paid great efforts on promoting energy efficiency in buildings.

Furthermore, the scientific evidence for climate changes and the associated impacts of greenhouse gas emissions are becoming increasingly obvious. One new

factor is the strengthening global impulse to reduce greenhouse gas emission in order to mitigate future climate change. In 1992 at the Environment and Development (UNCED 1992) conference in Rio de Janeiro, the European Union committed itself to stabilising and then reducing carbon dioxide and CFCs emissions into the environment. In addition, Kyoto Protocol was also established regarding the effects of the emissions from the burning of fuels and aimed to reduce the amount of CO₂ emissions.

The proliferation of energy consumption and CO₂ emissions in the built environment has made energy efficiency and savings strategies a priority objective for energy policies in most countries (Perez-Lombard et al. 2008). There are several advanced buildings design standards such as ECOhomes (BRE, UK), Passivhaus (Germany) AECB (UK) and LEED (USA) (Wang et al 2009). Commission of the European Communities stated that EU policy has identified increased energy efficiency for buildings as a key objective of EU energy and climate policy (Ekins and Lees 2008). In addition to this, in the EU, the main regulatory framework is the Energy Performance of Building Directive (EPBD) which is being adopted in December 2002 to improve the energy performance of buildings and which stresses the development of a common framework for the potential energy savings in the buildings sector throughout Europe (Ekins and Lees 2008). In this policy, all new buildings must be nearly zero energy buildings by 2018 and Member States shall set intermediate targets for 2018. A nearly zero energy building (ZEB) is a building that has a very high energy performance which means very low amount of energy required should be covered to a very significant extent by energy from renewable sources.

On the other hand, Building Regulations under UK Government is a standard for design and construction which apply to most new buildings and many alterations to existing buildings in England and Wales. Revisions Part L (conservation of fuel and power) also came into effect in October 2010 stating that “*reasonable provision shall be made for the conservation of fuel and power in buildings by limiting heat gains and losses through thermal elements and other parts of the building fabric; and from pipes, ducts and vessels used for space heating, space cooling and hot water services*”. When the proposed energy efficiency standards in Part L are strengthened, there is likely to be a tendency to more airtight buildings. This approach encourages the building design to adopt energy-efficient building material and technologies and at same time to ensure adequate means of ventilation is provided. In addition, Code for Sustainable Homes: an environmental impact rating system for housing in England & Wales, setting new standards for energy efficiency. Code levels pertaining to energy require a Dwelling Emission Rate (DER) a certain percentage higher than the Target Emission Rate (TER) as set in Part L1A of the Building Regulations. October 2010 saw Part L standards rise equivalent to Code level 3. Since this change Code level 4 requires 25% DER improvement over Part L1A TER standards and code level 5 is 100% improvement i.e. thermally twice as efficient. It is also anticipated that the Building Regulations as well as the minimum mandatory Code level will continue to improve until the 2016 target of 'net zero CO₂ emissions' per annum standard.

The “cradle to grave” term linked the building and construction sector to gain sustainable development. In regard to this, in the UK the “Building Regulation Approved Document L2A (2006) (Part L) took effect in 2006 and addresses the

conservation of fuel and power in the construction sector. This approach encourages the building design to adopt energy-efficient building material and technologies.

Besides, more attention has also recently been paid to the energy efficiency of buildings in China. For example, in 2005, the Ministry of Construction of the People's Republic of China published "Public Building Energy Efficiency Design Regulation" in order to improve the energy efficiency design standard (Wang et al. 2010) to improve the energy efficiency of public buildings by 50%. Energy Performance Norm (EPN) has been introduced in the Netherlands, a standard which is used to express the energy efficiency of a building in the number of energy performance coefficient (Brummelen 2006). Whilst in Malaysia, Low Energy Office (LEO) building initiated by the Ministry of Energy, Water and Communications (MEWC) has been adopted where the building is designed to achieve a building energy index of 40 kwh/m²/yr. A few facts put that in perspective: the benchmark to qualify as an energy efficient building (as defined in Malaysian Standards MS1525:2001) is energy consumption of not more than 135 kwh/m²/yr.

2.2.2.2 Awards as energy conservation instruments

Another instrument to promote energy conservation in built environment is energy awards or recognition where globally, many countries have organized energy awards to contribute towards energy sustainability (Manan et al. 2010). National Energy Efficiency Awards program has been introduced in 2006 in UK (www.energyaward.co.uk). The Malaysian Government under the Ministry of Energy, Green Technology and Water (MEGTW) has developed key policies and strategies for over 30 years to ensure energy security as well as sustainability, encourage energy

efficiency and mitigate environmental impact to meet its rising energy demand as shown in Figure 2.2 (Manan et al. 2010).

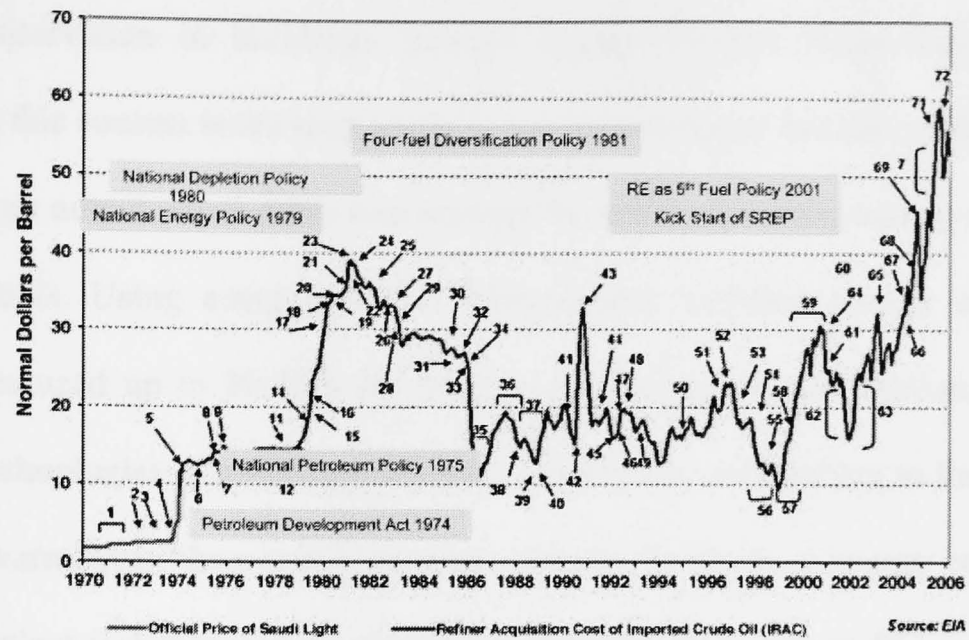


Figure 2.2 Evolution of Malaysia energy policy with crude oil price (Manan et al. 2010)

Whilst, Japan has introduced a national award system on Energy Conservation Excellence Cases in 1975 which is organised by the Energy Conservation Centre of Japan (ECCJ) (PROMEEC 2008). On the other hand, the Hong Kong Awards for Energy efficiency and Conservation were launched for the government sector in 2003 and for private sector in 2004 (www.eeawards.emsd.gov.hk). The Energy Conservation Award is one of the innovative schemes initiated by the Ministry of Power of India since 1991 to promote energy conservation (www.bee-india.nic.in). ASEAN Energy Awards have been given by the ASEAN Centre for Energy since 2001 (www.aseanenergy.org). The survey has shown that energy awards have made significant impact to achieve the objectives to adopt energy efficiency to the private and public sector (Manan et al. 2010).

2.2.2.3 Adoption of energy-efficient technologies

Owing to global energy crisis, various technical strategies are adopted for energy conservation in buildings through energy-efficient technologies. Energy-efficient in this context is the term given to the ratio between the energy input and the useful energy output which takes into account the form of primary energy source such as fossil fuels. Using energy-efficient technologies, building energy consumption could be reduced up to 20-30% by 2020. Furthermore, implementation of energy-efficient technologies in buildings will be a substantive contribution to the mitigation of global warming in the coming decades. In order to improve energy conservation, energy-efficient technologies can be used in building applications (Ke and Yanming 2009). However, energy efficient design can only be achieved successfully through careful design of built form and services using renewable or low energy sources (wind, water, solar energy, etc.) and passive solutions (Liddament 1996).

As we aware, total electrical energy demand in buildings is consumed by the air conditioner to maintain the comfort zone. For energy conservation and the protection of the environment, it becomes increasingly important to design air conditioning systems which save energy as well make comfortable air (Yoo and Kwon 2004). Wu et al. (2009) stated that evaporative cooling may be an alternative to mechanical refrigeration cooling for air conditioning as it is enhanced at the present status when energy saving and environmental preserving are two subjects in all engineering fields due to its characteristics of zero pollution, energy efficient, simplicity and good indoor air quality. Besides, to reduce the latent heat, desiccant dehumidification process can be added to the conventional air conditioning system

(Sukamongkol et al. 2010). Compared to cooling dehumidification, desiccant dehumidification has advantage in having greater energy saving potential (Liu 2007).

Besides, passive or natural ventilation also can reduce energy consumption on mechanical ventilation as well as improve indoor air quality. Natural ventilation is now one of the fundamental methods in the energy-efficient design of buildings (Khan et al. 2008). Wind-catchers/wind cowls or wind towers are the example of passive ventilation that have traditionally been used in the Middle East for many centuries to scoop the wind with no requiring energy to ventilate indoor space naturally. Recently, the wind-catcher systems have been increasingly installed in buildings around UK such as Queen's Building at De Monfort University, Jubilee Campus in Nottingham University and Inland Revenue building in Nottingham. In addition to bringing energy savings, these environmentally friendly technologies also help create healthier interiors for occupants (Elmualim 2006).

It comes to a brilliant state when the power of sun has a great effect on energy preserving and conserving. With this, the use of photovoltaic or solar panel in recent years has reached a remarkable edge (Thirugnanasamdandam et al. 2010). There are dense of research works have been done in this field for alternative energy to replace the scarcity of fossil fuels since electricity can be generated by converting energy from the sun using photovoltaic or solar cells. These works include solar water heaters (Chang et al.2002; Mathioulakis and Bellessiotis 2002), solar chimneys (Zhou et al. 2007; Changtawong et al. 2006; Ong and Chow 2003), solar air conditioning (Belusko et al. 2004; Gommed and Grossman 2007 and building integrated solar panel (Bazilian and Prasad 2002; Crawford et al. 2006).

With the growing demand for thermal, natural ventilated buildings, a standard requirement for future projects, regulatory and policy to meet, private and public awareness, less energy usage for conventional system, which are why energy-efficient technologies are becoming more popular. Since buildings have a long life span, lasting for 50 years (Wan et al. 2010) or more it is therefore, in conserving the energy, strategies to recover energy consumption in building is strictly important. From the reviewed literatures, it can be said that a large amount of energy is lost due to heating, air-conditioning and ventilation, it is thus very important to recover this energy by adopting heat recovery system for building applications. In addition, an approach is needed to integrate energy-efficient technologies in a way to meet high conservation of building energy consumption.

2.3 Heat recovery: An approach of energy-efficient technology for building application

In recent years, building ventilation loads are becoming more important as the indoor air quality standards and thus fresh air rates are increasing. Under these circumstances, more and more air handling units are equipped with heat recovery systems with the aim of decreasing the energy use in buildings (Hong 2009; Riffat et al. 2006)). Since all buildings require a source of fresh air, the need for heat recovery in ventilation system has become obvious. While opening a window does provide ventilation, the building's heat and humidity will then be lost in the winter and gained in the summer, both of which are undesirable for the indoor climate and for energy efficiency (<http://www.en.wikipedia.org>). Thus, heat recovery technology offers an optimal solution: fresh air, better climate control and energy efficiency (Shao et al. 1997).

Heat recovery in building applications comes into widespread use in some Europe countries, especially in the high latitude nations such as Germany and Sweden (Lazzarin and Gasparella 1998; Fehrm et al. 2003). Acknowledgement is worthwhile to new regulatory, policies, standards and energy-efficient technologies development on this field for the last decades, the heat recovery system has currently become a requirement in building designs. In Germany, the building code for the year 2000 contains prescripts for well insulated and tight buildings so the energy demand for heating from ventilation air tends to reach about 60% of the total annual energy demand for the building. Under these circumstances new buildings must install ventilation systems with heat recovery (Zhou et al. 2007). Using heat recovery it has been shown that the final energy consumption can be reduced up to 20% in cold climates (Fehrm et al. 2002). In China, more and more commercial buildings and single-family houses use air-to-air heat recovery ventilator as energy saving units for recovering heat from the exhaust air in ventilation systems in the current years (Ke and Yanming 2009).

2.3.1 Definition and concept of heat recovery

Heat recovery term in this study is refer to an air-to-air heat recovery system which is defined as the process of recovering energy (heat/mass) from a stream at a high temperature to a low temperature stream that is effective and economical to run (Riffat et al. 1998). On the other hand, Shurcliff (1988) defines that heat or energy recovery is any device that removes in terms of extracts, recovers or salvages heat or mass from one air stream and transfers it to another air stream. This means that the energy that would otherwise be lost is used to heat the incoming air, helping to maintain a comfortable temperature. Whilst in industries, it is abbreviated as HRV or

ERV (heat recovery ventilation) and became a general use within them. There are many different types of heat recovery systems are available for transferring energy from the exhaust air to the supply air or vice versa (Butcher and Readdy 2007; El-Baky and Mohamed 2007; Juodis 2006; Fehrm et al. 2002; Liu et al. 2006). These include sensible heat recovery and enthalpy (sensible and latent) heat recovery (Dieckmann et al. 2003). The heat transfer surfaces based in sensible heat recovery can only transfers sensible heat between the makeup and exhaust air, while in the enthalpy recovery, it can transfers both sensible and latent heat (moisture) however, have greater maintenance requirement and costly than sensible heat recovery (Lazzarin and Gasparella 1998). Above all, these systems are significantly proved as the most efficient single energy saving method of building in a cold climate.

Heat recovery systems typically recover about 60% to 95% of the heat in exhaust air and have significantly improved the energy efficiency of buildings. There are a number of possibilities and concepts for heat recovery from exhaust air in ventilation. The concept to be chosen depends on the possibilities for utilising the recovered energy (Shao et al.1997). Heat recovery systems are utilized to recover a fraction of the energy loss. Besides offering energy saving, this system also gives some advantages such as, reduces heat loss rather than create heat which is relatively to cost effective. This system also gives effective ventilation where open windows are security risk and in windowless room like bathrooms and toilets. It can also operate as ventilation system in summer, by passing the heat transfer system and simply replacing indoor air with fresh outdoor air. Whilst, during winter, it can reduce indoor moisture, as cooler outside air will have lower relative humidity. Heat recovery system certainly would save energy for fresh air treatment (Roulet et al. 2001; Zhang

et al. 2005). The efficiency of the heat recovery system is often used to calculate the energy saving (Routlet et al. 2001). The impact of unintentional airflows on the performance of ventilation units with heat recovery is discussed on the basis of single room ventilation units in Manz et al. (2001). It is shown that the unintentional airflows can considerably reduce the performance of ventilation units in terms of efficiency.

A typical heat recovery system in building consists of ducts for incoming fresh air and outgoing stale air, a heat exchanger core, where heat or energy is transferred from one stream to the other and two blower fans; one is to exhaust stale air and supply fresh air via the heat exchanger core. Figure 2.3 shows a typical heat recovery system installed in ventilation system. In the core, the fresh air stream is automatically preheated or pre-cooled (depending on the season) by the exhausted air and distributed to the interior part of the buildings. The outgoing and incoming air passes next to each other but do not mix in the heat exchanger. They are often installed in a roof space or within the building interior, recover heat from the internal air before it is discharged to the outside and warm the incoming air. In an advance design of this system, sometimes the incoming air is filtered to reduce the incidence of pollen and dust while the outgoing air is filtered to protect the heat exchanger and internal components. This system is also used in building HVAC energy recovery systems, where building exhaust heat is returned to the comfort conditioning system. This device lowers the enthalpy of the building supply during warm weather and raises it during cold weather by transferring energy between the ventilation air supply and exhaust air streams.

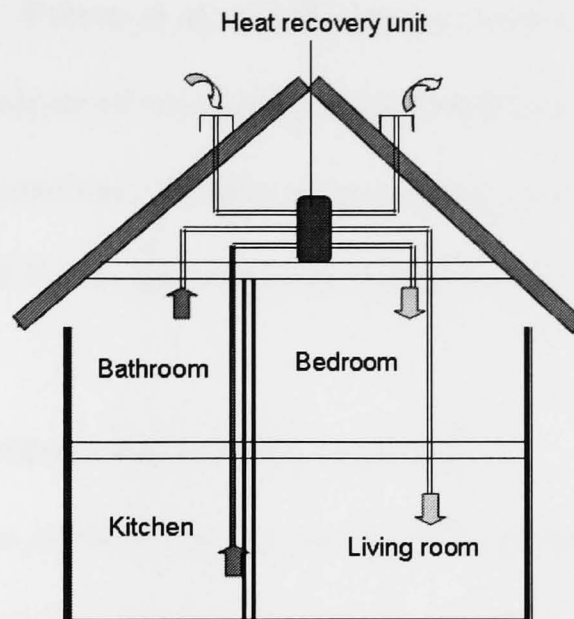


Figure 2.3 Heat recovery system

Researches on this field keep active in recent years and involve many theoretical and applied aspects of heat recovery system. Zhou et al. (2007) presented a simulation model of heat recovery system based on the new-generation dynamic building energy simulation program called EnergyPlus with the function of heat recovery called ERV in this context to reduce the fresh-air intake load via total heat recovery as shown in Figure 2.4.

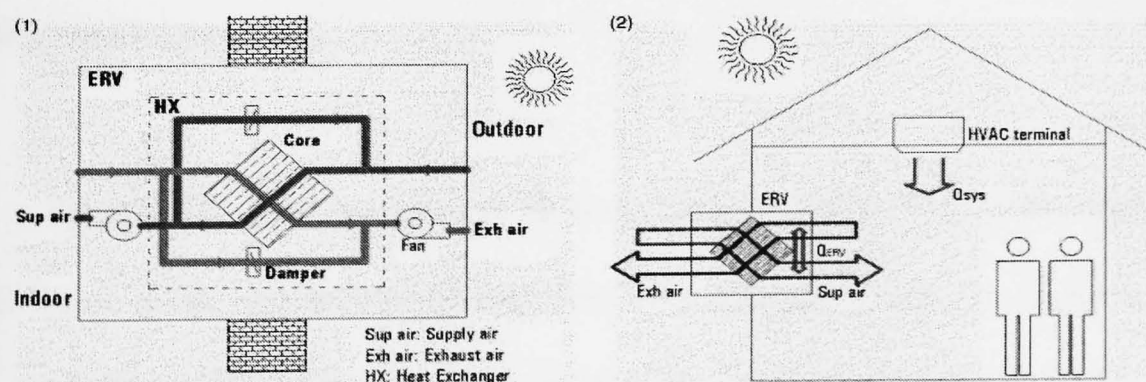


Figure 2.4 Structure (1) and air energy-flow (2) schematic diagram of ERV (Source: Zhou et al. 2007)

In order to evaluate the performances of heat recovery system in building ventilation system, Lazzarin and Gasparella (1998), discussed a technical and economical analysis to illustrate the possibility of using this system even for small

ventilation flow rates. Fehrm et al. (2002) gave a review on the development and economics of the technique of heat recovery in Sweden and Germany. In addition, Routlet et al. (2001) presented a theoretical analysis of real energy with air handling units and recommended for the heat recovery choice with the experimental data.

2.3.2 Types of heat recovery for building applications

Generally, these systems can be categorised according to their applications which are process to process, process to comfort and comfort to comfort. In process-to-process system, heat is captured from the process exhaust stream and transferred to the process exhaust stream and transferred to the process supply air stream. Equipment is available to handle high temperatures level. These devices generally recovers sensible heat and do not transfer latent heat. Whist, in process-to-comfort system heat is captured from a process exhaust heats building makeup air during winter. The process-to-comfort devices generally recover sensible heat only. Heat recovery device in comfort-to-comfort lowers the enthalpy of the building supply air during warm weather and raises it during cold winter and this system transfers both sensible and latent energy.

Specifically, heat recovery or air-to-air heat recovery systems are made in so many types, sizes, configurations and flow arrangements. There are many types of heat recovery units which are in use in building applications (Schild 2004). These types of heat recovery systems are depending on the heat exchanger core. Shah and Sekulic (2003) presented classifications of heat exchangers based on several features: geometry, flow direction, number of different working fluids and so on. Over the last few decades, several types of heat recovery systems such as fixed plate, heat pipe,

rotary wheel and run-around coil have been used to recover energy between the supply and exhaust airflows. The following discussion considers the classification based on construction type of heat exchanger which is the heart of heat recovery system.

2.3.2.1 Fixed-plate

Fixed-plate heat recovery is the most common type of heat recovery device which is obviously named by the construction of its exchanger. In this unit, the plate exchanger surfaces normally are constructed of thin plates that are stacked together or consist of individual solid panel with several internal airstreams (Figure 2.5). The plates maybe smooth or may have some form of corrugation. It operates by transferring thermal energy from outgoing to incoming air streams via plate heat exchanger surfaces. Figure shows the schematic diagram of heat transfer of fixed-plate. Typical effectiveness of sensible heat transfer is 50% to 80% and airflow arrangements are counter-flow, cross-flow and parallel flow (ASHRAE 2005).

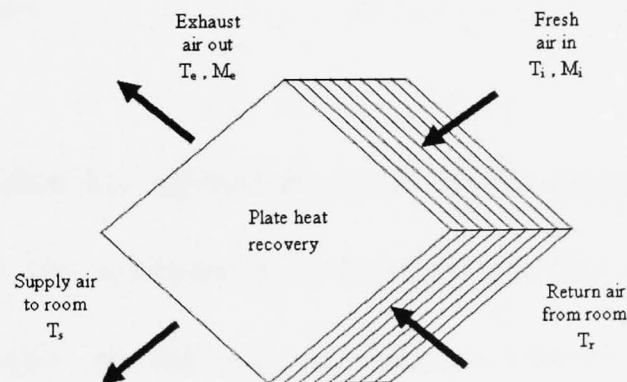


Figure 2.5 Fixed-plate heat recovery

Fixed-plate types provide an excellent means of achieving highly efficient heat recovery because their high heat transfer coefficients, coupled with counter-current flow, enable them to produce close end-temperature differences (Lamb 1982). One of

the earliest studied was carried out by Pescod (1979) to investigate the performance of sensible fixed-plate heat recovery or exchanger using numerical and experimental investigations. He conducted a series of studies on fixed-plate heat recovery unit and determined sensible heat transfer and pressure drop characteristics. His mathematical model predicts the fixed-plate exchanger performance using convective heat transfer coefficient equations and the results shows a good agreement with experimental results.

In another study, Svendsen (2005) has conducted a study of counter-flow plate heat recovery with 80-90% of efficiency in ventilation system in several experimental single-family houses to meet the new Danish energy requirement. His study addressed the aspects of minimizing the heat loss from the duct system and the heat recovery unit when placed in an unheated attic space in order to obtain an acceptable efficiency. In the study, he found that heat recovery in ventilation system has lived up to expectations corresponding to a good indoor climate, high efficiency and low electricity consumption.

Han et. al (2000) has performed a study to investigate the effect of outdoor weather conditions on the performance of the plate-type heat recovery ventilator. The experiments have been carried out to measure sensible, latent and enthalpy efficiencies by varying outdoor temperature and humidity conditions with the indoor conditions fixed at the standard heating or cooling conditions. They have introduced the coefficient of energy to quantify recovered energy in comparison with the electric power consumption. As a result, they have found that temperature exchange

efficiency under winter conditions shows larger values than in summer conditions due to the heat generation by an internal fan.

With the growing demand for fixed-plate sensible heat exchangers, heat recovery manufacturers produced different types of fixed-plate sensible heat exchangers. Field (1975) reported the use of glass sheets as the heat transfer surfaces in fixed-plate sensible heat exchanger in Switzerland since 1958. The effectiveness of such device is about 60% to 65% however, he did not specify at what air velocity this effectiveness was obtained. The payback period for such systems varies from a few months to 3.7 years. Nonetheless, he underlined that the payback period would be shorter when it is used in swimming pools, as condensation would occur on the glass surface which consequently releases heat and this heat will be added to the sensible heat and increases the amount of sensible energy transfer through the glass surface, as a result the effectiveness increases to 80%. This device has the advantage that it is easy to clean, has a long life and resists corrosion.

On the other hand, experiments were conducted by Persily (1982) to test the effectiveness of a cross-flow heat recovery which was constructed of plates and fins made from treated paper capable of moisture transfer. The heat recovery efficiency was determined by comparing the actual heat loss to that expected due to the mechanically induced ventilation and he had found that the exchanger (core of heat recovery) recovered 55% to 60% of the heat contained in the outgoing airflow depending on the fan speed. In another study, Zhang and Jiang (1999) conducted an experimental investigation of the performance of rectangular cross-flow fixed-plate made of membrane to study the heat transferred to recover energy in air conditioning

system. They have developed a numerical model and validated the data against the experimental results and found that the highest heat transfer occurred near the inlet area. In accordance to this study, Niu and Zhang (2001) investigated a similar study of a square shaped of fixed-plate made of the same membrane and found that the temperature in a cross flow heat exchanger configuration are more evenly distributed in comparison with Zhang and Jiang (1999) results.

With the motivation of fixed-plate made of membrane results, Nasif et al. (2010) then have come out with a thermal performance of a fixed plate utilized a porous membrane as the heat and moisture transfer surface that can recover both sensible and latent energy with new developed Z-flow configuration as shown in Figure 2.6. The effectiveness was found to approximately 75% for sensible and 60% for latent.

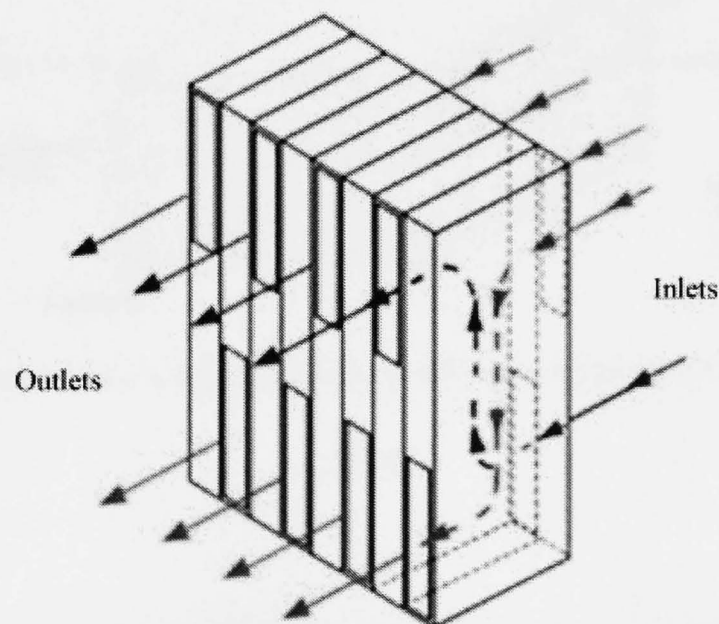


Figure 2.6 Z-flow fixed plate utilized a porous membrane as the heat and moisture transfer surface (Source: Nasif et al. 2010)

In another study, Min and Su (2010) have carried out a performance analysis of a fixed-plate called membrane-based energy recovery ventilator as shown in Figure

2.7 in order to investigate the effects of the membrane spacing (channel height) and membrane thickness on the ventilator performance under equal fan power conditions. The results found that for a fixed fan power, as the channel height increased, the total heat transfer rate initially increased.

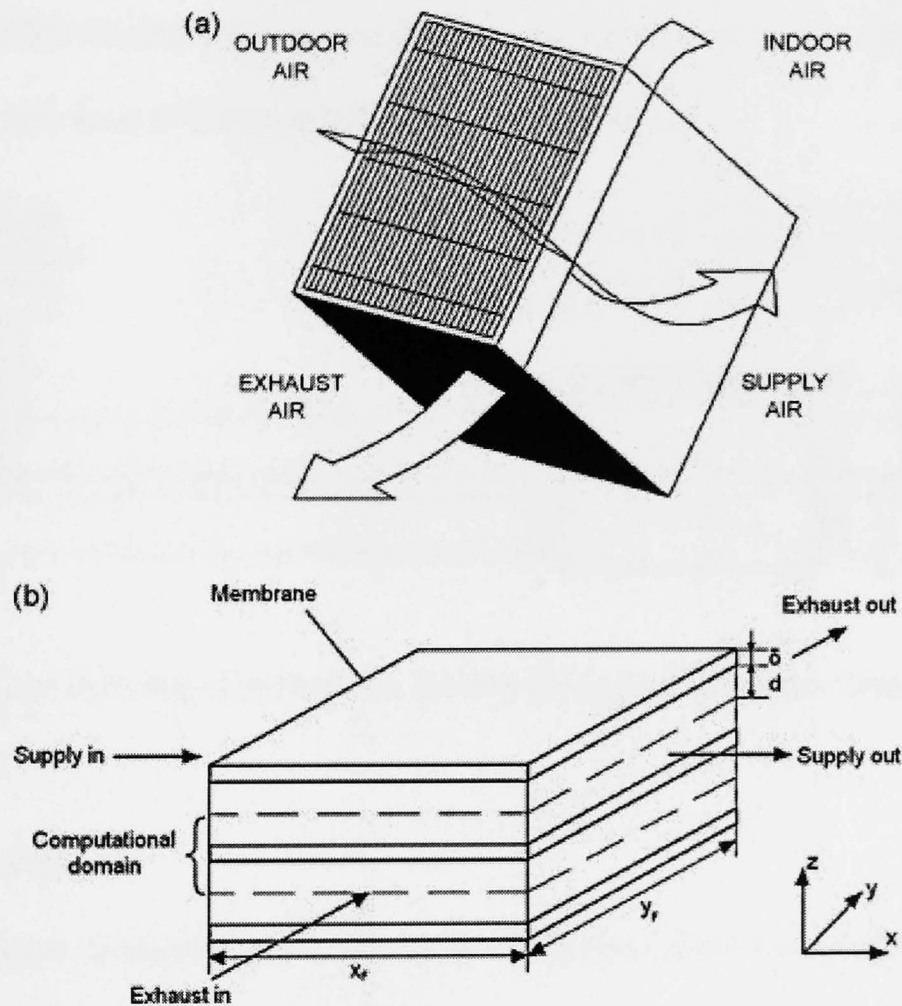


Figure 2.7 (a) The core of a typical MEE. (b) Physical model (Source: Min and Su 2010)

Recently, more options of fixed-plate material are introduced as the market growth. In regard to this, Lu et al. (2010) have developed and investigated the performance of a plastic film plate heat recovery ventilator that works under cross-flow mode by both simulation and experiment. The results indicated that the thin film vibrated when airflow passed through the channels which enhanced heat exchange

performance. In addition, the effectiveness of the heat recovery varies from 65 to 85% with airflow rate and the pressure drop is less than 20Pa. On the other hand, Fernandez-Seara et al. (2010) have conducted the experimental analysis of an air-to-air heat recovery unit equipped with fixed-plate heat exchanger made of a sensible polymer for balanced ventilation systems in residential buildings as shown in Figure 2.8. Results showed that relative humidity decreased from 95% to around 34%, the heat transfer rate were 672W and 80% of thermal efficiency.

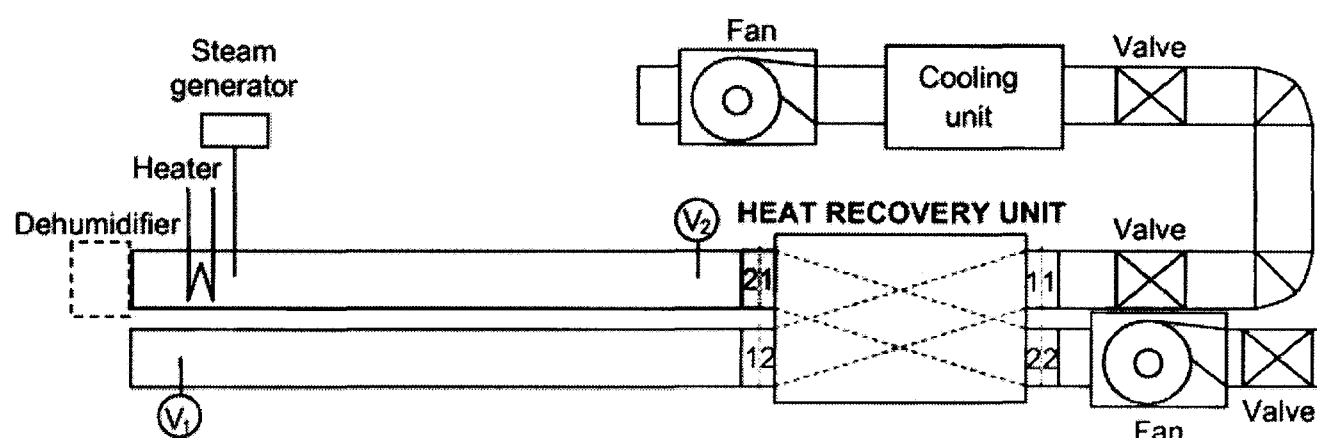


Figure 2.8 Layout of the experimental facility (Source: Fernandez-Seara et al. 2010)

2.3.2.2 Heat pipe

Heat pipe recovery is a sealed self-contained, fluid evaporating condensing system (Figure 2.9). It is a heat transfer device in which the latent heat of vaporization is utilized to transfer heat over a long distance with a corresponding small temperature difference (Yau and Ahmadzadehtalatapeh 2010). The unit is divided into two sections for heat/energy exchanges between exhausts and supply air which are evaporator and condenser. Heat is transferred from hot incoming gas to the evaporator section of the heat pipe. Thermal efficiency of heat pipes is between 45% and 55%. There are some advantages in term of flow resistance, such as no moving parts, no external power requirements and so high reliability, no cross contamination, compact and suitable for all temperature application in heating, ventilation and air-

conditioning, fully reversible and easy for cleaning. In addition, large quantities of heat can be transported through a small cross-sectional area over a considerable distance with no additional power input to the system (Brown et al. 1991).

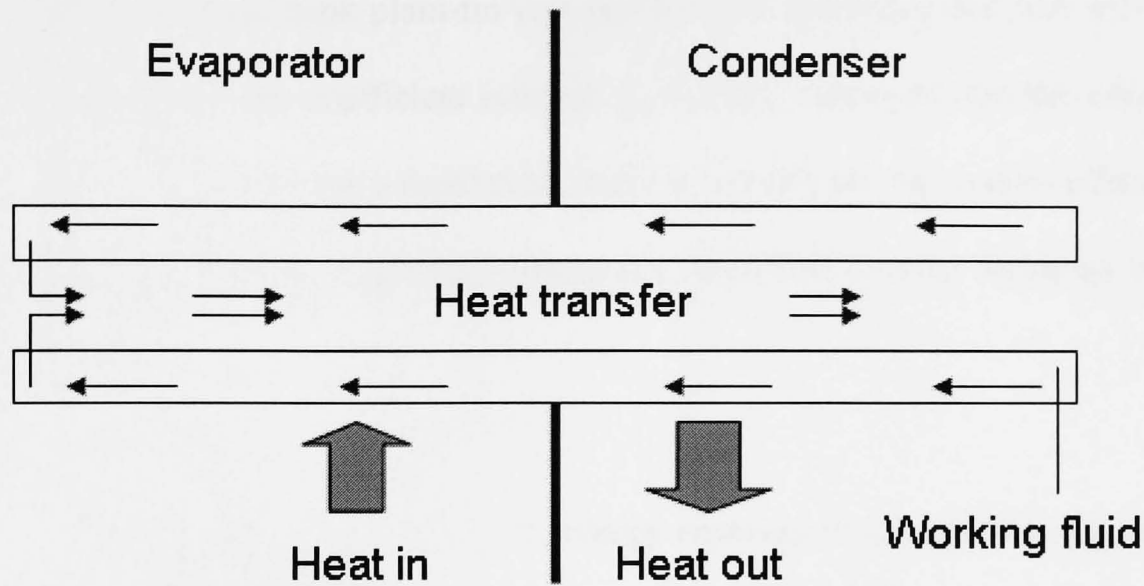


Figure 2.9 Heat pipe

Heat pipe recovery units are suitable to use in naturally ventilated buildings because of they offer several advantages over conventional heat recovery device (Shao and Riffat 1997). They have conducted a performance study of heat pipe recovery system in naturally ventilated building and found that the efficiency of 50% was achieved with the pressure loss about 1Pa. In another study, Gan and Riffat (1997) have investigated the performance of different heat pipe recovery units by experimental measurements and evaluate the pressure loss characteristics using CFD modelling in a two-zone chamber for naturally ventilated buildings. It was found that the effectiveness decreased with increasing velocity and poor thermal contact between fins and pipes drastically reduces the effectiveness of heat-pipe recovery unit. The numerical modelling indicated that at low velocities the pressure loss coefficient in heat pipe recovery unit decreases with increasing air velocity but the total pressure loss increase with the velocity.

On the other hand, Shao et al. (1998) have conducted a study of pressure loss and heat recovery efficiency of heat pipe units using experimental and computational approaches. The results found that heat recovery efficiency of close to 50% have been achieved for a single bank plain-fin unit and for a double bank unit was 40% higher with the pressure loss coefficient reduced as velocity increased. On the other hand, Yau (2001) has conducted a theoretical study to investigate the overall effectiveness of heat pipe exchangers operating in naturally ventilated tropical buildings based on NTU method.

Heat pipes are also suitable for energy recovery in air conditioning system in tropical countries where incoming fresh air at high ambient temperature could be pre-cooled by the cold exhaust air stream before it enters the refrigeration equipment (Francisco et al. 2003). El-Baky and Mohamed (2007) have carried out a study to investigate the thermal performance and effectiveness of heat pipe for heat recovery in air conditioning applications by measuring the temperature difference of fresh warm and return cold air through the evaporator and condenser site as illustrates in Figure 2.10. The results shown that the effectiveness and heat transfer for both evaporator and condenser sections have increased to about 48%. The temperatures change of fresh and return air was increased with the increasing of inlet temperature of fresh air.

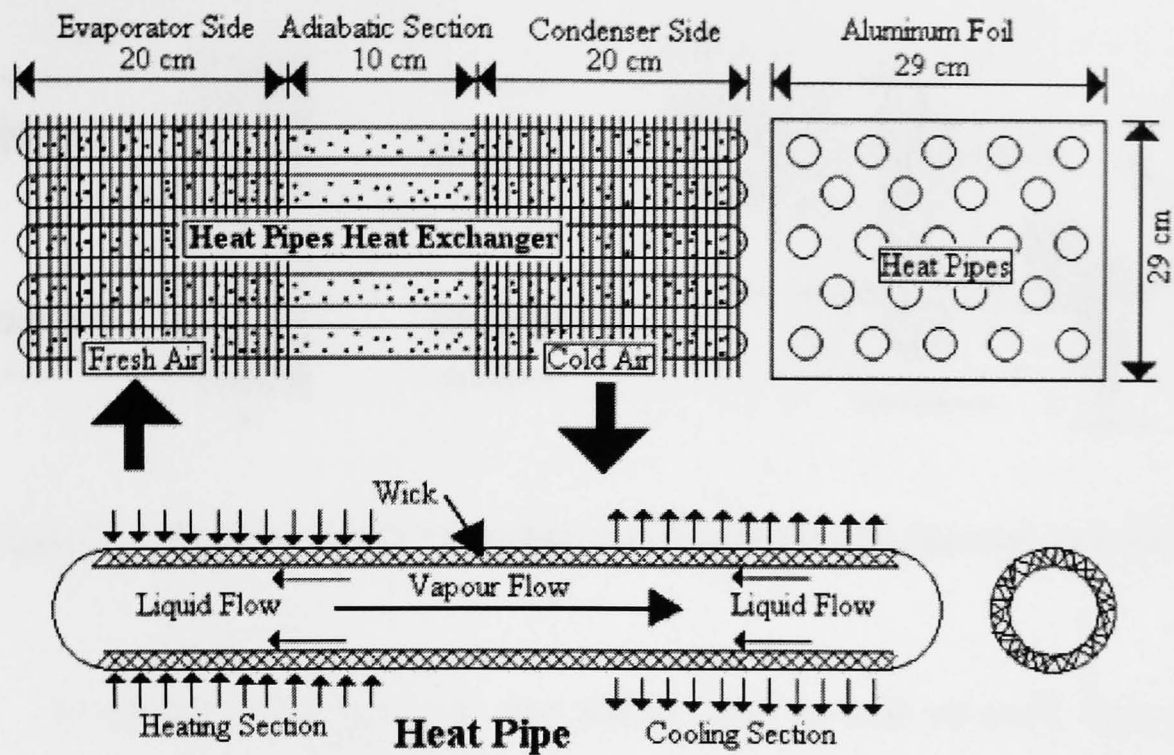


Figure 2.10 Heat pipe recovery in air conditioning system (Source: El-Baky and Mohamed 2007)

With the growing climate change and the thermal comfort issue in tropical hot and humid regions such as Malaysia and other South East Asian countries, heat pipe recovery has taken its place in dehumidification system. Yau (2007) has conducted a baseline performance characteristic study of heat pipe in dehumidification system for tropical climates as shown in Figure 2.11. By good results obtained, he has recommended that HVAC system in tropical climates should installed heat pipe in their dehumidification systems.

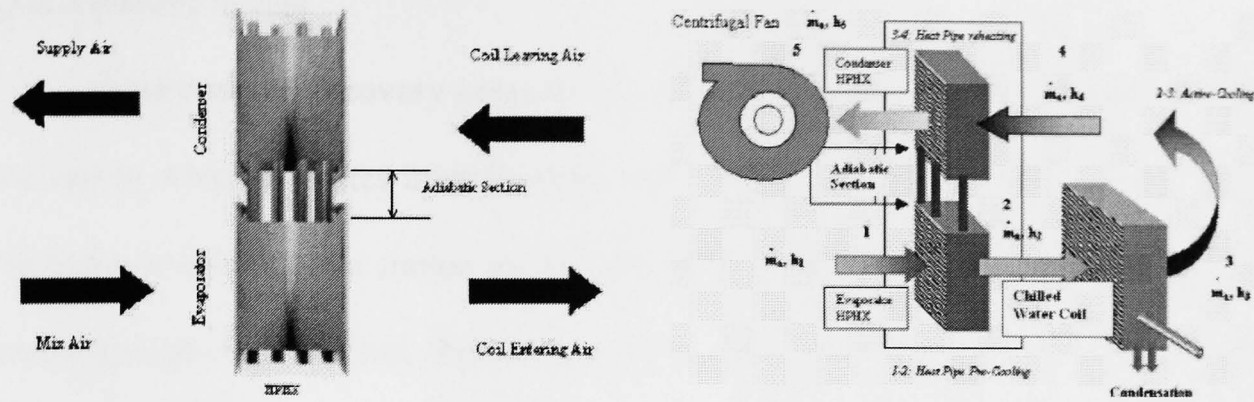


Figure 2.11 Heat pipe in HVAC system for tropical climates (Source: Yau 2007)

In addition, heat pipe are also widely used in heat recovery systems in domestic appliances such as dishwasher, air conditioner or freezer. In regard to this, Lin et al. (2005) provided a thermal model for simulating the performance of a heat pipe system for recovering waste heat in the drying cycle in a domestic appliance as presented in Figure 2.12. The results showed that the utilisation of heat pipe recovery in the drying cycle of domestic appliances might lead to a significant energy saving in the domestic sector.

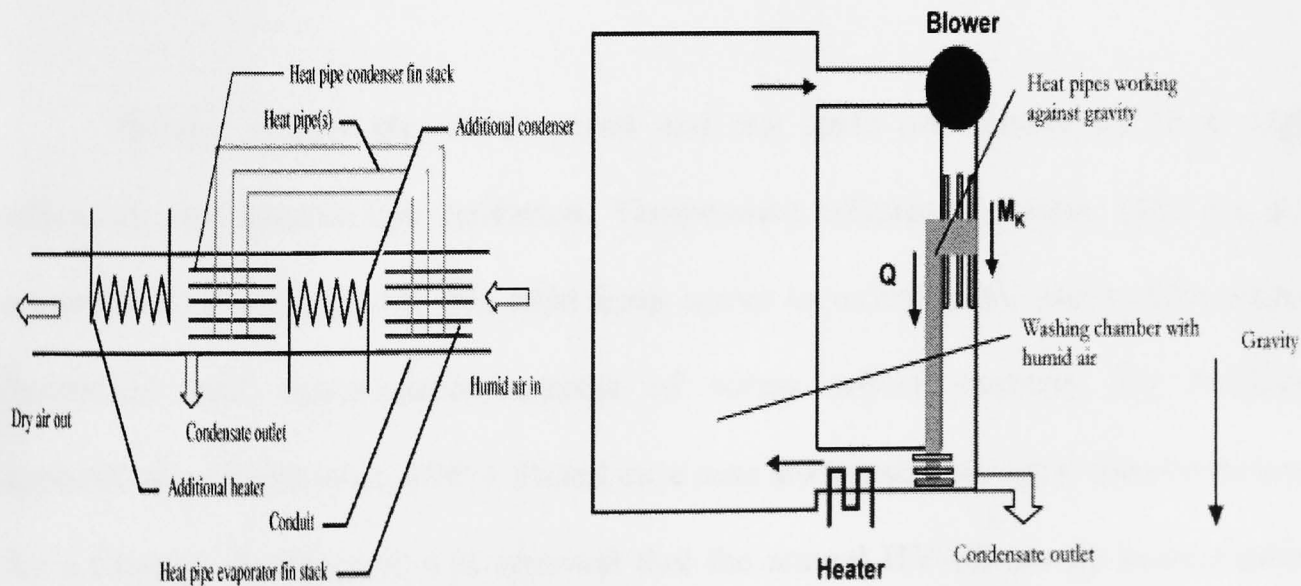


Figure 2.12 Heat recovery system using heat pipe solution in drying cycle (Source:

Lin et al. 2005)

2.3.2.3 Rotary wheel

Rotary wheel recovery consists of a rotor with permeable storage mass fitted in a casing which operates intermittently between a hot and cold fluid (Figure 2.13). The rotor is driven by a motor so that the exhaust air and fresh air are alternately passed through each section. Rotor speed is normally relatively low and in a range of 3-15rpm. A unique advantage of rotary wheels is the capability of recovering both sensible and latent heat.

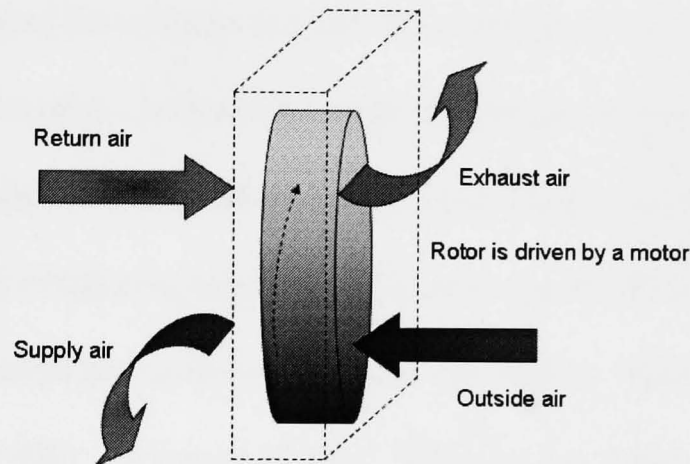


Figure 2.13 Rotary wheel recovery

Rotary wheels are widely used and the units are known for their high efficiency and trouble-free operation. Temperature efficiencies above 80% are not uncommon. Researches on this field keep active in recent years and involve many theoretical and experimental aspects of rotary wheel recovery for building applications. (Riffat et al. 1995). Based on a case study using a rotary wheel recovery for a Chicago building, it was reported that the annual HVAC energy consumption can be reduced between 31 and 64% (Mahmud et al. 2010).

One of the earliest investigations of rotary wheel recovery was performed by Sauer and Howell (1981). They used the AXCESS energy analysis computer program to evaluate the energy requirements of a two-story office building located in St. Louis on an hour-by-hour basis for a full year using local weather data. Their results showed that energy recovered by the rotary wheel was around 2.5 times greater than the heat recovered by a sensible heat exchanger. By looking to its mechanism, rotary wheel transfers energy from an exhaust to a supply air. The rotary wheel spans two adjacent ducts. One duct carries the exhaust air; the other carries the incoming air, which is to be heated. It also transfers moisture as well as sensible energy between air streams depending on the type of matrix (Holmsberg 1989). Rotary wheel was proven as one of the most efficient solutions to handle the moisture carried by the ventilation air as to dump the excess moisture within the fresh air supply back to the atmosphere (Waugamen et al. 1993). In regard to this, Nobrega and Brum (2009) developed a modelling and simulation to describe the heat and mass transfer in rotary wheel which was validated by comparing the work with independently obtained results. The results showed that heat wheels can be far less efficient than enthalpy recovery wheels depending on the atmospheric conditions.

In addition, in rotary wheel system, airflow arrangement is usually counter-flow and increases with rotation speed. Sorensen (2007) has done measurements of temperature distribution of rotary wheel of heat recovery units. The results show that the temperature profile is generally dependent in both the rotational speed of the wheel and flow rate. Ghodsipour and Sadrameli (2003) estimated maximum effectiveness as a function of rotational speed and hot/cold air velocities. In another

study, Simonson and Besant (1999) have presented the effectiveness correlations to predict sensible, latent and total effectiveness.

For balanced ventilation systems, the recovered heat power can be at the same rate. Unfortunately, the disadvantage of the rotary wheel is the greater cross-contamination between exhaust and fresh supply air. Due to the rotation device, there will always be a direct and indirect connection between exhaust and fresh supply air. Cross contamination through rotary heat recovery units comes from two mechanisms which are leakage and carryover. In conjunction to this, Hemzal (2006) has carried out a performance study of rotary wheel and found that the penetration of airflow (leakage) through the untightness were connected with transfer of contaminants and by the heat which influenced the efficiency.

With the encouraging previous results in its efficiency, some researches made intensive studies on the optimal operation of rotary wheel recovery. Dallaire et al. (2010) have portrayed a conceptual optimization of rotary wheel with a numerical model where internal structure was a porous medium in their research. The schematic presentation of the rotary wheel studied is shown in Figure 2.14. The numerical results showed that the figure of merit was substantially affected by both design variables and that optimal value of length and porosity could be obtained. On the other hand, San and Hsiau (1993) discussed the effects of NTU and Bi numbers on the performance with one dimensional model that included the axial heat and mass resistance. On the other hand, Abe et al. (2006) have presented the analytical model for predicting the effectiveness of rotating air-to-air energy wheels using the

characteristic measured on the same non-rotating wheels exposed to a step change in temperature and humidity.

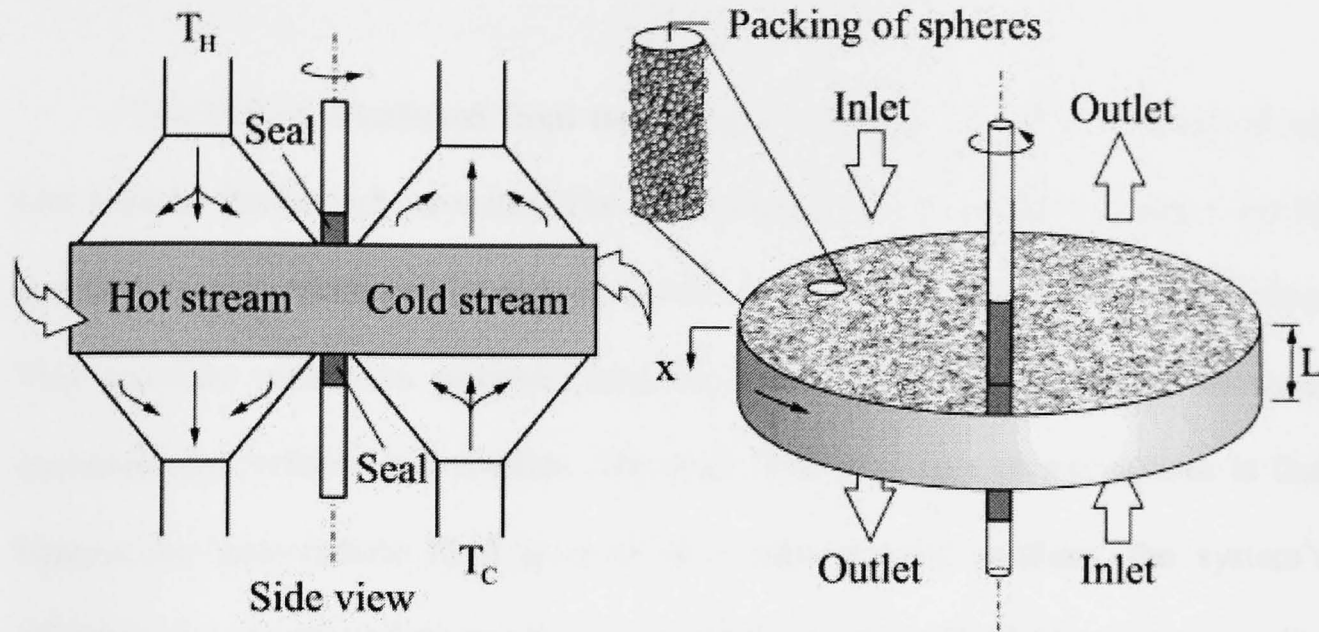


Figure 2.14 Schematic representation of the rotary wheel (Dallaire et al. 2010)

Nowadays, with the ability to recover both sensible and latent heat, rotary wheels have been used as desiccant wheels for humidity treatment for dehumidification (Tauscher et al. 1999; Zheng and Worek 1993; Zheng and Worek 1995) and enthalpy recovery (San and Hsiau 1993; Simonson et al. 1999).

2.3.2.4 Run-around

Run-around heat recovery system is the name given to a linking of two recuperative heat exchangers by a third fluid which exchanges heat with each fluid in turn as shown diagrammatically in Figure 2.15. Run-around heat recovery use two physically separated heat exchangers (coils) in the air supply and exhaust ducts to recover and transfer heat between them. This system may require an expansion tank to accommodate expansion and contraction of heat transfer fluid. Unlike other heat recovery devices, the run-around system does not require the supply and exhaust air

ducts to be located side by side. This gives run-around system an advantage over other available system when cross contamination is a concern (Vali et al. 2009).

The heat is transferred from the exhaust to supply air using an intermediate heat transfer fluids such as water. The main advantage of this system is that supply and extract duct can be physically separated, even in different part of the building. This provides maximum possible flexibility, as well as no possibility of cross contamination between air streams. The main disadvantages of this system is that because an intermediate fluid is used as a heat transfer medium, the system's efficiency is reduced and electricity is required for pumping fluid. However, pumping liquids remain significantly less energy-intensive than moving air with fans. Thermal efficiency of this type is normally from 45% to 65%.

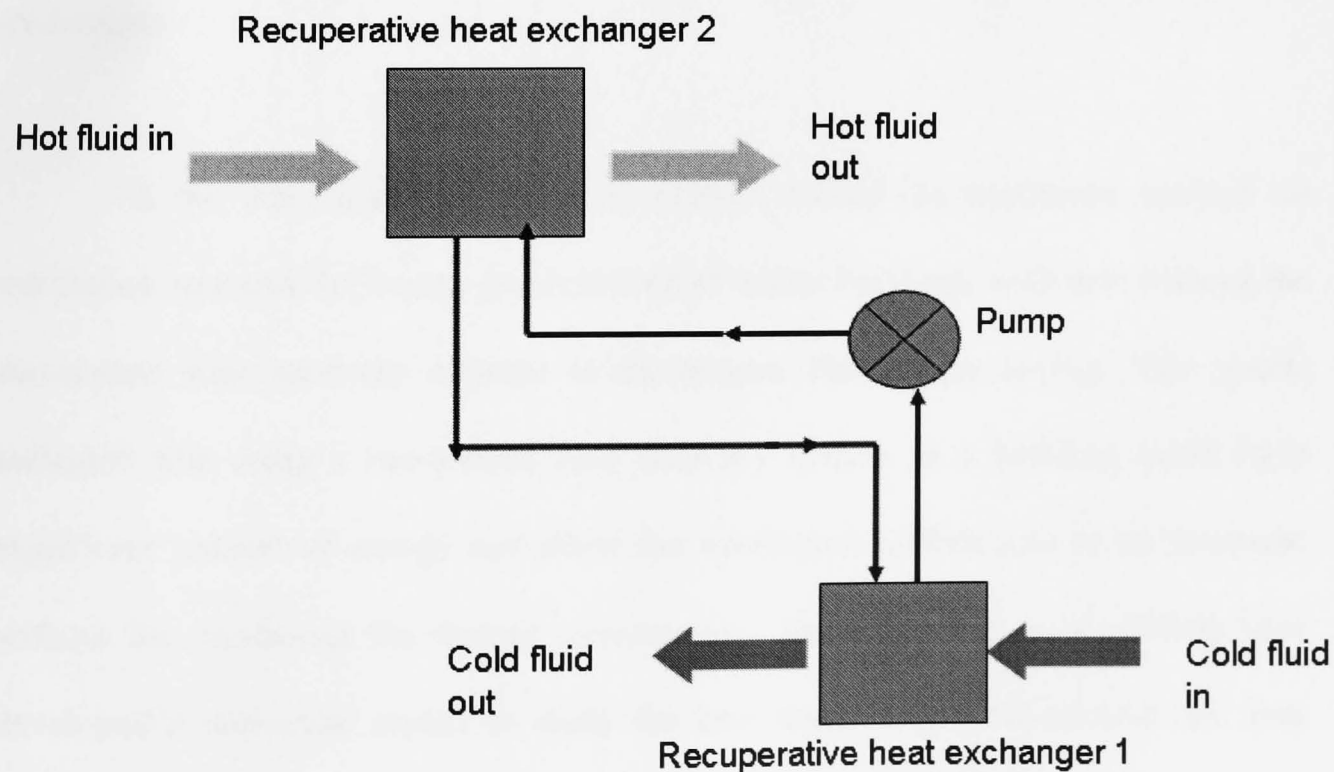


Figure 2.15 Run-around system

One of the first studies on the run-around heat recovery system was published by London and Kays (1951). It was found that at a constant NTU, the system had its

optimum performance when the heat capacity rates of the air and coupling liquid were equal. Emerson (1984) had developed a design of a run-around heat recovery system. He had found that the performance of a run-around coil system was sensitive to the rate of circulation of the secondary fluid and that the optimum rate changed with changes in the flow rates of the primary fluids or in the fouling resistances. He also suggested a simple method of monitoring the system to verify that the optimum rate of circulation. Wang (1985) has proposed a straight-forward explicit thermal design procedure in his study of run-around heat recovery system. Based on the allowable air pressure drop, the design started with a minimum number of rows and proceeds until all specifications have been met. Hence the smallest possible coil can be obtained by this approach. Forsyth and Besant (1988) then developed a numerical simulation to investigate the performance and design of run-around heat recovery with two coil heat exchangers.

On the other hand, Dhital et al. (1995) studied the maximum outdoor air ventilation rate and the energy performance of office buildings with and without the run-around heat recovery systems to investigate the energy saving. The results indicated that using a run-around heat recovery system in a building could have significant amount of energy and allow the ventilation airflow rate to be increased without the increasing the energy consumption. Recently, Vali et al. (2009) have developed a numerical model to study the heat transfer in a run-around coil heat recovery system with two combinations of counter and cross flow heat exchanger as shown in Figure 2.16. The simulated results showed that the effectiveness of each counter/cross flow heat exchanger and overall run-around system were used to develop effectiveness correlation. For a given total surface area of the exchangers, the

highest overall sensible effectiveness was achieved with exchangers which have a small exchanger aspect ratio. In another study, Ahmadi et al. (2009) have conducted an investigation on transient behaviour of run-around heat and moisture exchanger system.

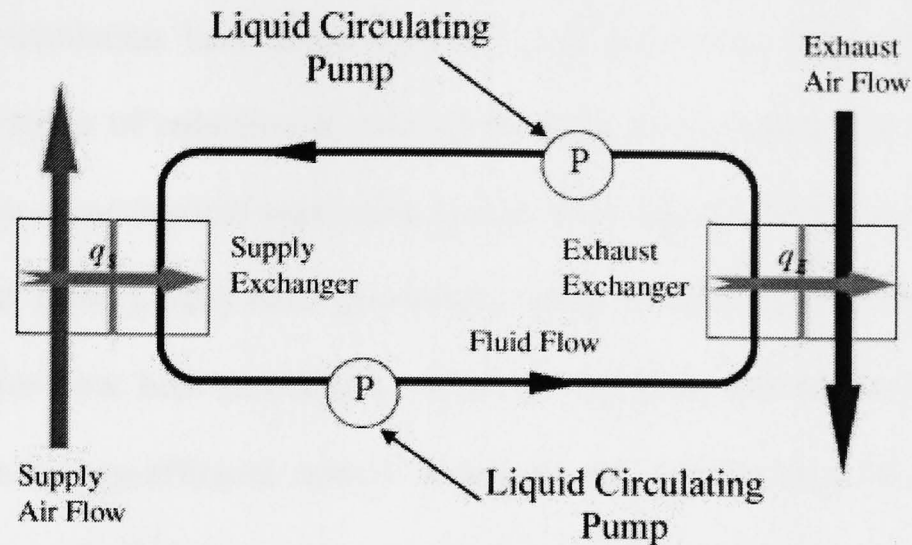


Figure 2.16 Schematic diagram of a run-around heat recovery (Source: Vali et al. 2009)

2.3.3 Heat recovery in integrated energy-efficient system for building application

Integrating heat recovery system in energy-efficient system represents significant progress for building applications. The integration of the system leads to a reduction of thermal ventilation losses of the building and to a reduction of the required energy support. This section reviews the previous works of various type heat recovery systems in combination with other low carbon technologies conducted by various researchers.

2.3.3.1 Heat recovery in mechanical ventilation system

Since more than 90% of a person's time is spent indoors, therefore it is substantial to maintain the indoor environment within comfortable conditions for the

occupants. For this purpose, mechanical ventilation system used in buildings to control indoor air quality and at the same time ventilates the indoor environment. Attempting to improve indoor air quality of buildings, the earliest study of mechanical ventilation system with heat recovery a study has been done in Denmark by using of mechanical ventilation heat pump recovery and the results demonstrated it was beneficial in terms of reduction in mite populations in mattresses and carpets. After that, the study of mechanical ventilation system with heat recovery was conducted by Nazaroff et al. (1981). They have presented a study of mechanical ventilation system with a counter-flow heat recovery in order to determine the effectiveness of this system as an energy-efficient control technique for indoor radon concentration in houses. As a result, they have found that the strategy of building tight houses and the use of mechanical ventilation systems with heat recovery may satisfy energy conservation goals in a cost-effective manner without comprising indoor air quality.

Mechanical ventilation consumes a large amount of electricity for input power and in some cases; it increased a household's electrical power consumption by up to 50% (Manz and Huber 2000). In respond to this, several researchers have investigated the ability of heat recovery unit coupled in this system to recover the energy loss. In mechanically ventilated buildings, heat recovery from ventilation air is the single most important means of reducing ventilation energy consumption (Liu et al. 2010). In regard to these, Nguyen et al. (2005) have studied the overall performance of mechanical ventilation heat pump system with heat recovery during forced ventilation. The methods for recovering sensible heat during ventilation process have been evaluated experimentally in four types of ventilation which are type A, B, C and D the results have been compared with the case of none heat recovery ventilation. For

type A, no heat recovery is used while in Type B, a separate sensible heat recovery was used. In type C, single heat recovery was used for recovery heat in an integrated heating-ventilation and in type D, double heat recovery was used to recover heat and heat pump as the second heat recovering mechanism as shown in Figure 2.17. In this study, it has been found that the integrated mechanical double heat recovery pump system is most efficient for saving energy for an indoor space.

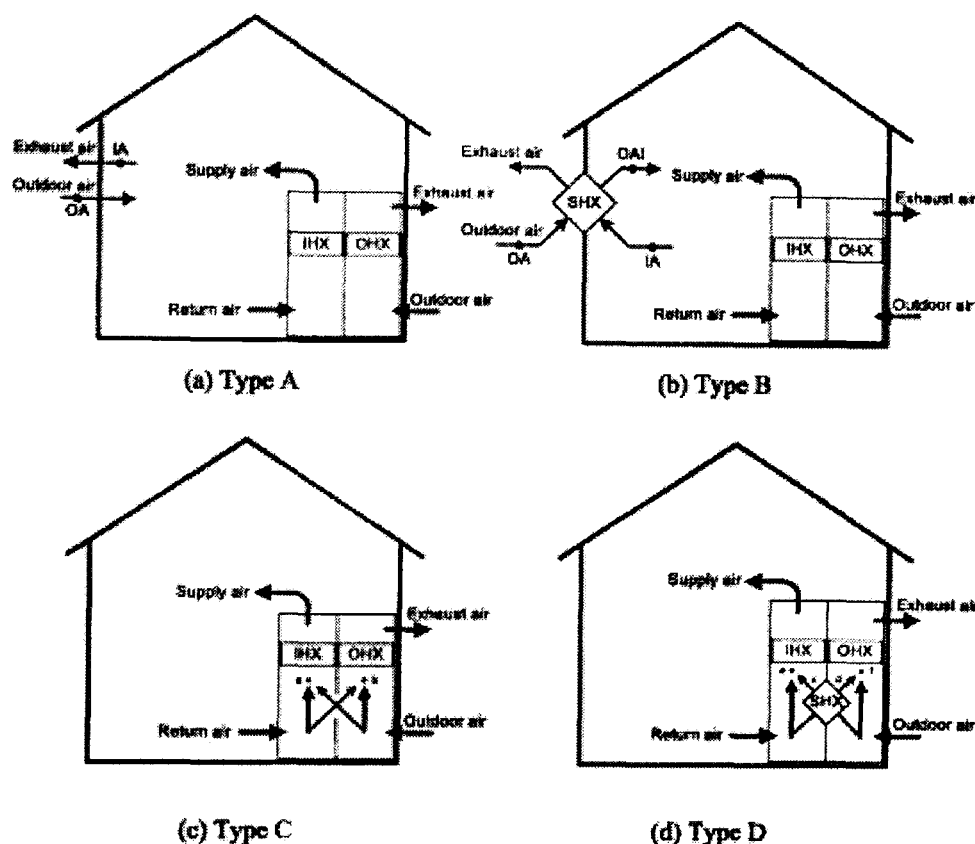


Figure 2.17 Mechanical ventilation heat pump system with four types of ventilation heat recovery (Source: Nguyen et al. 2005)

It is obviously known in literatures that mechanical ventilation with heat recovery system is efficient to remove pollutants and adequate sufficient ventilation to buildings. An advanced mechanical ventilation heat recovery incorporating heat pump system has been developed by Riffat and Gillott (2002) which has a low capital cost and little maintenance as shown in Figure 2.18. The results indicated that the air changes per hour complied with the ASHRAE Standard to maintain indoor air quality.

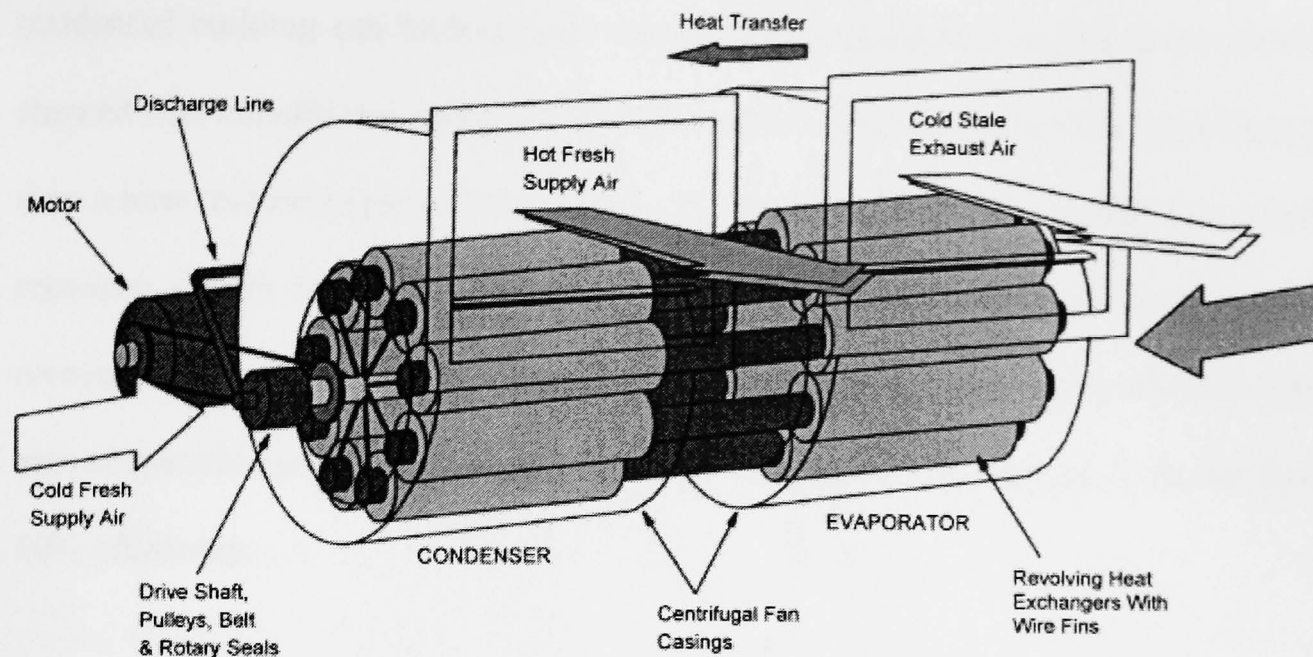


Figure 2.18 MVHR heat pump system (Source: Riffat and Gillott 2002)

Manz and Huber (2000) have presented mechanical ventilation that united two functions: fluid transport and heat recovery. This unit was investigated by means of experiments and simulations. It was shown that using this concept, it was possible to realize a mechanical ventilation unit with high efficiency of heat recovery. In another research, Manz et al. (2000) presented performance of single room ventilation units with recuperative or regenerative mechanical ventilation heat recovery by means of experiments and numerical simulations. It was shown that using these units, rooms could be efficiently ventilated at a good level of thermal comfort, temperature efficiencies up to 78% at low levels of electric energy input.

Jokisalo et al. (2003) on the other hand, have performed a simulation study using a dynamic thermal modelling of various mechanical supply and exhaust ventilation system incorporating heat recovery in typical Finnish residential apartment building in Finland. The systems studied were based on cost efficient realistic component available in the market. According to this study, energy efficiency in a

residential building can be improved remarkably by using this system as the results showed that a traditional exhaust ventilation system can use up to 67% more energy than a heat recovery system having 80% efficiency and 41% more energy than a heat recovery system having 60% energy recovery efficiency. The efficiency of heat recovery has a significant effect on energy consumption as the results showed total annual specific energy consumption at 80% temperature efficiency was 11% less than 60% efficiency.

Mechanical ventilation with heat recovery is often considered as one of the key elements of a low energy residential building in cold winter regions (Steimle and Roben 1992). However, in extremely cold or arctic climates where they have long winter season, it is difficult to obtain a traditional mechanical ventilation heat recovery system to operate as intended due to continuous moisture problems and inlet air below the freezing point. Researchers and designers devote much attention to frost formation and to means of getting rid of the frost. In response to these problems, Kragh et al. (2007) have constructed a novel mechanical ventilation heat recovery with the capability of continuously defrosting itself without using supplementary heating suitable for cold or arctic climates. The experiment's results showed that the heat recovery efficiency is still high and capable to defrost below the freezing point.

2.3.3.2 Heat recovery assisted passive ventilation

The term passive in this context indicates the opposite of active or mechanical ventilation where the fresh air is provided by fans or heat pumps. An early attempt in the field of heat recovery for passive or natural ventilation solutions was based on a vertical counter-flow air-to-air heat exchanger and achieved a heat recovery efficiency

of 40% (Schultz and Saxhof 1994). Riffat and Gan (1998) have been undertaking a project on heat pipe recovery with solar-assisted natural ventilation in a glazed solar chimney as an integral part of the system with heat recovery efficiency close to 43%. In this study, a heat pipe recovery unit used was a heat exchanger consisting of externally finned sealed pipe containing a volatile fluid such as methanol which has an operating temperature range from -40° - 100°C as shown in Figure 2.19. This unit was divided into evaporator and condenser sections. They have found that installing heat-pipe recovery in the chimney increased the flow rates in naturally ventilated buildings and also decreased the thermal buoyancy effect and thus they have suggested, in order achieving required airflow rates in naturally ventilated buildings with heat recovery, use should be made of wind forces.

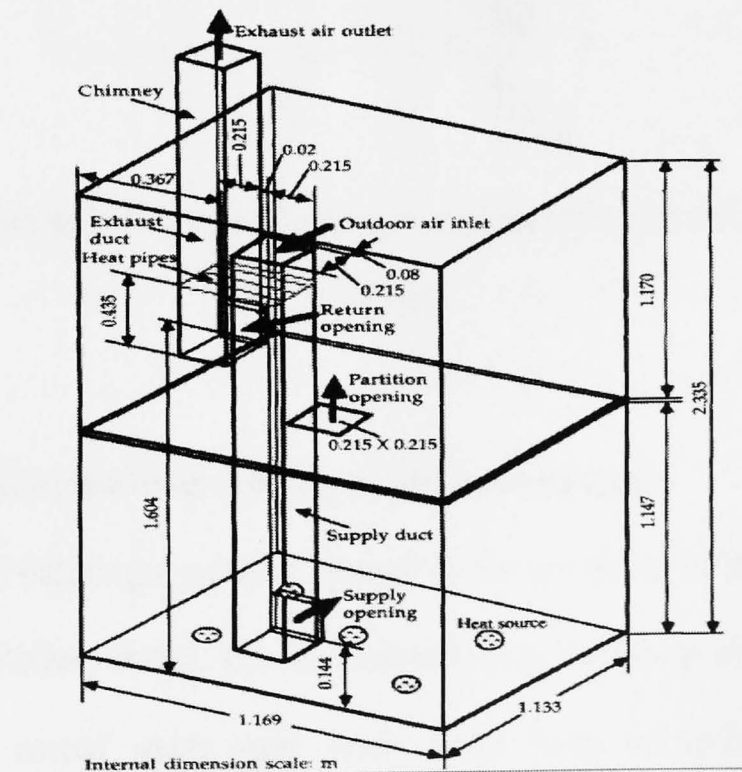


Figure 2.19 Schematic diagram of the naturally-ventilated room with heat pipe recovery unit (Source: Riffat and Gan 1998)

Recently, Hviid and Svendsen (2010) have presented an analytical and experimental analysis of heat recovery concept that has been developed for passive

ventilation systems suitable for temperate climates as shown in Figure 2.20. The total pressure loss and temperature exchange efficiency of heat recovery was measured and found to be 0.74Pa and 75.6%, respectively for a design flow rate of 560L/s.

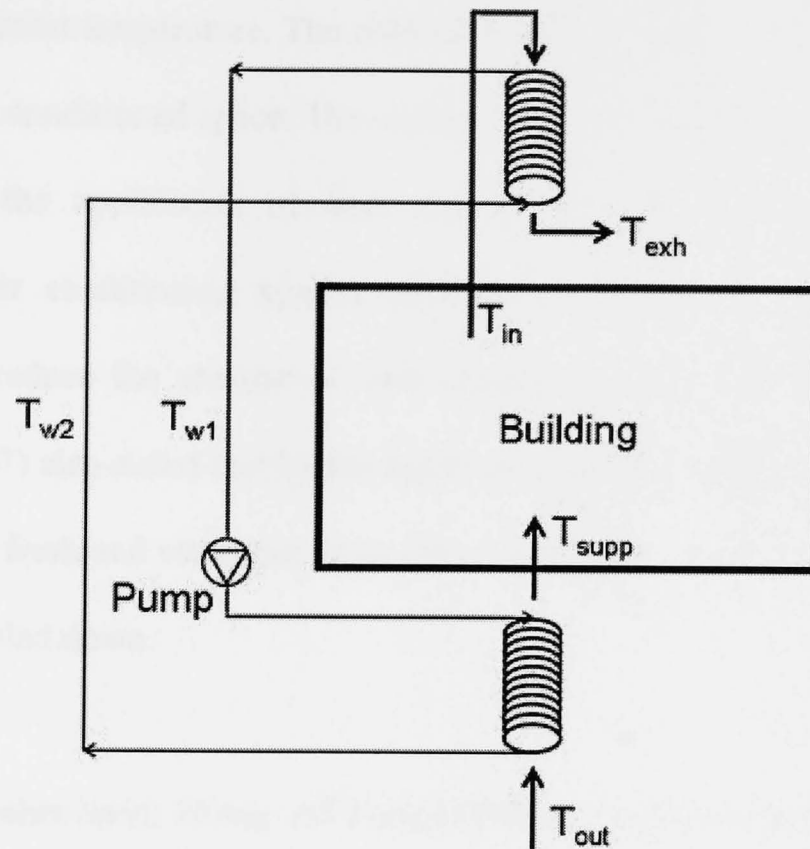


Figure 2.20 Schematic of the heat recovery concept (Source: Hviid and Svendsen 2010)

2.3.3.3 Heat recovery assisted-cooling or air conditioning

Within the buildings, most of energy is for provision of heating, cooling and air conditioning (Omer 2008). For air conditioning, buildings in warm climates or those with high casual gains may need some form of cooling to maintain a comfortable interior environment (Butcher and Readdy 2007; El-Baky and Mohamed 2007; Juodis 2006; Fehrm et al. 2002; Liu et al 2006). It is observed that plentiful waste condensing heat from traditional air conditioning system is directly exhausted to the environment, especially in summer time when the system operates on air conditioning mode (Gong et al. 2008). Many methods have been attempted to tackle

these problems. In regard to this, several researchers tried to add a heat recovery system on the air conditioning systems (Rasouli et al. 2010). In a conventional air conditioning system, the humidity is controlled by cooling the supply air stream below its dew point temperature. The cold air is then reheated to a temperature that is suitable for the conditioned space. The earliest study by McFarland et al. (1996) have declared that the application of heat recovery unit of heat pipe type in the conventional air conditioning system could be an efficient technique to control humidity and reduce the amount of heat energy required. Recently, El-Baky and Mohamed (2007) also stated that by the application of the heat pipe recovery between two streams of fresh and return air in an air conditioning system, the incoming fresh air could be cooled down.

On the other hand, Zhang and Jiang (1999) have presented a detailed heat and mass transfer model for an energy recovery ventilator with a porous hydrophilic membrane core to increase the efficiency of the air conditioning system. It is found that the sensible heat exchange, moisture exchange and the enthalpy exchange was promising. A study of window-type air conditioner with heat recovery system has been investigated by Liu et al. (2007) as shown in Figure 2.21. With the heat recovery system, they have found that the temperature of the mixed air would increase while in terms of relative humidity, would depend on the properties of the indoor air and outdoor air and their ratios. Whilst, Gu et al. (2004) have developed a heat recovery system using phase change materials (PCMs) to store rejected (sensible and condensation) heat from air conditioning system. A new heat recovery technique for air conditioning system was then proposed by Gong et al. (2008) employing a compound air-cooling and water cooling condensing module to replace the traditional

sole air-cooling condensing module. This proposed system was found had the ability to improve cooling and heating effects and recover condensing heat for heating sanitary water.

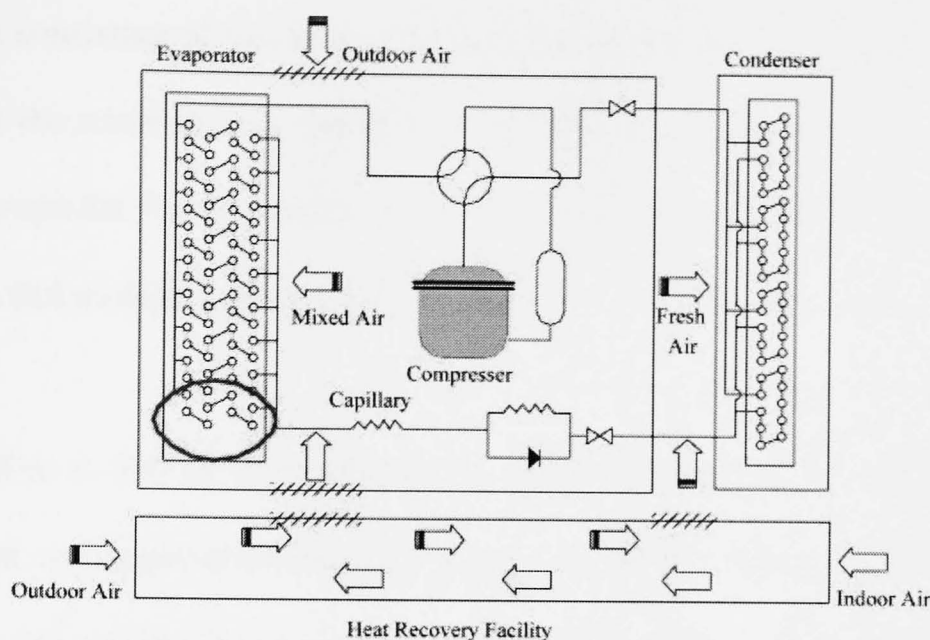


Figure 2.21 Schematic diagram of the window-type air conditioner with heat recovery facility (Source: Liu et al. 2007)

A heat recovery unit was installed in study of central forced-air heating and cooling system to control indoor air quality (IAQ) conducted by Emmerich and Persily (1984) in residential buildings. In this study, the heat recovery ventilator withdrew air from the return side of the forced-air system and replaced it with outdoor air drawn through the heat exchanger. The actual outdoor airflow rate during operation was selected to provide an air change rate of 0.35h^{-1} through heat recovery system. The outcome of this study stated that the tight Miami houses met the ASHRAE minimum air change rate on the hot day but still far short on the cold days.

In another study, Martinez et al. (2003) have designed a mixed-air heat recovery system, consisting of two heat pipes and indirect evaporative recuperators for air conditioning whereas the energy characterization of the mixed heat recovery system was performed by means of experimental design techniques. In their study,

they have analysed the influence of temperature, flow, relative humidity, and water flow on the basic characteristics defined by the mixed system. The results found that by application of the mixed heat recovery system in the air conditioning system installations consisting of two heat pipes and indirect evaporative systems, part of the energy from the return airflow could be recovered, thus improving energy efficiency. They also found that the heat recovery factors show a lineal dependence in relation to temperature and outdoor airflow factors.

Nasif et al. (2010) have performed experiments on thermal performance of an enthalpy heat exchanger as the heat and moisture transfer surface for air conditioning energy recovery systems as shown in Figure 2.22. It has been shown that in humid climate a saving of up to 8% in annual energy consumption can be achieved when this enthalpy exchanger used as a heat recovery instead of a conventional air conditioning system. Mahmud et al. (2010) have done a performance testing of a run-around heat recovery system for air conditioning which could transfer sensible and latent energy with non-adjacent ducting as shown in Figure 2.23.

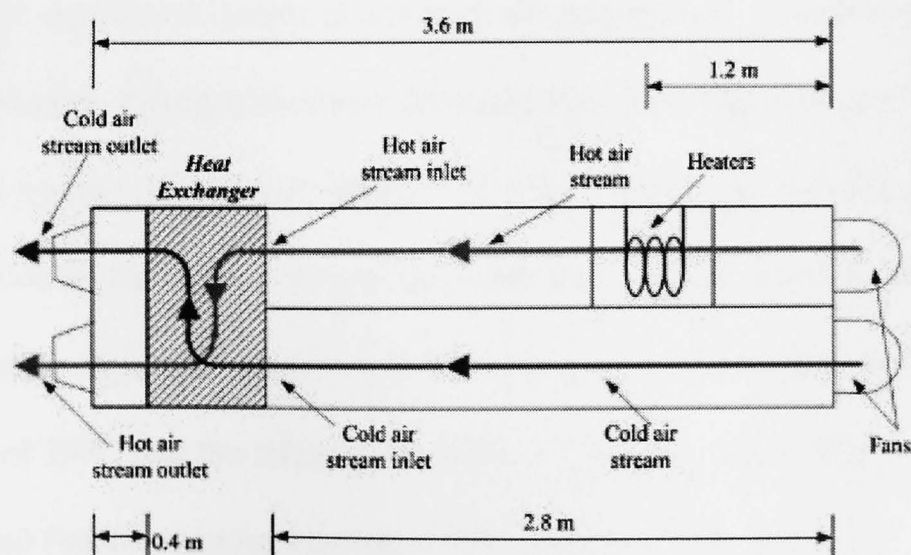


Figure 2.22 Heat and mass recovery system in air conditioning (Nasif et al. 2010)

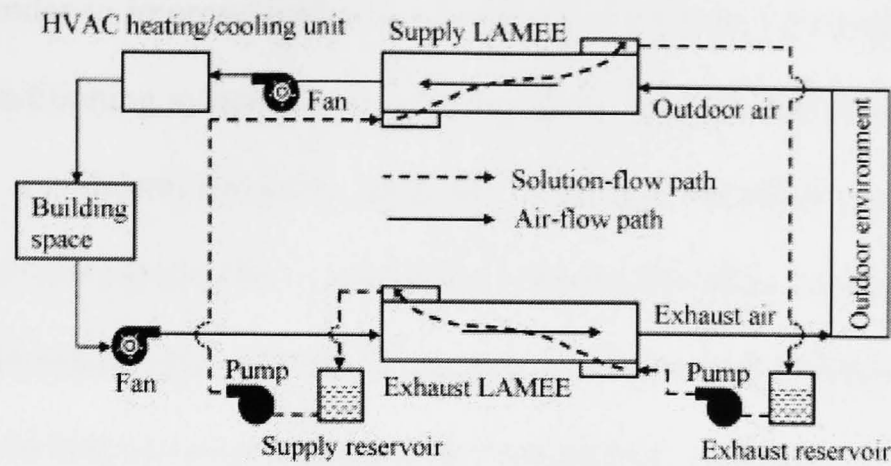


Figure 2.23 Schematic of a run-around heat recovery system in a air conditioning

(Source: Mahmud et al. 2010).

2.3.3.4 Heat recovery combined with dehumidification system

Due to the scarcity of conventional air dehumidification system, many efforts have been made since decades ago. Amongst these is the introduction of heat recovery in conventional system to recover the energy loss. The earliest study of heat recovery in dehumidification system was conducted by Abtahi et al. (1988) to investigate the dehumidifying characteristic of heat pipe recovery in humid climates. By using the heat pipe recovery between the warm return air and cold supply air, heat recovery was achieved with supply air reheat and return air pre-cooled. In another study, Kattar (1988) has tested dehumidification enhancement and energy saving for an air conditioning system in the sub-tropical Florida climate by installing a heat pipe recovery between the warm return air and cold supply air. He found that the dehumidification capability of the system was improved from 22 to 42% for the inlet temperature of 27°C and the relative humidity of 50%. In terms of energy saving, the results showed that the average saving of 75% over the 1985 and 1986.

With the demands of energy conservation in dehumidification system recently, Zhang et al. (2005) have proposed a fresh air processor with liquid desiccant total heat

recovery in order to improve indoor air quality and decrease the energy consumption of the air conditioning system. In another research, Zhang (2006) has proposed four independent air dehumidification systems with heat recovery strategies. These systems were compared with a mechanical dehumidification system with no heat recovery. The results showed that the system of mechanical dehumidification with membrane total heat recovery consumes the least primary energy.

Recently, a performance study involving modelling and experimental of air dehumidification system combined with membrane-based total heat recovery study was carried out by Liang et al. (2010) in order to improve the efficiency of a conventional dehumidification system in hot and humid regions as shown in Figure 2.24. The results indicated that as compared to conventional dehumidification system, the air dehumidification rate (ADR) of the new developed system is 0.5 higher and it has the ability to perform well under harsh hot and humid weather conditions.

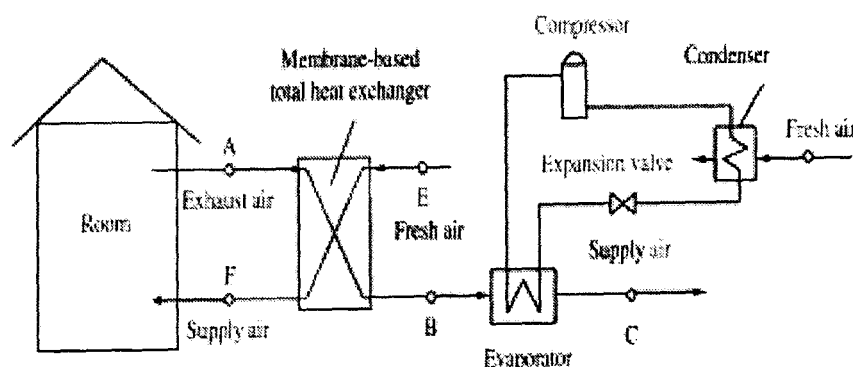


Figure 2.24 Schematic of air dehumidification system combined with membrane-based total heat recovery (Source: Liang et al. 2010)

Zhang and Niu (2002) in their paper presented the performance of rotary wheel so-called desiccant wheel for air dehumidification and enthalpy recovery as illustrated in Figure 2.25. Effects of rotary speed, number of transfer units and the specific area on the performance of the wheel were investigated and compared.

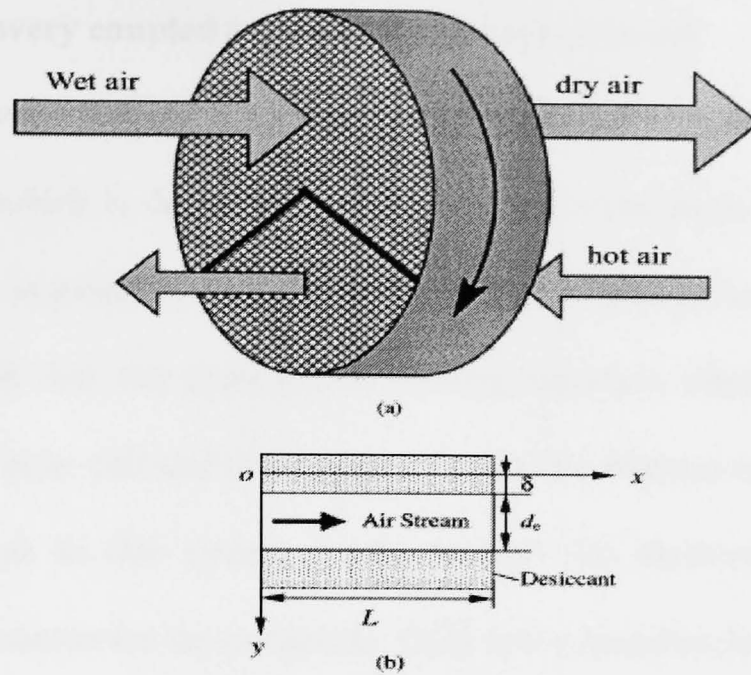


Figure 2.25 Schematic of the rotary desiccant wheel for dehumidification and enthalpy recovery (Source: Zhang and Niu 2002)

Liu et al. (2007) have combined a rotary wheel heat recovery with rotary desiccant wheel in a dehumidification system as shown in Figure 2.26 to analysis its energy consumption. The results showed that, compared to conventional system, energy savings were possible to be gained.

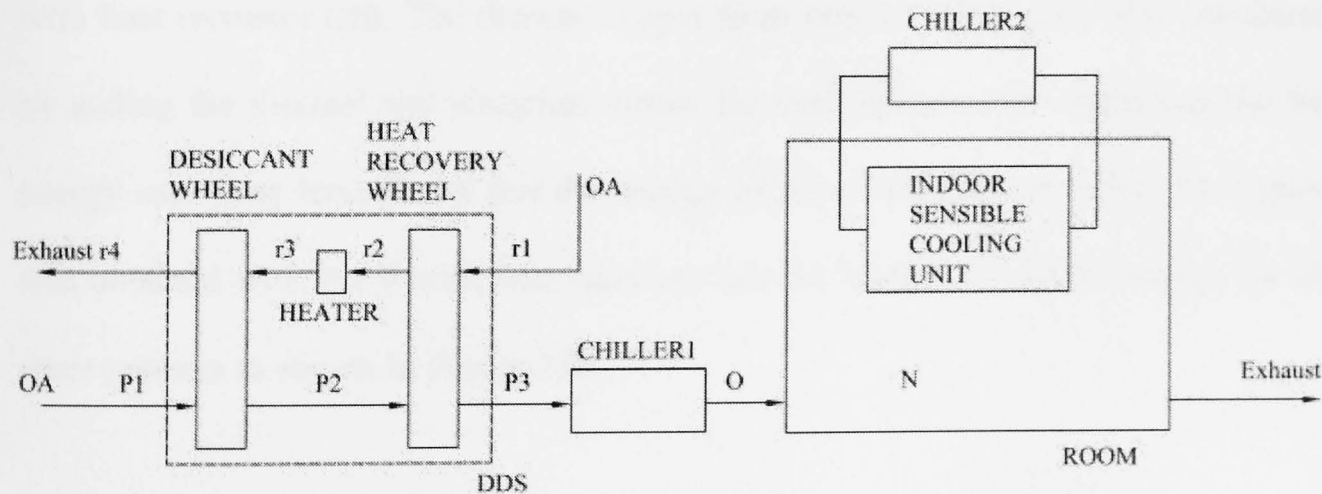


Figure 2.26 Schematic a rotary wheel heat recovery with rotary desiccant wheel in a dehumidification system (Source: Liu et al. 2007)

2.3.3.5 Heat recovery coupled with photovoltaic/solar panel

Heat recovery coupled with photovoltaic/solar panel is an advanced energy-efficient system which is developed in accordance to the weakness of solar panel when exposed to high temperature which resulting low efficiency. Luque (2003) has stated that the presence of cooling interface improves the electrical efficiency of the solar cell and in addition increase the lifetime of the system. Thus, heat recovery unit in this system works to cool the photovoltaic panels while providing a heat source for the occupants. Only few researches have been performed in the integration of heat recovery system with photovoltaic panel. Bazilian and Prasad (2002) have conducted a modelling study of a photovoltaic heat recovery system for buildings professional and validating with experimental data. The results indicated that the model helped to stimulate of a modular heat recovery unit addition to a building integrated photovoltaic system and could be customised to appropriately meet the needs of the users. On the other hand, Crawford et al. (2006) have presented the results of a life-cycle energy analysis of a building integrated photovoltaic system with heat recovery unit. The thermal output from heat recovery units was calculated by adding the thermal and electrical output for each system and subtracting the fan energy use. They have found that the energy pay periods between 4 and 16.5 years was obtained with BiPV with heat recovery has the highest embodied energy for all three systems as shown in Figure 2.27.

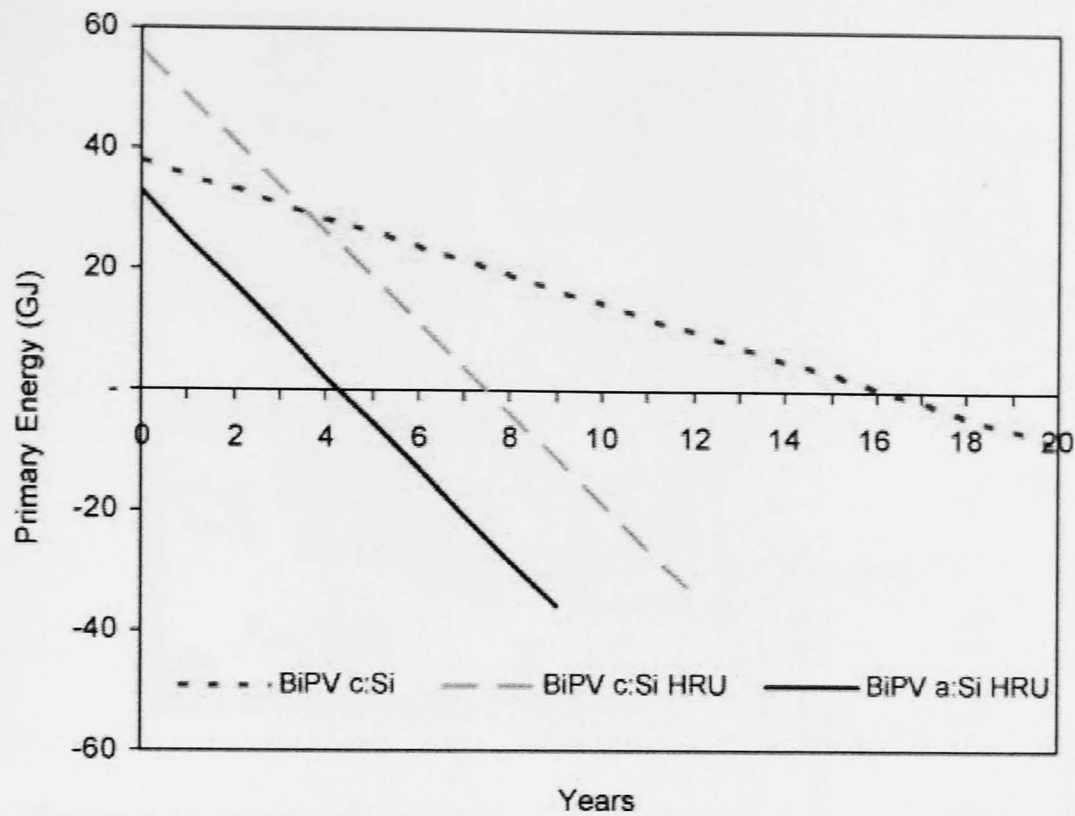


Figure 2.27 BiPV with heat recovery energy payback periods (Source: Crawford et al. 2006)

Recently, a study of condenser heat recovery with a PVT air heating collector has been conducted by Sukamongkol et al (2010) as shown in Figure 2.28. They have carried out an experimental test to investigate the validity of developed simulation model in predicting the dynamic performance of condenser heat recovery and found that the model agree satisfactorily with the results observed in experiments. This system can save energy by approximately 18% with the used of a photovoltaic thermal combined with the heat recovered from the condenser.

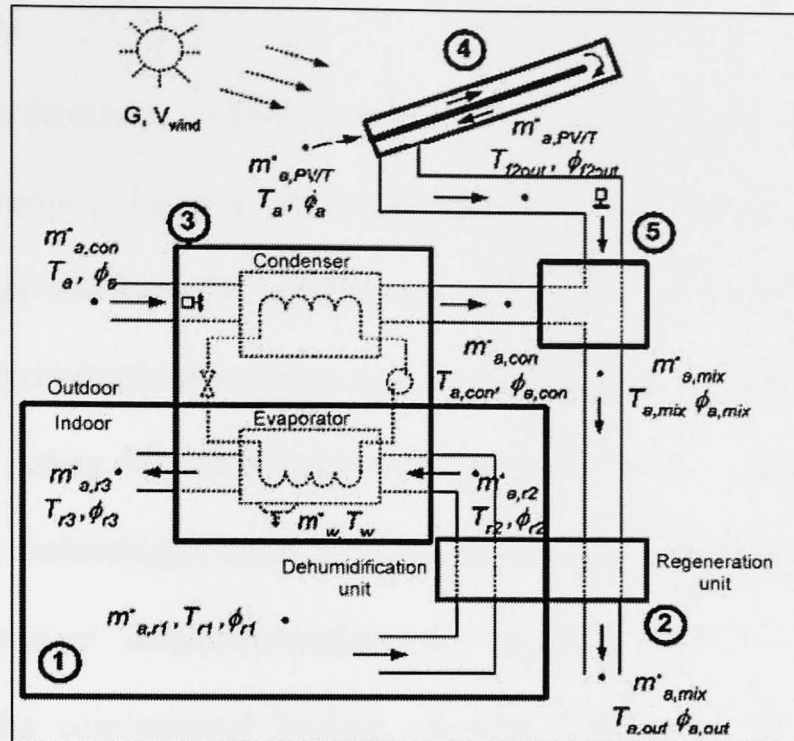


Figure 2.28 Schematic diagram of a condenser heat recovery with a hybrid photovoltaic/thermal (Source: Sukamongkol et al. 2010)

Another modelling and simulation of a hybrid photovoltaic module equipped with a heat recovery system was carried out by Maffezzoni (2009). Using the numerical model, he investigated the effects of temperature profile along the photovoltaic cells and the analysis of the model can be used to predict the current voltage levels that can be sustained by the solar panel. However, many aspects still need further investigations to include the direct heat exchange between the lower face of the photovoltaic cell and the air within the collector.

2.4 Summary

From the literature, it has been found that energy is consumed in buildings for space heating, cooling, lighting, air conditioning, and ventilation, water heating and general electrical services. To mitigate energy consumption in buildings, energy conservation, environmental concern and economic trends are the national energy regulatory and policy drivers of any country of the world. Besides, adoption of energy-efficient technologies such evaporative cooling, photovoltaic panel, passive ventilation, desiccant dehumidification etc would contribute to replace or as alternative to the conventional heating, cooling, ventilation and air conditioning system. In other context, significant energy savings for heating, ventilating and air conditioning purposes can be achieved by using heat recovery in building applications. Thus, heat recovery should be considered as part of an overall building application design strategy that attempts to meet energy conservation demands in buildings. A thorough review of the related knowledge regarding the heat recovery systems was then carried out. Findings from literature review shown that there are different of heat recovery types in the market nowadays such as fixed plate, heat pipe, and rotary wheel and run-around units utilized to recover energy loss. Table 2.2 summarized their efficiency and advantages.

Table 2.2 Heat recovery types, efficiency and advantages

Types of heat recovery	Typical efficiency	Advantages
Fixed-plate	50 to 80%	Compact, highly efficient due to high heat transfer coefficient, no cross contamination, can be coupled with counter-current flow which enabling to produce close in-temperature differences
Heat pipe	45 to 55%	No moving parts, no external power requirements, high reliability, no cross contamination, compact, suitable for naturally ventilated building, fully reversible, easy cleaning
Rotary wheel	Above 80%	High efficiency, capability of recovering sensible and latent heat
Run-around	45 to 65%	Does not require the supply and exhaust air ducts to be located side by side, supply and exhaust duct can be physically separated, no cross contamination

Throughout the literatures, it is found many works have been done since 1980s' related to heat recovery systems. In the past, the works had emphasized more on heat/mass transfer in heat exchanger until the buildings standards are introduced then the efficiency and performance of heat recovery in building applications such as ventilation, air conditioning and dehumidification systems come into concerns. For natural/passive ventilation heat pipe recovery has been used since no moving part is required in this system. For mechanical ventilation, researchers tend to integrate heat pump so-called mechanical ventilation heat pump recovery whilst rotary wheel recovery has widely been used in desiccant dehumidification to recover heat and moisture.

On the other hand, many theoretical and experimental works in literature has been conducted for integration heat recovery system with mechanical ventilation.

natural ventilation, air conditioning and dehumidification systems. However, combination of heat recovery with low carbon technologies such as evaporative cooling and desiccant dehumidification is just a handful amount and very limited studies have been done to integrate them in one system. Besides, the integration of heat recovery with photovoltaic panel is still new and only few researches have been found. In addition there is no practical study for integration of heat recovery with low carbon technologies to become one device with multifunction (heat recovery/cooling/air dehumidifier) in one system and no work has been found on building integration of heat recovery system.

As a conclusion, the building energy consumption will continue to increase during the coming years due to the expansion of built area and associated energy needs. Private initiative together with government intervention through the promotion of energy efficiency, new technologies for energy production, limiting energy consumption and raising social awareness on the rational use of energy will be essential to make possible a sustainable energy future. Therefore the improvement of energy efficiency of buildings becomes an urgent issue to the world nowadays.

CHAPTER 3

Review on Theoretical Studies of Heat Recovery System

3.1 Introduction

As mentioned earlier in Chapter 2, heat recovery system is classified into two major categories: sensible heat recovery and enthalpy (sensible and latent) heat recovery (Dieckmann et al. 2003). In order to give further understanding of heat recovery system, theoretical background study has been conducted by reviewing the physical parameters, heat and mass transfer, flow and pressure drop inside the ducts, performance parameters, efficiency and energy calculations.

3.2 Physical parameters

Heat recovery system has particular physical components, which makes it unique in its operation and behaviour. The physical conditions and characteristics of the elements that configure the heat recovery determine how it behaves in terms of performance. As discussed before, the whole typical heat recovery is a system composed of ductwork for inlets and outlets, fans and the most important is the core which is the heat exchanger. Overall, each component has its own physical parameters that need to be considered to obtain good overall efficiency of heat recovery system. The parameters involve size, material and configuration (flow arrangement).

3.2.1 Size

The heart of heat recovery system is the heat exchanger. Thus, size of heat exchangers used in heat recovery systems is very important parameter. Generally, by increasing the heat transfer area or size of heat exchanger, the efficiency would also

increases but this will add to the bulk and cost of the equipment. Soylemezy (2000) has conducted a study on the optimum heat exchanger sizing for heat recovery for three different unmixed type heat exchangers which are counter-flow, parallel-flow and single fluid as shown in Figure 3.1.

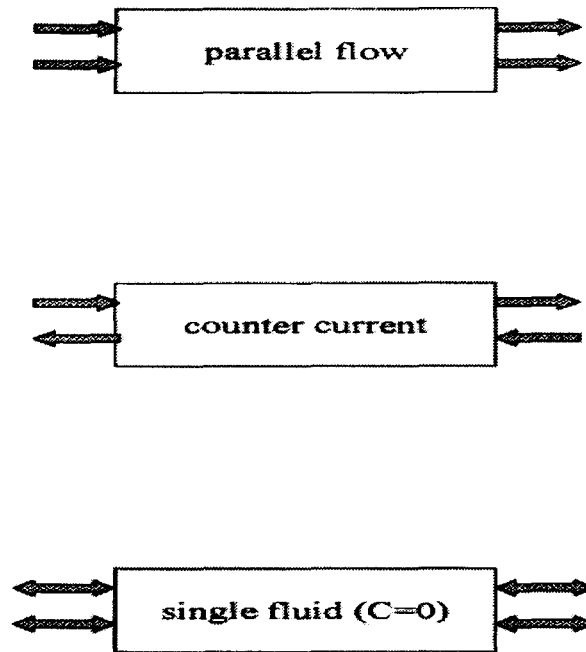


Figure 3.1 Types of heat exchangers (Source: Soylemez 2000)

In the study, he has developed a thermoeconomic optimization analysis for calculating the optimum heat exchanger/recovery size at which maximum savings occur using the P_1 - P_2 together with effectiveness-NTU method. The results illustrated that heat transfer surface area or size of the heat exchanger affects the effectiveness of heat recovery, which is an important performance indicator as shown in Figure 3.2.

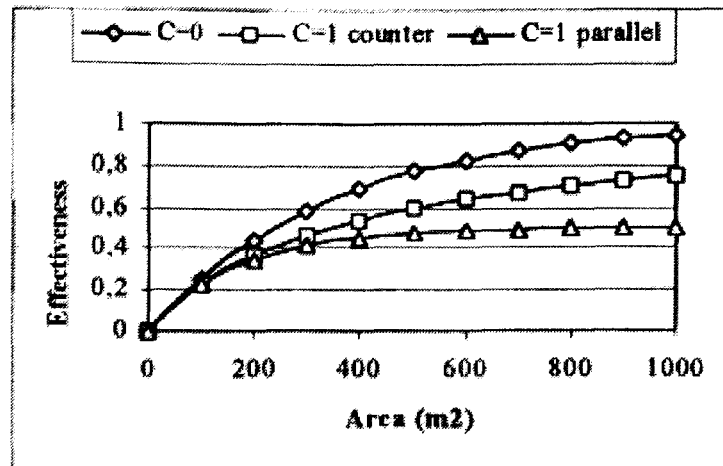


Figure 3.2 Effect of heat transfer area on effectiveness (Source: Soylemez 2000)

It was proven that the effectiveness of heat recovery increased as the area increased. He also concluded that the initial and operational cost of the heat recovery system mainly depends on the size of the heat exchanger itself (Figure 3.3).

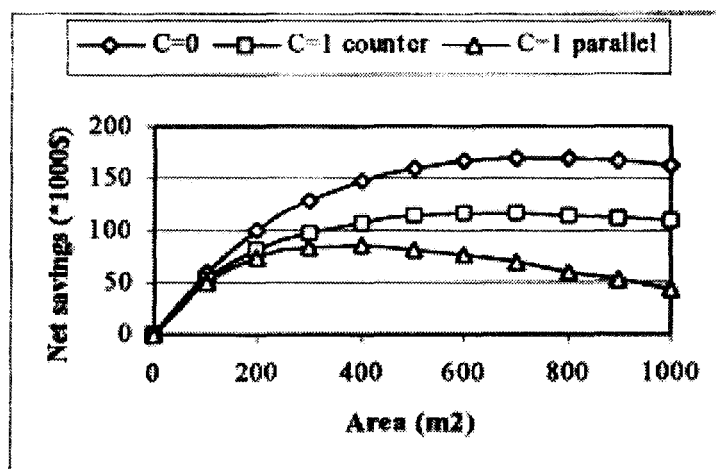


Figure 3.3 Effect of heat transfer area on net energy savings (Source: Soylemez 2000)

Manz and Huber (2000) in their study have proved that the length of heat exchanger has an impact on the effectiveness in terms of temperature efficiency as shown in Figure 3.4. In another study, Nasif et al. (2010) has discussed the effect of varying the heat exchanger face area on energy consumption where Kuala Lumpur, Malaysia weather data is used as a bench mark. The results indicated that as the heat transfer area of exchanger increased, the amount of energy saved increased as shown

in Figure 3.5. In heat pipe recovery unit, size is termed by the number of rows and it has been proven that as the number of row increased, the effectiveness would also increased (Yau 2001; Riffat and Gan 1997, Shao et al. 1998). The logical explanation for this phenomenon is that, with increased number of rows, the overall heat transfer area has been increased, thus increasing the heat transfer between the airflow and heat pipes (Yau 2001).

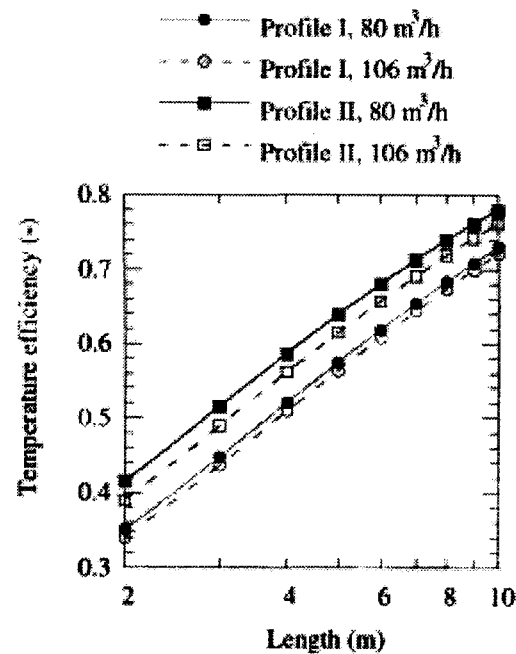


Figure 3.4 Temperature efficiency η as a function of heat exchanger length for two profile types (Source: Manz and Huber 2000)

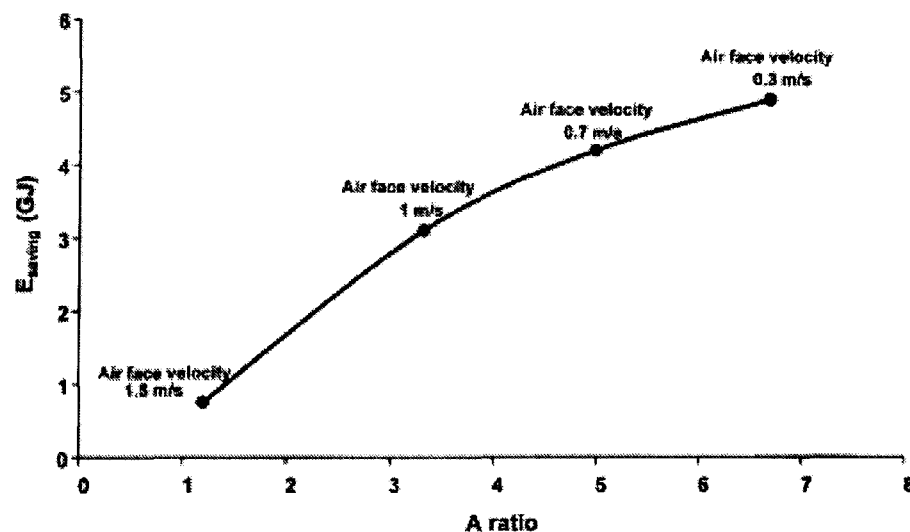


Figure 3.5 Effect of changing heat exchanger face area on annual energy saving in Kuala Lumpur (air face velocity indicated on top of each point) (Source: Nasif et al. 2010)

On the other hand, it is also important to take into account the size of the fan with high energy efficiency. Depending on the size of the fan, the size of duct in terms of diameter can be determined needed for this system for the case when the installation of the fans is in the ductwork. As suggested by Shurcliff (1988), ducts should be short and free of sharp bends as feasible and of ample diameter in order that the pneumatic resistance will be low and fans or blowers of small, low power, quiet type will suffice. Usually, the air flowing in the ducts is turbulent and the duct length range from 3 to 18m and duct diameters of 0.1 to 0.2m are satisfactory, producing pressure drops at a low flow rate.

Besides, the duct structure and material will influence the flow distribution and are also substantial in order to minimize the heat loss from the duct system. Otherwise, the heat loss can reduce the total efficiency of the system significantly. In addition, duct cross-sections are the predominant factor influencing pressure drop and heat transfer coefficient (Zhang 2009). This will be discussed further in another section. In literatures, there are several of duct cross-sections investigation have been done either experimentally or numerically (Shah and London 1978; Incropera and Dewitt 1996; Chen et al. 2000; Zhang 2007).

3.2.2 Structure and material

From the engineering approach, structure and materials are selected by how they perform because this will bring some significant effects to their surroundings or how they physically resist the influence of the surroundings. Capillary forces or porosity and pore diameter of the materials play significant role in moisture transfer. Higher porosity material can hold more transfer and bigger pore diameter has lower

mass flow resistance (Liu 2008). Besides, thickness of the heat/mass transfer surface/membrane heavily affects the heat and mass transfer resistance. On the other hand, durability of material is another important part to evaluate the optimization and economic performance of the heat recovery.

3.2.1.1 Metal type

Copper and aluminium are most common material used in design of heat exchanger. However, these materials have less porosity to retain the condensed moisture from the hot and humid air. Thus, to increase transfer surface, porous structure is considered to replace the smooth surface of the sheet or tube (Tadris et al. 2004) such as wickered metal, foams or wools or fins. The porous metal have thermal conductivity from 29.43 to 400Wm/K. Experimental and numerical study has been carried out by Manz and Huber (2000) involving aluminium fins of heat recovery system used as combined duct and heat exchanger as shown in Figure 3.6. These aluminium fins were 2.2mm thick. The results showed that by using this concept, heat recovery up to 70% at a duct/heat exchanger length of 6m could be achieved for building ventilation. In another study, the heat pipe recovery consists of 25 copper tubes with the evaporator and condenser sections were finned with 50 square aluminium sheets of 0.5mm thickness were used in research work by El-Baky and Mohamed (2007).

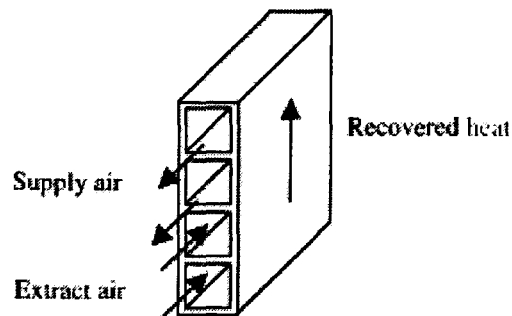


Figure 3.6 Segment of an extruded aluminium profile used as a combined duct and heat exchanger (Source: Manz and Huber 2000)

3.2.1.2 Polycarbonate

Polycarbonate is a particular group of thermoplastic polymers which easily worked, moulded and thermoformed. Thermoplastic is the term used for polymers that soften when heated and become firmed again when cooled. Polycarbonate has good chemical resistance to acids but poor resistance to alkalis and solvents and able to prevent corrosion. Polycarbonate normally has service temperature ranged of -4 to 135°C. Because of its low thermal conductivity around 0.19 to 0.22W/mK, it finds many applications. It is shown that it do hold promise for use in the construction of heat exchangers in HVAC and heat recovery applications (T'Joen et al. 2009). For instance, a study of polycarbonate plates in heat exchanger has been performed by Kho et al. 1997. On the other hand, Kragh et al. (2007) has conducted a performance investigation of a polycarbonate fixed-plate heat exchanger with 0.5 wall thickness as shown in Figure 3.7 for heat recovery of mechanical ventilation in arctic climates.

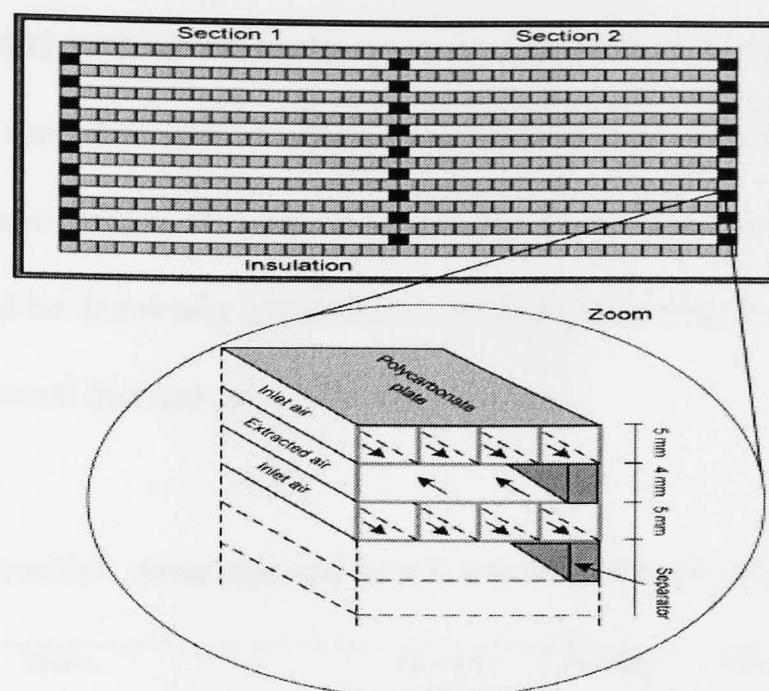


Figure 3.7 Horizontal cross-section of the exchanger (Source: Kragh et al. 2007)

3.2.1.3 Fibre

Fibre material such as paperboard, cloth, wood or glass fibre and natural fibre have relatively high hydrophilic and lower thermal conductivity and hardness. It is found that fibres have much lower thermal conductivity than metals, ranging from 0.01 to 0.3W/mK (Zhao et al. 2008; Zhao et al. 2009). The pore size of various fibres is thin enough to carry the heat/mass transfer with less resistance and have strong absorption ability (Idicula et al. 2006). Table 3.1 shows the porosities, pores size and membrane thickness (Liu 2008). On the other hand, Wang et al. (2006) stated that the effective thermal conductivity decreases with increasing of porosity of fibrous material. Even though thermal conductivities of the fibres are lower than that of metals, the porosities of most fibres are enough to absorb moisture from the humid air and the pores size of fibre are bigger than the liquid water molecular diameter. In terms of hardness, most fibre materials are not strong enough for use as exchanger plates and the lifespan of the fibre exchanger is short as it is easy to be deformed or damaged when being soaked by water. (Fend 2005). In term of cost, the fibres are

extremely cheap and so frequent replacement is affordable that could overcome the disadvantages of short life span. Dallaire et al. (2010) have presented a conceptual optimization of porous core of rotary wheel. They found that the performance of a rotary wheel could be drastically improved by properly selecting its thickness and the porosity of the internal thermal mass.

Table 3.1 Porosities, pores size and membrane thickness (Source: Liu 2008)

Fibres	Pore size ($\times 10^{-6}m$)	Porosity	Membrane thickness (mm)
Woven fibre	0.3~2.5	>50%	0.86
Randomly oriented ultra-fine fiber	0.2~0.4	52~83%	0.15~0.3
Carbons fibres	> 0.000137	0~95%	1.6
Hardwood fibre	2~5	63~71%	<15
Si-Al-C fibres	0.1	>10%	0.394~0.706
Porous paper	0.05~0.1	<90%	$0.2\sim 2.0\times 10^{-3}$
Pigment-filled polymer coated paperboard	0.08~0.14	>70%	0.3
Paper board	0.01~0.06	30~95%	0.012~0.5
Natural fibre (Banana, Pineapple, Sisal, etc.)	0.1~5	<50%	0.015~0.5

3.2.1.4 Wick structure

Wick is one of the structures that could increase the heat/mass transfer area and at the same time increase the capillary force. Wick porosities are enough to contain the condensed moisture. Metal wick structure famously used in heat pipe exchanger. The present of wick structure in heat pipe exchanger would results to a larger surface area and would increase the effectiveness (Yau 2001). Figure 3.8 shows the wick structure with heat and fluid flow paths in the evaporation surface studied by Hwang et al. (2007).

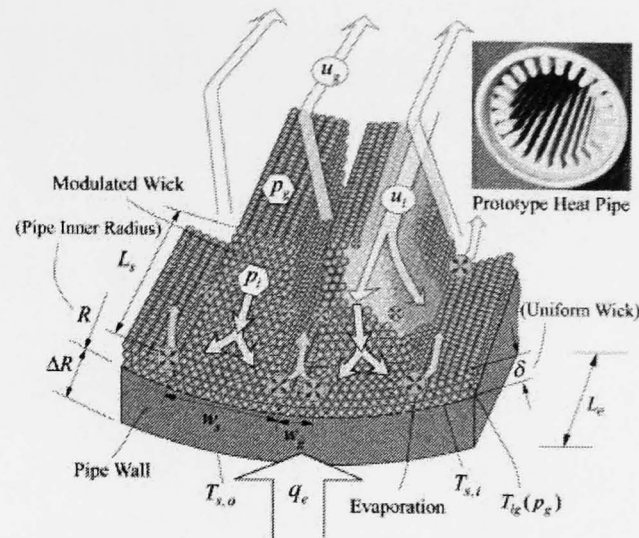


Figure 3.8 Schematic of the wick geometry in the evaporator of heat pipe (Source: Hwang et al. 2007)

3.2.1.5 Corrugated structure

Corrugated structures are basic channels construction in fixed-plate exchangers (Zhang 2005). The corrugations force the flow in the plate channels to experience a continuous change in direction and flow area (Kho et al. 1997). The benefits of this geometry are that they have efficient heat exchange capabilities and strong mechanical strength, even with very thin material wall thickness. There are a lot of studies in literatures have been conducted to investigate the performance of corrugated structures of heat exchanger's channel such as Okada et al. 1972; Focke et al. 1985; Stasiek et al. 1996; Ciofalo et al. 1996; Muley and Manglik 1997); Zhang (2005). In order to achieve enhanced heat transfer, Islamoglu (2003) has applied a design of corrugated structure in construction of channels in his study as shown in Figure 3.9.

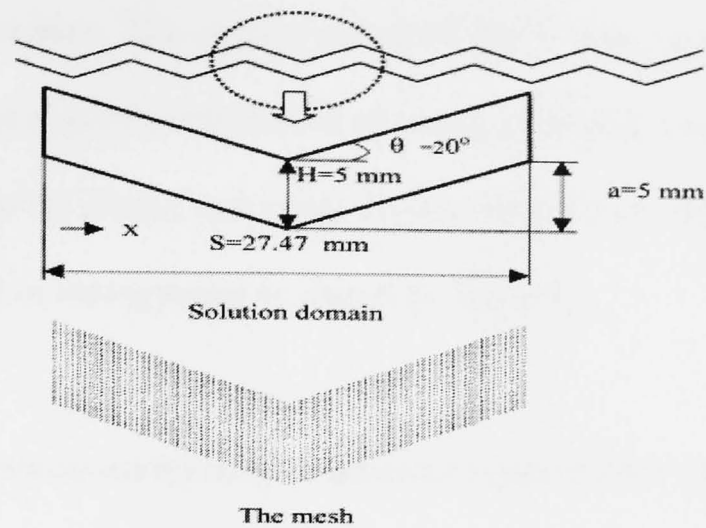


Figure 3.9 A schematic representation corrugated structure channel (Source: Islamoglu 2003)

3.2.1.5 Membrane based

Membrane-based material is a new approach to heat/mass transfer in heat recovery whereas this material has the capability as an enthalpy recovery. Heat exchanger made of vapour permeable membrane such as treated paper or new microporous polymeric membrane to transfer both heat and moisture from one air stream to the other, thus providing total enthalpy energy exchange (Min and Su 2010). The membrane-based can economically achieve high sensible heat recovery and high total energy effectiveness because they have only a primary heat transfer surface area separating the air streams and are therefore not inhibited by the additional secondary resistance inherent in other exchanger types. There are many studies have been done in this field. For example, Niu and Zhang (2001) has performed a theoretical model to evaluate the performance of a membrane-based energy recovery ventilator and investigated the effects of the entrance states of the two airstreams. Zhang and Niu (2002) further developed performance correlations for quick estimates of the enthalpy effectiveness of a membrane-based energy recovery ventilator. Min and Su (2010) have carried out a numerical investigation to study the effects of membrane spacing

and membrane thickness. The results indicated that it was necessary to use a thin membrane to obtain a good performance of energy recovery ventilator. Performance comparison is made by Zhang and Jiang (1999) among heat recovery with different core material and flow arrangement as shown in Table 3.2.

Table 3.2 Performance comparison of different types of ERV (Source: Zhang and Jiang 1999)

Performance comparisons of different types of ERV			
Types of ERV	SE	ME	EE
Sensible only ERV	0.762	0	0.154
ERV with paper core	0.691	0.362	0.433
ERV with membrane core (cross)	0.752	0.748	0.743
ERV with membrane core (counter)	0.821	0.816	0.818

3.2.3 Configuration/Flow arrangement

It is believed that flow arrangements have direct impact on heat exchanger effectiveness. In addition, heat transfer efficiency is maximized if the two airstreams have opposite direction in airflow arrangement (Shurcliff 1988). There are numerous possibilities exist for airflow arrangement in heat exchanger for heat recovery system. Parallel-flow is a flow configuration where the hot and cold fluids enter at the same end of heat exchanger, flow through in the same direction and leave together at the other end. Another famous configuration in heat recovery system design is counter-flow heat exchanger. As the name implied, in this configuration, the hot and cold fluids enter in the opposite ends of the heat exchanger and flow in opposite direction. Cross flow has been the predominant flow arrangement for heat exchanger where in this configuration, the two fluids usually flow at right angles to each other and the flow can be called as mixed or unmixed flow. Figure 3.10 illustrates the airflow arrangement described above. By comparing the effectiveness of these three flow

arrangement, a counter-flow arrangement is the best. It is well known, effectiveness of a cross-flow heat exchanger is 10% less than of a counter-flow heat exchanger and the maximum effectiveness is confined to 0.8. For parallel flow, it is confined to 0.5 (Incropera and Dewitt 1996).

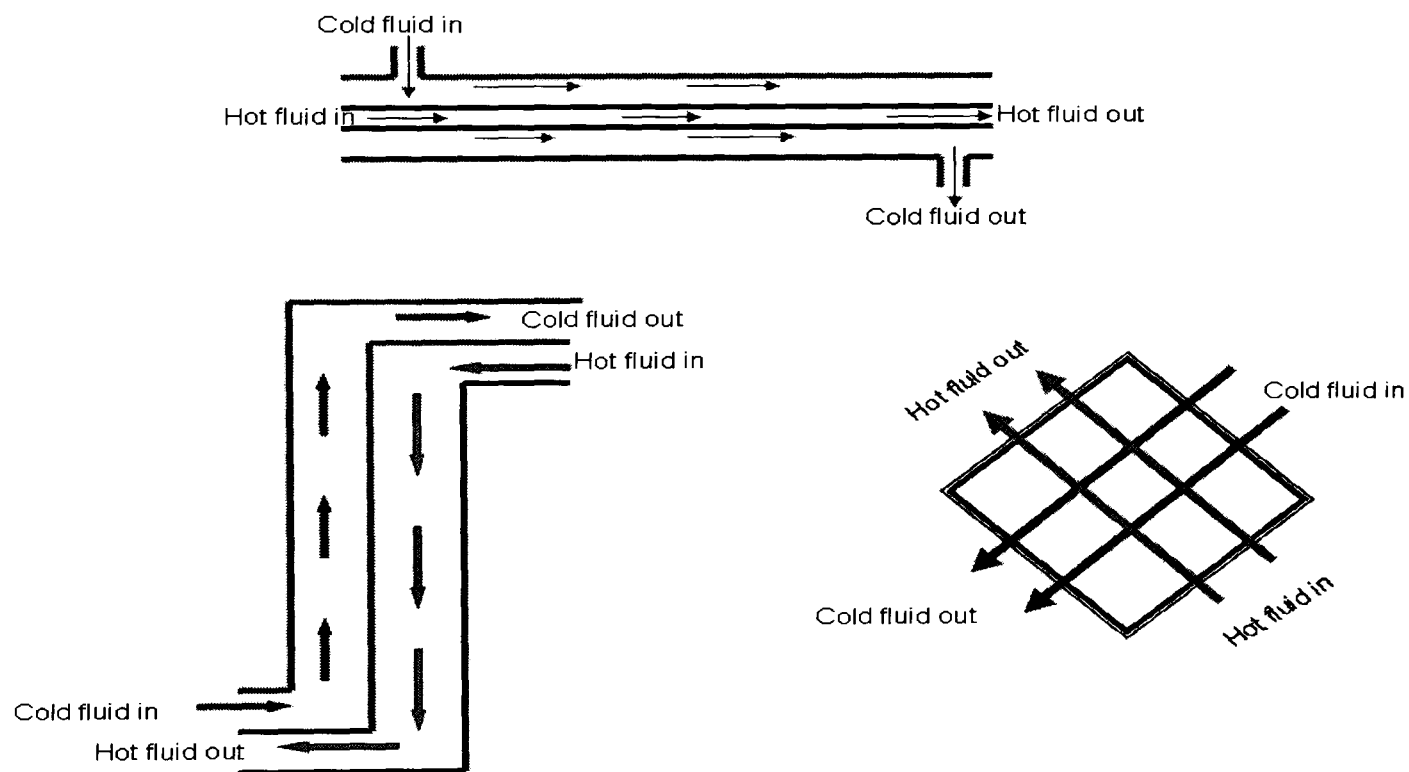


Figure 3.10 Flow arrangements

Optimization of the fixed-plate heat exchanger flow arrangement to yield a minimum annual operating cost was studied by Jarzebski and Wardas-Kozziel (1985). Kandlikar and Shah (1989) analyzed several usual configurations and presented guidelines for selecting appropriate flow arrangement from among those considered. It was verified that in most cases symmetric configurations with counter-flow yielded the highest effectiveness. Pinto and Gut (2002) presented a optimization method for determining the best flow configuration.

Recently, advanced flow arrangements have taken their part in heat exchanger such quasi-counter flow arrangement as shown in Figure 3.11. Zhang (2010) have

developed a mathematical model and experiments to investigate the performance of quasi-counter flow membrane-based exchanger. The results found that the effectiveness of the arrangement lie between those for cross flow and counter-flow arrangements. The comparisons of flow arrangements in case of effectiveness were also conducted in their study and generally shown that sensible and latent effectiveness were improved by 5% in quasi-counter flow arrangement. On the other hand, Nasif et al. (2010) have conducted an investigation of advanced Z-flow configuration heat exchanger which provides counter-flow arrangement over most of the transfer surface to maximized heat and moisture transfer.

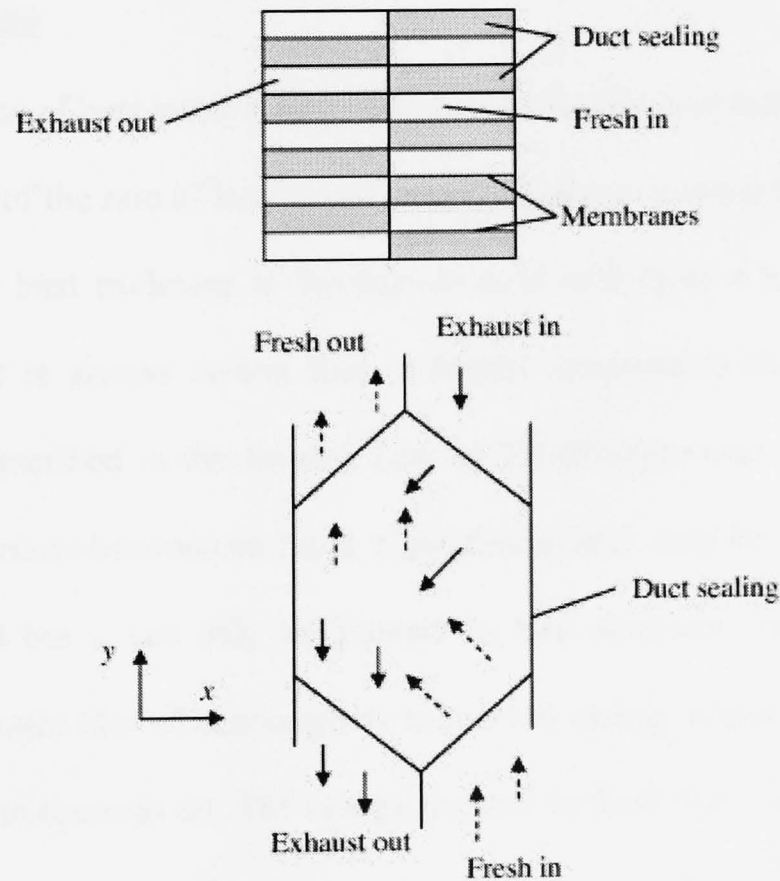


Figure 3.11 Schematic of a quasi-counter flow parallel-plates total heat exchanger

(Source: Zhang 2010)

3.3 Heat/mass transfer

The concept of energy is used in thermodynamic to specify the state of a system. It is a well-known fact that energy is neither created nor destroyed but only

changed from one from to another. The science of thermodynamics deals with the relation between heat and other forms of energy. In this section the theoretical analysis has been done in accordance to heat and mass transfer or in other words these also could be called as sensible and latent heat. In heat recovery system, sensible and latent heat will be treated differently. Sensible heat is heat that can be sensed by thermometer or our fingertip while latent heat is heat that has converted a solid to a liquid or has converted a liquid to a gas (Shurcliff 1988). Heat/mass transfer in heat recovery core is of interest to predict energy recovery efficiencies.

- Heat transfer

The science of heat transfer or is also called sensible heat transfer is concerned with the analysis of the rate of heat transfer taking place in a system. Heat transfer or is also known as heat exchange is the transition of heat from a hotter surface to a cooler surface. It is always occurs from a higher temperature surface to a cooler temperature as described in the Second Law of Thermodynamics. Where there is a temperature difference between surfaces in proximity, heat transfer between them can never be stopped but it can only be slowed. In heat recovery system for building application, the basic idea of exchanger is to transfer energy where heat is recovered from hot airflow to the cold air. The energy transfer by heat flow cannot be measured directly, but the concept has physical meaning because it is related to the measureable quantity called temperature. In reality, temperature distribution in a medium is controlled by combined effects of these three modes of heat transfer which is conduction, convection and radiation. However in this chapter, heat transfer by convection mode is only discussed which occurs between the air and the heat transfer surface of heat exchanger in heat recovery system. Convection is the transfer of heat

energy when fluid flows over a solid body or inside a channel while temperatures of the fluid and the solid surface are different. In this mode, heat transfer between the fluid and the solid surface takes place as a consequence of the motion of fluid relative to the surface. Figure 3.12 shows the example of the heat transfer mechanism on a fixed-plate heat exchanger. As fluid motion goes more quickly the convective heat transfer increases.

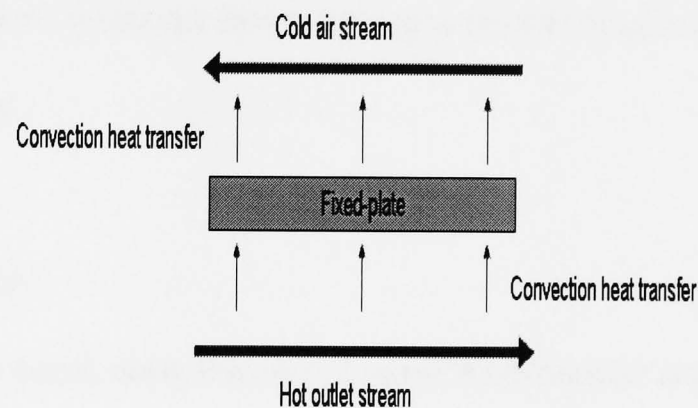


Figure 3.12 Heat transfer mechanism in fixed-plate

There are two types of convective heat transfer which are:

- Natural convection which occurs when the fluid motion is caused by buoyancy forces that result from the density variations due to variations of temperature in the fluid.
- Forced convection which occurs when the fluid is forced to flow over the surface by external source such as fans and pumps.

Generally, the formula for rate of convective heat transfer when there is no condensation or evaporation on the heat transfer surface is defined as:

$$q = UA(T_s - T_f) \quad (3.1)$$

The heat transfer coefficient here varies with the type of flow (laminar or turbulent) and also depends upon physical properties of the fluid such as temperature and physical situation whether the mechanism of heat transfer is by forced convection such as blower fan or a heat pump or by natural buoyancy. Therefore, the heat transfer coefficient must be derived or found experimentally for every system analyzed. For laminar flows the heat transfer coefficient is rather low compared to the turbulent flows due to turbulent flows having a thinner stagnant fluid film layer on heat transfer surface

- Mass transfer

On the other hand, mass transfer or latent heat transfer is related to the transfer of moisture with the difference in temperature of heat/mass transfer surface. Mass transfer is often described by Sherwood correlations in which the Sherwood number, Sh as presented in the following:

$$Sh = kD_h/D_{va} \quad (3.2)$$

The convective mass transfer can be an analogy to convective heat transfer (Incropera and Dewitt 1990) and thus, we have:

$$Nu = Sh \quad (3.3)$$

$$Nu = kD_h/D_{va} \quad (3.4)$$

$$\text{where } k = h/\rho_a C_p Le \quad (3.5)$$

Le is the Lewis number which is defined as :

$$Le = \lambda_a/\rho_a C_p D_{va} \quad (3.6)$$

There have been numerous investigations of the heat/mass in heat exchanger for heat recovery (Zhang 1999; Zhang 2005; Zhang 2007) Recently, Zhang (2010) has

conducted a heat and mass transfer study of a membrane based total heat exchanger for heat recovery in air conditioning system. A detailed heat and mass transfer study has been study by Zhang and Jiang (1999) of a novel porous hydrophilic polymer membrane for two different flow arrangement. The results showed that for the cross flow arrangement, the membrane area is not effectively used either for sensible heat or for moisture transfer as compared to counter-flow flow arrangement.

- Temperature, humidity and moisture content

Temperature is very important parameters in heat/mass transfer study. Note that in this thesis, the term “temperature” used is referred to dry bulb temperature (DBT) unless stated as wet bulb temperature (WBT). Another parameter that has significant role in heat/mass transfer is humidity especially for study the enthalpy recovery. There are two measures of humidity: absolute humidity and relative humidity. Absolute humidity means the actual absolute amount of water in a kg of air while relative humidity (RH) is a ratio of actual amount of water contained in the given body of air or the greatest amount of water that this air at its given temperature and pressure can hold. Whilst, moisture contents of air are easily solved with the aid of the Psychrometric Chart as shown in Figure 3.13 and which depends on dry bulb temperature and relative humidity. In fact it shows the relationships between four key quantities: temperature, relative humidity, absolute humidity and enthalpy (Shurcliff 1988).

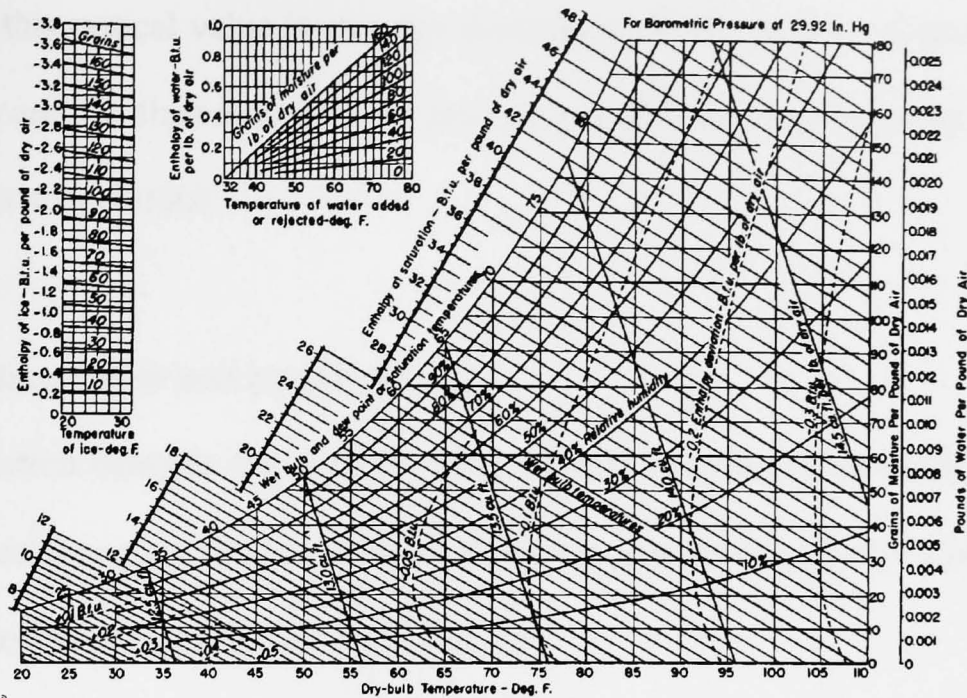


Figure 3.13 Psychrometric chart (Source: www.truetex.com)

3.4 Flow inside a duct

3.4.1 Velocity boundary layer

The fluid flow in the duct has a uniform velocity, V_0 at the duct inlet. As the fluid enters the duct a velocity boundary layer starts to develop along the wall surface. The velocity of fluid particles at the wall surface becomes zero and that at the vicinity of the wall is retarded; as result, the velocity in the central portion of the duct increases to satisfy the requirement of the continuity of flow. The thickness of the velocity boundary layer δ , continuously grows along the duct surface until it fills the entire duct. For flow inside the duct, the Reynolds number defined as:

$$Re = VD_h/\nu \quad (3.7)$$

This Reynolds number is used as a criterion for change from laminar to turbulent flow. The turbulent flow is usually observed for:

$$Re = Vd_h/\nu > 2300 \quad (3.8)$$

However, this critical value is strongly dependent on the surface roughness, the inlet conditions and the fluctuations in the flow. In general, the transition may occur in the range $2000 < Re < 4000$

3.4.2 Friction factor and pressure drop

Friction between the fluid flowing through a duct and its inside wall causes losses, which are quantified as pressure drop. The pressure drop over a length of duct can be determined using the following step :

- Calculation of Reynolds Number (Re)
- Calculation of friction factor (f)

The formula used to calculate the friction factor is dependent on the magnitude of the Reynolds Number. If the Re greater than 2300 but less than 100,000, it means the flow is turbulent. Thus the following formula can be used to calculate the friction factor :

$$f = 0.3164 \times Re^{-0.25} \quad (3.9)$$

- Calculation of pressure drop

Pressure drop, ΔP (N/m²) can be calculated using following formula:

$$\Delta P = \frac{V^2 f L \rho}{2D} \quad (3.10)$$

If Q is the flow rate in cubic meters per second through the duct, the electric power, P_f (Nms⁻¹ or W) required to get the fluid through the duct against the ΔP becomes:

$$P_f = Q \Delta P \quad (3.11)$$

3.4.3 Flow inside the ducts of various cross sections

The Nusselt number, Nu and the friction factor for laminar flow in ducts of various cross sections have been determined in the region where velocity and temperature profiles are fully developed. If the duct cross section for flow is not circular, then the heat transfer and friction factor for many cases of practical interest, can be based on the hydraulic diameter, D_h defined as:

$$D_h = 4A_f/p \quad (3.12)$$

Then the Nu is :

$$Nu = \alpha D_h / \lambda_f \quad (3.13)$$

3.5 Performance parameters

This section comprises certain proven techniques of monitoring the performance of heat recovery system from existing established data and previous works in the literatures. The performance parameters of heat recovery discussed in this section is defined by five parameters, which are as follows: the efficiency, effects of airflow, effects of temperature, pressure drop and electrical consumption.

3.5.1 Efficiency/Effectiveness

Efficiency of heat recovery system is usually defined with respect to balanced airflows and the performance of this unit can be studied by a simple mass and energy balance as shown in Equation 3.15 and 3.16 without no leakage flow between supply and exhaust air stream.

$$M_{E'} = M_r - M_e \quad (3.14)$$

$$M_{S'} = M_s - M_i \quad (3.15)$$

3.5.1.1 Sensible heat recovery

Energy balance of sensible heat recovery unit is shown when heat transfer through a casing by air leaks and heat conduction is not taken into account. In that case, sensible heat (recovered heat) from return air, q is equal to sensible heat transferred to supply air.

$$q = M_{E'} C_{p_{E'}} (T_r - T_e) = M_{S'} C_{p_{S'}} (T_s - T_i) \quad (3.16)$$

When only sensible heat is transferred and specific heat of exhaust air stream and supply air stream are equal, Equation 3.16 reduces to

$$q = M_{E'} (T_r - T_e) = M_{S'} (T_s - T_i) \quad (3.17)$$

Heat capacity of supply and exhaust air stream are defined as

$$C_{E'} = M_{E'} C_{p_{E'}} \quad (3.18)$$

$$C_{S'} = M_{S'} C_{p_{S'}} \quad (3.19)$$

Heat capacity ratio, C of supply and exhaust air stream is

$$C = C_{\min} / C_{\max} \quad (3.20)$$

where, C_{\min} and C_{\max} are the smaller and larger of two magnitudes of $C_{E'}$ and $C_{S'}$. The air that might undergo the maximum temperature difference is the air having the minimum heat capacity ratio, C_{\min} . Therefore, thermodynamically limited maximum possible heat transfer is defined as

$$q_{\max} = C_{S'} (T_r - T_i) \text{ if } C_{S'} < C_{E'} \quad (3.21)$$

$$= C_{E'} (T_r - T_i) \text{ if } C_{E'} < C_{S'} \quad (3.22)$$

Sensible heat efficiency is the ratio of the actual amount of heat transfer (recovered) from the exhaust air to the maximum possible amount of this heat transfer (Incropera and DeWitt 1996) as the following:

$$\varepsilon_S = q/q_{\max} \quad (3.23)$$

Substituting for q and q_{\max} from equation 3.18 and 3.24 and assuming $C_{pE'} = C_{pS'}$, equation 3.24 gives for sensible heat recovery without condensation (ASHRAE 1999).

$$\varepsilon_S = \frac{M_{S'}(T_s - T_i)}{M_{\min}(T_r - T_i)} = \frac{M_{E'}(T_r - T_e)}{M_{\min}(T_r - T_i)} \quad (3.24)$$

According to ASHRAE Standard (2005), sensible heat recovery effectiveness, ε_S is expressed by the temperature ratio or temperature efficiency when mass flow rates of supply and exhaust air are equal as the following:

$$\varepsilon_S = \frac{(T_s - T_i)}{(T_r - T_i)} = \frac{(T_r - T_e)}{(T_r - T_i)} = \varepsilon_{S,S'} = \varepsilon_{S,E'} = \varepsilon_S \quad (3.25)$$

3.5.1.2 Enthalpy recovery/Total recovery

Sensible heat recovery as mentioned earlier in literatures does not transfer moisture. Latent heat is transferred only when the warmer air stream is cooled below its dew point and condensation occurs. Sensible heat recovery is used where heat transfer without moisture is desired. Enthalpy recovery such as rotary wheel, fixed-plate with membrane based is used to transfer both moisture and heat between air streams (ASHRAE 2005).

Moisture balance of enthalpy recovery device is

$$M_{E'}(\omega_r - \omega_e) = M_{S'}(\omega_s - \omega_i) \quad (3.26)$$

Moisture/Latent efficiency is defined as

$$\varepsilon_L = \frac{M_{S'}(\omega_s - \omega_i)}{M_{\min}(\omega_r - \omega_i)} = \frac{M_{E'}(\omega_r - \omega_e)}{M_{\min}(\omega_r - \omega_i)} \quad (3.27)$$

When mass flow rates of supply and exhaust air are equal, moisture efficiency which is calculated based on the amount of moisture transferred and is presented by

$$\varepsilon_L = \frac{\omega_s - \omega_i}{\omega_r - \omega_i} \quad (3.28)$$

Enthalpy balance of total recovery is

$$M_{E'}(H_r - H_e) = M_{S'}(H_s - H_i) \quad (3.29)$$

Enthalpy efficiency or energy efficiency can be defined as

$$\varepsilon_H = \frac{M_{S'}(H_s - H_i)}{M_{\min}(H_r - H_i)} = \frac{M_{E'}(H_r - H_e)}{M_{\min}(H_r - H_i)} \quad (3.30)$$

3.5.1.3 The Effectiveness-NTU method

A second definition of efficiency was originally made by Nusselt (1985), called number of transfer units (NTU). The method of NTU is based on the fact that the inlet/exit temperature change (difference) of a heat exchanger or heat recovery core is a function of NTU and capacity rate ratio, C from Equation 3.21. The NTU is a non-dimensional expression which depends on the heat transfer area and the overall coefficient of heat transfer from fluid to fluid and has been the most convenient methodology to predict performance (Zhang 2009). When the NTU is small the efficiency of heat recovery unit is low, and when the NTU is large the effectiveness approaches asymptotically the limit defined by flow arrangement and thermodynamic

considerations. In addition, NTU is changed numerically by changing the convective heat transfer coefficients, the transfer area and the mass flow rate of dry air (Niu and Zhang 2001). NTU is defined as:

$$NTU = \frac{AU}{C_{\min}} = \frac{1}{C_{\min}} \int_A U(dA) \quad (3.31)$$

The overall heat transfer coefficient is defined as:

$$U = \frac{1}{1/h_{cold} + s/\lambda + 1/h_{hot}} \quad (3.32)$$

On the hand, in case where U cannot be treated as constant, the definition of second equality applies. The product of A and U is defined as a conductance of heat recovery unit as presented in the following equation:

$$G = AU = A \frac{1}{R} \quad (3.33)$$

where R = thermal resistance of heat recovery core, m²K/W which can be calculated as:

$$R = \frac{1}{\alpha_E} + \frac{s}{\lambda} + \frac{1}{\alpha_S} + m_f \quad (3.34)$$

The universal correlations for convection heat transfer cannot necessarily be applied in calculation of NTU, because the flow may not be fully developed or condensation may occur or heat transfer surfaces are shaped and so on. However, the correlations, can be used when necessary and they are usually presented as

$$Nu = C Re^n Pr^m \quad (3.35)$$

where C , n and m are constant, Nu is Nusselt number, Re is Reynold number, Pr is Prandtl number and can be calculated as:

$$Nu = \alpha D_h / \lambda_f \quad (3.36)$$

$$Re = VD_h / \nu \quad (3.37)$$

$$Pr = \nu / \alpha_D \quad (3.38)$$

Thus, the efficiency of heat recovery using effectiveness-NTU method can be defined with the following equation when the flow arrangement, NTU and the heat capacity ratio, C are known (Kays and London 1984). It can be noted that flow arrangement is unimportant when $C=0$. This corresponds to the situation when one fluid undergoes a phase change where specific heat capacity of the fluid may be thought to be infinite.

For the cross-flow heat recovery, when both air streams are unmixed, $C = 0$, the effectiveness is defined as:

$$\varepsilon_{NTU} = 1 - \exp\{NTU^{0.22}[\exp(-NTU^{0.78}) - 1]\} \quad (3.39)$$

For parallel flow heat recovery, the effectiveness is:

$$\varepsilon_{NTU} = \frac{1 - \exp(-NTU(1 + C))}{(1 + C)} \quad (3.40)$$

For counter-flow heat recovery, the effectiveness is as follows:

$$\varepsilon_{NTU} = \frac{1 - \exp(-NTU(1 - C))}{1 - C \cdot \exp(-NTU(1 - C))} \quad (3.41)$$

And when $C = 1$, the effectiveness is presented as:

$$\varepsilon_{NTU} = \frac{NTU}{1 + NTU} \quad (3.42)$$

There are massive of works conducted in the literatures related to effectiveness-NTU method of heat exchangers. For instance, Nellis and Pfotenhauer (2005) have performed an analytical study of effectiveness-NTU relationship for a counter-flow heat exchanger which subjected to an external heat transfer. On the other hand, Wetter (1999) has conducted a simple simulation model of air-to-air plate heat exchanger to be used for yearly energy calculations where the effectiveness-NTU relations were used to parameterize the convective heat transfer for a cross-flow with both streams unmixed. Niu and Zhang (2001) have discussed the influence of NTU number on the effectiveness as shown in Figure 3.14. It can be seen that the effectiveness increased with increasing NTU number.

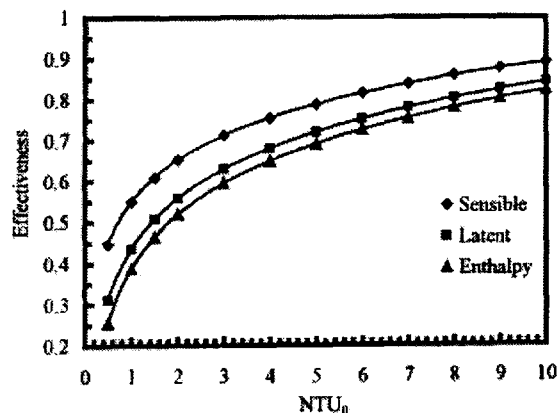


Figure 3.14 Effects of total number of heat transfer units on the effectiveness (Source: Niu and Zhang 2001)

3.5.1.4 Global efficiency

Another way to calculate efficiency was introduced by Roulet et al. (2001) by conducting measurements of the heat recovery system as shown in Figure 3.15. In the

study, he has suggested a global efficiency of heat recovery system which depends significantly on the air infiltration and exfiltration. The global efficiency of the heat recovery system, ϵ_G is defined as follows:

$$\epsilon_G = \frac{[1 - \gamma_{exf} - R_e R_{ie}](\gamma_{inf} - \gamma_{exf})(1 - R_{xs})}{1 - R_e R_{ie}(\gamma_{inf} - \gamma_{exf}[R_e + R_{xs}(1 - R_e)])} \epsilon_{HR} \quad (3.43)$$

$$\text{where, } \gamma_{inf} = \frac{M_{inf}}{M_a} \quad (3.44)$$

$$\text{and } \gamma_{exf} = \frac{M_{exf}}{M_a} \quad (3.45)$$

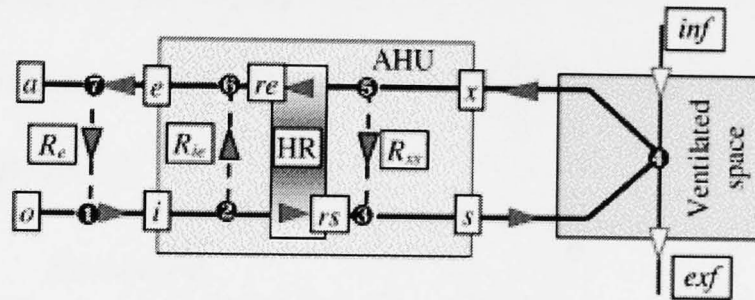


Figure 3.15 The tested system (Source: Roulet et al. 2001)

However, when there is no external recirculation ($R_e = 0$), Equation 3.46 can be simplified as follows:

$$\epsilon_G = \frac{(1 - \gamma_{exf})(1 - R_{xs})}{1 - R_{xs}\gamma_{exf}} \epsilon_{HR} \quad (3.46)$$

By taking the infiltration and exfiltration rate, the global heat recovery efficiency was between 60 to 70% for units having 80% nominal heat recovery efficiency (Roulet et al. 2001). On the other hand, Jakisalo et al. (2003) were comparing global efficiency with temperature efficiency and annual efficiency of heat recovery installed in mechanical ventilation system.

3.5.2 Effect of airflows

The airflow rate has a significant effect on the efficiency of heat recovery. Shao et al. (1998) has conducted a study on heat pipe recovery with low pressure loss for natural ventilation and air velocity in the system was measured around 0.5 to 1m/s. The results indicated that, the heat recovery efficiency decreased with increasing air velocity as shown in Figure 3.16. Nasif et al. (2010) have conducted the experiments of thermal performance of enthalpy/membrane heat exchanger for heat recovery. The measurements were performed for air face velocity ranging from 0.3 to 2.89m/s. The results discovered that as the air velocities increases, the effectiveness declines as for this range of air velocities the larger the resident time, the higher the heat transfer and effectiveness (Figure 3.17).

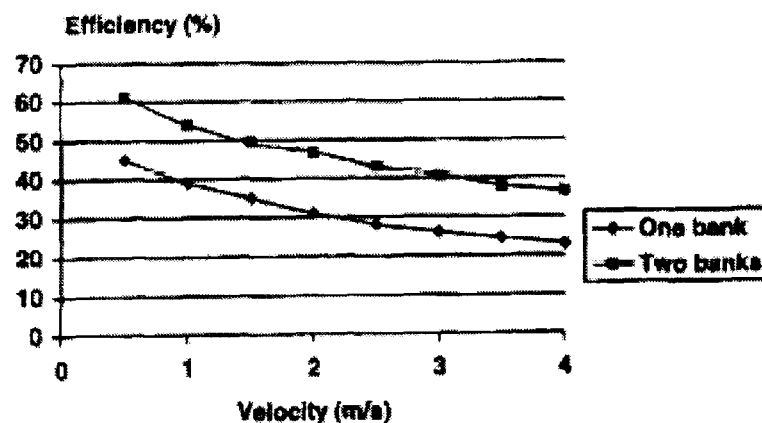


Figure 3.16 Heat recovery efficiency of plain fin unit (Source Shao et al. 1998)

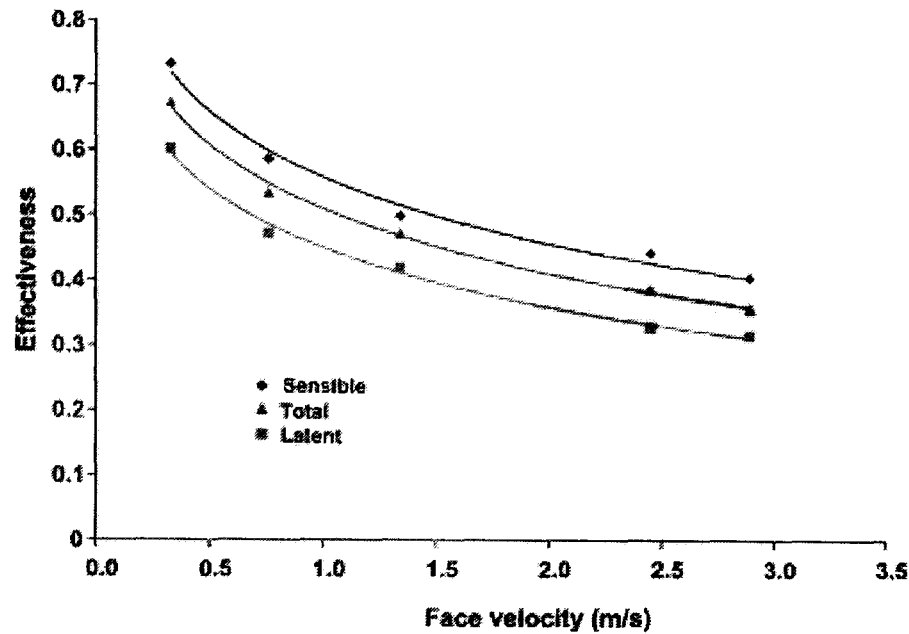


Figure 3.17 Experimental sensible, latent and total effectiveness for 60gsm paper heat exchanger (Source: Nasif et al. 2010)

In contrary to this, heat transfer in terms of heat recovered increased with increasing airflow rates. Hviid and Svendsen (2010) have compared the heat transfer against airflow rate in his their study with several of literature sources as shown in Figure 3.18.

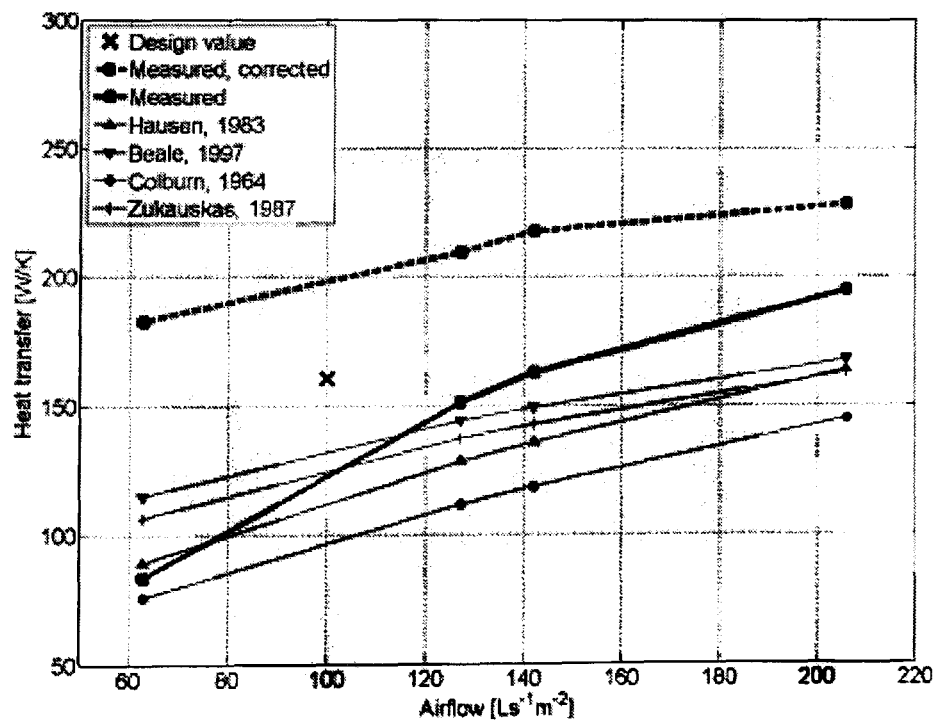


Figure 3.18 Comparison of measured heat transfer with the literature (source: Hviid and Svendsen 2010)

On the other hand, airflows also have significant effects on the pressure loss of heat recovery system. As airflow increases, the pressure loss increases as shown in Figure 3.19 (Shao et al. 1998). In addition, it has been proven that the temperature of air after the heat recovery unit (supply air to room) vary with air velocity (Riffat and Gan 1998).

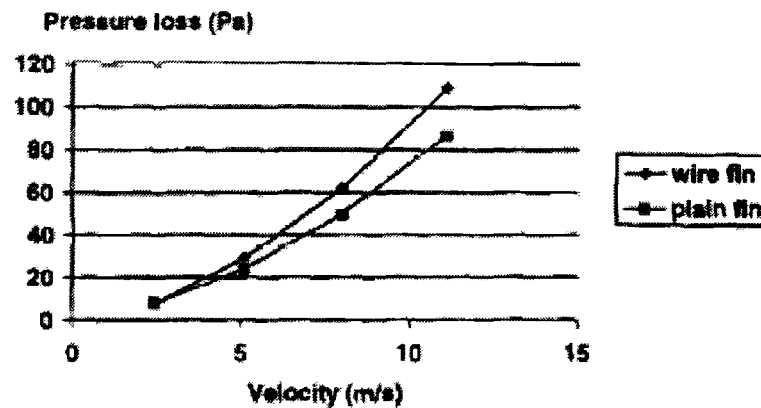


Figure 3.19 Pressure loss against velocity (Source: Shao et al. 1998)

For difference case, Manz et al. (2001) have conducted a study to observe the impact of unintentional airflows on the ventilation unit with heat recovery system on the energy requirement for heating. The system studied is shown in Figure 3.20. The results found that intentional airflows can considerably reduce the performance of ventilation units in combination with unintentional heat flows through the casing.

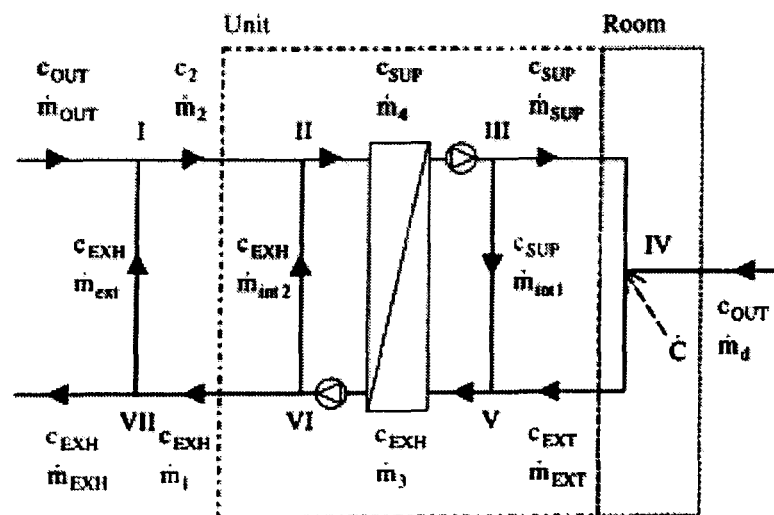


Figure 3.20 Main and unintentional air flows in a system consisting of a ventilation unit, room and outdoor space (Source: Manz et al. 2001)

3.5.3 Effects of temperature

In order to determine the sensible and total efficiency, temperature in terms of dry bulb and wet bulb must be known. In theoretical point of view, the performance of heat recovery system should not be affected by inlet temperatures. For both sensible and total efficiency, the temperature of the inlet air appears to have minor influence (Yau 2007) in heat recovery system used in natural ventilation system. On the other hand, the effect of heat-pipe inlet temperature was studied by Shao and Riffat (1997) for six cases in naturally ventilated buildings and results indicated that the temperature of heat pipe had a small effect on flow loss performance and pressure loss as shown in Table 3.3.

Table 3.3 Effect of temperature on flow loss and pressure loss of heat pipe recovery

(Source: Shao and Riffat 1997)

	IPL (Pa)	IFL (%)
HP1	0.103	17.1
HP2	0.062	8.8
HP3	0.047	20.0
HP4	0.096	15.4
HP5	0.103	14.3
HP6	0.107	6.5

However, the efficiency of heat recovery system in real situation varies with the temperature of supply and return air (temperature difference) (Gan and Riffat 1997) and because of air leakage, motor heat generation and so on (Han et al. 2007). In heat recovery system used to recover energy in air conditioning, El-Baky and Mohamed (2007) proved that the inlet fresh air temperature is the dominant parameter to enhance the heat transfer rate in the evaporator side of the heat pipe recovery and the effectiveness is increased with increasing the inlet fresh air temperature as presented in Figure 3.21. In addition, the temperature change increases with increasing the inlet fresh air temperature as shown in Figure 3.22.

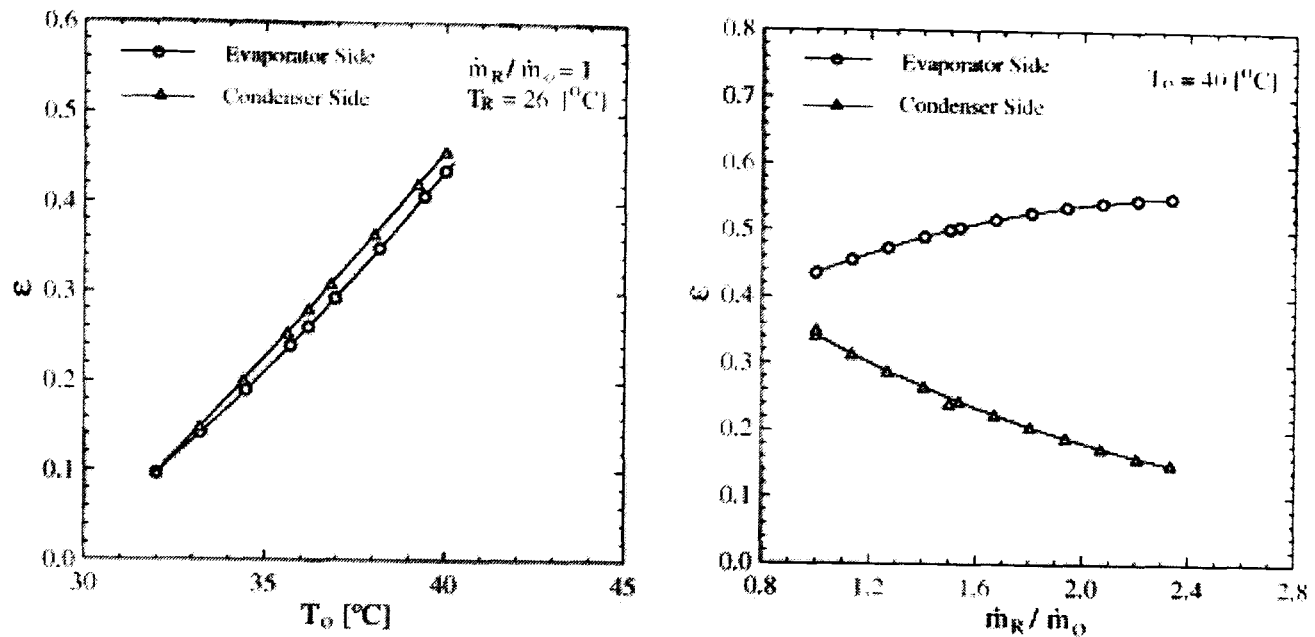


Figure 3.21 Effect of fresh air temperature and return air mass flow on effectiveness, ϵ

(Source: El-Baky and Mohamed 2007)

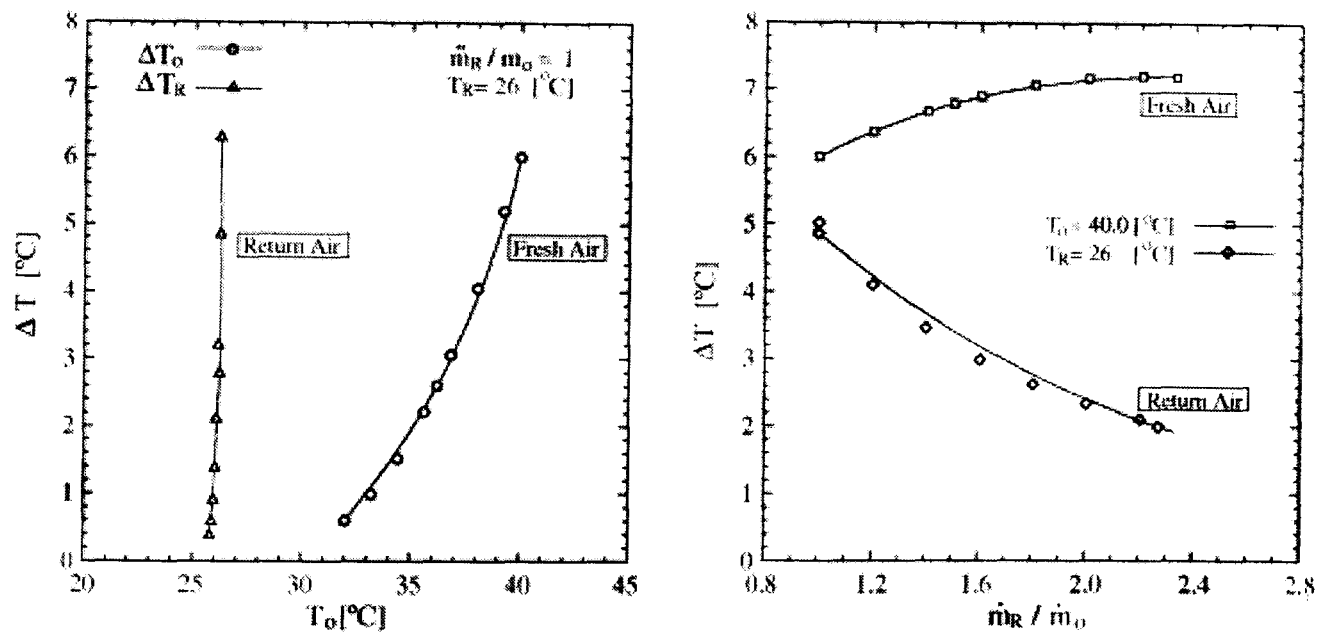


Figure 3.22 Effect of fresh air temperature and mass ratio on ΔT_O and ΔT_R (Source:

El-Baky and Mohamed 2007)

3.5.4 Effects of humidity

Effects of supply air humidity has been studied by Niu and Zhang (2001) and found that the supply air humidity has slight effects on the sensible efficiency but it

has a major influence on the latent effectiveness. Figure 3.23 shows the results of the experiments.

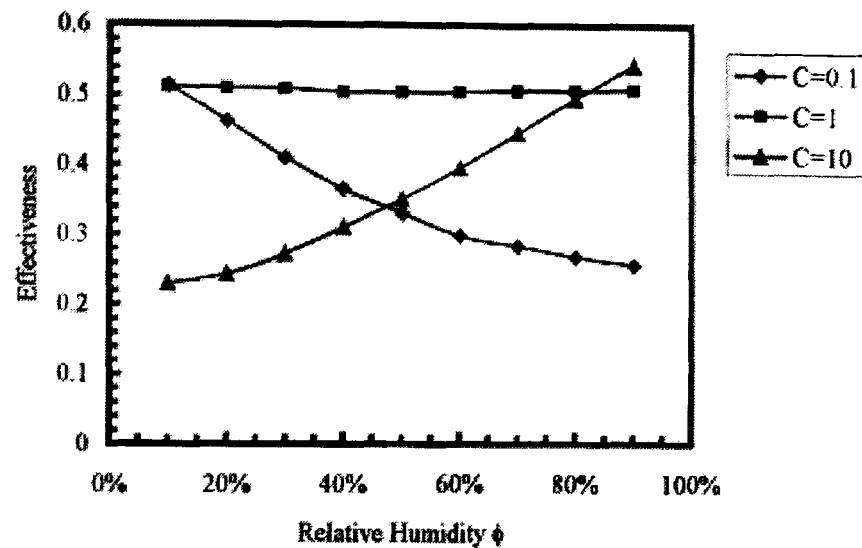


Figure 3.23 Effects of relative humidity of supply air on effectiveness with supply in temperature (35°C) (Source: Niu and Zhang 2001)

3.5.5 Pressure drop

Experimental measurements of pressure losses across heat pipe recovery unit were carried out by Shao et al. (1998). The results shown that, the pressure loss coefficient reduced as velocity increased as shown in Figure 3.24. In another study, pressure drop across the membrane-based heat exchanger for energy recovery has been measured by Nasif et al. (2007) in their study. The results indicated that pressure drop is proportional to the air velocity as shown in Figure 3.25.

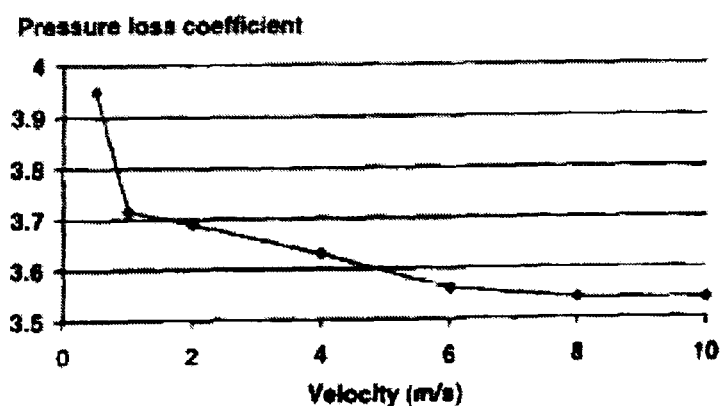


Figure 3.24 Reduction of pressure loss coefficient with increasing air velocity

(Source: Shao et al. 1998)

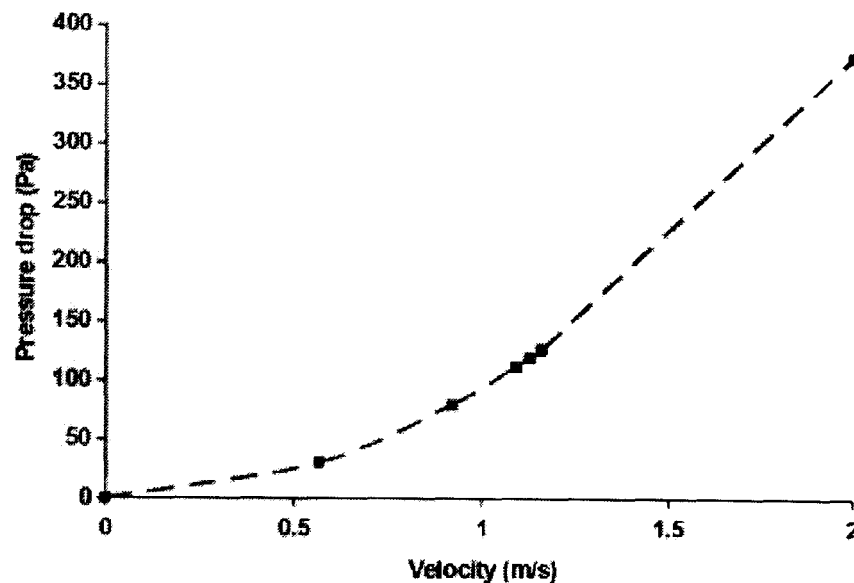


Figure 3.25 Pressure drop measurements (Source: Nasif et al. 2010)

3.5.6 Electrical consumption

Thermal energy recovered by using heat recovery systems is a crucial issue in building ventilation and this may result in a consumption of electrical energy (Kang et al. 2010). The electrical power necessary to overcome the pressure drop in a heat recovery system is defined as:

$$P_f = \frac{Q_a \Delta P}{\varepsilon_f} \quad (3.47)$$

The ratio between the heating load reduction due to mechanical ventilation with heat recovery and the electrical power consumed by the fans named electro-thermal amplification (ETA) was introduced by Manz et al. (2001). It is defined as:

$$ETA = \frac{Q_{h,0} - Q_h}{P_{el}} \quad (3.48)$$

3.6 Energy calculation

Jakisalo et al. (2003) stated that energy calculations are usually carried out with degree day method or using temperature differences based on hourly or monthly weather data. The use of degree day method is based on the fact that energy consumption of heating and ventilation is nearly proportional to the average temperature difference of indoor and outdoor air. Daily or hourly average values of outdoor temperatures are usually used for calculating heating degree days

$$S_{Ti} = \sum(T_R - \bar{T}_e)\Delta t \quad (3.49)$$

With the energy calculation by degree day method, ventilation heating energy consumption can be calculated as :

$$Q_{\text{vent}} = MCp(1-\varepsilon)t_{\text{op}}S_{Ti} \quad (3.50)$$

where, T_{op} = operating time of air handling unit per day, h/day. Degree day method do not distinguish day-time and night-time operation.

On the other hand, Soylemez (2000) has developed the formulation to calculate the amount of annual total energy saved by the heat recovery system as the following:

$$Q = \varepsilon(MCp)_{\text{min}}\Delta T_{\text{max}}\Delta t \quad (3.51)$$

The economics of the heat recovery application in terms of energy savings was discussed by Soylemez (2000) by introducing the formula combining effectiveness-NTU method with P_1 - P_2 method as:

$$S = P_1C_EQ - P_2C_AA \quad (3.52)$$

The net savings function can be interpreted as:

$$S = P_1 C_{EE} (\text{MCp})_{\min} \Delta T_{\max} \Delta t - P_2 C_{AA} \quad (3.53)$$

The net energy recovery savings with lifetime of the heat recovery system was presented in the study as shown in Figure 3.26 for three unmixed type of heat recovery core. The results indicated that the longer the lifetime, the more is the net energy savings.

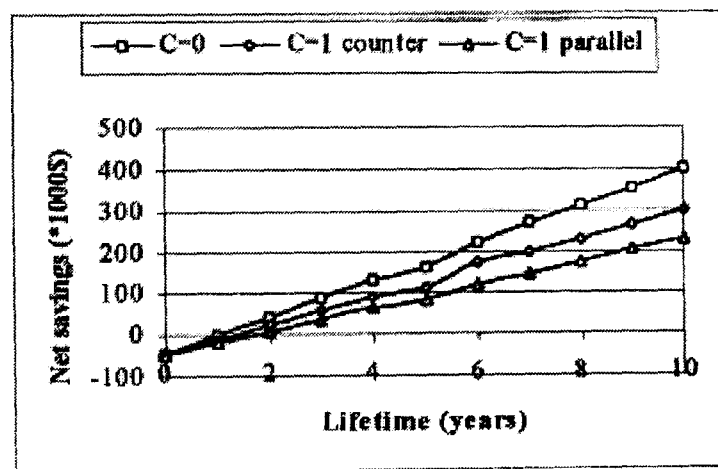


Figure 3.26 Effect of lifetime on net energy savings (Source: Soylemez 2000)

In another study, Roulet et al. (2001) have introduced a specific net saving energy (SNES) per cubic meter of outdoor air in and can be calculated by:

$$SNES = \frac{\rho \eta_G Q_{vent} + P_f (f_r - f_p)}{M_a} \quad (3.54)$$

where, f_r = factor relates to the part of the fan power recovered which is close for one for supply fans and zero for exhaust fans, f_p is production factor. The results data for their experiments is shown in Table 3.4.

Table 3.4 Results of SNES (Source: Roulet et al. 2001)

Outdoor air efficiency η_a , exfiltration and infiltration ratios γ_{ext} and γ_{int} , external and internal recirculation rates R_e , R_{ex} and R_{in} , heat recovery effectiveness ϵ_{HR} , global heat recovery efficiency η_G , specific net energy saving SNES in $W\ h/m^3$, and coefficient of performance COP, of audited air handling units.

Unit	η_a (%)	γ_{ext} (%)	γ_{int} (%)	R_e (%)	R_{ex} (%)	R_{in} (%)	η_a (%)	ϵ_{HR} (%)	η_G (%)	SNES	COP
B30	97	16	0	6	7	0	86	70	56	1.55	6.5
TP	92	47	9	20	5	0	59	70	39	1.35	8.0
BH	100	29	7	0	5	0	72	90	62	1.18	5.2
CS	68	77	76	55	1	0	31	30	9	-0.05	3.3
E1	98	8	17	0	7	0	92	80	69	1.92	6.7
E2	97	43	8	0	6	0	61	90	52	0.69	4.5
E12	100	14	0	4	2	0	87	80	68	1.45	5.5
E13	97	25	0	0	0	0	77	70	54	1.17	5.5
E14	95	97	49	0	0	0	10	50	5	-0.37	1.8
E15	93	91	18	100	6	0	18	50	8	-0.92	1.5
HA	74	8	0	0	33	0	94	63	40	1.37	6.2
HB	57	2	0	0	44	4	99	80	44	2.21	6.8
HC	68	0	0	0	39	25	100	90	55	2.69	8.2

By neglecting the heat storage effects in the building conservation, transmission and infiltration heat losses, solar gains and internal gains from people and appliances, Manz et al. (2001) have suggested the heating load reduction (energy savings) with heat recovery which can be calculated by:

$$Q_h = M_{Exh} C_p (T_{Exh} - T_{out}) - P_{el} \quad (3.55)$$

The efficiency of heating load reduction with heat recovery is defined as:

$$\eta_{heatingloadreduction} = \frac{Q_{h,0} - Q_h}{Q_{h,0}} \quad (3.56)$$

The annual energy consumption of an air conditioner coupled with enthalpy recovery was studied by Nasif et al. (2010) using modified HPRate software for Kuala Lumpur and Sydney cases. On the other hand, the annual energy consumption of the heat recovery was studied by Jakisalo et al. (2003) in mechanical ventilation of buildings apartment in Finland. The results showed that the efficiency of heat recovery has a significant effect on energy consumption.

3.7 Summary

To study the performance of heat recovery system either sensible or enthalpy, important parameters that should be emphasized are:

- Size, structure and material of heat exchanger,
- Size of ducts and fans
- Flow arrangement
- Heat and mass transfer
- Flow and pressure drop in the ducts
- Temperature and humidity
- Airflow rates

It was proven that the effectiveness of heat recovery increased as the area increased. Besides, the selection of fans should be considered since depending on the size of the fan, the size of duct in terms of diameter can be determined needed for this system for the case when the installation of the fans is in the ductwork. Usually, the air flowing in the ducts is turbulent. Besides, the duct structure and material will influence the flow distribution and are also substantial in order to minimize the heat loss from the duct system. Otherwise, the heat loss can reduce the total efficiency of the system significantly. In addition, material and structure of heat exchanger are the predominant factor the heat and mass transfer. Capillary forces or porosity and pore diameter of the materials play significant role in moisture transfer. Recently, membrane-based material is a new approach to heat/mass transfer in heat recovery whereas this material has the capability as an enthalpy recovery. It is believed that flow arrangements have direct impact on heat exchanger effectiveness. In addition, heat transfer efficiency is maximized if the two airstreams have opposite direction in

airflow arrangement. The effectiveness of these three flow arrangement, a counter-flow arrangement is the best.

Heat recovery efficiency can be determined by application of three suggested method as following:

- ASHRAE Standard method which can be defined in terms of sensible/temperature efficiency, latent efficiency and enthalpy (total) efficiency.
- Effectiveness-NTU method by which defined by the calculation of NTU and heat capacity ratio, C when flow arrangement is known.
- Global efficiency which takes into account the exfiltration and infiltration rate in ventilation system

In any heat recovery system, reducing airflow rates always increases efficiency. On the other hand, airflows have significant effects on the all types of heat recovery efficiency, pressure loss and transferred (recovered) heat/mass. For both sensible and total efficiency, the temperature of the inlet air appears to have minor influence in heat recovery system. However, the efficiency of heat recovery system in real situation varies with the temperature of supply and return air (temperature difference). In addition, the temperature change increases with increasing the inlet fresh air temperature. On the other hand, the economics of the heat recovery application in terms of energy savings can be calculated by several methods such as degree day method, net saving combination of P_1 - P_2 method, specific net energy saving (SNES) and heating/cooling load reduction method.

Thus, as a conclusion, the energy saving performance of the heat recovery is related to the ambient climatic condition in terms of temperature and relative humidity, effects of airflows, pressure drop and fan power. The larger the indoor-outdoor enthalpy (temperature and humidity) difference, or the higher efficiency, or the lower fan power, or the lower the airflow, or the larger the surface area, the more energy can be saved. However, it will also cost more in high level heat recovery type and high performance of fan. Thus, to improve saving performance, more efficient heat transfer materials and more efficient fans must be explored.

CHAPTER 4

Performance Investigation of an Individual Heat Recovery Unit

4.1 Introduction

In this chapter, triggered by good numerical results by various past researchers and the intention to understand the performance of various parameters of individual heat recovery system in recovering heat, a fixed-plate heat recovery unit has been experimentally investigated. The heat performance has been analysed based on the calculation analysis provided by literatures. The experimental tests were conducted on a cross-flow configuration heat recovery unit that utilises cellulose fibre papers (pads) as the heat transfer surface. An overview of the experimental techniques used to investigate the performance of heat recovery including the details of experimental set up, procedures and instrumentations used in a laboratory are presented and experimental results are outlined and discussed.

4.2 Description of the heat recovery core

The heat recovery core used in this investigation is called Micro Heat and Mass Cell Cycle Core (MHM3C) which has overall geometrical dimensions of 445mm height, 545mm width (w_1), 300mm width (w_2), 245mm (w_3) and 645mm length. In this 3C (cell, cycle, core) unit, on one side of the wall, there is one air stream which is stale air from the room, exchanging heat that circulate to the other side of the wall. On the other side of the partition wall, another stream which is fresh air from outside, will exchange heat from the opposite side of the wall as shown in Figure 4.1.

In each small triangular channel, the height of the triangle is 6.5mm. This MHM3C core has a diamond shape which is an enhanced version of the conventional fixed-plated sensible heat recovery core and has the ability to overcome the disadvantages of the rotary wheel heat recovery. It is worth mentioning that the core was built in China.

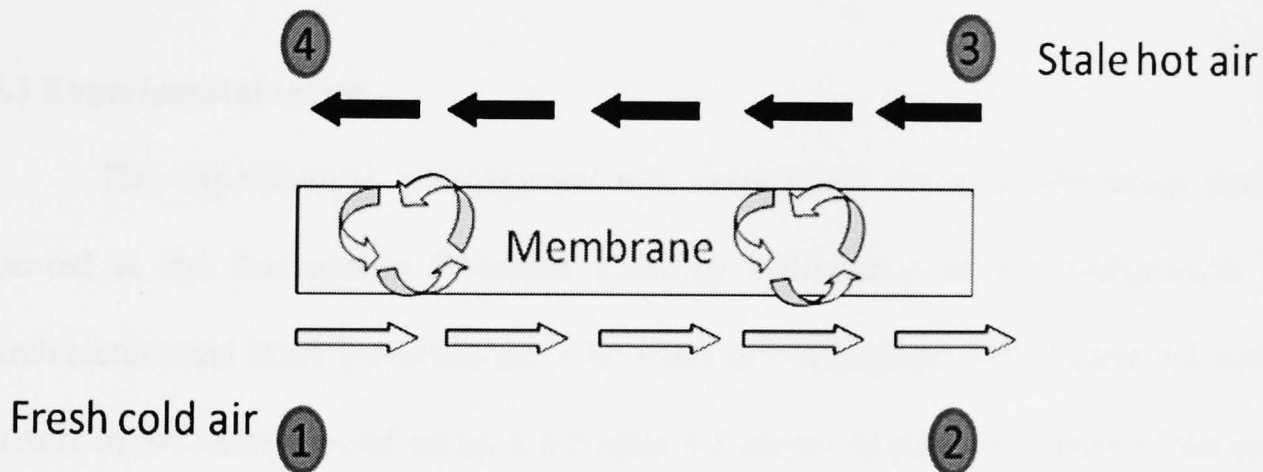
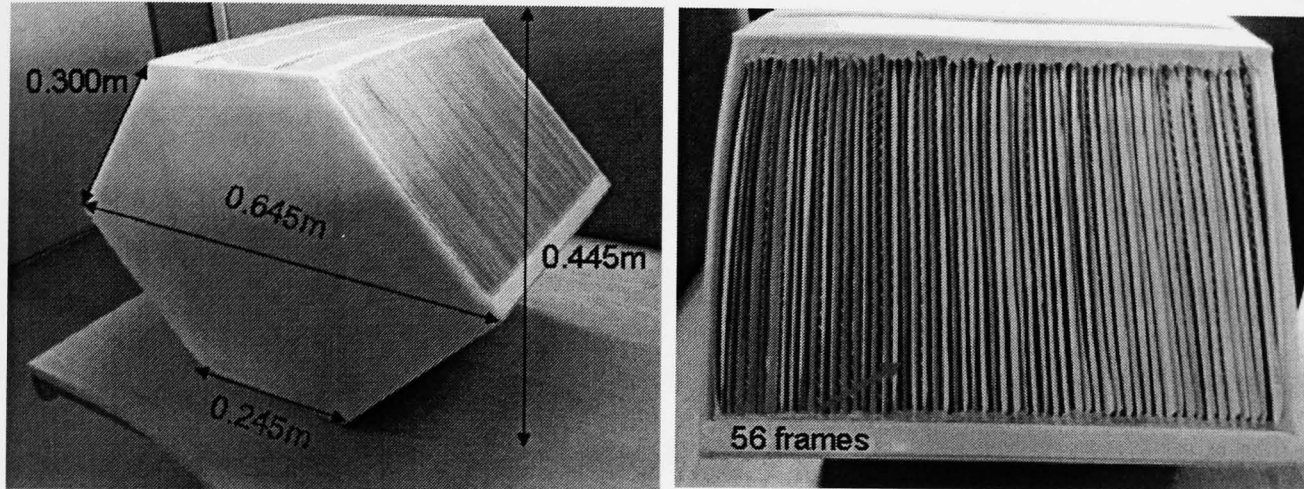


Figure 4.1 MHM3C core

The heat transfer surface of this MHM3C core is made of cellulose fibre papers (pads) that allow heat to be transferred with 0.198m^2 of heat transfer surface area. Hence, sensible heat or energy is recovered. The papers are separated by thin plastic sheets and impregnated with unique ingredients and additives to achieve high performance and structural strength. The pads were assembled together in a special way of cross-flow arrangement consist of 56 frames with 28 air channels so that the

inlet air is divided into two streams. The waveform stand or plate-fin supports two pieces of fibre paper to divide each air tunnel into a large number of small triangular channels. The thickness of the cellulose fibre papers is 0.5mm. As stated by the manufacturer, the special way of cross-flow design of the diamond shape could optimize the amount of surface area to hold the heat which the air flows over because of the number of fibre paper used. Besides, the angles in this configuration cause the air to change direction in a way that ensures sufficient air comes in contact with the heat transfer surface before leaving the core. Thus, the air exits the core with the maximum amount of recovered energy. This MHM3C core also has the ability to improve indoor air quality as well as recovering operating cost as the media acts as a self-cleaning air filter that purifies the supply air.

4.3 Experimental set up

The experimental investigation was carried out using a laboratory model located at the Sustainable Research Building Laboratory of the Department of Architecture and Built Environment, University of Nottingham, UK. Figure 4.2 is the picture of the experimental set up and Figure 4.3 shows its schematic view of the heat recovery system. The system includes a test room of 2m x 2m. The test room was made of plywood and there was 50mm layer of expanded polystyrene insulation on the interior of the chamber to reduce the influence of surroundings. A heat recovery unit was housed on top of the test room and consists of two separate air ducts (supply and exhaust). The heat recovery unit was sealed by wooden boxes from the top to the bottom. Insulations were attached on the inside surfaces of the boxes to keep the temperature and humidity uniform and steady. The ducts walls are made of 25mm

thick polystyrene sandwich panels with thin steel sheet and have a diameter of 100mm.

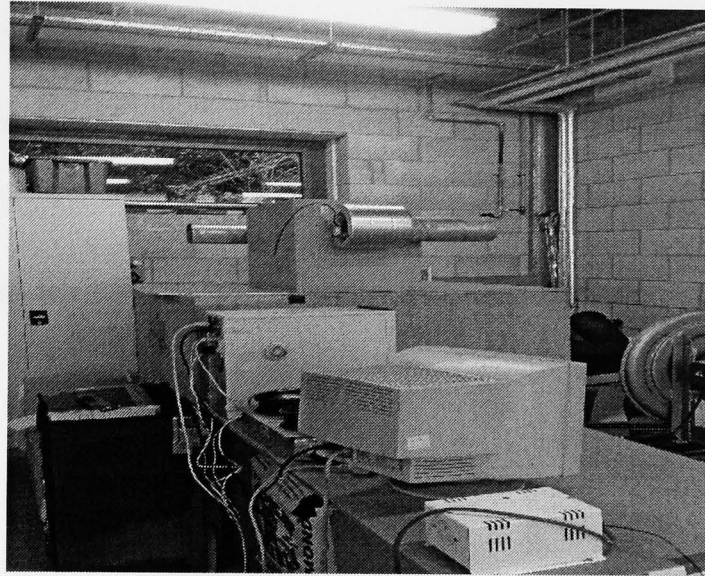


Figure 4.2 Laboratory experimental rig

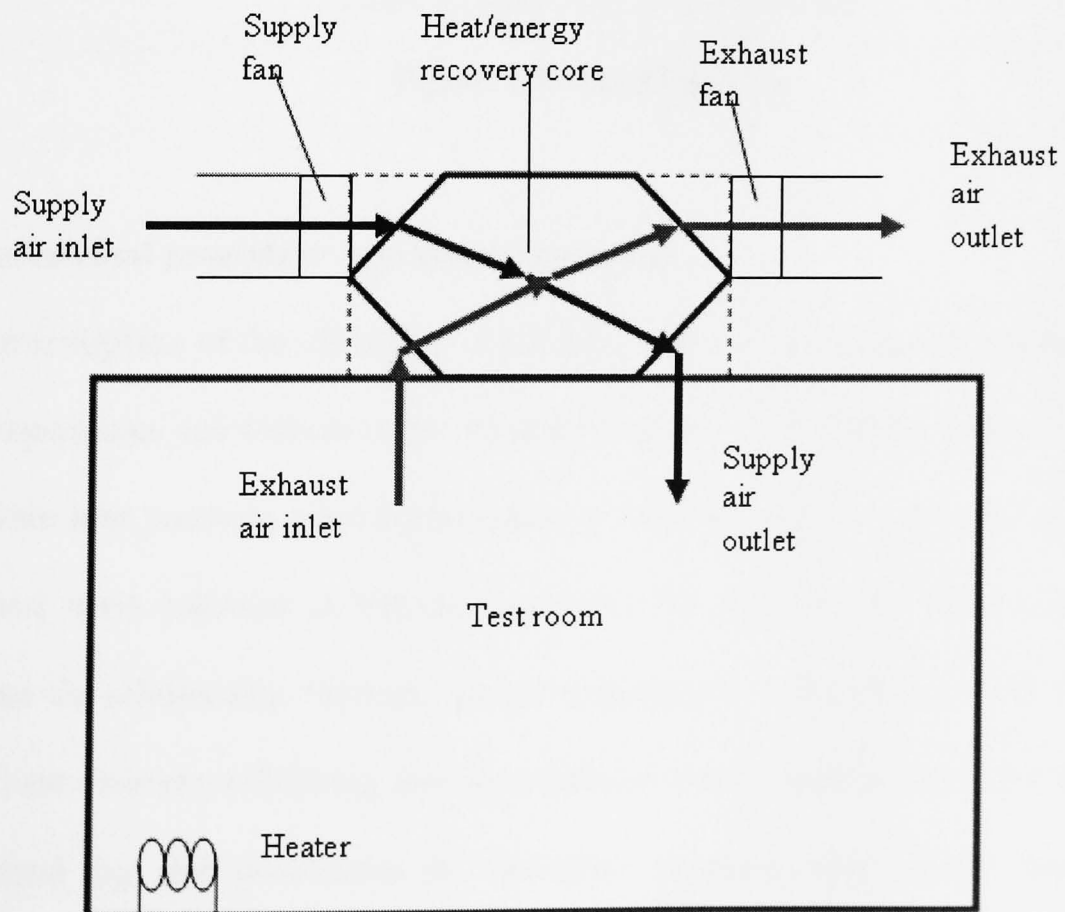


Figure 4.3 Schematic view of experimental set up

Two 2kW centrifugal fans were installed in supply and exhaust ducts to assist airflow and to distribute the air through the heat recovery unit and the duct (Figure 4.4). The supply fan pulls the air coming through the supply duct and the heat recovery core into the test room. The exhaust fan pulls the air and blows it out from the system through the exhaust duct. In order to test the performance of the heat recovery unit at different airflows, two speed controllers were connected to the fans. A heater of 2kW was placed to simulate heat production in the test room.

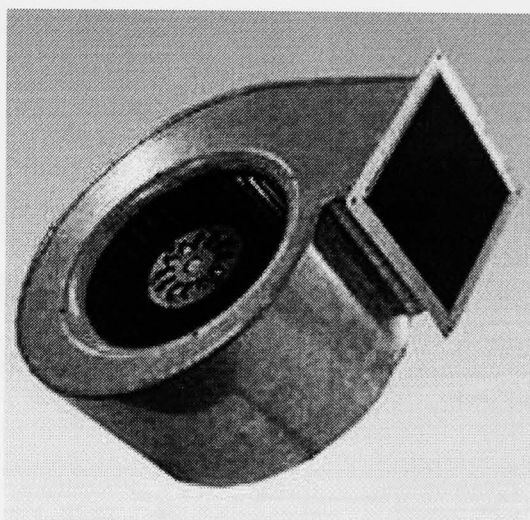


Figure 4.4 Centrifugal fan

4.4 Experimental procedure and instrumentation

Investigation of the efficiency of the heat recovery unit requires measurement of air temperatures and airflow rates. As stated by Fisk et al. (1985), measurement of the sensible heat recovery core performance is difficult, due to the need to achieve energy and mass balances in the measurements. In order to get reliable data and investigate the relationship between the air temperature, humidity and airflow speed with the heat recovery efficiency, two air condition control systems were set up in the experimental rig and procedures as described in sub-section below have been conducted. Measurement for sensible efficiency was carried out under different air velocities ranged from 1 to 3m/s.

Temperature measurements were carried out at different points across the experimental rig. Velocity measurements were conducted in the supply and exhaust duct at the same position of temperature measurements. First, the experimental rig was operated until the setting conditions were maintained to ensure consistent conditions throughout the laboratory experimental measurement system. The fans were switched ON and the fan speeds were adjusted in order to obtain equal airflow rate in both streams. Power was then supplied to the heater and the test room was heated. The experimental rig was allowed to come to steady state condition which was established after about 30 minutes. Measurements were taken after the system reached steady state conditions. Air temperature values outside the test room, inside the test room and in the inlet and outlet streams were measured.

4.4.1 Data acquisition

The data logger used was a dataTaker (DT500 series) as shown in Figure 4.5. It was used as an interface between a personal computer and the temperature sensors. It is an instrument that acquires data from the thermocouples and transfers the data via a serial link to a control programme in the PC which it records the data using “DeLogger™ 4 Pro software an enhanced graphical package that allows reporting to a data base and also offers remote dataTaker management features. The data-logging equipment used for the data collection and storage is shown in Figure 4.6. Data collection through data-logging was carried out and the results were analysed to evaluate the heat recovery performance. The data was collected over a period of 2 hours for each test.



Figure 4.5 DataTaker

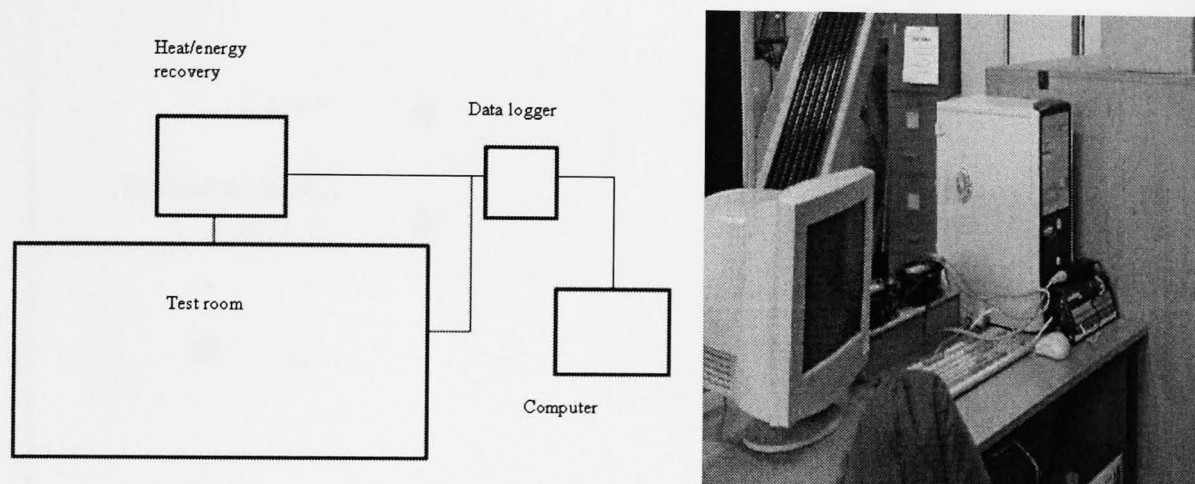


Figure 4.6 Data-logging equipments

4.4.2 Temperature measurement

Temperature measurements were taken using K-type thermocouples (22 points) which were calibrated with the accuracy within 0.1°C . Figure 4.7 shows the positions of thermocouples in the experimental rig. The temperature measurement system consisted of:

- four points of thermocouples in the supply air in side, $T_{s \text{ in}}$ (1,2,3,4)
- four points of thermocouples in the supply air out side, $T_{s \text{ out}}$ (5,6,7,8)
- four points of thermocouples in the exhaust air in side, $T_{e \text{ in}}$ (9,10,11,12)
- four points of thermocouples in the exhaust air out side, $T_{e \text{ out}}$ (13,14,15,16)
- four points of thermocouples in the test room, T_{room} (17,18,19,20)

- two points of thermocouples of ambient air, T_{ambient} (21,22)

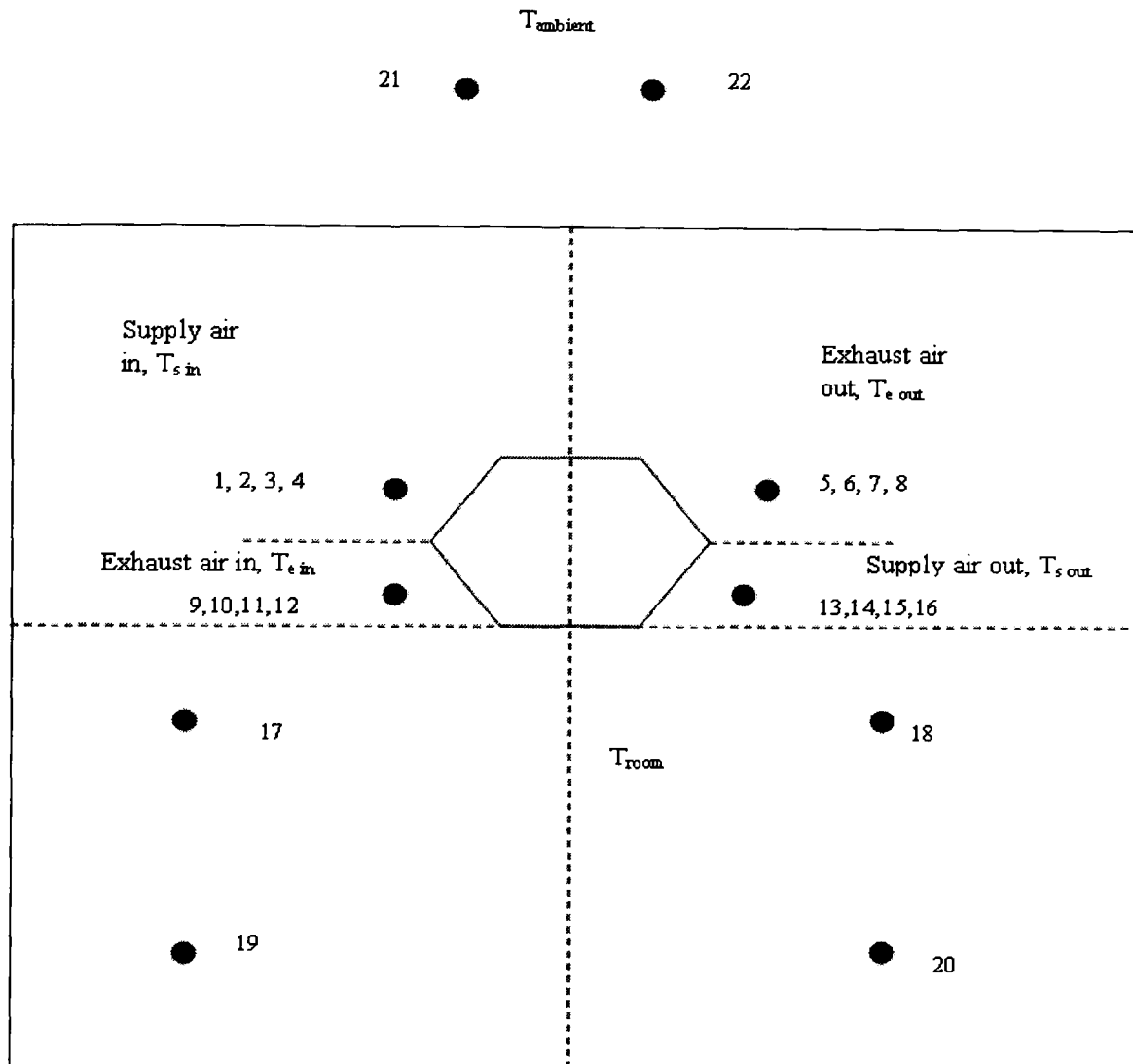


Figure 4.7 Positions of thermocouples in the experimental rig

4.4.3 Airflow measurement

Efficiency of a heat recovery is usually defined with respect to balanced airflows (the rate of exhaust air is the same as the rate of supply air) as shown in Figure 4.8. Investigation of the performance of a heat recovery unit can be studied by a simple mass and energy balance.

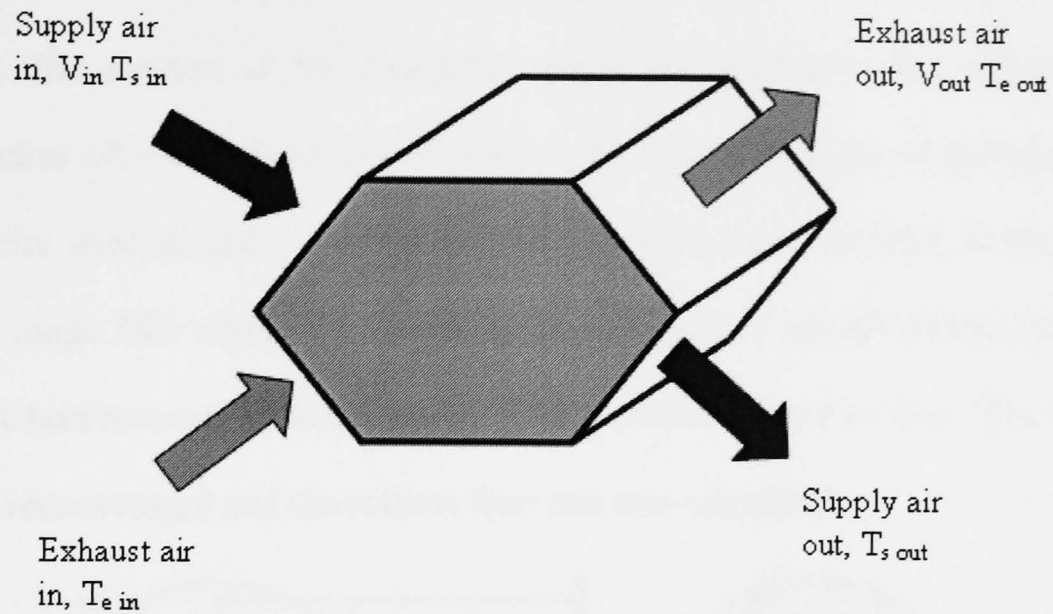


Figure 4.8 Airflow through heat recovery core

In order to determine the airflow measurements, a hand-held hot wire anemometer with an accuracy of 0.03m/s as shown in Figure 4.9 was used to measure the velocity of the air stream at the inlet and outlet at the same locations as the temperature measurements.



Figure 4.9 Hot wire anemometer

In order to obtain accurate air velocity in the ducts, log-Tchebycheff method was used. The position of the measuring points corresponds to the values of the relative radius r/R_j or of the relative distance to the wall y/D as shown in Figure 4.10. The velocity used in this measurement was ranged from 1 to 3m/s which is this operating range falls within the operating range specified by ASHRAE (2000) for fixed plate heat recovery/exchanger system which varies from 1 to 5m/s. The velocity readings were averaged and the volume flow rate was calculated.

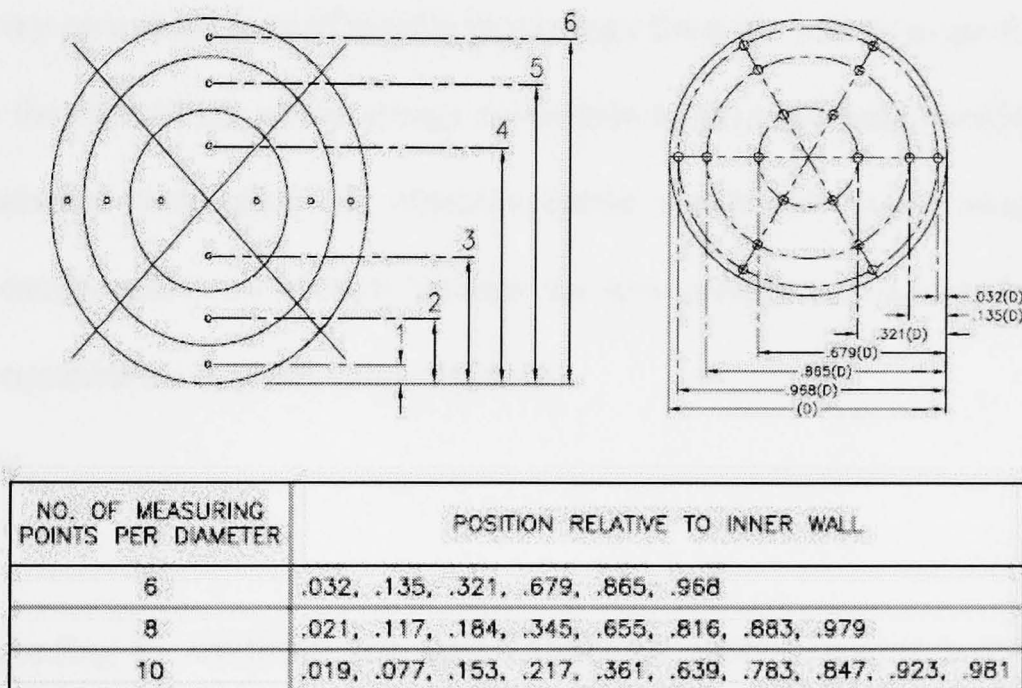


Figure 4.10 Measuring points for circular duct

4.4.4 Pressure measurement

The static pressure difference was measured between the supply air stream to the heat recovery unit and the ambient using a differential pressure meter connected with a pitot-tube for variations in supply airflow.

4.5 Performance Calculation Model

Performance in terms of heat recovery unit can be studied by a simple mass and energy balance when there is no leakage airflow between supply and exhaust air streams.

4.5.1 Efficiency

Efficiency is a dimensionless parameter which quantifies how efficient the heat recovery core is in terms of transferring energy from one stream to another and is defined as the ratio of the actual energy transferred to the maximum possible energy transfer between airstreams. To obtain accurate results for every measurement recorded, energy and mass balance between the two streams was achieved as in the following equation for sensible energy balance.

$$M_s = M_e \quad (4.1)$$

According to ASHRAE Standard (ASHRAE 1999), sensible heat recovery efficiency or temperature efficiency is expressed by the temperature change of supply air to the temperature difference of the exhaust air and thus calculated by the following equation

$$\varepsilon_s = \frac{T_{sout} - T_{sin}}{T_{ein} - T_{sin}} \quad (4.2)$$

4.5.2 Recovered/Transferred energy

Sensible heat recovered or transferred when heat transfer through a casing by air leaks and heat conduction is not taken into account is shown by the following expression

$$q_s = M_a C p_a \Delta T \quad (4.3)$$

$$q_s = M_a C p_a (T_{ein} - T_{eout}) \quad (4.4)$$

4.6 Test results and performance analysis

The tests were conducted for the heat recovery performance comprising a cross-flow MHM3C core which also called as enthalpy core by measuring temperature and airflow rate at the supply and exhaust streams at steady state conditions. Based on the measurements results, the following parameters were calculated using appropriate theoretical expressions as described in Chapter 3.

- Temperature change
- Efficiency
- Recovered/transferred energy
- Pressure drop

4.6.1 Temperature data

The tests were carried out at ambient temperature of between 23 to 24°C and test room temperature at 30°C. Table 4.1 shows the temperature measurements data.

Table 4.1 Temperature measurements data

Velocity m/s	Q l/s	M kg/s	T _{ambient} °C	T _{s in} °C	T _{s out} °C	T _{e in} °C	T _{e out} °C
1.0	7.90	0.010	23.8	23.5	26.4	27.9	25.0
1.5	11.8	0.015	23.7	23.5	26.7	28.6	25.6
2.0	15.7	0.020	24.0	23.8	27.5	30.0	26.4
2.5	19.6	0.026	23.9	23.5	27.5	31.0	27.1
3.0	23.6	0.031	24.2	23.4	27.6	32.0	28.1

The temperature change (ΔT) which is $T_{s\ in} - T_{s\ out}$ across the heat recovery unit was recorded. The temperature change presenting the change between exhaust air in and exhaust air out. From the temperature measurement, it denotes that the temperature change increases with increasing air velocity. For air velocity of 3.0m/s, a change of 4.3°C was recorded which the highest value corresponding to the highest air velocity.

4.6.2 Heat recovery efficiency

Tests were carried out to investigate the effect of the airflow rate on the efficiency under balanced airflow rate. The airflow rates for this investigation was ranged from 0.010 to 0.031kg/s which equivalent to 1 to 3m/s. The intake air (outdoor air) temperature was keeping unchanged at 23°C, the room temperature was 30°C. The efficiency of the cross-flow heat recovery is evaluated using Equations 4.2 based on the measurements data. Table 4.2 summarized the results of the calculation for the air velocities tested.

Table 4.2 Efficiency calculation results

Velocity	Sensible efficiency
1.0	65.9
1.5	62.8
2.0	59.6
2.5	53.3
3.0	47.8

4.6.2.1 Effects of airflow rates

Figure 4.11 shows the variation of the efficiency of the cross-flow heat recovery with air velocity in the duct. It can be seen that the air velocity or airflow rate of air has a big impact on the efficiency. The efficiency ranged from 48% at air velocity of 3.0m/s to 66% at 1.0m/s. It can be seen that the efficiency decreases with increasing velocity, which is due to the amount of residence time within the heat recovery core.

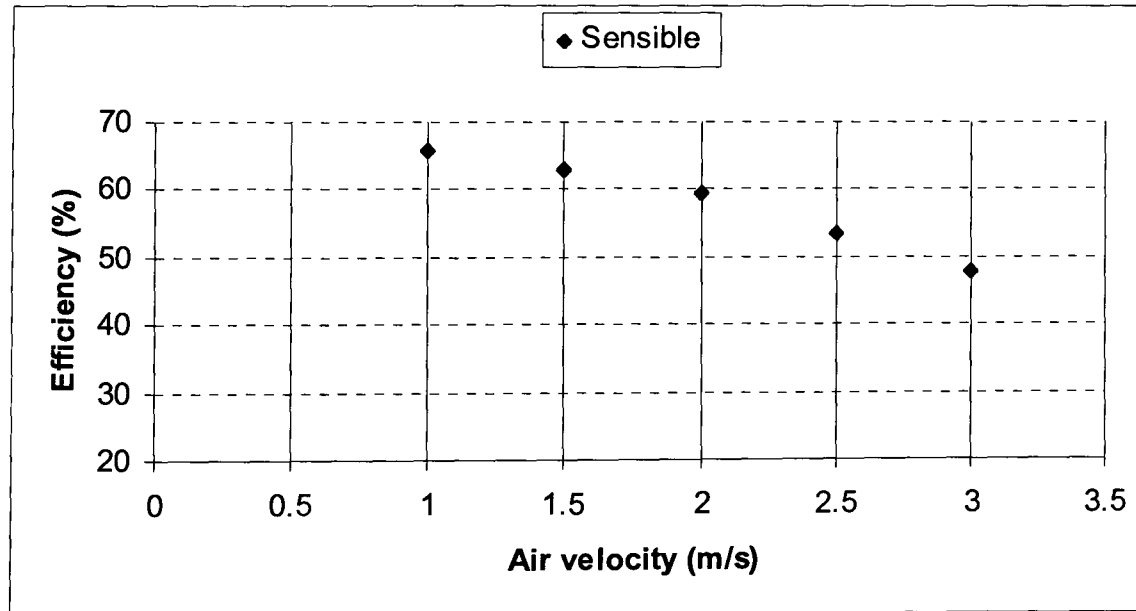


Figure 4.11 Variation of the efficiency of the cross-flow heat recovery with air velocity

For this range of air velocities, the larger the residence time, the higher the efficiency. Thus, the air velocity has a significant effect on the efficiency of heat

recovery unit. The relationship between the efficiency and air velocity in this experiment can be expressed by the following correlations for the velocity tested:

$$\varepsilon_s = 2.26V^2 - 0.11V + 68.26 \quad (4.5)$$

4.6.2.2 Effects of supply air inlet temperature

The effects of the supply air inlet temperature on the efficiency are analysed in this investigation. The experiments were conducted with supply air inlet temperature ranging from 24 to 30 °C, room temperature at 20°C and air velocity constant at 1.0m/s. The efficiency remained at 65.7%. This shows that the efficiency of this heat recovery has not affected by changing the supply air in temperature.

4.6.3 Recovered/Transferred energy

Recovered or transferred energy is the amount of energy needed to cool or heat the air. It is the transition of thermal energy or simply heat between the heat transfer surface and air at different temperature. Figure 4.12 shows variation of sensible energy recovered with different values of air velocities ranging from 1.0 to 3.0m/s. The trend shows that the sensible energy recovered increases linearly with increasing air velocity due to the enhancement of heat transfer. The following trend correlation is presented by:

$$q_s = 6.76V + 27.99 \quad (4.6)$$

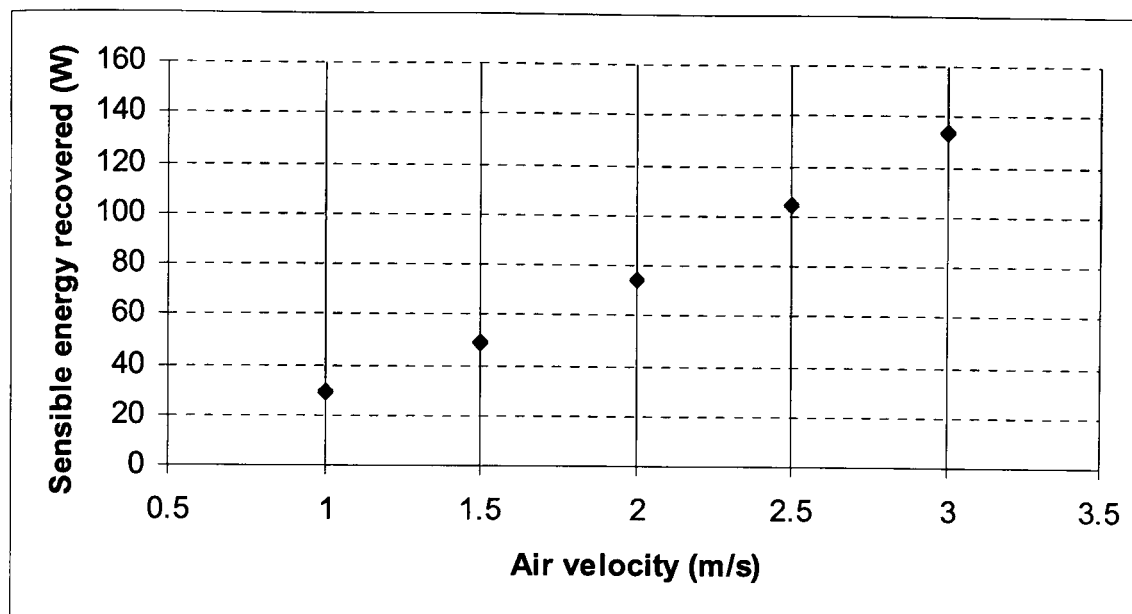


Figure 4.12 Variation of sensible energy recovered with air velocity

Figure 4.13 shows the impact of temperature change to the sensible energy recovered. Maximum sensible energy recovered of 134W was calculated at 4.3°C temperature change across the heat recovery unit at 3.0m/s air velocity. This is due to the air has more residence time in heat recovery core and more heat transfer takes place and thus more heat can be recovered with higher temperature change.

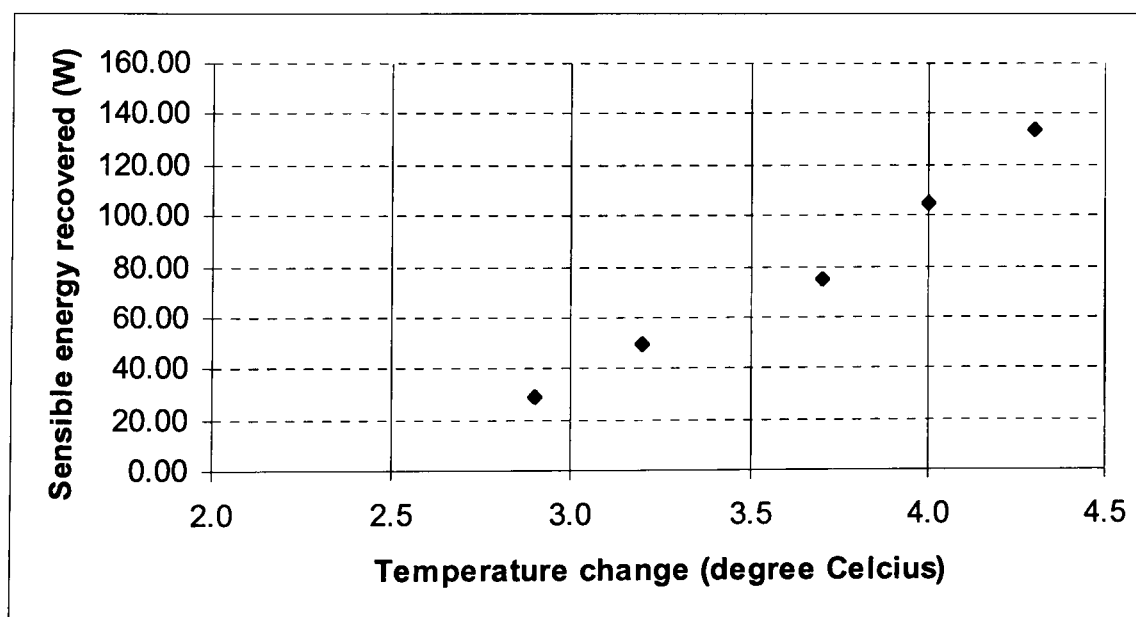


Figure 4.13 Impact of temperature change to the sensible energy recovered

4.6.4 Pressure drop (ΔP)

Experimental measurements of static pressure drop between the supply air stream to the heat recovery unit and the ambient were also carried out and the results are shown in Figure 4.14. It can be seen that, at air velocity 1.0m/s, the pressure drop was 8Pa which is response to the lowest air velocity tested, and 30Pa of pressure drop was observed at 3.0m/s. Thus, it denotes that pressure drop of between the supply air stream to the heat recovery unit and the ambient increases with increasing air velocity in the duct. As the velocity increases, the pressure increases with increasing rate.

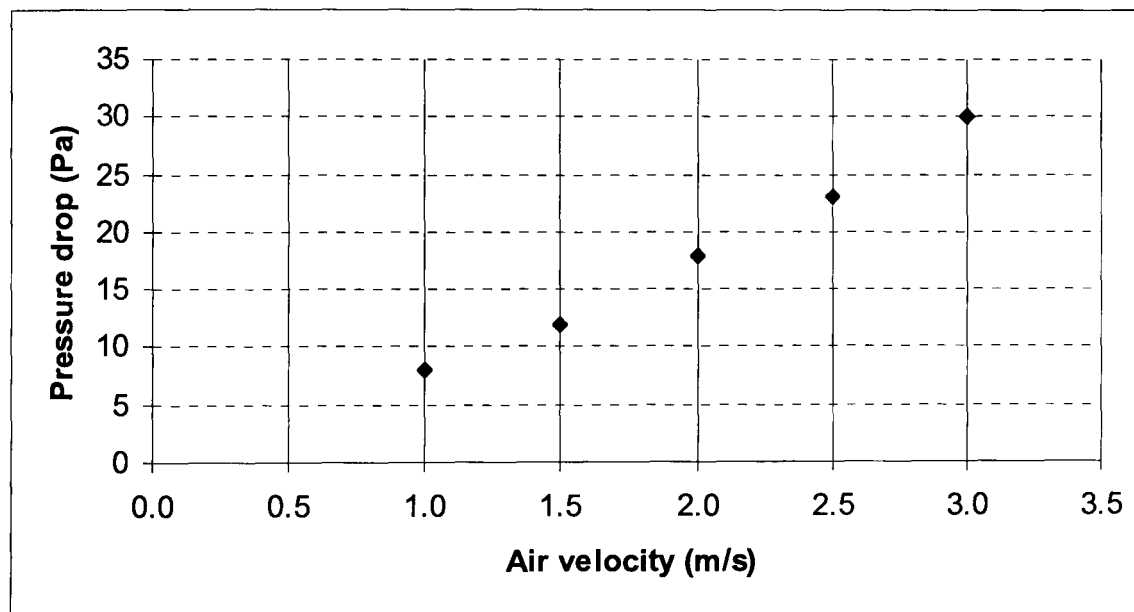


Figure 4.14 Pressure drop between the supply air stream to the heat recovery unit and the ambient

The pressure drop through the duct is also investigated for the velocity ranged from 1.0 to 3.0m/s where the duct has 100mm diameter. Pressure drop through the duct is presented by the pressure loss coefficient or f factor as follows:

$$f = \Delta P 2D / V^2 f L \rho \quad (4.7)$$

Figure 4.15 shows the pressure drop coefficient through the duct. It can be seen that the pressure drop coefficient decreases with increasing air velocity in the duct. The overall reduction is around 7 to 8 % for the velocity range.

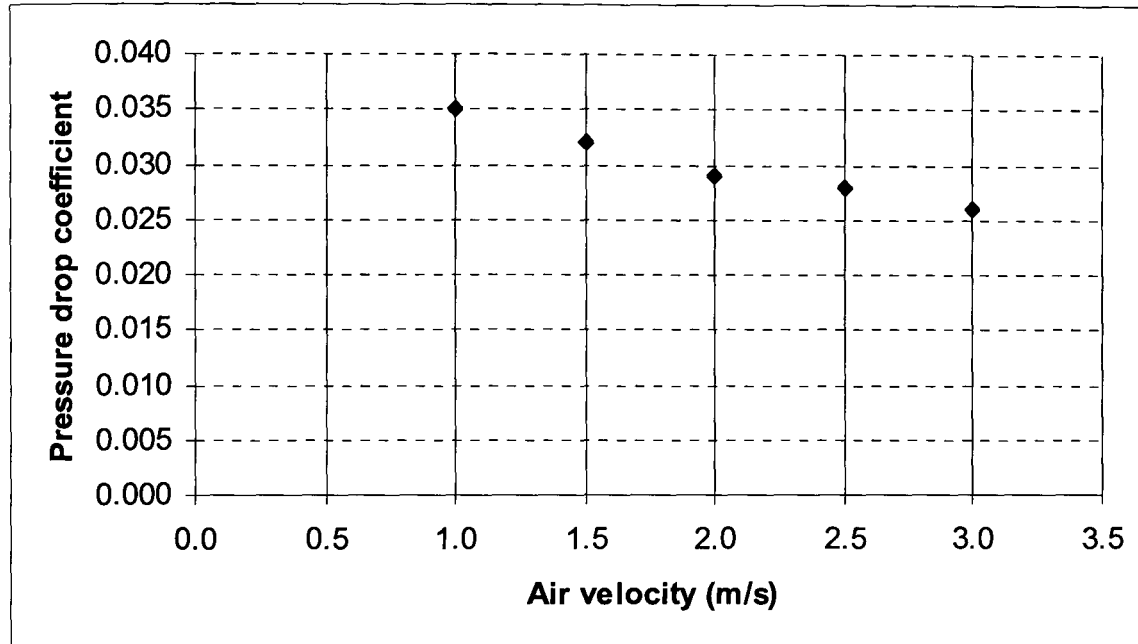


Figure 4.15 Pressure loss coefficient in the duct

Figure 4.16 shows the pressure drop through the duct. The increasing trend in pressure drop with increasing velocity can be seen and it was found that at highest velocity of 3.0m/s, pressure drop of 0.26 Pa occurred. This is due to the increasing of Reynolds number, $Re > 2300$ as the airflow increases.

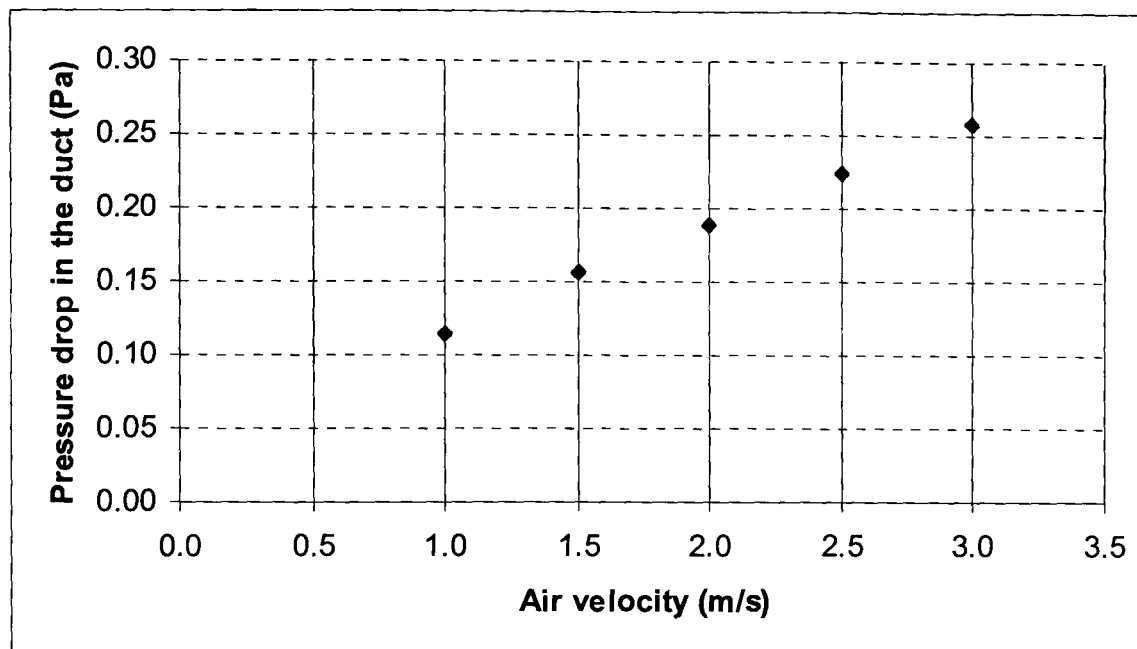


Figure 4.16 Pressure drop in the duct against velocity

4.7 Summary

This chapter discussed experimental work on heat recovery performance of a cross-flow MHM3C. The unit was classified according to the way installed in a laboratory model. The unit was tested in an environmental control chamber for two different conditions; varying airflow rate and constant airflow but varying supply air in temperature. The data recorded was then analysed and the major results are summarized as follows:

- As the airflow rate and temperature change increase, the efficiency decreases and recovered energy increases.
- At air velocities ranged from 1.0 to 3.0m/s, the efficiency ranged from 66 to 48%,
- Increasing the airflow rate from 0.010 to 0.031kg/s results in a decrease of 18.1% in the efficiency.
- Maximum recovered energy of 134W for sensible energy was calculated at 3.0m/s air velocity.

- Temperature change ranged from 2.9 to 4.3°C was observed for the air velocities tested.
- This system is a static device which can achieve high efficiency, easy to maintain and cheap.
- The experimental analysis presented in this chapter provides a guide in the improvements and applications of heat recovery unit using paper sheet as the heat transfer surface in order to fulfil energy-efficient technology demands.

CHAPTER 5

Integrated Heat Recovery System Associated with Wind-catcher and Evaporative Cooling

5.1 Introduction

Increased global warming and deterioration of the ozone layer have stimulated interest in the use of low carbon technologies. Today's high cost of energy together with its environmental impact are reasons enough to warrant a reduction in energy consumption in current air conditioning systems or those at design stage. Wind-catcher is increasingly being employed in modern buildings to release the harmful emissions to the environment. However, most of ventilation system contributes to energy loss. On the other hand, frequent summer warm spells, improved insulation of buildings and growth of indoor facilities have lead to an increased requirement for air conditioning of the indoor environment. The conventional mechanical compression air conditioning systems consume huge amount of electrical energy that is largely dependent upon fossil fuel. This mode of air conditioning is therefore, neither sustainable nor environmental friendly. In order to overcome this problem, evaporative cooling system has been introduced in decades ago. Evaporative cooling utilise the latent heat of water evaporation to perfume air conditioning of buildings and is therefore a potential replacement of existing systems. In this chapter, experimental investigations on integrated heat recovery system with combined wind-catcher and evaporative cooling were carried out. The desire is to have an integrated system operating at low energy with use of energy-efficient technology based on new materials and methods. The chapter presents the system description, experimental installation and the results gained for the integrated system.

5.2 System description

The major materials used in these investigations are the wind-catcher unit, heat recovery unit and indirect evaporative cooling unit and are described in the following section.

5.2.1 Wind-catcher unit

Wind-catchers as proved by literatures have been used for centuries in the hot arid regions especially Middle East to create natural ventilation in buildings or passive cooling and hence thermal comfort. Wind-catcher can capture the wind at roof level and direct it down to the rest of the building (Khan et al. 2008). There are a lot of research works involving wind-catcher in literatures (Elmualim 2006; Montazeri and Azizian 2008; Montazeri et al. 2010; Jones and Kirby 2009; Su et al. 2008). For this research, a square MonodraughtTM wind-catcher with a size of 600mm x 600mm and a length of 1500mm was used as shown in Figure 5.1. The square wind-catcher was divided into four equal quadrants each with an area of 0.06m². The quadrants ran the full length of the wind-catcher. Each quadrant comes with 10 weatherproof louvers.

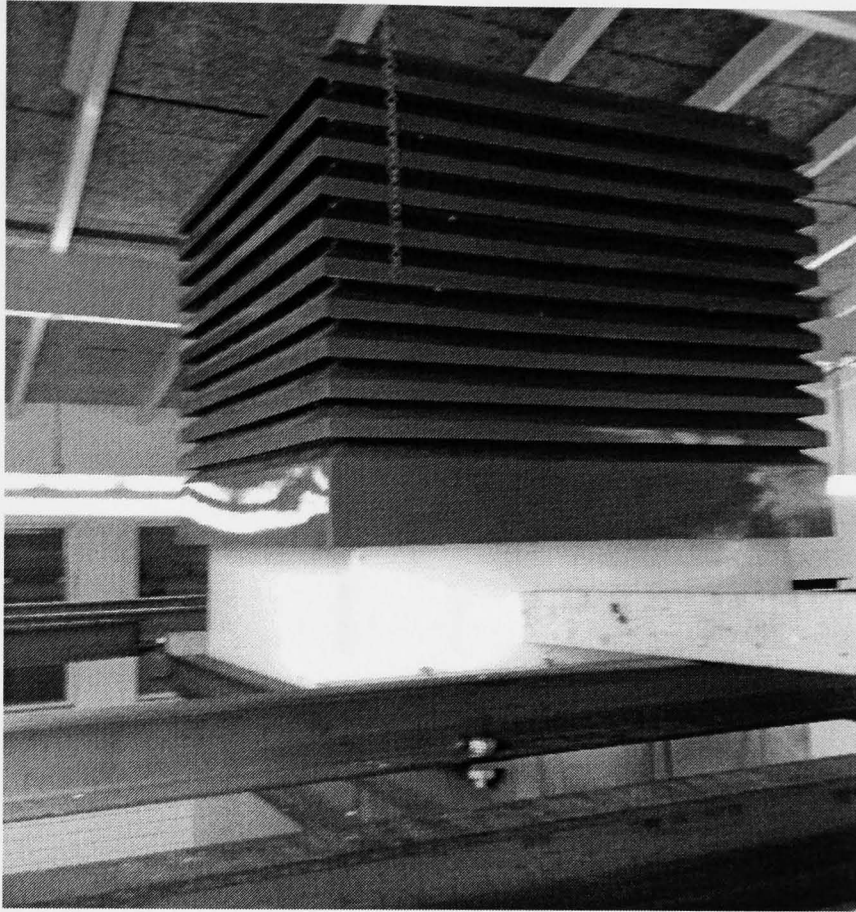


Figure 5.1 A square Monodraught™ wind-catcher

The wind-catcher's design combines the two ventilation principles of wind tower and passive stack into one design around a stack that is divided into four quadrants acting as supply or extract for the air with the division running the full length of the stack. The unit captures the wind at roof or top level and direct it down to the building to provide ventilation. Figure 5.2 shows the operational principle of ventilation mode of wind-catcher in this system. Fresh air is drawn in at the windward side and is directed into the building interior. Stale air is extracted at the leeward side. The differential air temperature and hence pressure inside and outside the building force warmer air to rise and exit through the extract quadrants or passive stack. The system is divided into four quadrants which run the full length of the body and become air intakes or extractors depending on wind direction thus making the wind-

catcher system less vulnerable to periodic wind changes and negating the need for any possible rotation to face the wind.

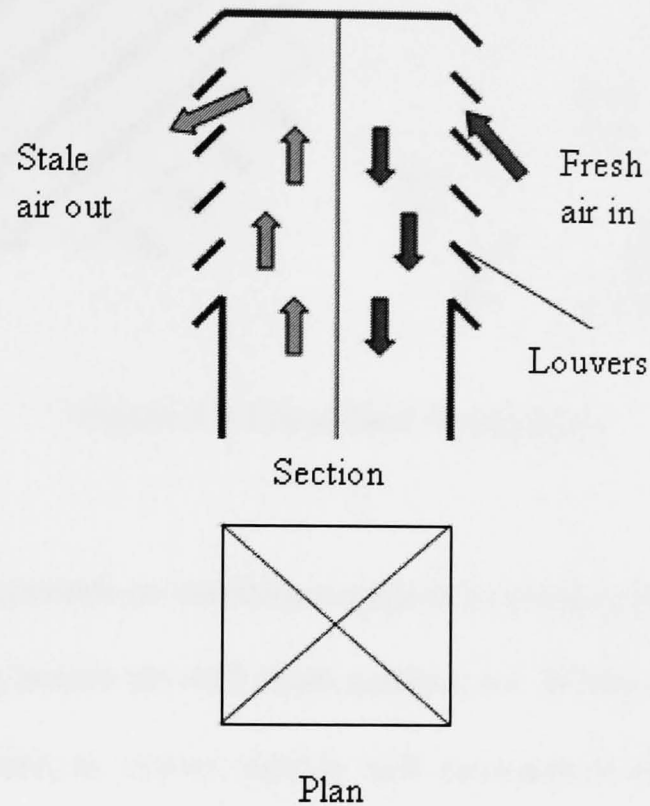


Figure 5.2 Operational principle of ventilation mode of wind-catcher in this system

5.2.2 Heat recovery unit

Heat recovery unit in this system is utilized to recover a fraction of the energy loss. Besides offering energy saving, this unit also gives some advantages such as, reduces heat loss rather than create heat which is relatively to cost effective. In this system, heat recovery unit used is a cross-flow fixed-plate type which has a dimension of 600mm x 600mm x 300mm and made up of 21 polycarbonate plastic frame flow-channels with 20 air passage as shown in Figure 5.3.

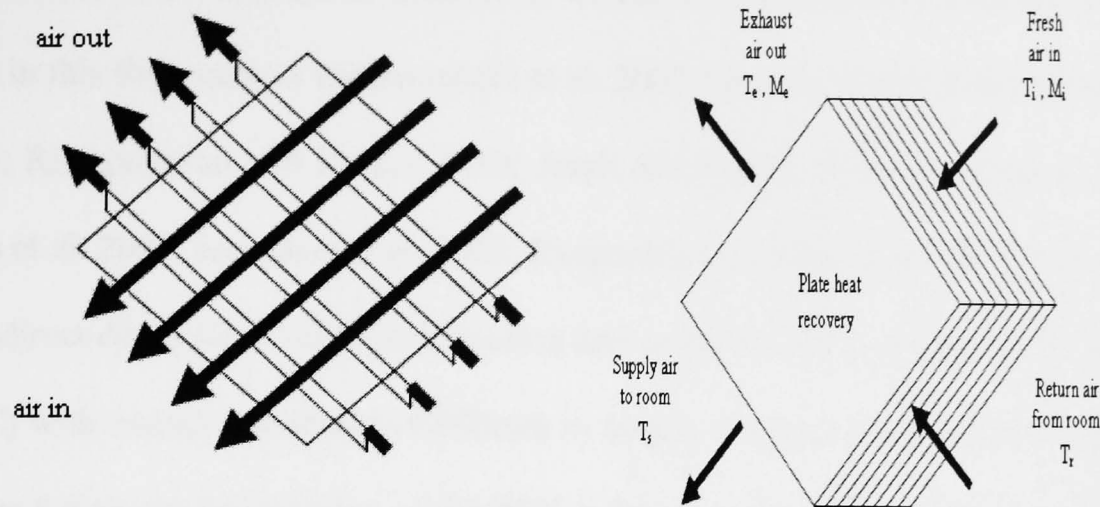


Figure 5.3 Cross-flow fixed-plates

In hot air, it operates as ventilation system by passing the heat transfer system and simply replacing indoor air with fresh outdoor air. Whilst, during cold air, it can reduce indoor moisture, as cooler outside will have lower relative humidity. Heat recovery unit in this investigation consists of ducts built in wind-catcher unit for incoming fresh air and outgoing stale air, a heat exchanger core, where heat or energy is transferred from one stream to the other and two blower fans; one is to exhaust stale air and supply fresh air via the heat exchanger core. In the core, the fresh air stream is automatically preheated or pre-cooled (depending on the season) by the exhausted air and distributed to the interior part of the building. The outgoing and incoming air passes next to each other but do not mix in the heat exchanger core.

5.2.3 Evaporative cooling unit

Evaporative cooling has long been recognised as the most efficient ecological and safe method that can be cheaply exploited. By definition evaporative cooling is the exchange of sensible heat in air for the latent heat of vaporisation of water droplets on wetted surfaces. Two common types of evaporative cooling system are

direct and indirect system. In literatures, we can found a massive of works have been done in this field such as Hettiarachchi et al. 2007; Qiu and Riffat 2006; Johnson et al. 2003; Riangvilaikul and Kumar 2010; Joudi and Mehdi 2000; Martinez et al. 2003; Zhao et al. 2009; and Zhao et al. 2008. Evaporative cooling unit used in this system is an indirect dew point evaporative cooling unit consists of Psychrometric Energy Core (PEC) with overall dimension of 850mm in length, 400mm in width and 260 in depth. Figure 5.4 shows the diagram of the PEC indirect evaporative cooling unit. This PEC core is made of corrugated cellulose paper impregnated with wetting agents. Polygonal sheets were stacked to form channels and to provide counter flow heat exchange between two adjacent sheets. A water proof coating was applied to one side of the polygonal sheets to prevent water penetration. Two adjacent channels provide a dry side and wet side for airflow. In this system, intake air is brought into the dry channels from the lower part of the right-hand side of the stack. The air flows through the channels and is divided into two parts at the opposite end of the channels. One part of the air stream moves in the same direction and is delivered to the space where cooling is required, whilst the other part of the air stream is diverted into the adjacent wet channels where the surfaces are wetted by water. The wet channels allow heat to be absorbed through the channel walls by vaporising the water on the surfaces. The air in the wet channels flows in a reverse direction and is finally discharged to atmosphere from the upper part of the right side of the stack. In this design, the dry channels contain both product and working air and the wet channels take only working air. Because of the heat transfer between the dry-channels and their adjacent wet-channels, the product air in the dry channels will be cooled and the working air in the wet channels will be humidified and heated.

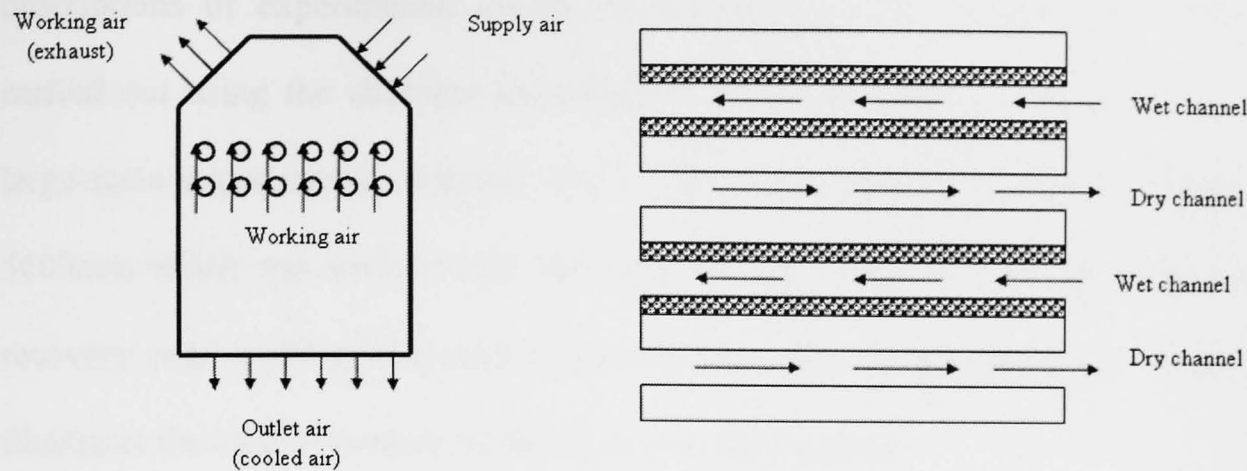


Figure 5.4 Working process of the PEC indirect evaporative cooling unit

5.2.4 Capital cost of the system

The capital cost involves in the construction of integrated heat recovery with wind-catcher and evaporative cooling are details in the following:

Wind-catcher unit	= £3300
Heat recovery unit	= £100
Evaporative cooling unit	= £320
Sum	= £3720

The capital cost of the integrated heat recovery associated with wind-catcher and evaporative cooling system is quite expensive about £3720 since it is employing a big size of wind-catcher unit. However, this system could be installed in high buildings and for long term it will benefit the buildings in terms of energy saving.

5.3 Experimental installation

The experimental investigation was carried out using a large-scale laboratory model located at the Energy Learning Laboratory of the Department of Architecture and Built Environment, University of Nottingham, UK. This section presents detail

descriptions of experimental set-up of this system. The experimental study was carried out using the chamber illustrated in schematic diagram in Figure 5.5. This large-scale experimental chamber has a total dimension of 3000mm x 3000mm x 5600mm which was divided into three zones: wind-catcher or ventilation zone, heat recovery zone, indirect evaporative cooling zone and a single test room. Figure 5.6 illustrates the total dimension of the experimental chamber.

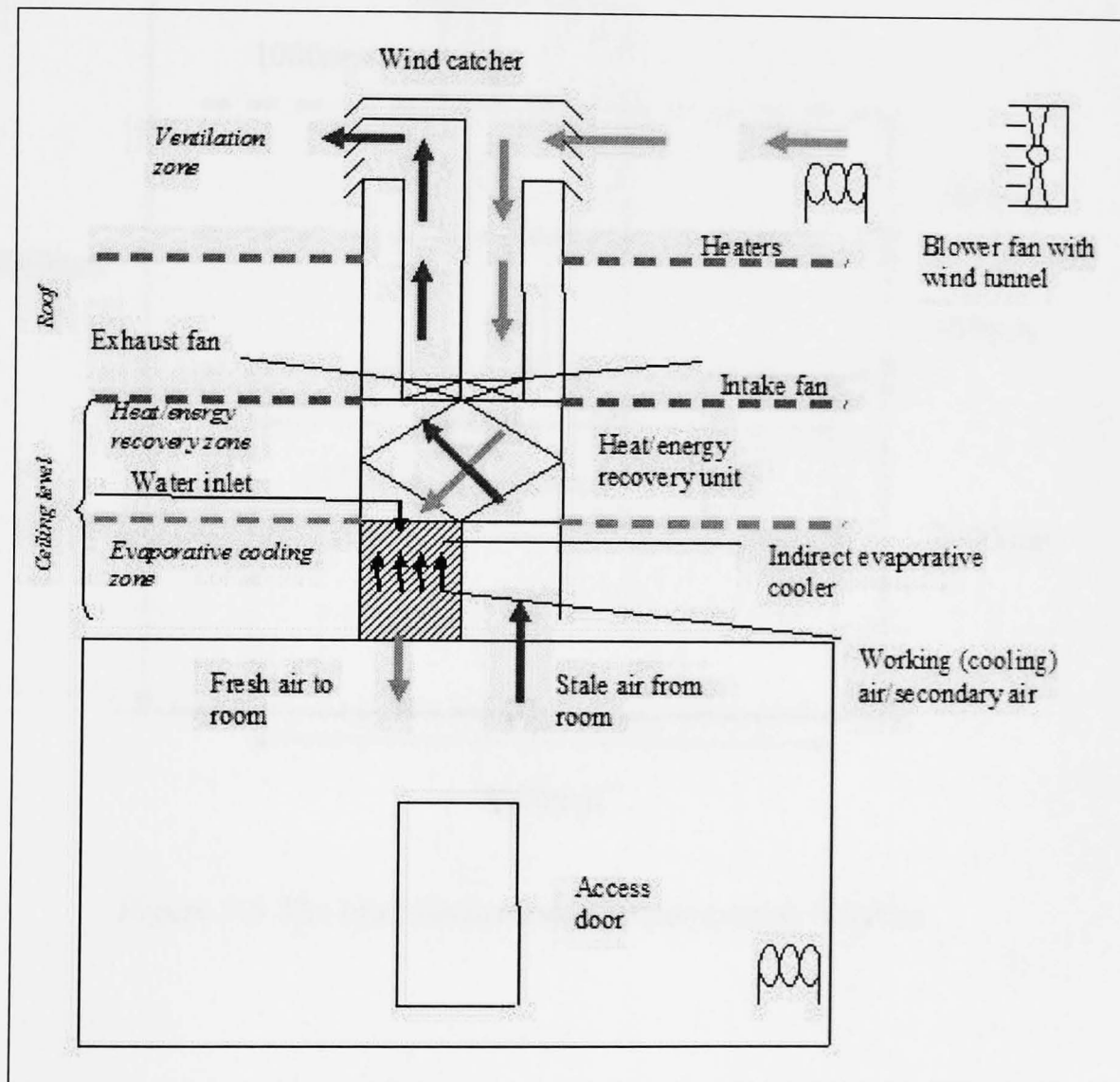


Figure 5.5 The schematic diagram of experimental chamber

The chamber has a single cubic test room of 3000mm x 3000mm floor area and 2400mm high (Figure 5.7). The walls of test room were constructed of 100mm thick of expanded polystyrene sandwich panels with plasterboard. The insulation material was used to reduce the influence of surroundings. The ceiling was made of

timber panel on the external skin and plasterboard on the internal part. The silicon sealants and duct tapes were used to seal the gap in the test room.

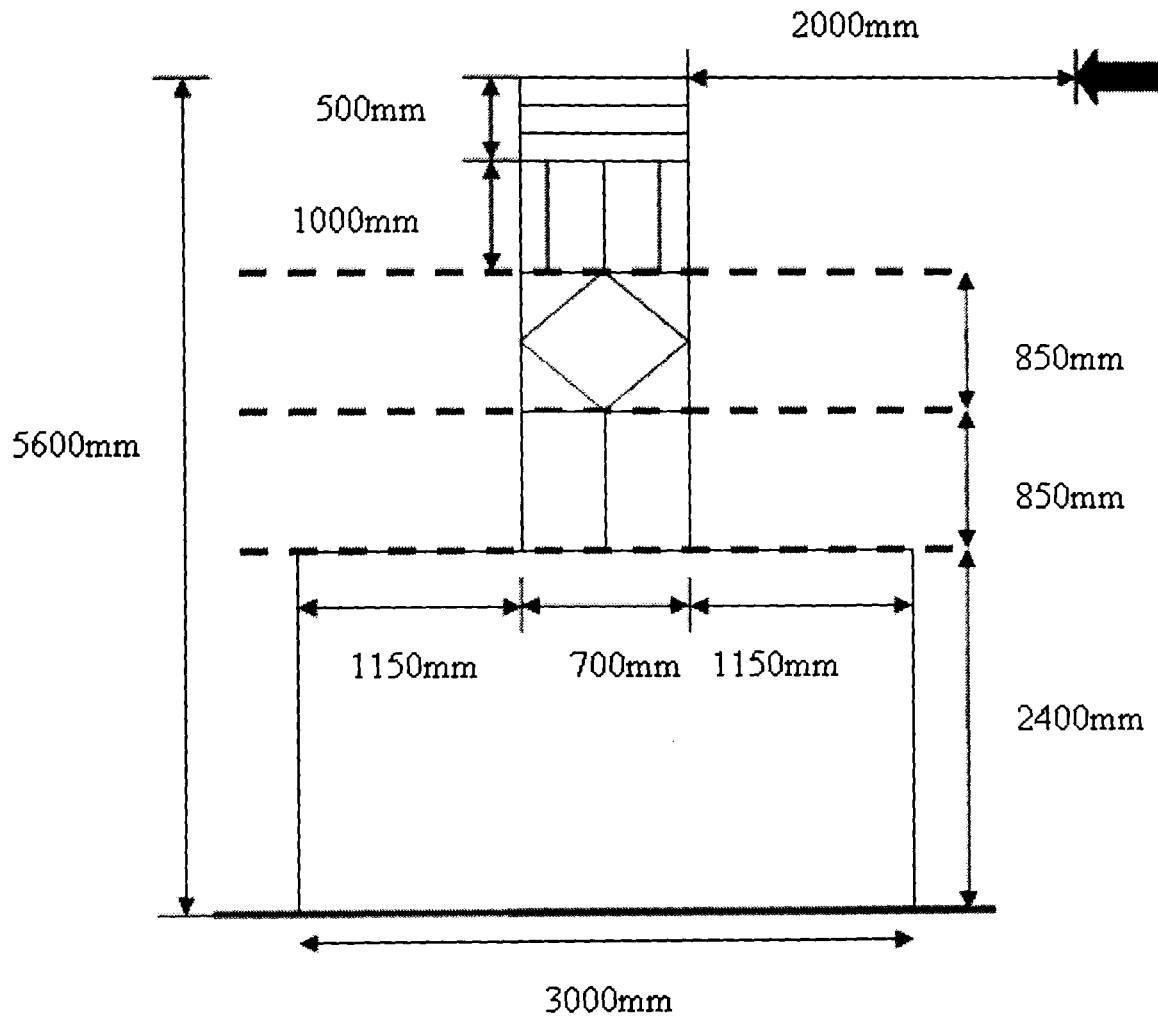


Figure 5.6 The total dimension of experimental chamber

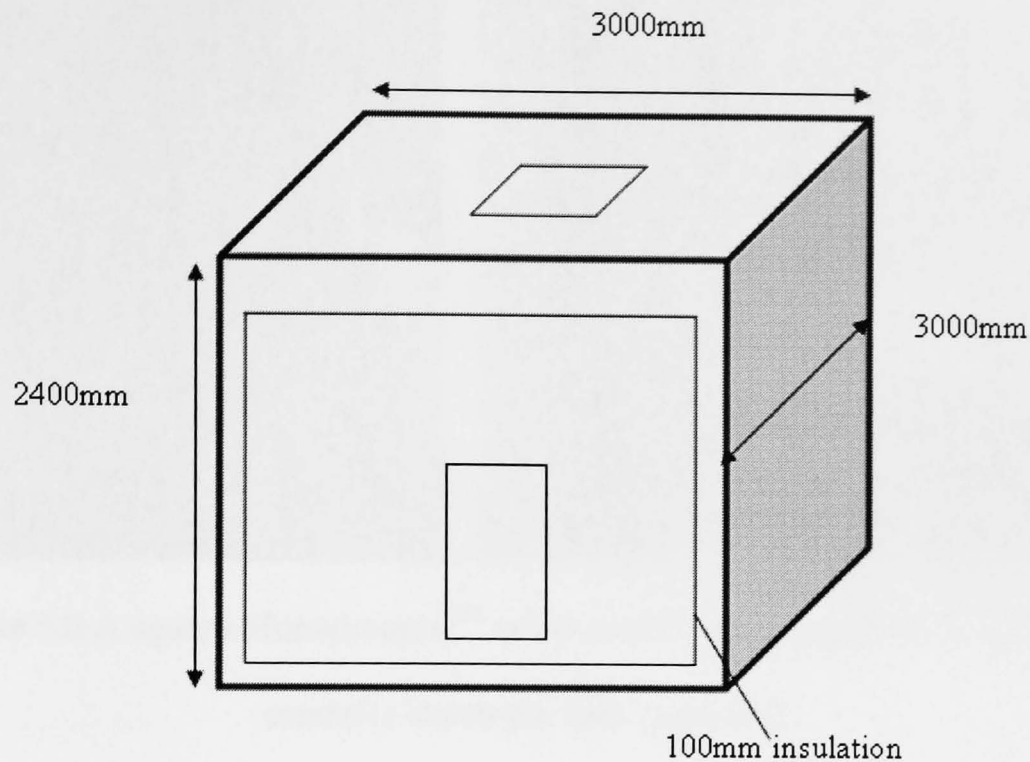


Figure 5.7 Test room

For ventilation and to assist airflow in and out of the heat recovery unit, a square Monodraught™ wind-catcher with a size of 600mm x 600mm was installed and positioned centrally above the cubic test room as shown in Figure 5.8. The purpose of combination of wind-catcher with heat recovery unit is to assist airflow in and out from the system. In order to achieve this, two ducting system consist of intake and exhaust duct were constructed in the middle of wind-catcher unit. These two ducts are made of steel sheets and each duct has a diameter of 225mm (Figure 5.9).



Figure 5.8 A square Monodraught™ wind-catcher was installed and positioned centrally above the cubic test room

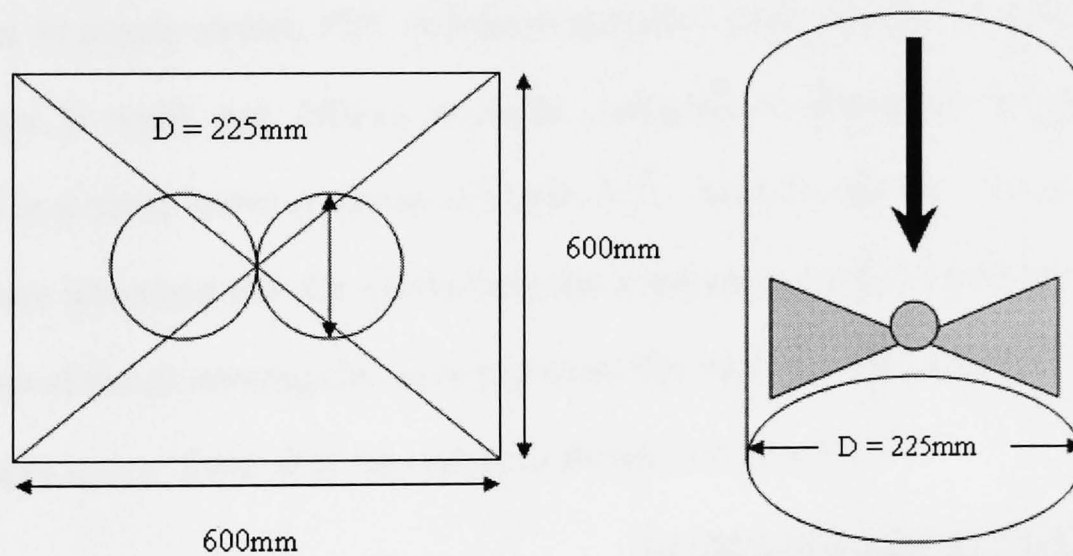


Figure 5.9 The diagram of duct

For heat recovery purpose, a cross-flow fixed-plate heat recovery unit which has a dimension of 600mm x 600mm x 300mm and made up of 21 polycarbonate frame flow-channels with 20 air passage was mounted centrally in the ceiling level as shown in Figure 5.10.

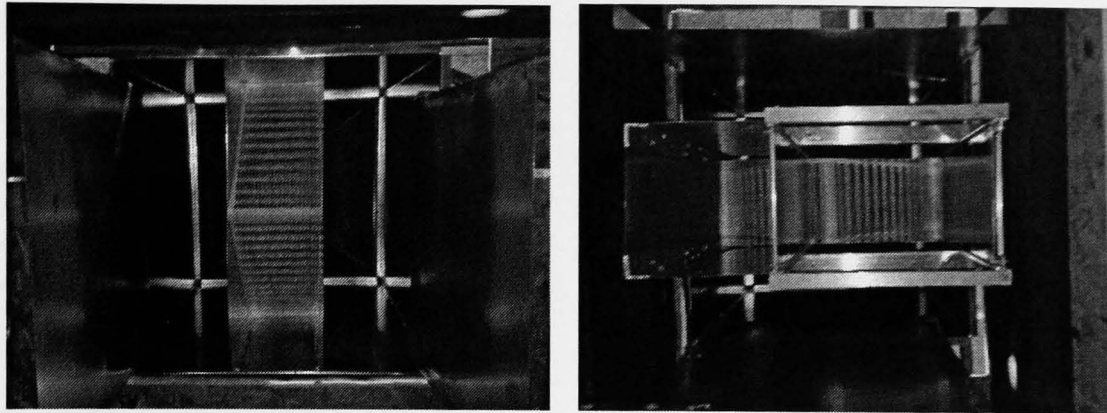


Figure 5.10 Cross-flow fixed plate Heat recovery was mounted centrally in the ceiling level

Two separated streams were built below the heat recovery unit which are supply stream and return stream. Supply stream functions to duct fresh air in to the test room. In supply stream, PEC indirect evaporative cooler which has a dimension of 400mm in width and 260mm in depth contained in aluminium housing was installed in a metal frame as shown in Figure 5.11. The heat recovery unit and PEC cooler were integrated into the system between wind-catcher and the ceiling so that a proportion of the air entering the room is cooled. The unit then was connected directly to a damper system fitted with the ceiling as shown in Figure 5.12.

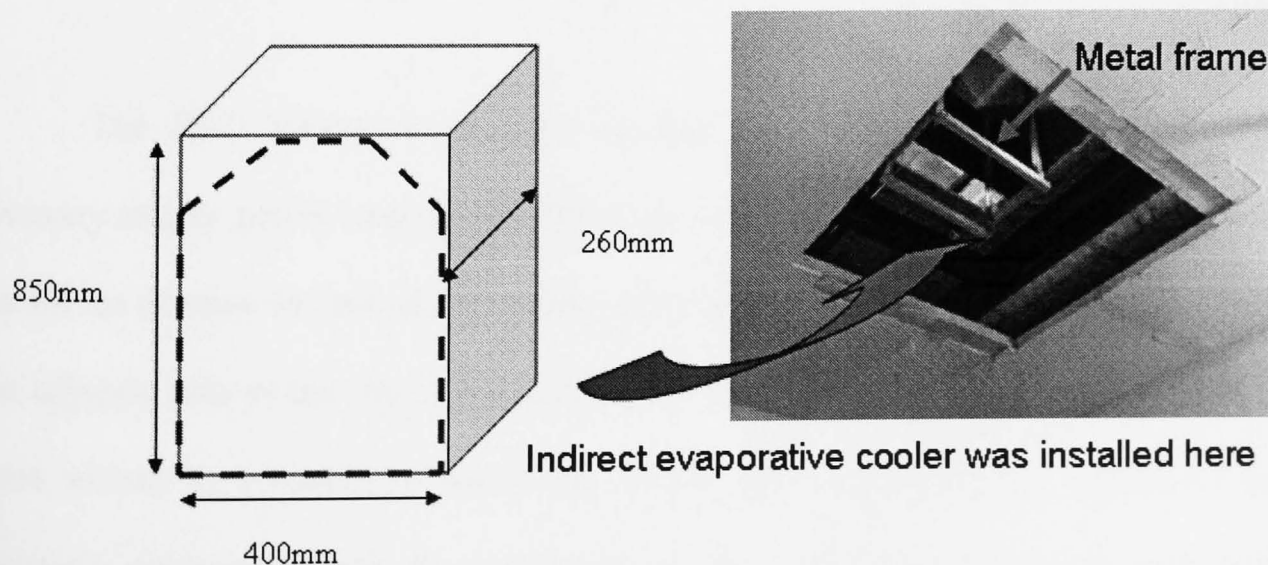


Figure 5.11 : Supply stream where indirect evaporative cooling unit was installed

PEC indirect evaporative cooler

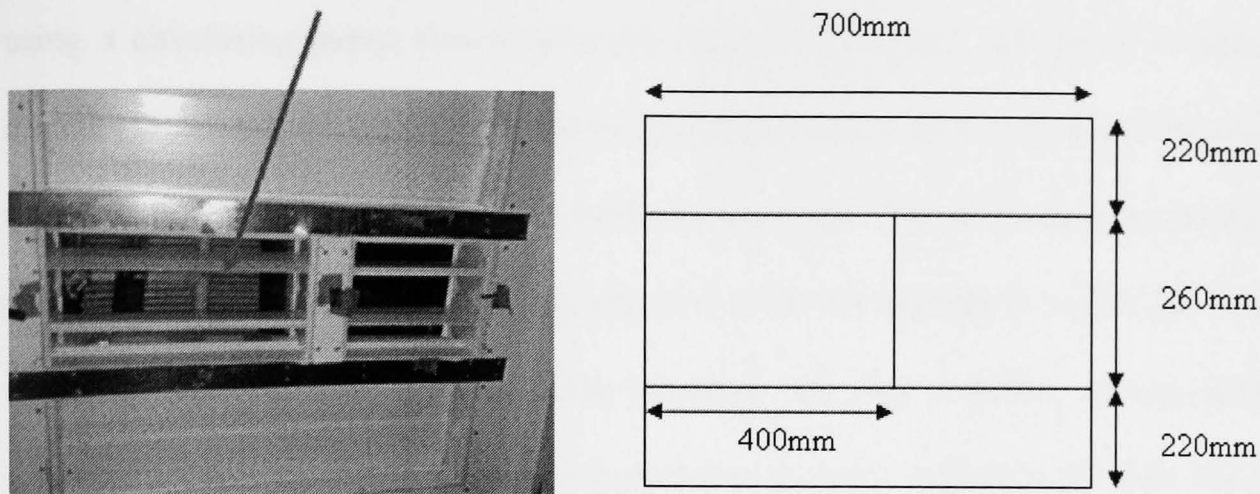


Figure 5.12 A damper system fitted with the ceiling

Figure 5.13 presents the schematic diagram of the system with the PEC indirect evaporative cooling experimental set up. As presented in figure, water is pumped from a water tank and is used for the purpose of evaporative cooling in the PEC indirect evaporative cooler. Water flow was controlled by a glove valve. (Figure 5.14). Excess water from the wet channels and any water entering the dry channels was collected at the base of the PEC indirect evaporative cooling unit and drained to a water tank positioned below the apparatus.

The PEC indirect evaporative cooling unit took incoming air from heat recovery supply stream and passes it through a series of channels called the dry side. As the air reaches the end of the cooler, some of the air was diverted to channels on the adjacent side to the dry side and flows in the opposite direction. These channels were wetted by a supply of water and as the air flows across the surface of the channels, evaporation from the surface causes heat transfer across the channel walls and provides a cooling effect to the air in the dry channels. At the base of the PEC indirect evaporative cooling unit, the flow was directed to the test room.

In cooling mode, water is sprayed over the pads along the vertical channels using a circulating pump allocated in the supply water tank. Air which is taken in system (intake air) passes through the wind-catcher inlet's port at the top of the wind-catcher and then passes through the heat recovery unit. The air is then drawn by the supply zone of heat recovery unit through the indirect evaporative cooler and is split into two streams. One stream flows through the wet channels in the indirect evaporative cooling unit to enhance evaporation of water sucked in the unit and thus cools the other stream in the dry channels within the indirect evaporative cooler. The cooled air stream will then flow into the room carrying the warm exhaust air inside the room to rise through the heat recovery unit exhaust channel and leave the wind-catcher through the exhaust air outlet by the help of the exhaust fan.

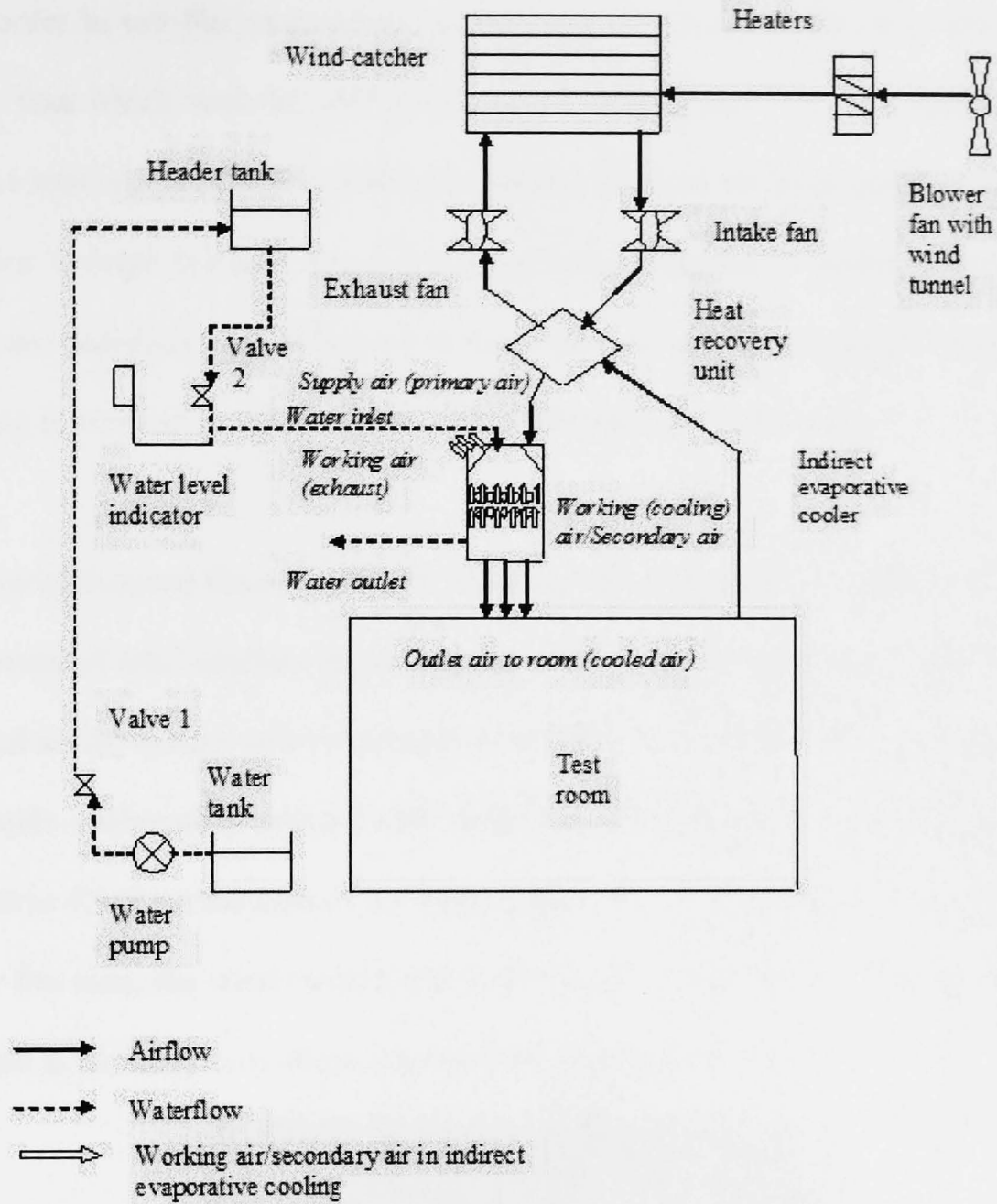


Figure 5.13 Schematic diagram of the system with the PEC indirect evaporative cooling experimental set up

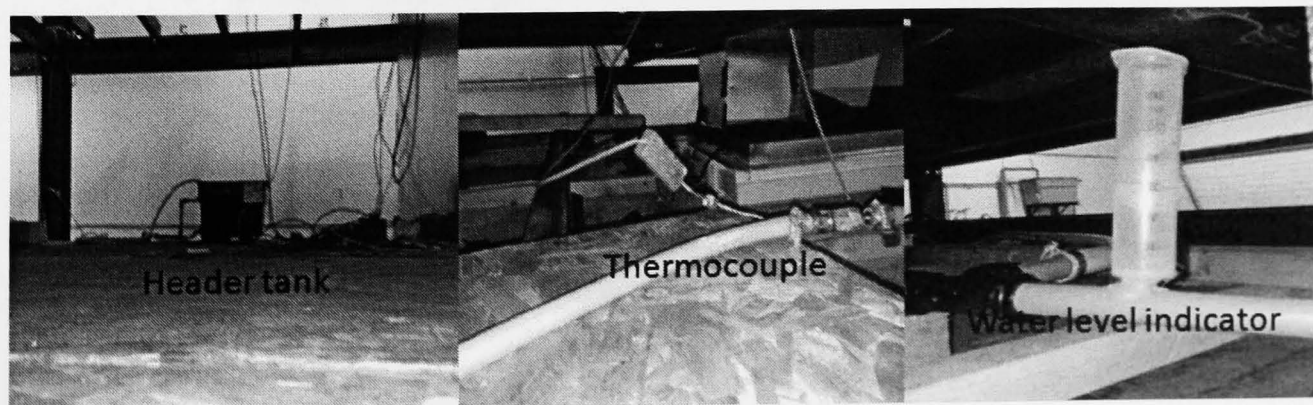


Figure 5.14 Evaporative cooling experimental set up

In order to test the performance of the system at variable airflows, two low energy DC fans which each fan has dimension of 225mm and 12V with adjustable power input were installed in the intake and exhaust ducts in the wind-catcher unit to assist airflow through the heat recovery unit and was designed to produce 100 L/s. These fans are necessary to distribute air through the heat recovery unit and were also used to bring in fresh air to the test room and to exhaust stale air to outside.

A variable-speed blower fan with wind tunnel was positioned 2000mm away from the centre of wind-catcher. In practice, the system will be installed on top of the building and so the system will be subject to different wind speeds. The experiments was run inside a laboratory assisted with wind tunnel to provide varying wind speed between 1.6 to 4.5m/s at the inlet of the wind-catcher, as shown in Figure 5.15. When the blower fan runs, the wind-catcher will function to induce fresh air flow through the test room at the windward and exhausted stale air flow at the leeward.

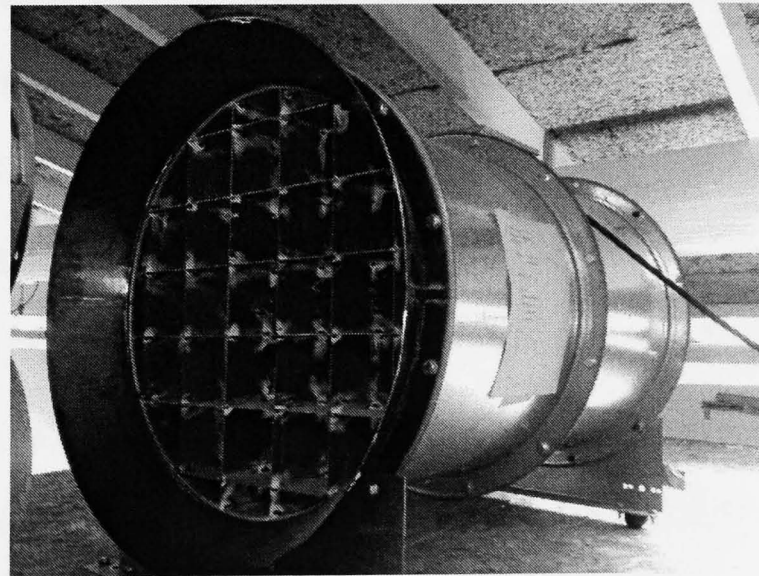


Figure 5.15 Wind tunnel with blower fan

For heat generation purpose, a 3kW heater was place in the test room and 3 heaters of 2kW were placed in between wind tunnel and wind-catcher to warm the

ambient air for warm air intake condition and to vary the intake temperature at wind-catcher zone (Figure 5.16).

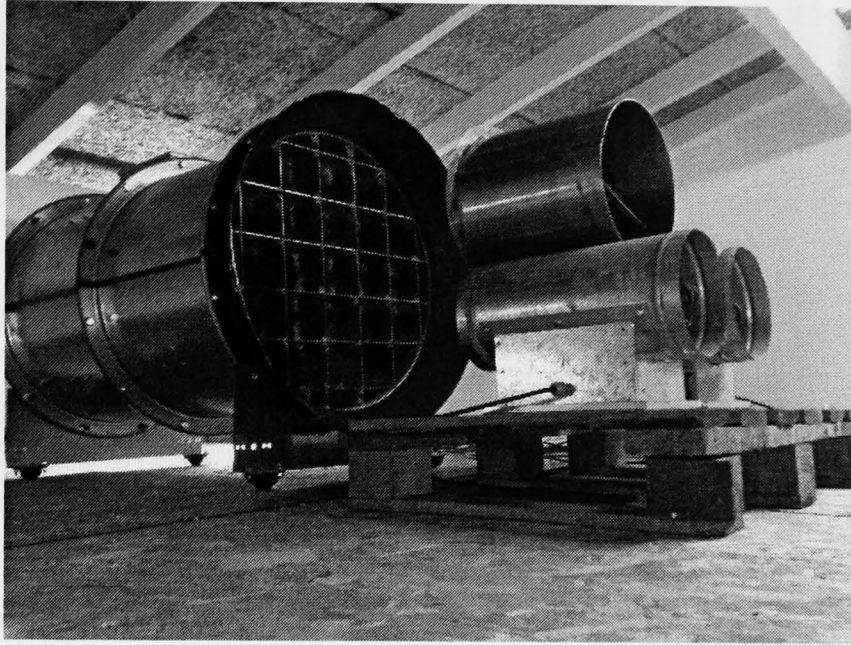


Figure 5.16 Heaters used to generate warm air

5.4 Measurement procedures

Tests were carried out at mean air velocities ranging from 1.2 to 3.1 m/s. First the system was operated until the setting conditions were maintained. The heat recovery unit was then switched on and measurements were taken for two different conditions of air intake which are cold air condition and warm air condition without the operation of evaporative cooler. The tests were carried out under different wind speeds, and different intake and exhaust fan rated power. Air temperatures were measured across the experimental rig using thermocouples and airflows were measured using hot wire anemometer. The procedures and instrumentation used in this investigation for heat recovery performance are similar to the procedure discussed in Chapter 4. Figure 5.17 shows the position of airflow measurements in the intake and exhaust ducts.

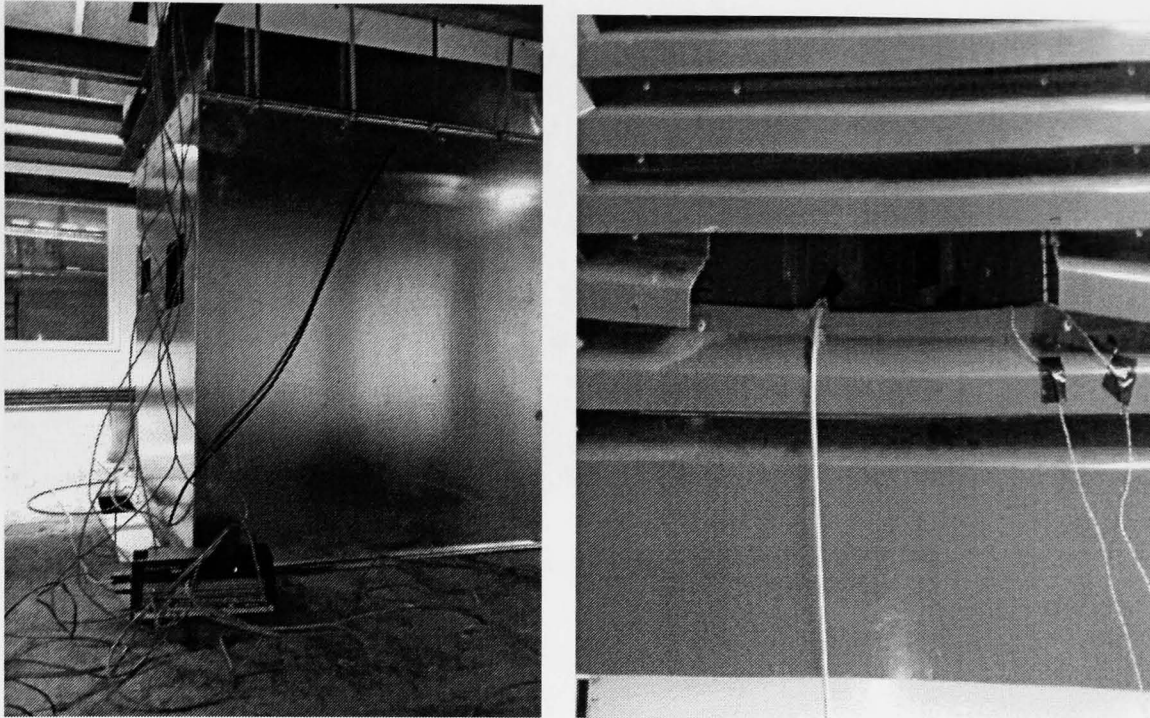


Figure 5.17 Position of airflow measurements in the ducts

The test then carried out with the operation of PEC indirect evaporative cooling unit. The performance of PEC indirect evaporative cooling unit was investigated. First the system was operated until the setting conditions were maintained without the added of water into the cooling unit. The cooling system was then switched on and measurements were taken until steady state is achieved. The parameters studied are the temperature, relative humidity and airflow. The humidity and temperature probes were connected to a DT500Datataker so that a log of the test data can be recorded (Figure 5.18). Airflows at the supply and outlet streams were estimated by measuring the velocity of flow at various positions across each hole and calculating the average flow. The velocity was measured by a hot wire anemometer.

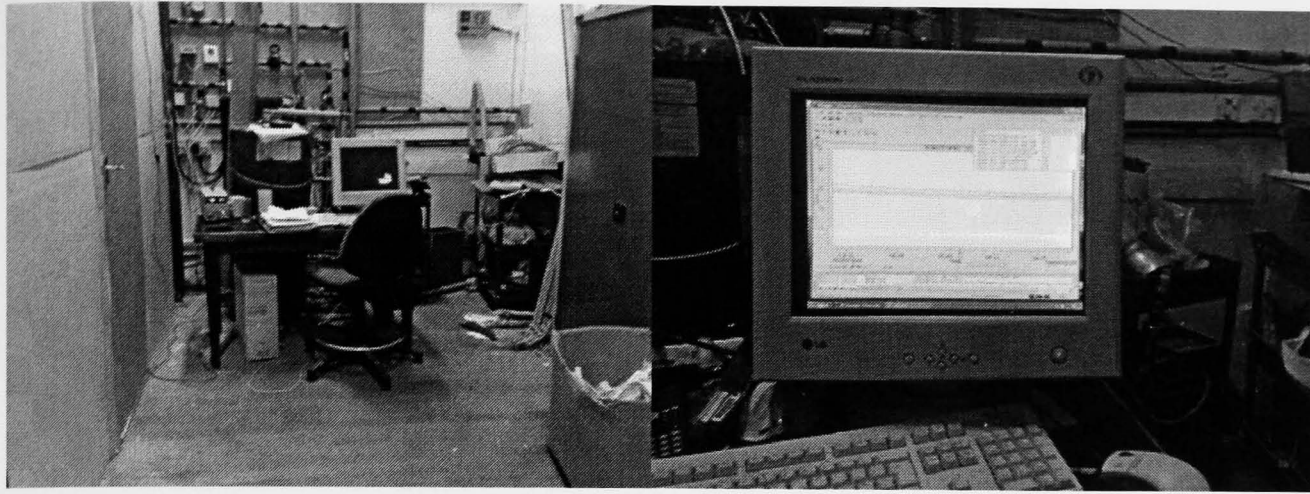


Figure 5.18 Data acquisition equipment

5.4.1 Temperature measurements

Figure 5.19 illustrates the schematic of the set up for temperature measurements and Figure 5.20 shows the picture of thermocouples position across the system. For warm air condition, air was heated using three heaters. While for cold air condition, the ambient air was used. Before each experiment, the test room was heated to reach a steady for 30 minutes. The temperature measurement system consisted of :

- four points of thermocouples at the wind-catcher fresh air inlet (T_1, T_2, T_3 and T_4)
- four point of thermocouples in the intake side of heat recovery unit (T_i)
- four point of thermocouples in the supply side of heat recovery unit (T_s)
- four point of thermocouples in the return side of heat recovery unit (T_r)
- four point of thermocouples in the exhaust side of heat recovery unit (T_e)
- four points of thermocouples in the room (T_5, T_6, T_7 and T_8)

- four points of thermocouples at the outlet stream of PEC indirect evaporative cooling unit (T_9, T_{10}, T_{11} and T_{12})
- four points of thermocouples at extract air stream from the room (T_{13}, T_{14}, T_{15} and T_{16})

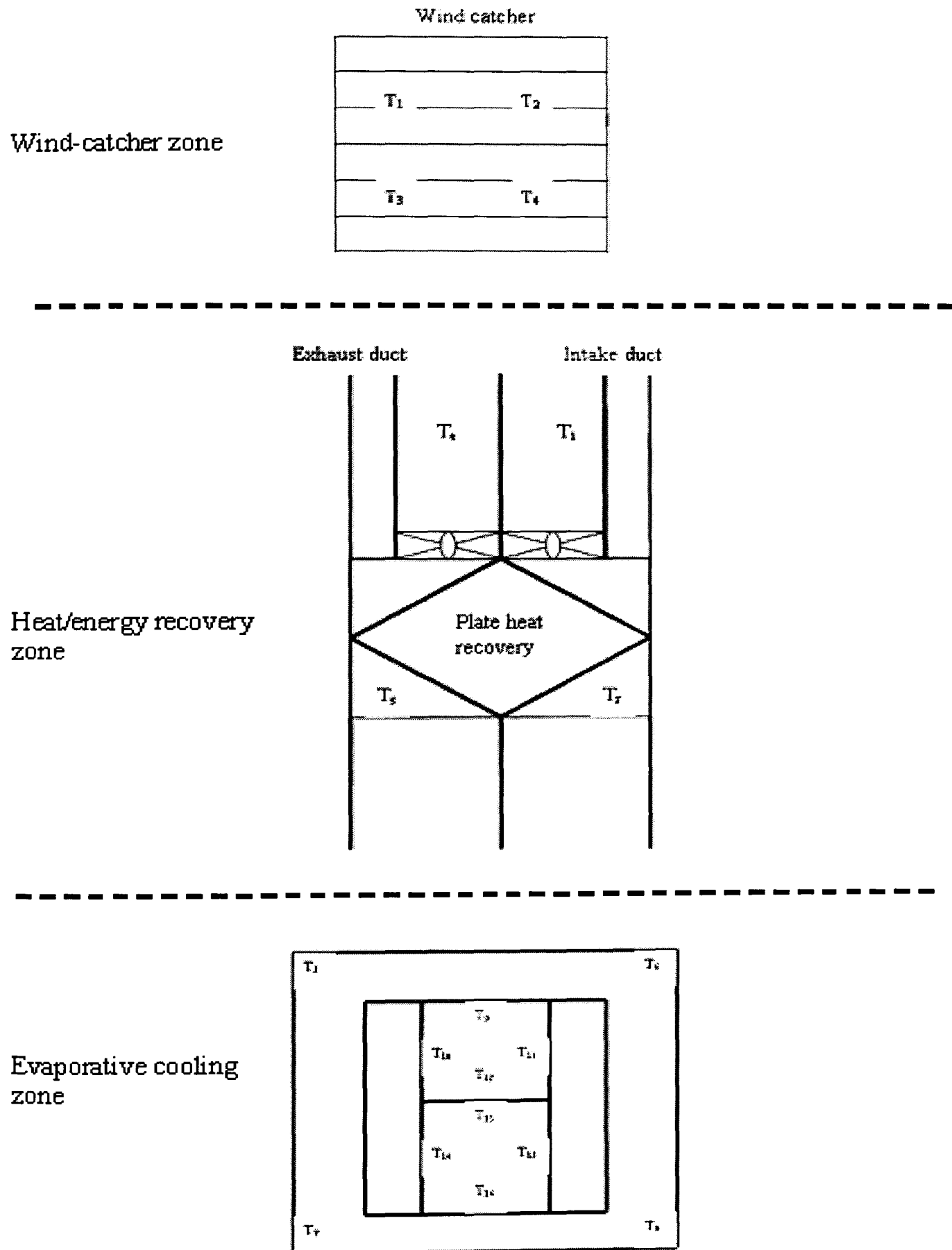


Figure 5.19 Schematic of the set up for temperature measurements

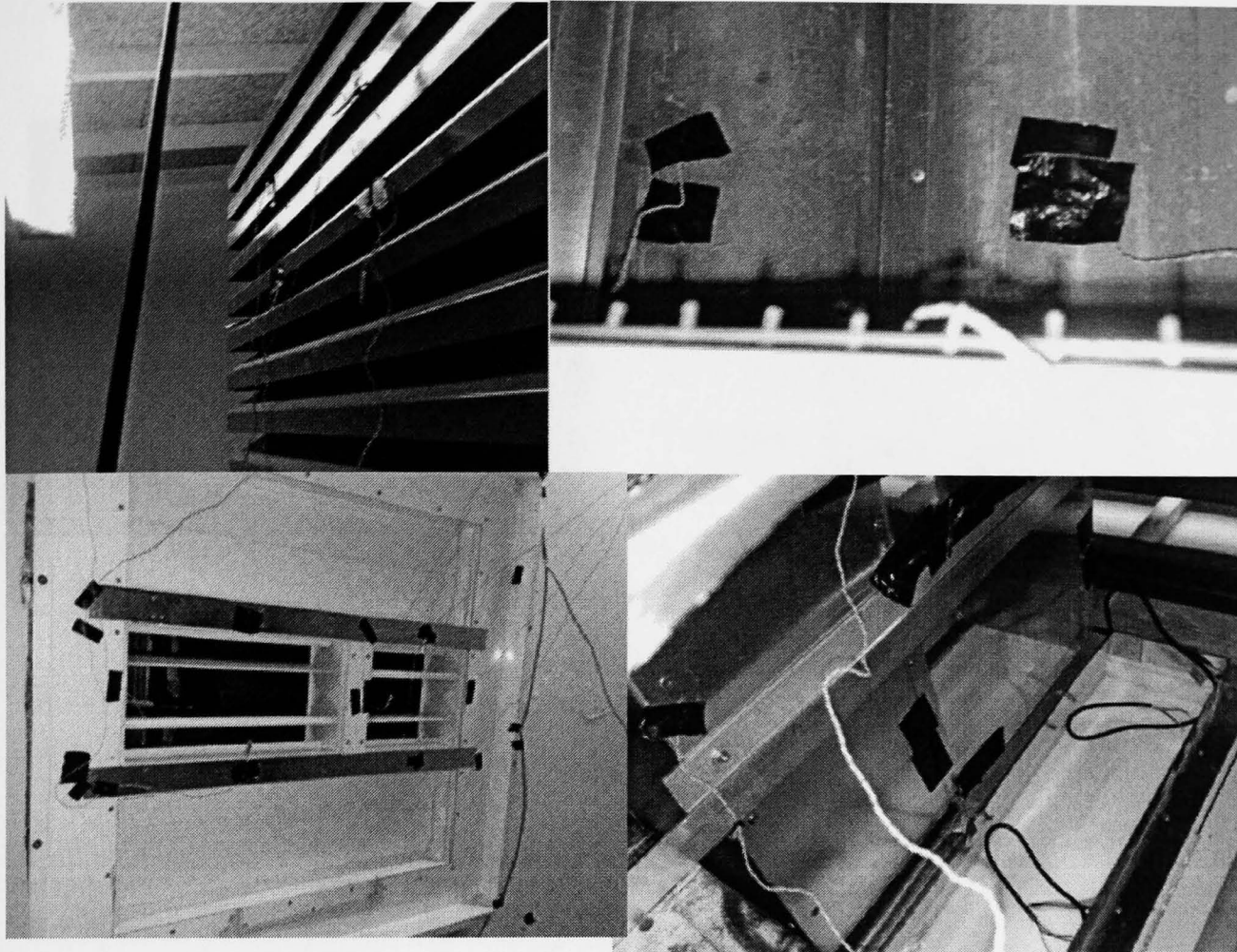


Figure 5.20 Picture of thermocouples position across the system

5.4.2 Relative humidity measurements

Measuring was carried out using Vaisala HUMICAP HMP45A/D humidity probe connected to a data logger and a PC. Figure 5.21 shows the position of relative humidity measurement.

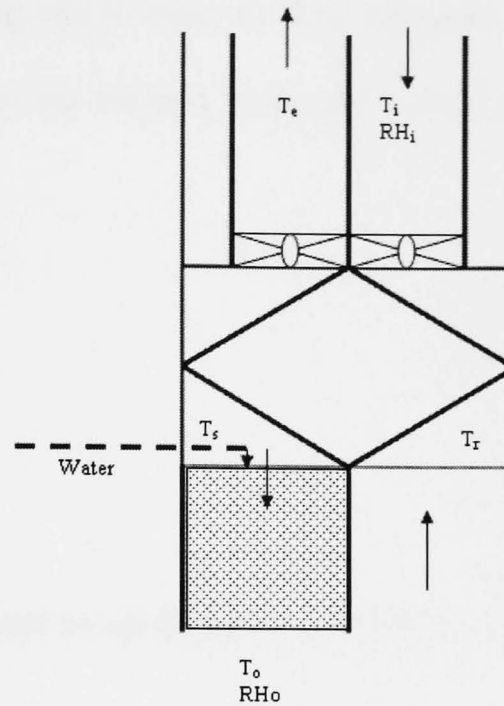
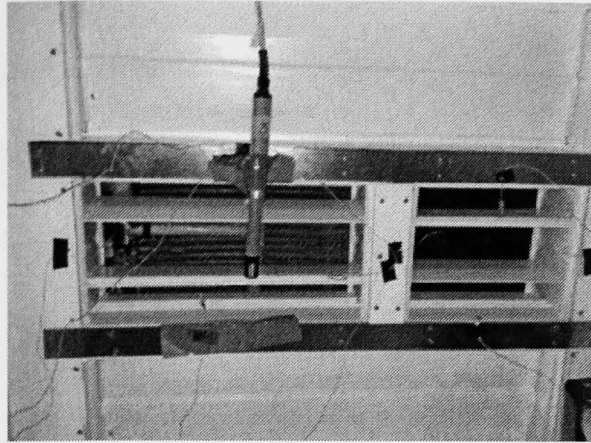


Figure 5.21 The position of relative humidity measurement

5.5 System performance calculation model

The performance of integrated heat recovery system associated with wind-catcher and evaporative cooling is evaluated based on the following calculation model:

- Heat recovery efficiency in this system is expressed calculated by the following equation

$$\epsilon_{HR} = \frac{(T_s - T_i)}{(T_r - T_i)} \times 100 \% \quad (5.1)$$

- Cooling capacity

Basic calculations for cooling system capacity flow rates and Psychrometric processes are based on mass flow and enthalpy. A practical method of using volume but still including mass so that accurate results are obtained is the use of volume values based on measurement at ASHRAE standard conditions. As a result of

difference in enthalpy between the incoming and leaving air flow obtained from the Psychrometric Chart, the cooling capacity of the indirect evaporative cooling system can be calculated as follow:

$$\text{Cooling capacity, } q_c = M_a \Delta H \quad (5.2)$$

$$= M_a (H_s - H_o) \quad (5.3)$$

- Cooling efficiency

The cooling efficiency can be evaluated by applying the following expression:

$$\varepsilon_{\text{C-wet bulb}} = \frac{(T_s - T_o)}{(T_s - T_{wb})} \quad (5.4)$$

$$\varepsilon_{\text{C-wet bulb}} = \frac{(T_s - T_o)}{(T_s - T_{dp})} \quad (5.5)$$

- Water consumption rate

In evaluating the performance of evaporative cooling system either direct, indirect or combination total evaporative water mass is one of the important parameters. Basically, the water consumption or requirement of an evaporative cooling system can be evaluated by the application of the Equation 5.6 (Rao 2003, Moran 1995) as follows:

$$M_w = M_a (\omega_o - \omega_s) \quad (5.6)$$

- Coefficient of performance (COP)

Coefficient of performance is the dimensionless number defined by efficiency ratio of the amount of heating or cooling provided by a heating or cooling unit to the energy consumed by the system. This term is universal in its use but not in its meaning. For cooling, COP is defined as the ratio of the rate of heat removal to the

rate of energy input. For purpose of comparison, the higher value of COP shows the more efficient the system. For mathematical purposes, COP can be treated as efficiency. COP is calculated by dividing the amount of heat produced by a heating system divided by the amount of energy put in to it. COP of the system is calculated as:

$$\text{COP} = \frac{\text{Cooling capacity (W)}}{\text{Power input (W)}} \quad (5.7)$$

where, power input is the electrical energy consumed by the fan and the water pump.

5.6 Results and discussion

Experimental performance tests were conducted to analyse different parameters that are crucial in evaluating the performance of integrated heat recovery system associated with wind-catcher and indirect evaporative cooling. Typical results of different values of intake temperatures, relative humidity and corresponding outlet condition were recorded. The experiments were carried out under the following conditions:

- Heat recovery performance under two different intake air conditions: cold and warm without the operation of evaporative cooling unit
- Heat recovery performance with the operation of evaporative cooling unit
- Evaporative cooling performance under varying airflow rate and constant airflow rate
- System performance

5.6.1 Heat recovery performance

First experimental tests were conducted on the heat recovery unit when the indirect evaporative cooling unit was not operated. This test was conducted to investigate the performance of heat recovery unit. The tests were carried out for the heat recovery unit performance for two different intake air conditions which are cold air and warm air condition without the operation of evaporative cooling unit. The heat recovery performance of the system was evaluated by measuring the temperature and airflow rate at the intake and exhaust air streams at steady conditions.

Tests were performed at mean air velocities ranging from 1.2 to 3.1 m/s and room temperature ranges from 23 to 25°C for both conditions. Volume airflow rate is calculated using Equation 5.8 by multiplying cross sectional area of the duct (225mm of diameter) and the average air velocity measured at the duct.

$$Q = VA \quad (5.8)$$

Table 5.1 and 5.2 presents a summary of these results during cold air condition and warm air condition respectively.

Table 5.1 Results of cold air

Intake air velocity, V_i (m/s)	Volume airflow rate, Q_i m^3/s l/s		Mass airflow rate, M (kg/s)	T_{wc} °C	T_i °C	T_s °C	T_r °C	T_e °C
1.2	0.0478	47.80	0.058	14.9	15.0	19.3	21.0	16.8
1.5	0.0597	59.70	0.072	15.0	15.2	19.6	22.0	17.5
2.3	0.0915	91.50	0.110	15.2	15.6	20.6	24.2	19.2
3.1	0.1234	123.4	0.148	15.2	15.5	20.6	25.8	20.6

Table 5.2 Results of warm air

Intake air velocity V_i (m/s)	Volume flow rate		Mass airflow rate, M (kg/s)	T_{wc} °C	T_i °C	T_s °C	T_r °C	T_e °C
	m^3/s	l/s						
1.2	0.0478	47.80	0.062	34.8	29.9	26.1	24.3	28.1
1.5	0.0597	59.70	0.078	34.9	30.1	26.1	23.9	28.0
2.3	0.0915	91.50	0.119	34.5	29.8	25.3	22.2	26.7
3.1	0.1234	123.4	0.160	34.2	30.5	25.9	22.5	27.1

The temperature change (ΔT) across the heat recovery unit was observed shown in Figure 5.22. In figure, it can be seen that temperature change between return air to heat recovery unit and extract air from heat recovery unit to outside increases with increasing air velocity. For cold air condition, a change ranged from 4.2 to 5.2°C was recorded with the highest value corresponding to 3.1m/s air velocity. Whilst for warm air condition, temperature change ranged from 3.8 to 4.6°C was observed.

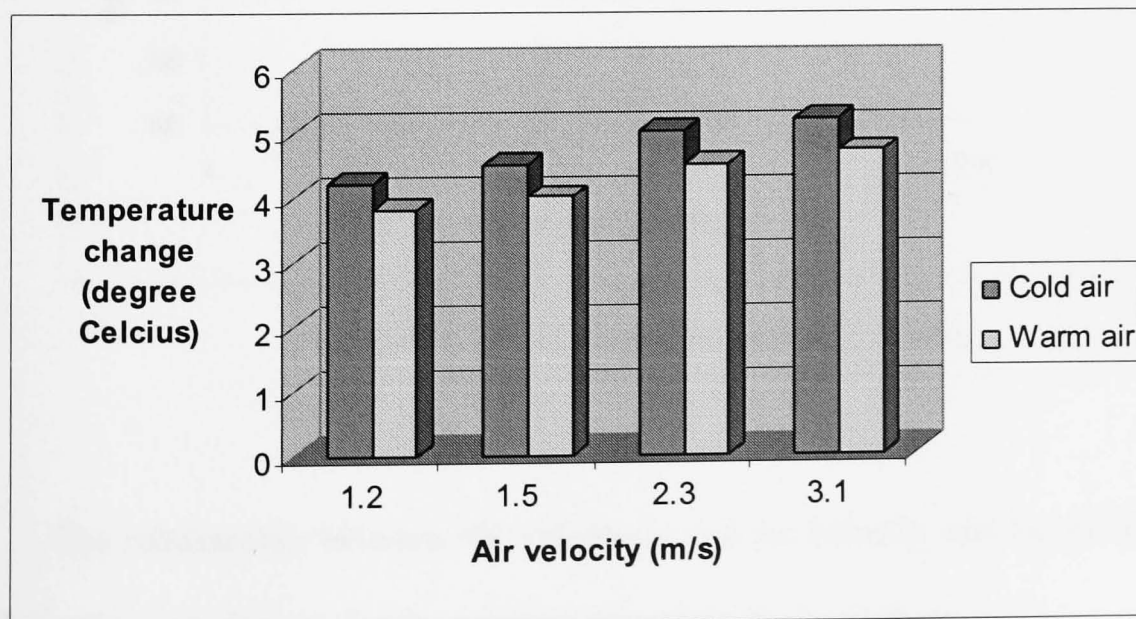


Figure 5.22 Temperature change across the heat recovery unit

5.6.1.1 Heat recovery efficiency

When mass flow rates of intake and exhaust air are equal, the heat recovery efficiency, ϵ_{HR} was determined using equation 5.1 where it is called temperature efficiency. Figure 5.23 illustrates the variation of the cross-flow heat recovery efficiency for cold air condition and warm air condition with respect to air velocity in the duct. The efficiency ranged from 70% at average velocity of 1.2 m/s to 50% at 3.1 m/s during cold air condition. Whilst, during warm air condition, the efficiency ranged from 69% at average velocity of 1.2m/s to 49% at 3.1m/s. In both conditions, it can be seen that the air velocity has a significant effect on the efficiency of cross-flow heat recovery. The efficiency decreases with increasing air velocity due to short residence time when the velocity was high.

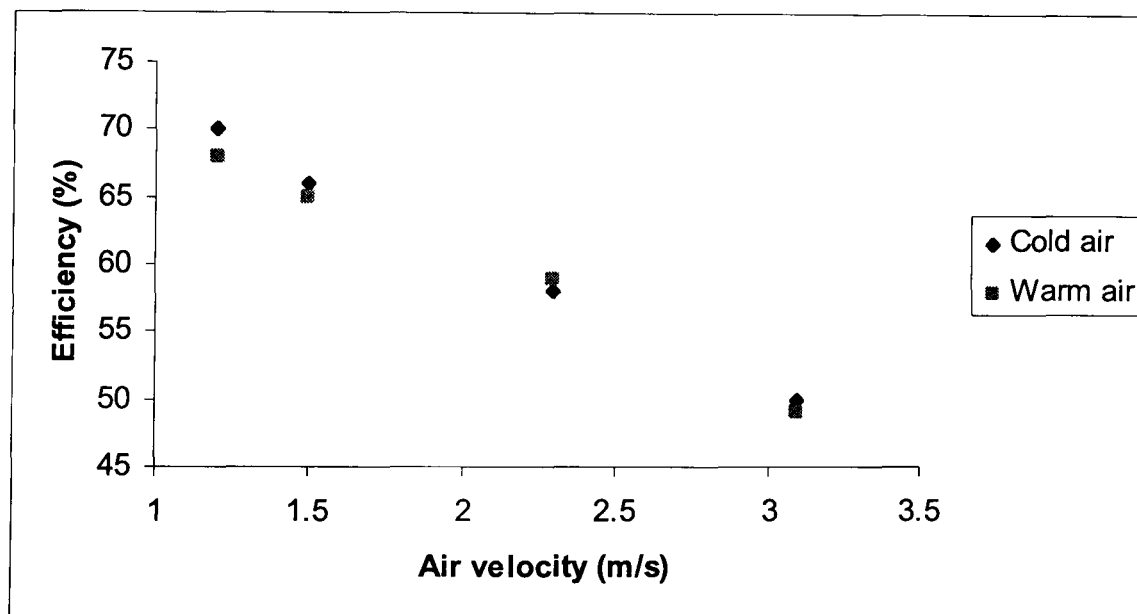


Figure 5.23 Efficiency against air velocity

The relationship between the efficiency and air velocity can be presented by the following correlations for the velocity range tested; for cold air intake,

$$\epsilon_{HR} = 0.63V^2 - 13.1V + 84.59 \quad (5.9)$$

for warm air intake,

$$\epsilon_{HR} = 1.99V^2 - 1.16V + 71.87 \quad (5.10)$$

5.6.1.2 The sensible transferred energy (heat) (q_{HR})

Table 5.3 shows the sensible transferred energy (heat) during cold air condition and warm air condition.

Table 5.3 Sensible transferred energy (heat)

Volume airflow rate (l/s)	Transferred energy (heat) (W)	
	Cold air	Warm air
47.8	244.6	237.1
59.7	325.3	312.0
91.5	552.2	535.5
123.4	772.9	757.6

Figure 5.24 illustrates the variation of transferred heat during both air conditions. It can be seen that, the transferred heat gives higher value in higher airflow rate, due to enhancement in heat transfer coefficient.

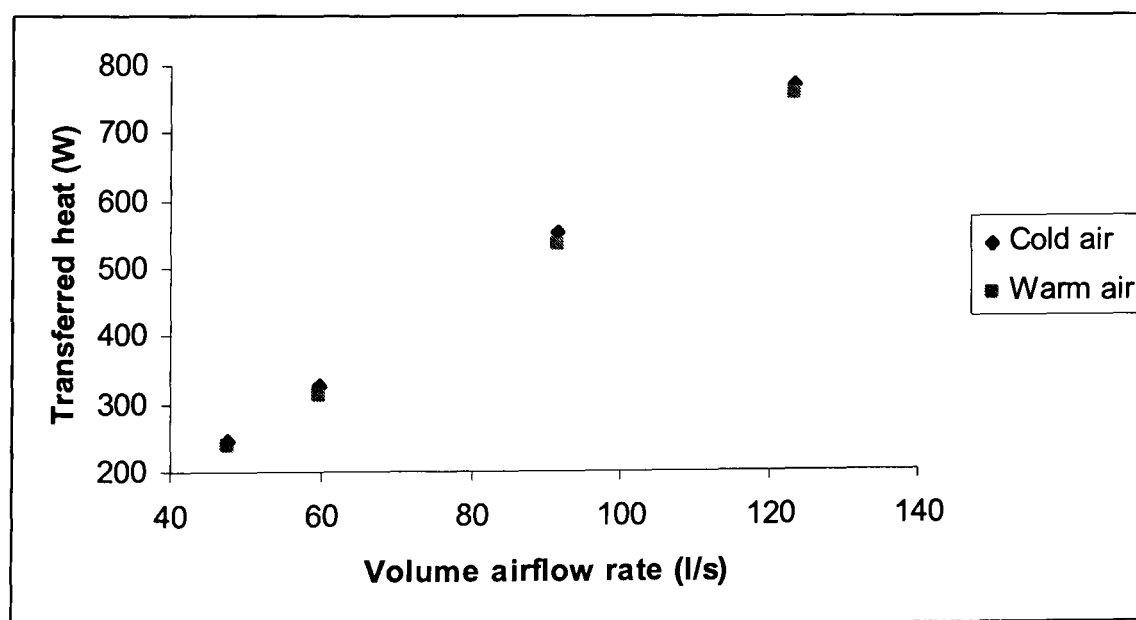


Figure 5.24 Sensible transferred heat vs airflow rate

Figure 5.25 shows the impact of temperature change to the sensible heat transferred for cold and warm air intake conditions. It can be seen that a maximum of 772.9W was obtained at 5.2°C temperature change for cold air condition and a maximum of 757.6W was calculated at 4.7°C of temperature change for warm air condition.

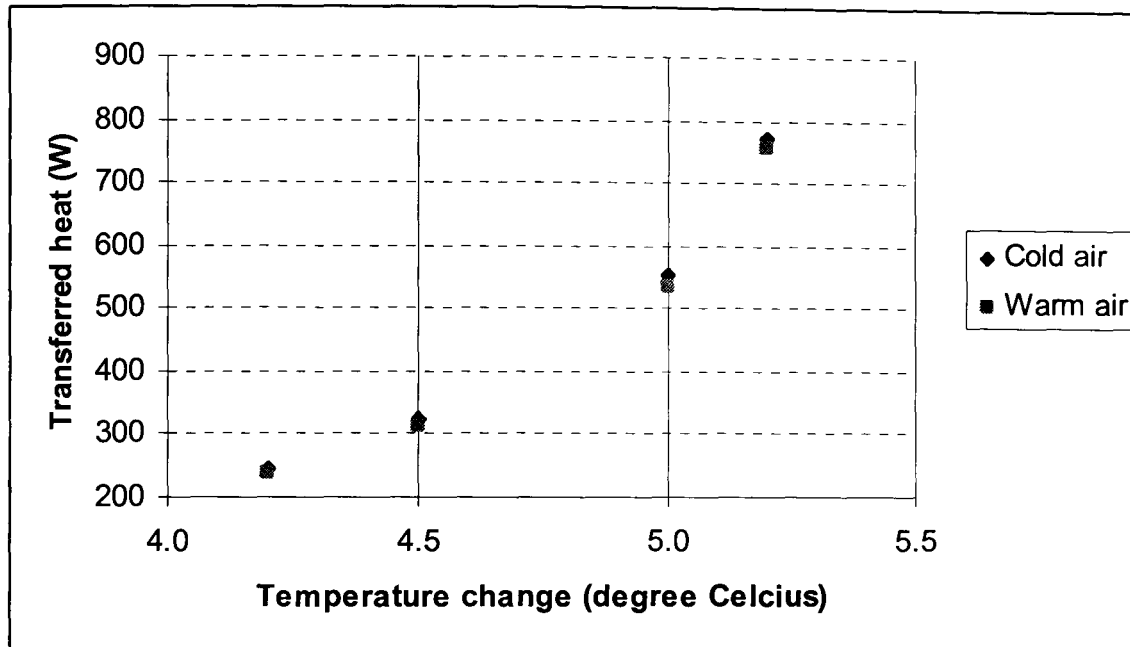


Figure 5.25 Impact of temperature change to the sensible heat transferred for cold and warm air intake conditions

5.6.1.3 Pressure drop

The difference between static pressure at the inlet to the heat recovery unit and the ambient was measured for variations in intake airflow as can be seen in Figure 5.26.

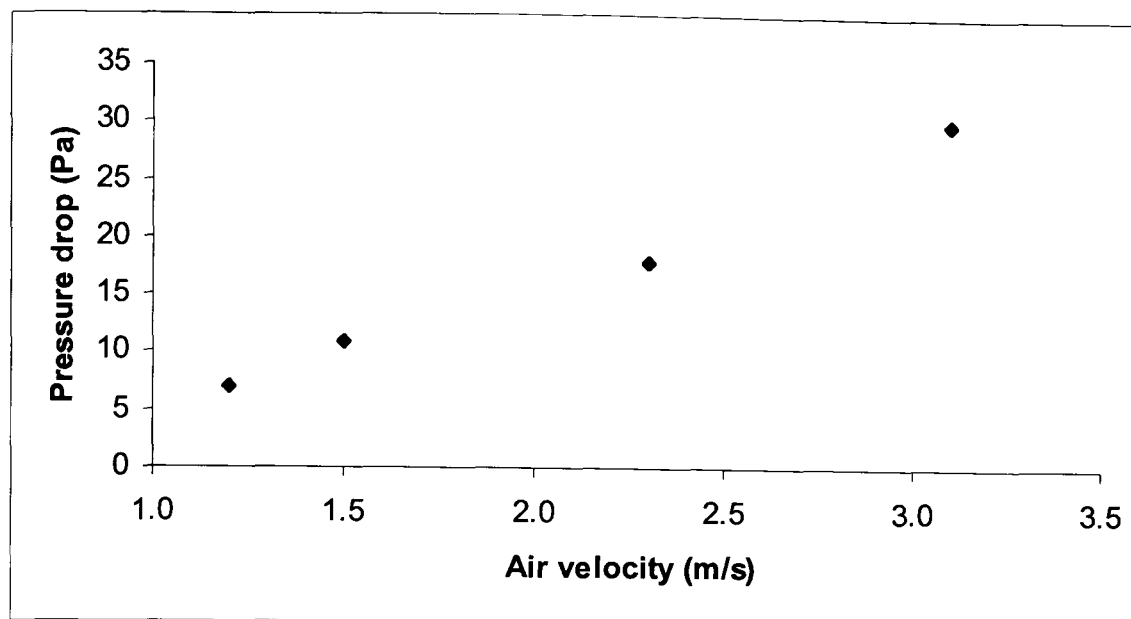


Figure 5.26 Pressure drop versus air velocity

Intake airflow was varied between 1.2 and 3.1m/s and it can be observed that the pressure difference increased from about 7 to 30Pa in that flow range. This shows that the pressure drops are low for moderate to high inlet airflows. This means that the power required to drive air through the unit is low.

5.6.2 Cooling performance

The performance of indirect evaporative cooling unit was conducted to analyse different parameters that are crucial in evaluating the performance of the integrated system. Tests were performed at different velocities range from 1.5 to 3.1m/s, water temperature ranges from 18 to 19°C, room temperature was at 29° and ambient temperature ranges between 34 to 35°C. The mass flow is calculated using the cross sectional area of the outlet stream (0.076m²) and the average working air velocity measured at the outlet stream of indirect evaporative cooling unit. Table 5.4 and 5.5 present the summary of these results.

Table 5.4 Airflow experimental results

Supply air velocity, V_s (m/s)	Working air velocity, V_o (m/s)	Supply air volume flow rate, Q_s (m^3/s)	Working air volume flow rate, Q_o (m^3/s)	Supply air mass flow rate, M_s (kg/s)	Working air mass flow rate, M_o (kg/s)
1.5	0.4	0.0597	0.030	0.078	0.040
2.3	0.7	0.0915	0.053	0.119	0.069
3.1	0.9	0.1234	0.068	0.160	0.089

Table 5.5 Temperature and relative humidity results

V_s (m/s)	T_s ($^{\circ}C$)	RH_s (%)	T_o ($^{\circ}C$)	RH_o (%)
1.5	32.0	32	24.3	50.3
2.3	31.5	37.1	26.2	56.0
3.1	30.5	40.1	26.3	60.2

Tests were also carried out to investigate the effect of supply air temperature and relative humidity under constant air velocity. Table 5.6 shows the values obtained from the tests under the conditions that the intake air velocity is constant at 3.1m/s and the cooling water temperature is between 18 to 19 $^{\circ}C$.

Table 5.6 Testing data

T_s	T_o	RH_s	RH_o
25.1	22.0	40.2	65.0
27.8	24.1	40.0	64.7
29.6	25.6	39.8	63.5
30.1	25.9	38.5	62.7
31.4	27.0	36.8	61.8
32.3	27.4	34.7	60.6
33.7	28.7	33.0	60.0
34.6	29.0	32.6	59.7
35.8	29.8	31.5	59.2
36.8	30.6	30.3	58.0

5.6.2.1 Temperature profiles

The temperature change across the indirect evaporative cooling unit was observed. From the measurements the temperature change decreased with increasing air velocity. For air velocity range from 1.5 to 3.1m/s, a different of 4.2 to 7.7°C was recorded with the highest value corresponding to the minimum air temperature velocity.

Figure 5.27 shows the timely variation of supply and outlet air temperatures across the indirect evaporative cooling unit where the intake air velocity is constant at 3.1m/s and the cooling water temperature is between 18 to 19°C whilst, Figure 5.28 shows the variation of outlet air conditions with supply air temperature. The temperature change increased with increasing supply air temperature. For supply air temperature range of 25.1 to 36.8°C, a change of 3.1 to 6.2°C was recorded with the highest value corresponding to the maximum supply air temperature. It denotes that the temperature change increases with increasing supply air temperature. Considering

the supply and outlet temperature, decrement becomes higher as inlet air temperature increases, so cooling efficiency becomes higher with increasing supply air temperature.

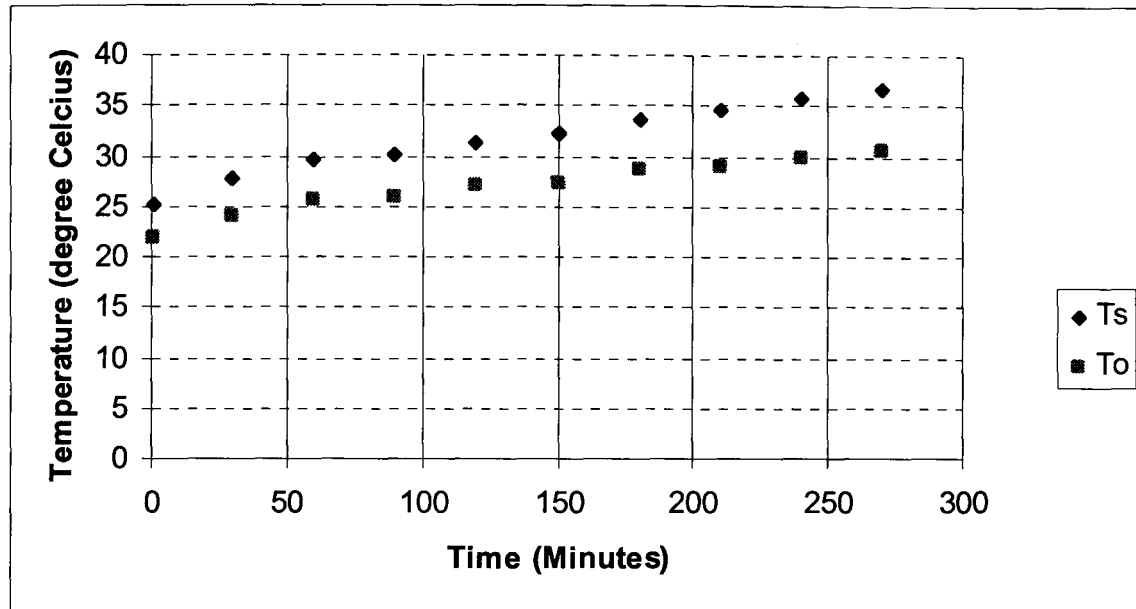


Figure 5.27 Temperature vs time

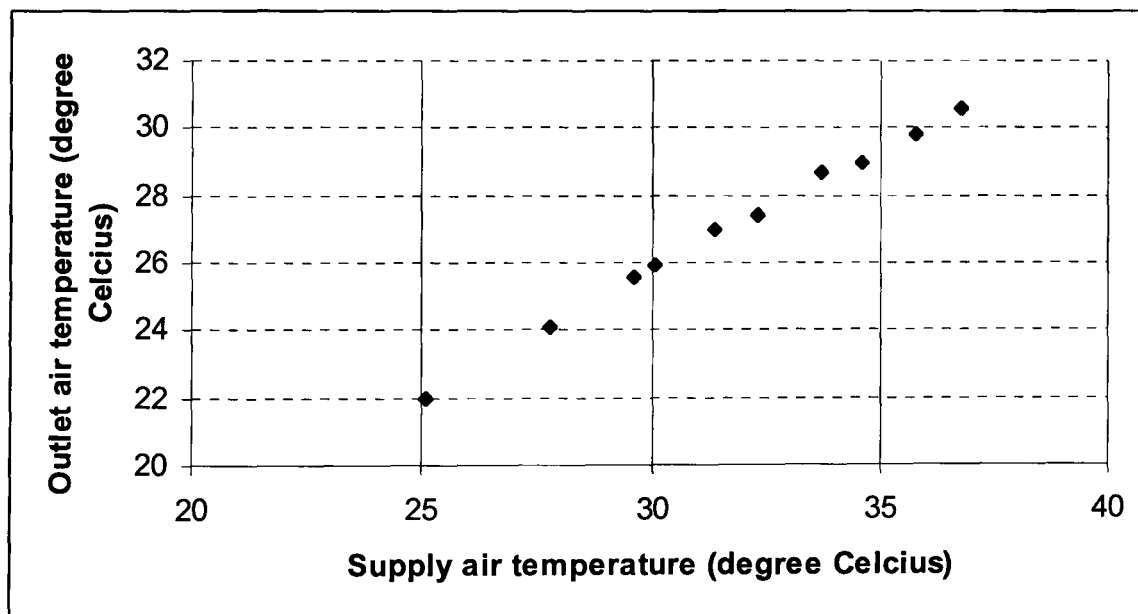


Figure 5.28 Outlet air temperature vs supply air temperature

5.6.2.2 Relative humidity profiles

For supply relative humidity ranges from 32 to 40.1% corresponding rise of 18.3 to 20.1% was observed at the outlet which is the supply air stream to the test room.

Figure 5.29 shows the combined temperature and relative humidity profiles at the supply and outlet streams operating conditions of the system. The main characteristic of this result is that the air temperature change decreases while the relative humidity difference increases between the supply and outlet streams of the system.

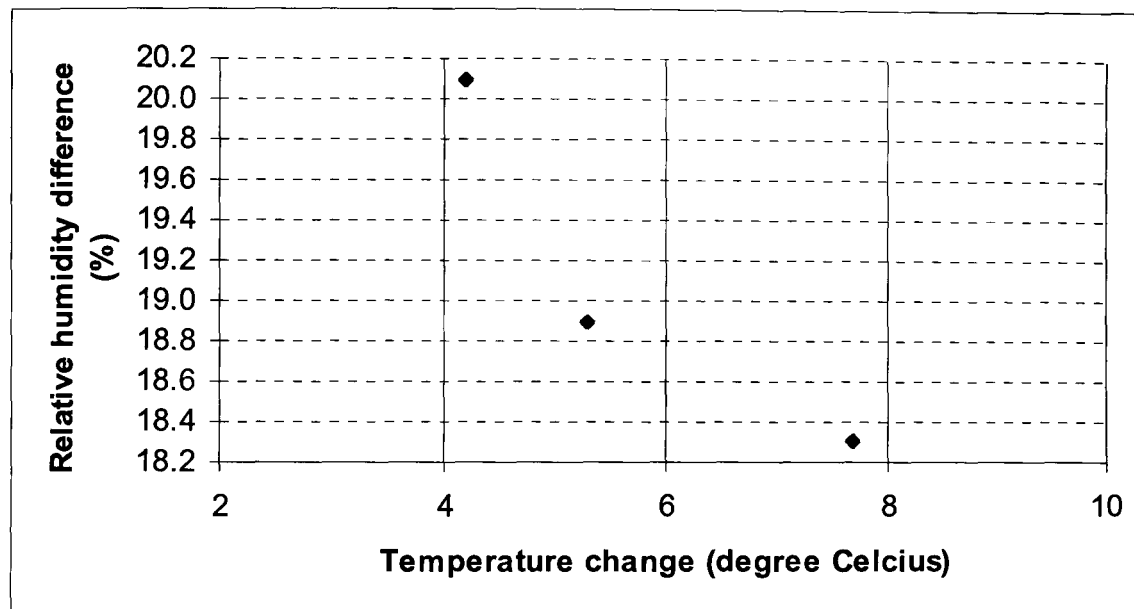


Figure 5.29 Variation of relative humidity difference with temperature change of the evaporative cooling system

Similar to temperature effect test above, corresponding relative humidity outlet conditions were also observed under constant intake air velocity of 3.1m/s. Figure 5.30 shows the timely variation of supply and outlet air relative humidity across the indirect evaporative cooling unit. With a supply air range of 30.3 to 40.2%, the variation showed corresponding range of 58 to 65% at the outlet conditions. The increase in relative humidity was therefore 24.8 to 27.7% as the outlet conditions were approaching saturation. This performance indicated the efficiency of the system in minimising the rise in relative humidity that can be supplied to the building environment. It also showed that even at a low level of supply relative humidity, the system can provide outlet values within the range of comfort limits.

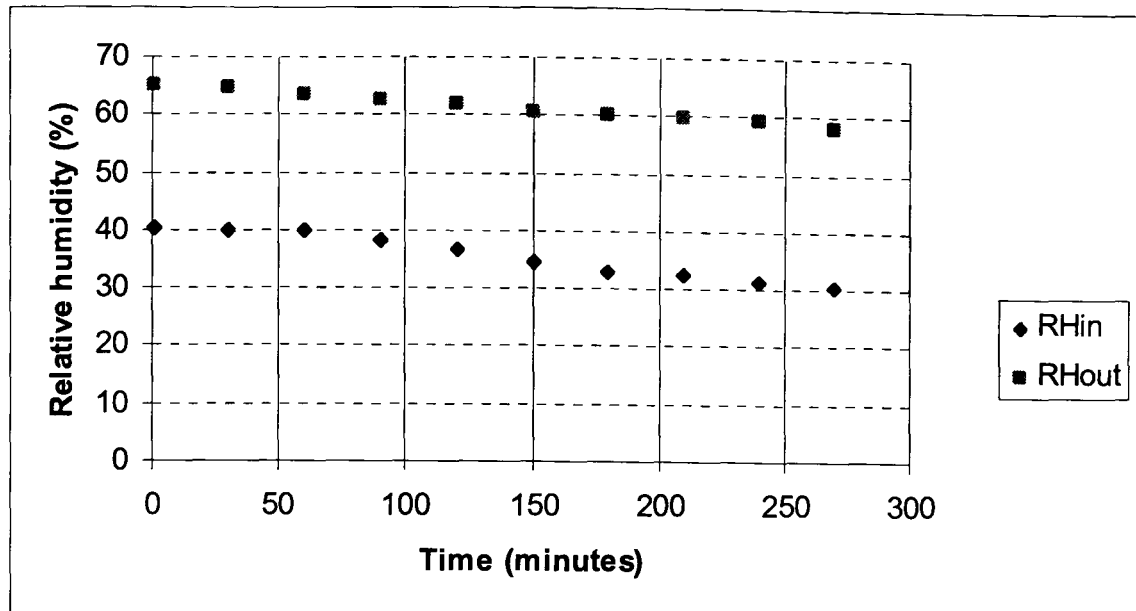


Figure 5.30 Timely variation of supply and outlet air relative humidity across the indirect evaporative cooling unit

5.6.2.3 Cooling capacity

Figure 5.31 shows variation of cooling capacity with different values of supply air velocities ranging from 1.2 to 3.1 m/s. The trend shows that the cooling capacity increases linearly with increasing air velocity as a result of the enhancement of heat and mass transfer. The main reason for that was due enthalpy difference between the supply and outlet air with larger airflow is higher, resulting in bigger cooling capacity.

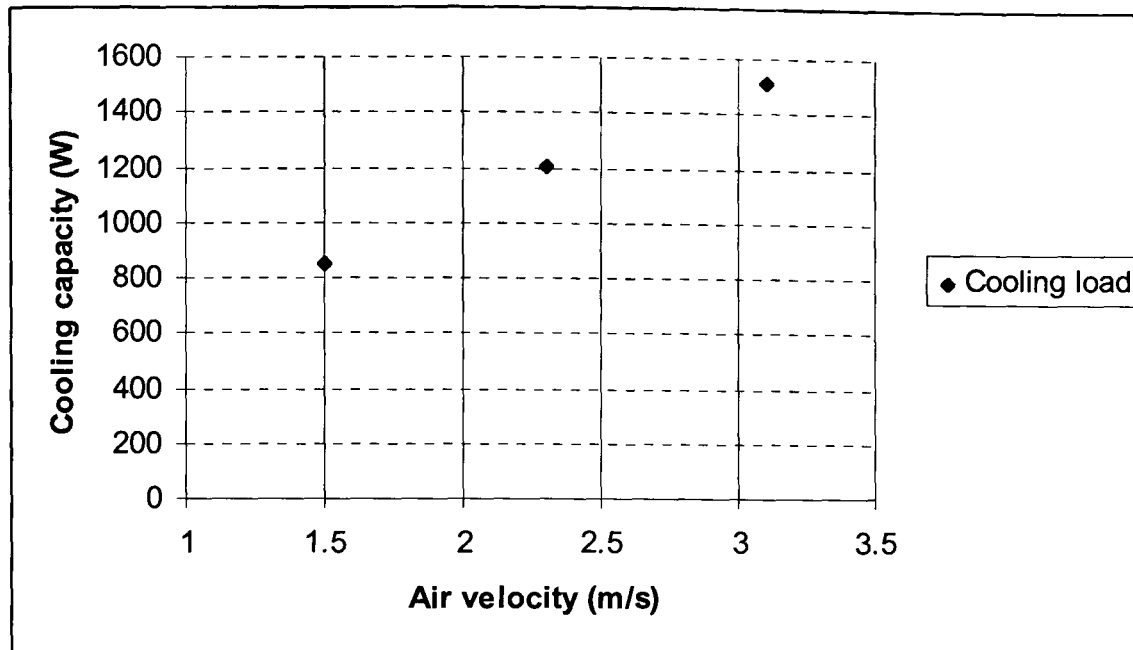


Figure 5.31 Variation of cooling capacity at different air velocity

Figure 5.32 plots show the cooling capacity variation with supply temperature. From the figure, it can be seen that, maximum cooling capacity of 1512.5W was calculated at 4.2°C temperature different and 18.3% rise in relative humidity across the indirect evaporative cooling unit at 3.1m.s of air velocity and 30.5°C supply air temperature.

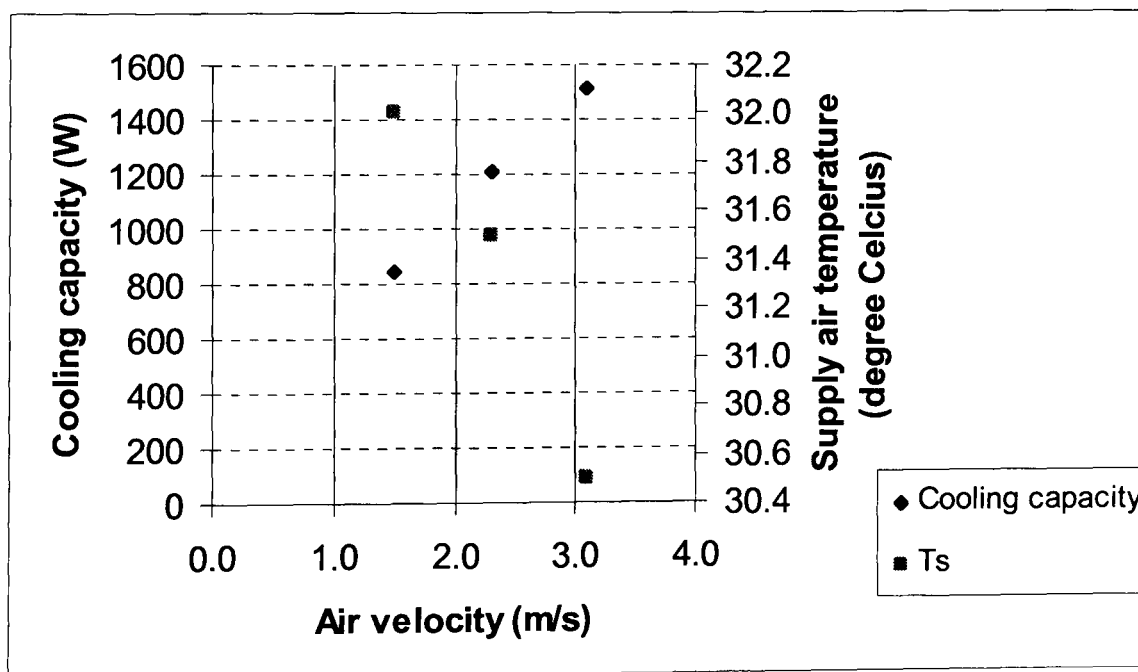


Figure 5.32 Cooling capacity variation with supply temperature

5.6.2.4 Water consumption rate

Table 5.7 contains the experimental results for the water consumption analysis of the system. Figure 5.33 plots show the difference between supply air and outlet air temperatures variation with water consumption rate. The maximum water consumption rate of 0.446g/s occurred at the highest airflow rate of 3.1m/s corresponding to 30.5°C of supply air temperature.

Table 5.7 Water consumption rate of the system

Air velocity (m/s)	T _s (°C)	T _o (°C)	Water consumption rate, M _w (g/s)
1.5	32.0	24.3	0.214
2.3	31.5	26.2	0.360
3.1	30.5	26.3	0.446

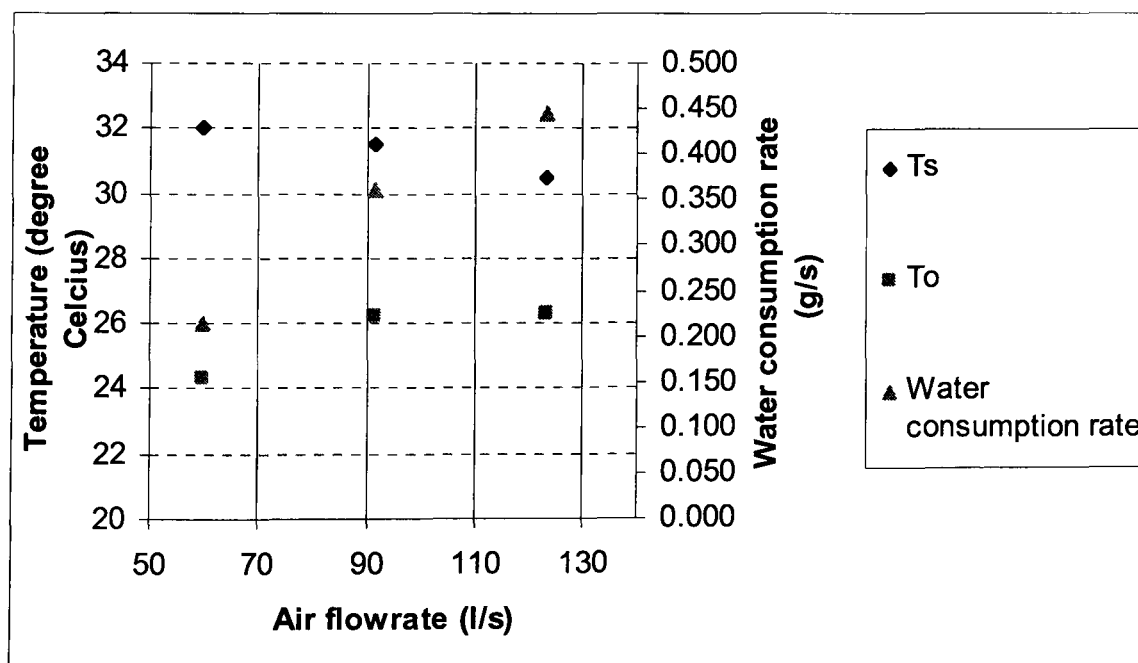


Figure 5.33 Effect of supply air and outlet air temperatures on water consumption rate

Figure 5.34 shows that as the difference between supply air and outlet air temperature increases the water consumption rate reduces. This is because the higher the temperature change lowers the temperature of the indirect evaporative cooling unit surface, hence lowers the evaporation rate.

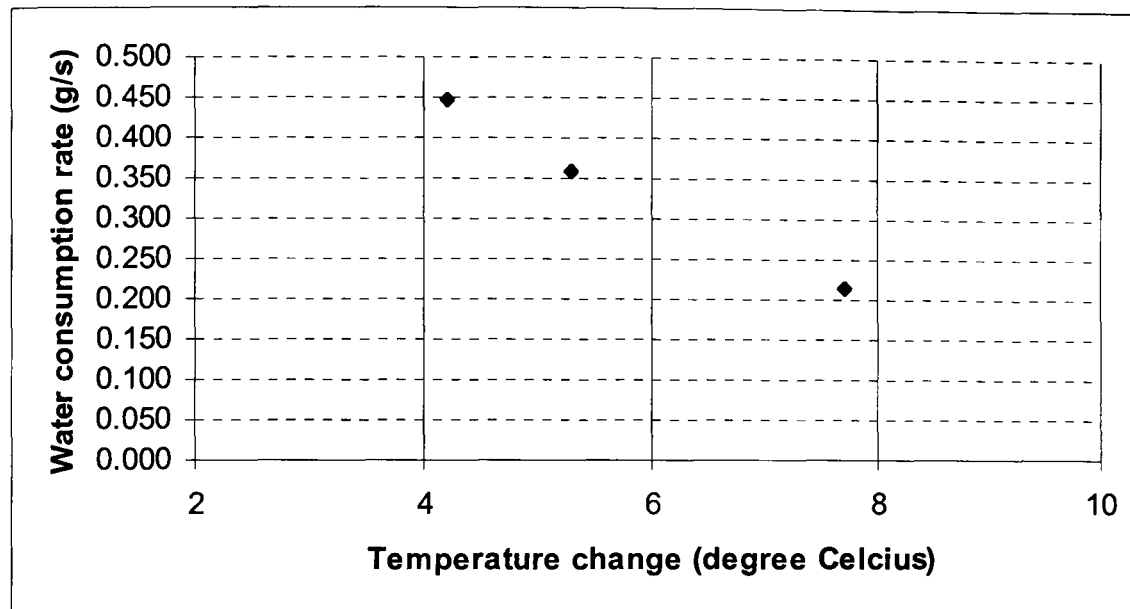


Figure 5.34 Water consumption rate versus temperature change between supply air and outlet air temperatures

5.6.2.5 Cooling efficiency

The cooling efficiency was calculated for varying air intake velocity which ranged from 1.5 to 3.1m/s in terms of dew point and wet bulb, while keeping the indoor temperature at 29°C. It can be seen that both dew point and wet bulb cooling efficiency decrease with increasing air velocity as illustrated in Figure 5.35. The dew point cooling efficiency ranged from 47% at air velocity of 1.5 to 29% at 3.1m/s. Whilst, the wet bulb cooling efficiency ranged from 54% at air velocity of 1.5m/s to 31% at 3.1m/s. As the air velocity decreases the air has more residence time in the cooling core, hence more heat and moisture transfer takes place.

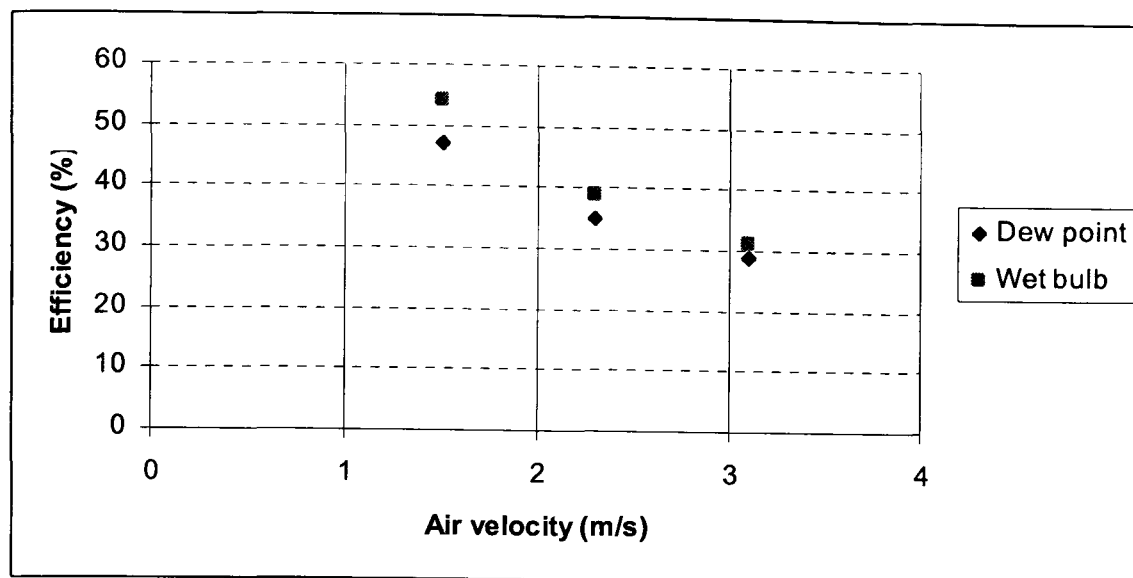


Figure 5.35 Cooling efficiency vs air velocity

5.6.3 Coefficient of performance

Tests were done at four different air intake velocities which are 1.2m/s, 1.5m/s, 2.3m/s and 3.1m/s. Table 5.8 summarize the results of coefficient of performance.

Table 5.8 The results of coefficient of performance

Air intake velocities (m/s)	Cooling capacity (W)	Power input (Fans and water pump) (W)	COP
1.5	847.7	25.80	32.86
2.3	1208.0	42.36	28.52
3.1	1512.5	68.52	22.07

5.6.4 System performance

The air velocities were varied and the corresponding temperature values were recorded. Table 5.9 shows the temperature values of the system for different air velocities. The wind-catcher or ambient temperature was recorded at 37°C and room temperature was at 29°C. From the table, a drop ranged from 0.9 to 1.8°C was observed when the warm air entered the intake duct in the wind-catcher unit. This

shows that the wind-catcher helped to reduce the temperature of incoming warm air. When the air passed through the heat recovery unit, a drop ranged from 4.1 to 4.7°C was recorded as heat transferred occurred via the core. A drop of 4.2 to 7.7°C was then gained after the air passed through the indirect evaporative cooler. Thus, it can be seen that, from the beginning air entered the system until supplied to the room; a drop of 11.5 to 12.7°C was gained.

Table 5.9 The temperature values of the system

Air velocity (m/s)	T_{wc}	T_i	T_s	T_o	T_r	T_e
1.5	37.0	36.1	32.0	24.3	29.9	33.9
2.3	37.0	36.9	31.5	26.2	29.3	33.8
3.1	37.0	35.2	30.5	26.3	25.5	30.2

The tests were also conducted under dry condition that is without water added to the indirect evaporative cooling unit. Figure 5.36 shows the variation of temperature change of heat recovery unit and indirect evaporative cooling unit. From the figure, the temperature change for heat recovery unit ranged from 4.0 to 4.7°C. Whilst, the temperature change between supply air and outlet air of indirect evaporative cooling unit under dry condition ranged from 2.0 to 2.5 °C and with water added, the temperature ranged from 4.2 to 7.7°C providing very acceptable indoor conditions.

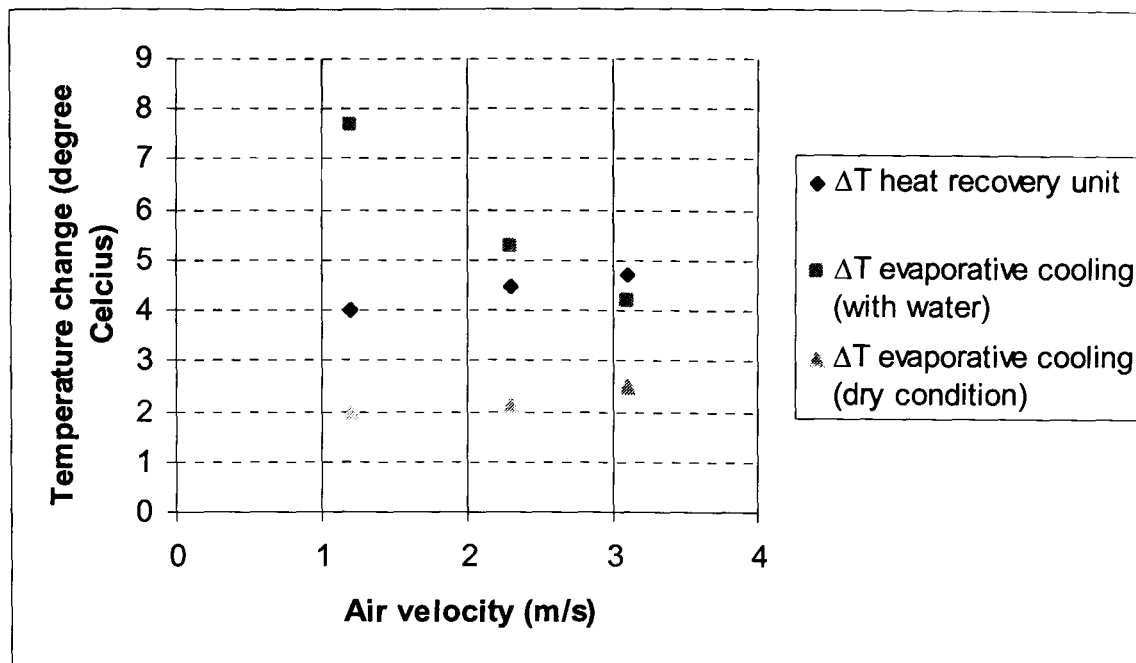


Figure 5.36 Variation of temperature change of heat recovery unit and indirect evaporative cooler

The performance results of this integrated heat recovery system associated with wind-catcher and indirect evaporative cooling are summarized in Table 5.10 and Figure 5.37 plotted the capacity of energy of this system.

Table 5.10 Performance results

Air velocity (m/s)	Transferred heat, q_{HR} (W)	Cooling capacity, q_c (W)	ϵ_{HR} (%)	ϵ_{C-wet} bulb (%)	ϵ_{C-dew} point (%)	ΔT_{HR} (°C)	ΔT_C (°C)
1.5	312.0	847.7	64	54	47	4.0	7.7
2.3	535.5	1208.0	58	39	35	4.5	5.3
3.1	757.6	1512.5	47	31	29	4.7	4.2

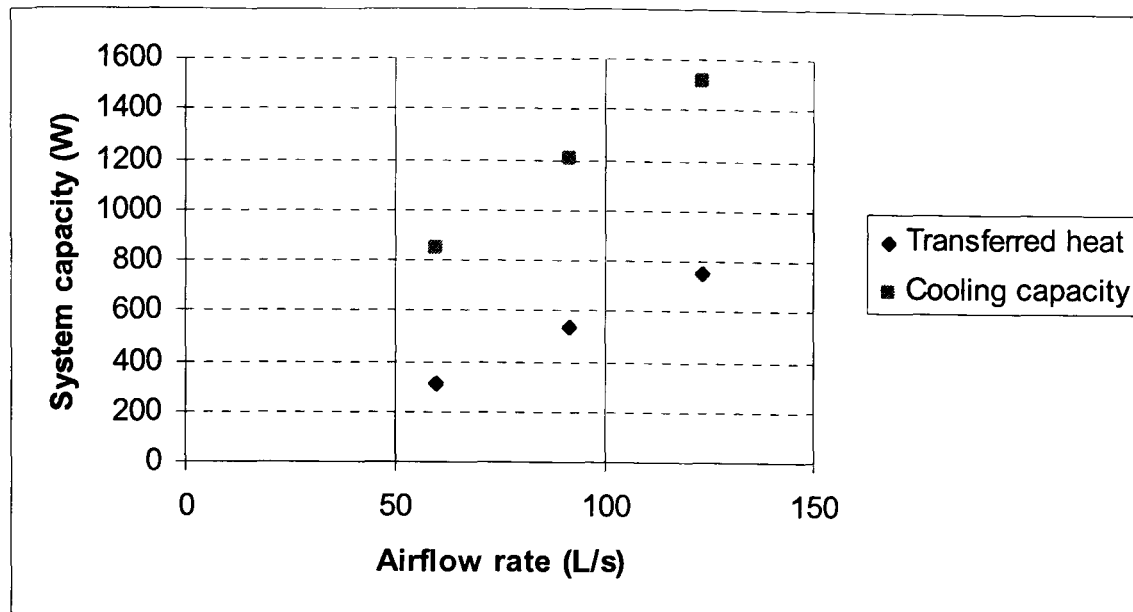


Figure 5.37 System capacity vs volume airflow rate

5.7 Summary

This chapter explored development and experimental work of an integrated system of three major working units; heat recovery, wind-catcher and evaporative cooling which have been combined together. The system was investigated in a large-scale model under laboratory condition. The main conclusions that can be drawn from the results obtained during this investigation are that the integrated heat recovery system associated with wind-catcher and evaporative cooling, allow part of the energy from the return airflow to be recovered, thus improving energy efficiency and reducing environmental impact and for long term it has the ability to be cost effective in energy saving. The combination of wind-catcher with heat recovery unit helps to assist airflow in and out. On the other hand, the combination of wind-catcher with heat recovery unit has devoted the decreasing of incoming warm air temperature which ranged from 0.9 to 1.8°C. More dropping of warm air temperature observed as it passed through the heat recovery core. Thus, generally it can be said that from the beginning warm air entered the system and until supplied to the room, a drop of 11.5 to 12.7°C was gained. This concludes that wind-catcher and heat recovery unit

themselves also contributed to the decreasing of incoming warm air temperature as a result of convection between air and material surface.

At air velocities ranged from 1.2 to 3.1m/s, heat recovery efficiency ranged from 70 to 50% for cold air condition and 69 to 49% for warm air condition. This results show that as the airflow rate increases, the efficiency decreases. The maximum recovered energy of 772.9W was obtained at 5.2°C temperature change of heat recovery unit. From this investigation it can be concluded that the cooling capacity of indirect evaporative cooling unit employing dew point PEC core increases linearly with increasing air velocity as a result of the enhancement of heat and mass transfer in wetted pads. The maximum cooling capacity of 1.5kW was calculated at 4.2°C temperature change and 18.3% rise in relative humidity across the indirect evaporative cooling unit at 3.1m/s of air velocity and 30.5°C supply air temperature. The dew point cooling efficiency ranged from 47% at air velocity of 1.5 to 29% at 3.1m/s. Whilst, the wet bulb cooling efficiency ranged from 54% at air velocity of 1.5m/s to 31% at 3.1m/s. In addition, it is observed that the temperature change for heat recovery unit ranged from 4.0 to 4.7°C.

Besides, the novel feature of this system is low water consumption for evaporative cooling system and less energy consumption as DC power fan has been used. Thus, this system could fulfil the needs of energy-efficient system as it is developed by combining of three different low carbon technologies. Another alternative that can be done to this system is the application of wind cowl or wind turbine to replace the wind-catcher unit.

CHAPTER 6

Development and Performance Investigation of Novel Building Integrated Heat Recovery (BIHR) System

6.1 Introduction

Virtually every aspect of a building's design, construction and service has an effect on its energy consumption. In order to reduce the energy consumption to a minimum, whilst maintaining comfort standards, it is important to identify the design aspect in energy performance. For instance, thermal insulation technology is one of design aspect that can be applied to reduce thermal losses or gains in buildings through the envelope. The advanced technology in thermal insulation and airtightness of buildings' envelopes, which greatly reduce thermal losses and air filtrations, increases ventilation requirements and consequently, raises the thermal losses associated with the ventilation system (Liddament, 1998). On the other hand, in a modern building, the ventilation losses may become more than 50% of total thermal losses (Routlet 2001). Taking into account the above cited facts, to reduce these losses and to reach a low energy standard for the building, integration of a heat recovery system and improvement of the efficiency in building ventilation systems are required. In addition, buildings also have advantages in relation to the implementation of building integrated system where these systems can make a significant percentage contribution to overall home energy loads.

Integrating heat recovery system into a building envelope represents significant progress in energy-efficient technologies. In this configuration it is not only acts a heat recovery, but also as a contribution to building thermal insulation.

The integration of this system leads to a reduction of thermal ventilation losses of the building and to a reduction of the required energy support. The integration of existing structural elements like walls, roofs and floors within the building and its foundation can lead to economically and ecologically optimised solutions.

By taking into account all the requirements of energy-efficient, the need for balanced ventilation, the problems facing by individual MVHR system, thermal loads in terms of losses and gains, in this chapter the integration of heat recovery system with building part so-called building integrated heat recovery (BIHR) was explored, developed and investigated. It introduces a new approach to MVHR system, an established technology that uses a modified insulation panel, linking the inside and outside of a building, to recover heat or energy while extracting waste air and supplying fresh air. The chapter presents the design, development, description, and experimental work of prototype unit, full-scale measurements on real buildings, investigation of the system with photovoltaic power, construction and investigation of improved system, economic analysis and the development of the system with fibrous material in the internal channels adaptable for cooling and dehumidification. The work in this chapter aims to integrate heat recovery with building envelope (roof/wall/floor) to become one device with multifunction (building integrated heat recovery/cooling/air dehumidifier) in one system.

6.2 System design features and construction

The incorporation of heat recovery unit into buildings, referred to as building integrated heat recovery (BIHR), replaces conventional building elements such as

roof tiles, floor or wall that perform the same functions but also provide energy-efficient system to recover wasted heat or energy.

Building integrated heat recovery (BIHR) panel is a system that provides insulation, ventilation and heat recovery in one integrated panel. This invention relates to improvements or relating to insulating panels where it can be fitted within the building (wall, floor or roof) to recover heat or energy at near maximum efficiency, reduce cooling loads on air-conditioning and benefit both building and occupants from improved air quality. The system comprises an insulating and ventilating system in which the system includes a plurality of insulating panels formed from a substantially rigid insulating material such as polystyrene and having an internal channel. The double function of BIHR gives us new intelligent solutions, an improvement of the eco-efficiency and an increase in value of modern sustainable buildings.

Thus, this system provides an improved insulating panel with economic use and positioning of thermal insulation additionally comprises thermally efficient means for ventilating a building using counter-flow heat exchange. The material used to thermally insulate a building envelope can, at the same time, be used to house and insulate a MVHR unit. By the diagonal insertion, through an exterior element (wall, roof or floor), of a counter-flow air to air heat exchanger, using one pass in each direction (forming a double duct), waste internal air can be exchanged with fresh external air whilst recovering heat.

The diagonal positioning of the double duct connects the internal conditioned space of the building with the outside, for ventilation purpose, while also insulating the duct as heat transfer takes place between the two temperature profiles (the mean temperature of the airflows along the duct being one, the other being the temperature profile through the building element). Figure 6.1 shows the schematic diagram of the BIHR panel. The constructions of the system are described as follows:

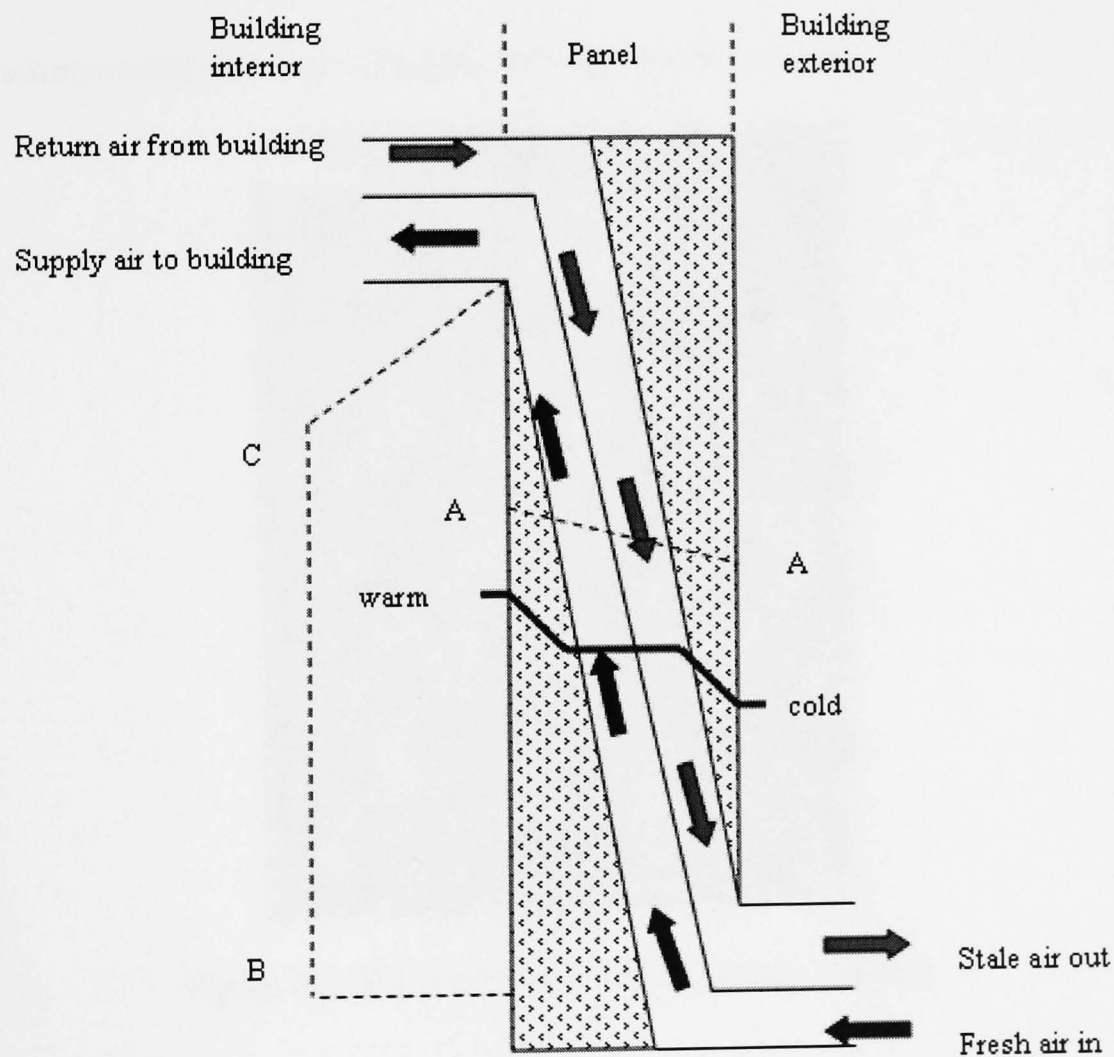


Figure 6.1 Schematic sectional view of building integrated heat recovery panel

- The panel was designed as a counter-flow configuration to recover exhaust heat in order to preheat supply air for buildings.

- The layered panel consists of a sheathing plate and insulating panel in which the insulating was mounted on spacer members, attached to its first face, to the rear surface of the sheathing plate.
- The insulating panel used to form part of an exterior element (wall or roof) of a building for thermal insulation and ventilation and heat recovery purpose comprising two wedges shaped layers of thermal insulation material that sandwich an air duct. The wedge shaped (Figure 6.2) layers opposed such that their combined thickness and consequently their insulating effectiveness, was substantially the same throughout the length of the panel.



Figure 6.2 The wedge layer of insulation material

- Figure 6.3 shows the schematic sectional view of internal channels along the line A-A. The internal channel of BIHR comprises an air-intake channel, which permits an airflow from the exterior to the interior of a building in which the system was installed and air-extract channel which permits an air-flow from the interior to the exterior of the building. The internal channel was

divided into the air-intake channel and air-extract channel by a heat transfer surface which provides a substantially air-tight seal between the air-intake and air-extract channel and in use, permits the transfer of heat energy between airflows within the respective channels.

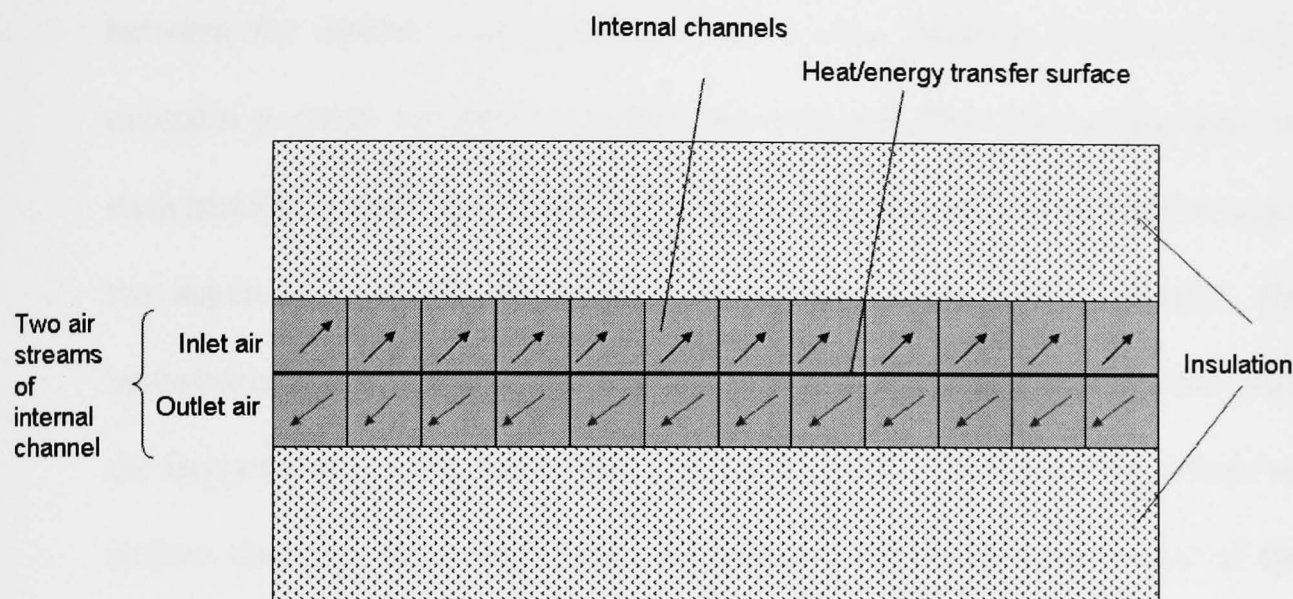


Figure 6.3 Schematic sectional view along the line A-A

- The heat recovery core is made of polycarbonate and insulated with insulation material. The insulation material was utilised to separate the two layers and their corresponding airflows, with the insulation material interposed between the ventilation layers to reduce heat transfer between each ventilation layer and control relating to condensation rather than to provide fresh air for the occupants. The insulation material is made of expanded plastics foam which is polystyrene. The insulating panels were adapted for insertion between adjacent trusses of a roof or between stud-work or within a cavity of an external wall structure.
- The air duct being divided along the same plane as the sandwich layering to provide separated airways/streams for fresh air to enter the building and for stale air to exit the building. The dividing layer, used to facilitate heat transfer

between the counter flowing airstreams and being of a nominal thickness would preferably have reinforcement that would laterally separate the individual airflows.

- In used of the described system, a number of insulating panels were interposed between the interior and exterior structure of a building in order to help maintain a stable temperature within the building. The internal channels of each insulating panel were preferably arranged so that as heat transfer between the separated airflows takes place along the length of the channel, the temperature of the respective airflows within each channel corresponds with the temperature profile across the insulating panel. That is to say, where an airflow through the channel has a temperature which is close to that of the temperature inside the building, the degree of insulation between the channel (and thus the airflow) and the inside of the building is less than corresponding degree of insulation between the channel and the outside of the building.
- According to this arrangement, the degree of insulation on the side of the insulating panel exposed to the exterior of the building decreases from B to C along the length of the panel. Conversely, the degree of insulation on the side of the insulating panel exposed to the exterior of the building increases from B to C as the temperature of the airflow tends towards the external air temperature.
- Due to the graduation of the thickness of insulating material on each side of the air ducts, uniform heat transfer across the panel is maintained, optimising the insulating material used in the panel, reducing fabric heat losses or gains. Besides, due to the graduation of the thickness of insulation material on each

side of the air ducts, the heat transfer process is insulated therefore reducing ventilation heat losses or gains.

- In this system, independent ducts are connected via a manifold to each respective channel to isolate the respective air-flow through channels. In turn, the ducting was subsequently connected to one or more ventilation intake/extract ports within a room. The manifold comprises a system control means for isolating a flow of air through ducting connecting particular ventilation extract/intake ports from a specific location within the building. This arrangement facilitates modification of the system to provide a plurality of multiple closed ventilation system to avoid noise transfer, for example that associated with a fan operating in bathroom or kitchen, through the ducting to a quiet room such as a bedroom.

Referring to Figure 6.4, there is shown the air flow within insulation material of heat recovery core. The panel was designed as a counter flow heat exchanger to recover exhaust heat to preheat supply air for buildings.

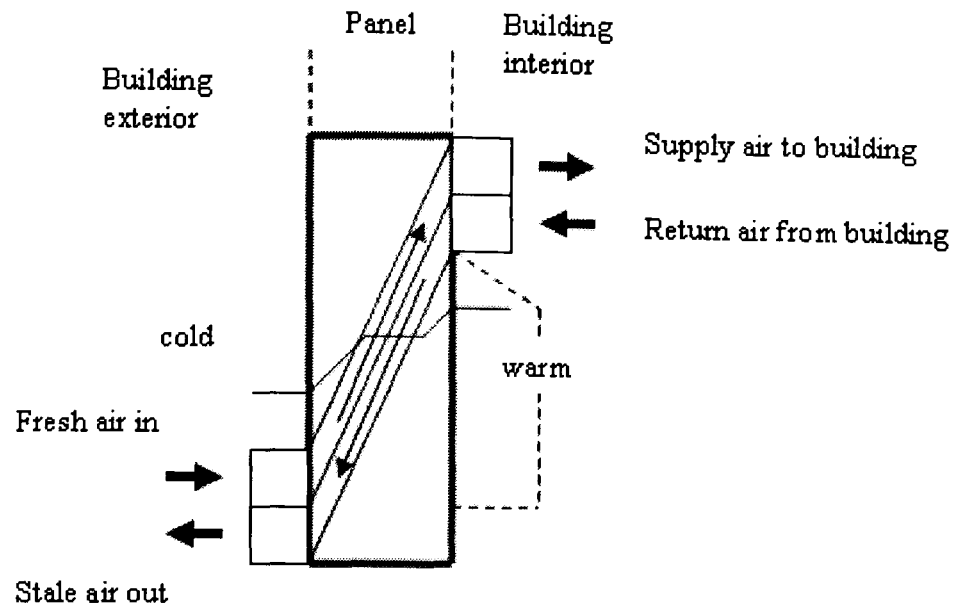


Figure 6.4 The internal channel of insulating panel

6.3 Laboratory investigation of BIHR prototype panel

A prototype of BIHR has been constructed and laboratory tests were performed in Energy Learning Unit Laboratory in Department of Architecture and Built Environment, University of Nottingham. A test room was built which has a dimension of 3000mm x 1500mm x 2400mm (L x W x D) and BIHR prototype has been placed as shown in Figure 6.5.

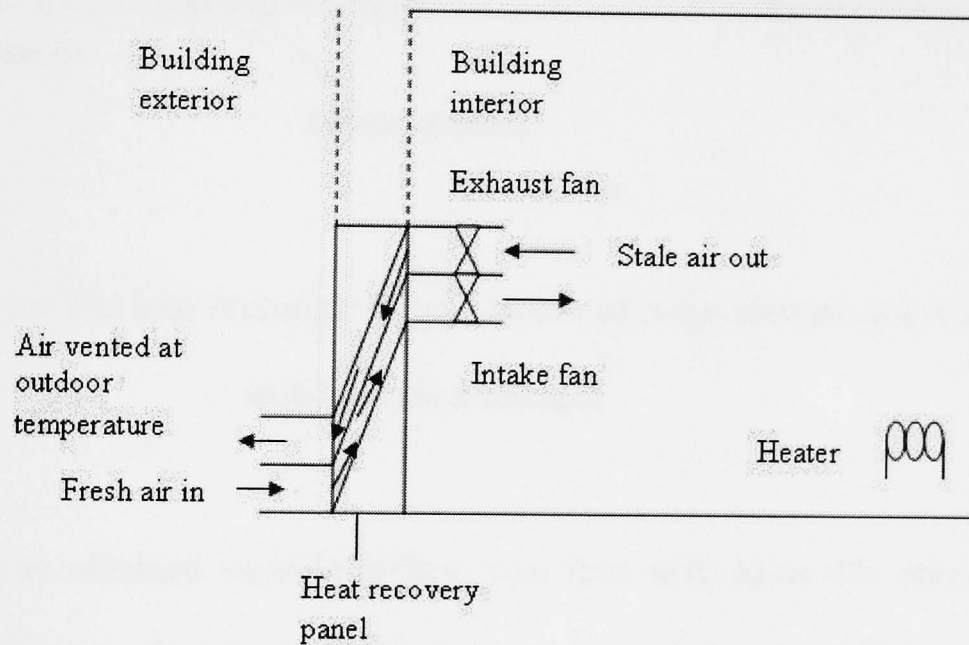
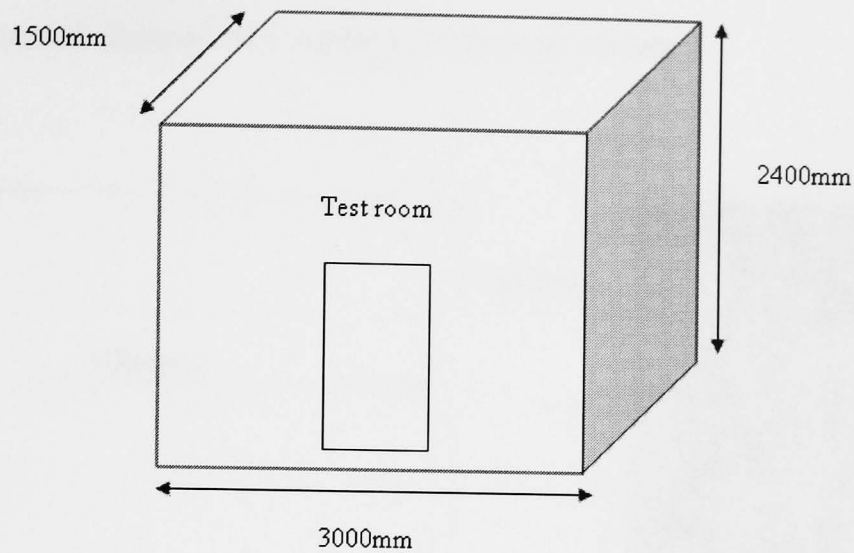


Figure 6.5: Experimental rigs for testing structural insulated heat recovery panel performance

Figure 6.6 shows the BIHR prototype panel which has overall dimensions of 1000mm x 1000mm x 16mm. This panel is made of polycarbonate and insulated with expanded polystyrene. The stream was divided into the air intake stream and air exhaust stream by a 2mm thick heat transfer surface which provides a substantially air-tight seal between the air intake and air exhaust stream and permits the transfer of

heat energy between airflows within the respective streams. The heat transfer surface has 45 effective internal channels for supply/exhaust air stream.

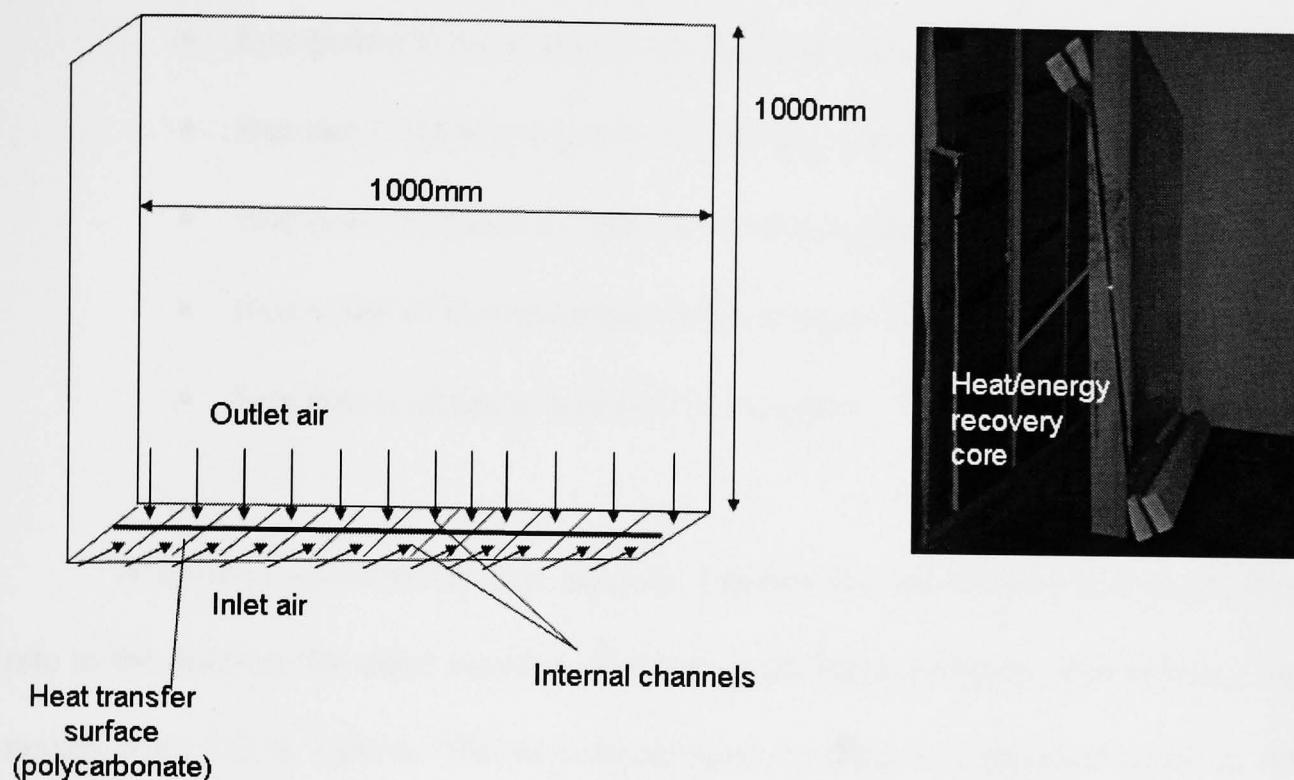


Figure 6.6 The heat exchanger (core) is made of polycarbonate and insulated with insulation material

In order to obtain variable airflow, two fans with adjustable speed were installed in the 100mm of intake and exhaust ducts and each duct has 1000mm length ($A=7.9 \times 10^{-3}$). The fans were used to circulate air throughout the test room and to exhaust stale air from room to outside. A heater was used to generate heat production in the test room. The performance was evaluated by calculating the sensible effectiveness from airflow rate and temperature measurements of the intake and exhaust air streams of the heat recovery core. Thermocouples were used to measure the temperatures at different points across the airflow ducts before and after the heat exchanger and were recorded by a data logger with accuracy $\pm 1\%$ and of 0.1°C

resolution. This set up is shown in Figure 6.7. The temperature measurement system consisted of:

- four points of thermocouples for ambient air
- four point of thermocouple in the intake side
- four point of thermocouple in the supply side
- four point of thermocouple in the return side
- four point of thermocouple in the exhaust side
- four points of thermocouples in the room

A hotwire anemometer was used to measure the air velocity and hence flow rate in the ducts at the same location of temperature measurements. The velocity was ranged from 1.0 to 2.0m/s. The procedures used in chapter 4 repeated again in this investigation in order to gain accurate results.

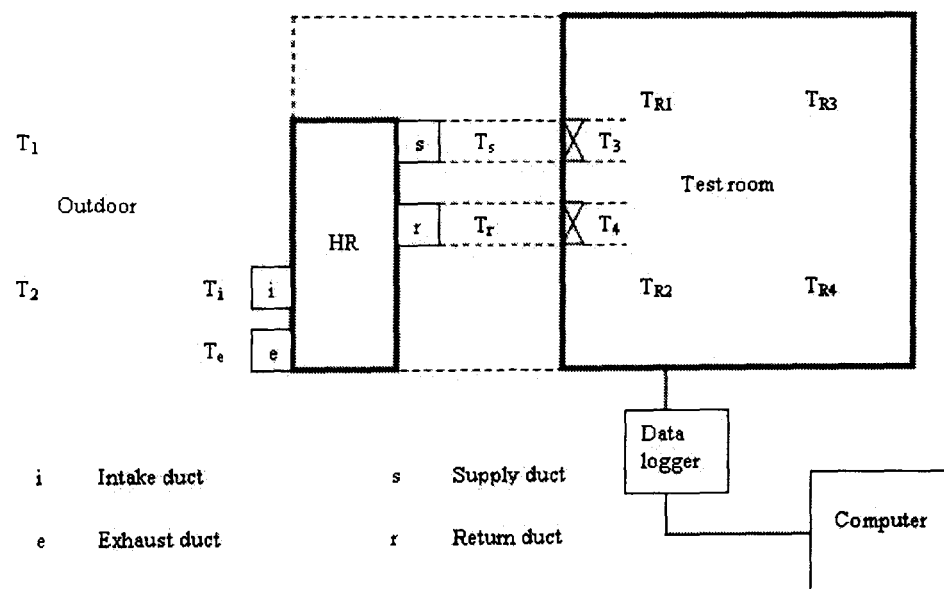


Figure 6.7 Schematic of the set up for temperature measurements

6.3.1 Analysis and results

Tests were performed at mean air velocities ranging from 1.0 to 2.0m/s and the room temperature was kept constant about 23°C. The temperature values of fresh intake air, T_i , supply air to room, T_s , return air, T_r , exhaust air, T_e and ambient air at various airflow rate are shown in Table 6.1.

Table 6.1 Experiments data of prototype

Velocity m/s	Volume airflow rate m ³ /s	T_i °C	T_s °C	T_r °C	T_e °C	Ambient °C
1.0	0.0079	16.9	19.0	20.5	18.3	16.1
1.5	0.0118	17.5	20.1	22.2	19.5	16.2
1.8	0.0141	17.7	20.7	23.3	20.3	16.4
2.0	0.0157	17.6	20.6	24.4	21.0	16.2

Note : Air property calculation at the point where velocity measurements were done

Without the operation of BIHR system, the temperature of fresh ambient air was at 16.1°C and the indoor air temperature was 23°C. The different between both temperatures is 6.9°C. With the installation and operation of BIHR system, for instance at 1.0m/s air velocity, the fresh ambient air coming in changed about 0.8°C at the intake air of BIHR then supplied to room with 19.0°C. Thus, the different between supply air and indoor air was became 4°C showing a smaller value compared to the value without BIHR system. By taking into account all the temperature changes, it can be seen that about 2.1°C has been recovered in supply air streams with the installation and operation of BIHR system. The temperature change across the heat recovery unit was recorded. The temperature change presents the difference between

the return air to heat recovery core and the exhaust air. It was found that the temperature change increased with increasing airflow rate which ranged from 2.2 to 3.4°C with the lowest value corresponding to 0.0079m³/s airflow rate.

The calculated results of BIHR efficiency are indicated in Figure 6.8 with respect to airflow rate in the duct. It was found that the BIHR efficiency decreased with increasing airflow rate which ranged from 50% at airflow rate of 0.0157m³/s to 61.1% at airflow rate of 0.0079m³/s. Also, The BIHR efficiency decreased by about 3.7% with increasing temperature change.

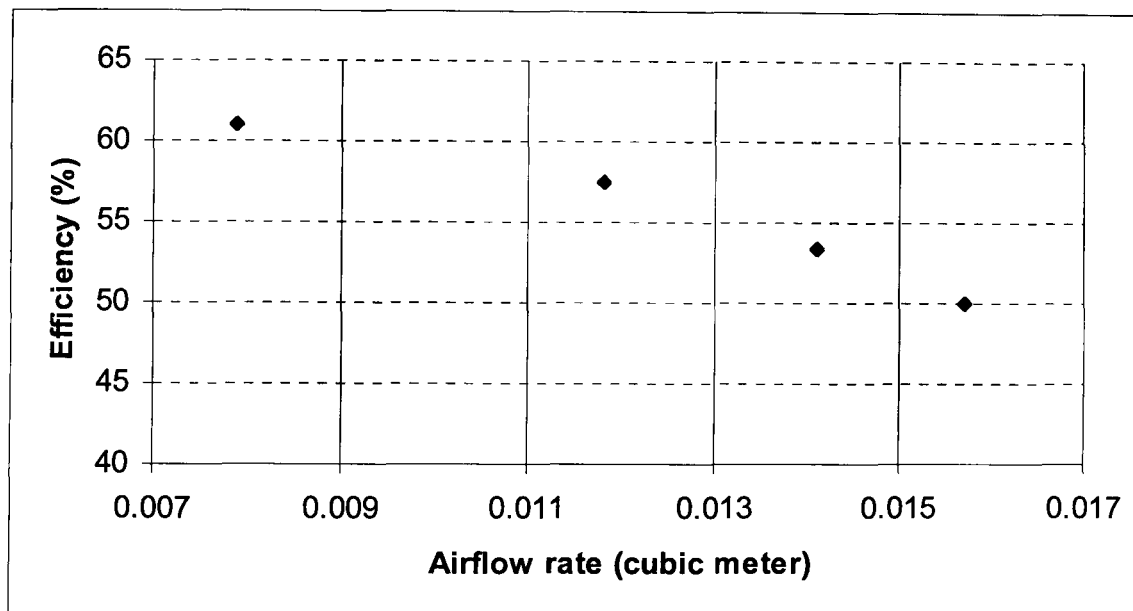


Figure 6.8 BIHR prototype's efficiency

The values of recovered heat or energy through polycarbonate surface are illustrated in Figure 6.9 with respect to airflow rate. The data was taken at supply air of 20.5 to 24.4°C. The trend shows that the recovered heat increases linearly with increasing airflow rate. The maximum recovered heat of 70W was gained at 3.4°C temperature change and a minimum of 22.8 W was calculated at 2.2°C temperature change. This is due to the increases in temperature change or temperature gradient of

the airflow circulating around the panel and as a result the greater heat transmission can be gained.

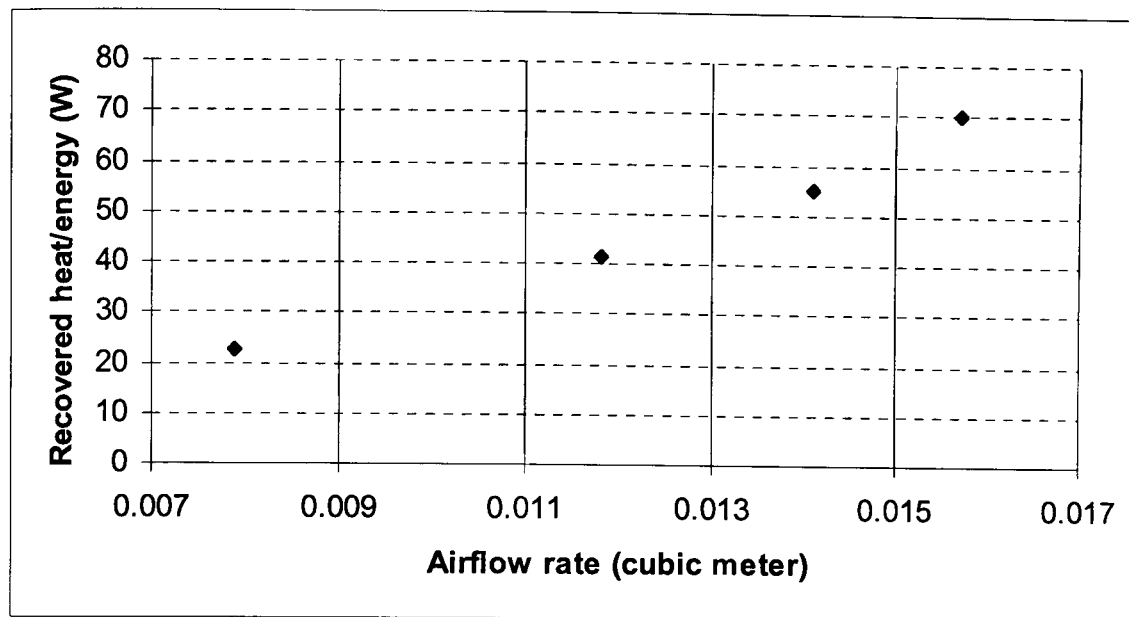


Figure 6.9 Recovered heat of BIHR prototype

Figure 6.10 shows the pressure drop through the duct of BIHR prototype system. The increasing trend in pressure drop with increasing velocity can be observed due to the increasing of flow pattern in the duct and it denotes that at highest velocity of 2.0m/s, pressure drop of 1.14 Pa occurred.

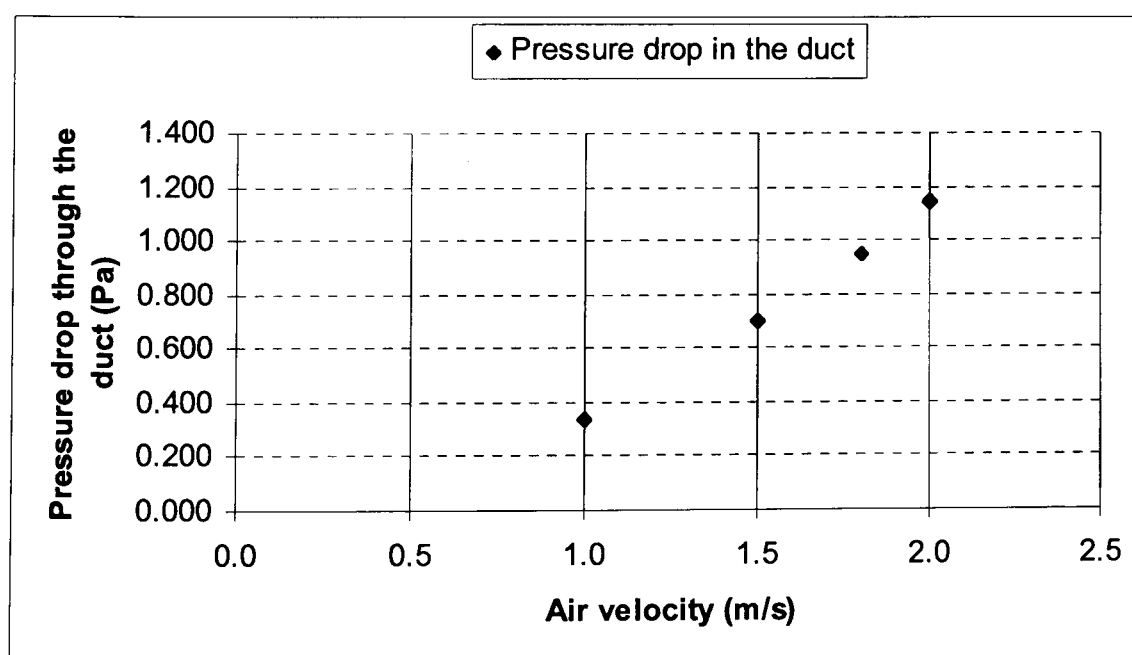


Figure 6.10 Pressure drop through the duct of BIHR prototype system

6.4 Case study I: Full-scale measurements of BIHR panel on a real building in Ashford, Kent (Forstal Farm House)

This section outlines full-scale measurements of the performance of BIHR undertaken on a real building in Forstal Farm, Kent commencing in October 2009. The full-scale test structure and its location are detailed, followed by the experimental techniques applied.

6.4.1 Description of the building

The building has a dimension of 9000mm x 4000mm x 2000mm located at Forstal Farm, Ashford, Kent (Figure 6.11). The wall and the roof of the building were constructed with two layer of plasterboard for the interior part and sterling board (OSB) for the exterior part with a 100mm insulation (ECOTHERM) of expanded polystyrene foam layer in between to reduce the influence of surroundings (Figure 6.12). The floor was made from concrete for the bottom part insulated with a 50mm insulation material and chipboard flooring and was insulated with 50mm insulation material. The insulating panel helps to prevent heat loss from a building in terms of any accumulated heat within a loft space. Figure 6.13 gives all the necessary dimensional information of the building.

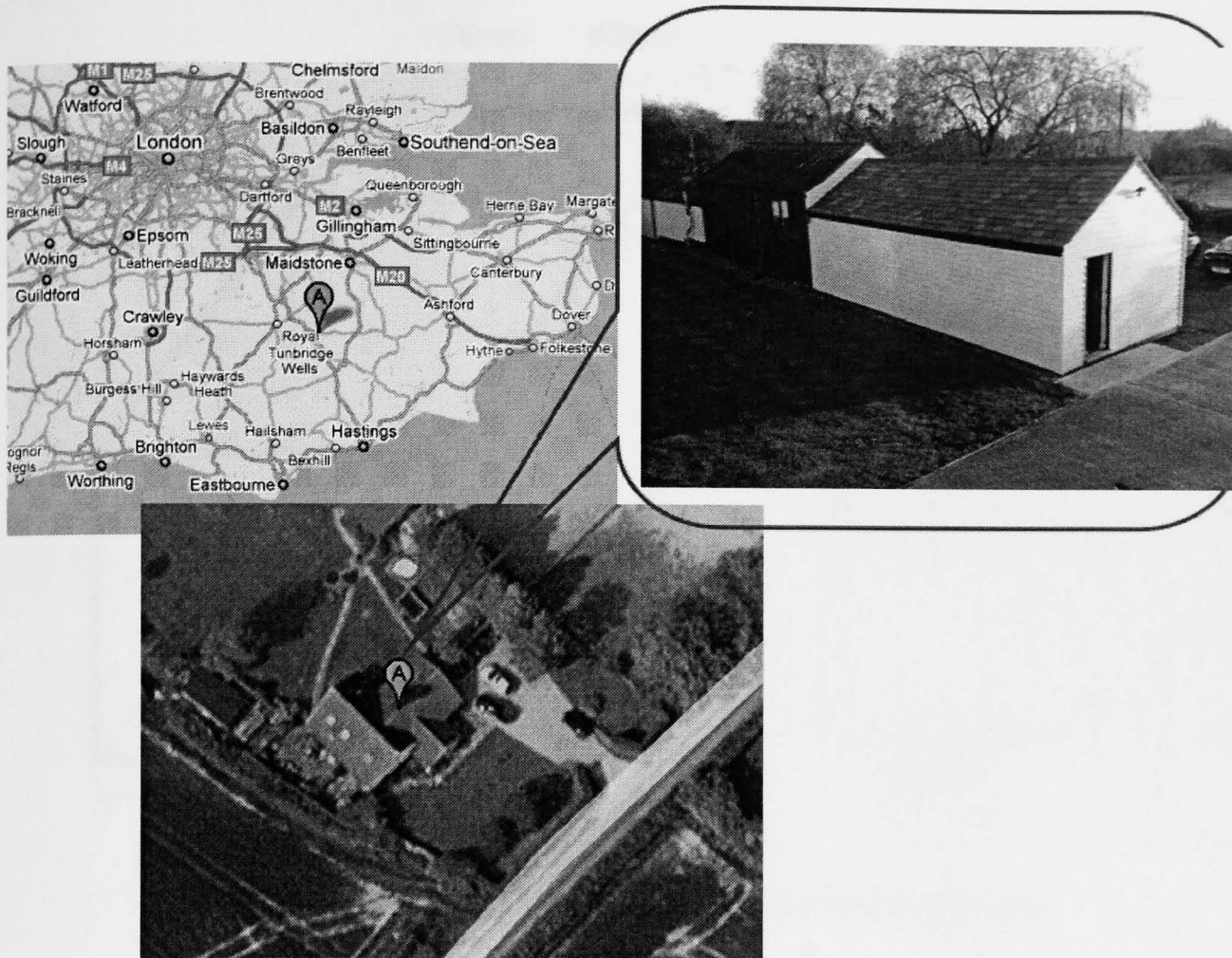


Figure 6.11 Building studied located at Forstal Farm, Kent, UK

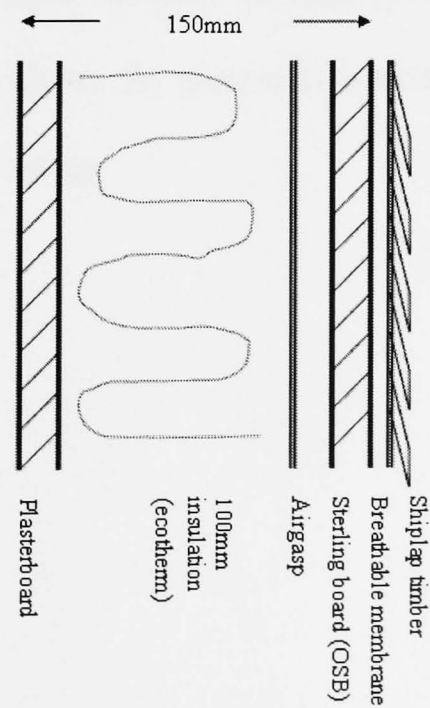


Figure 6.12 Wall structure

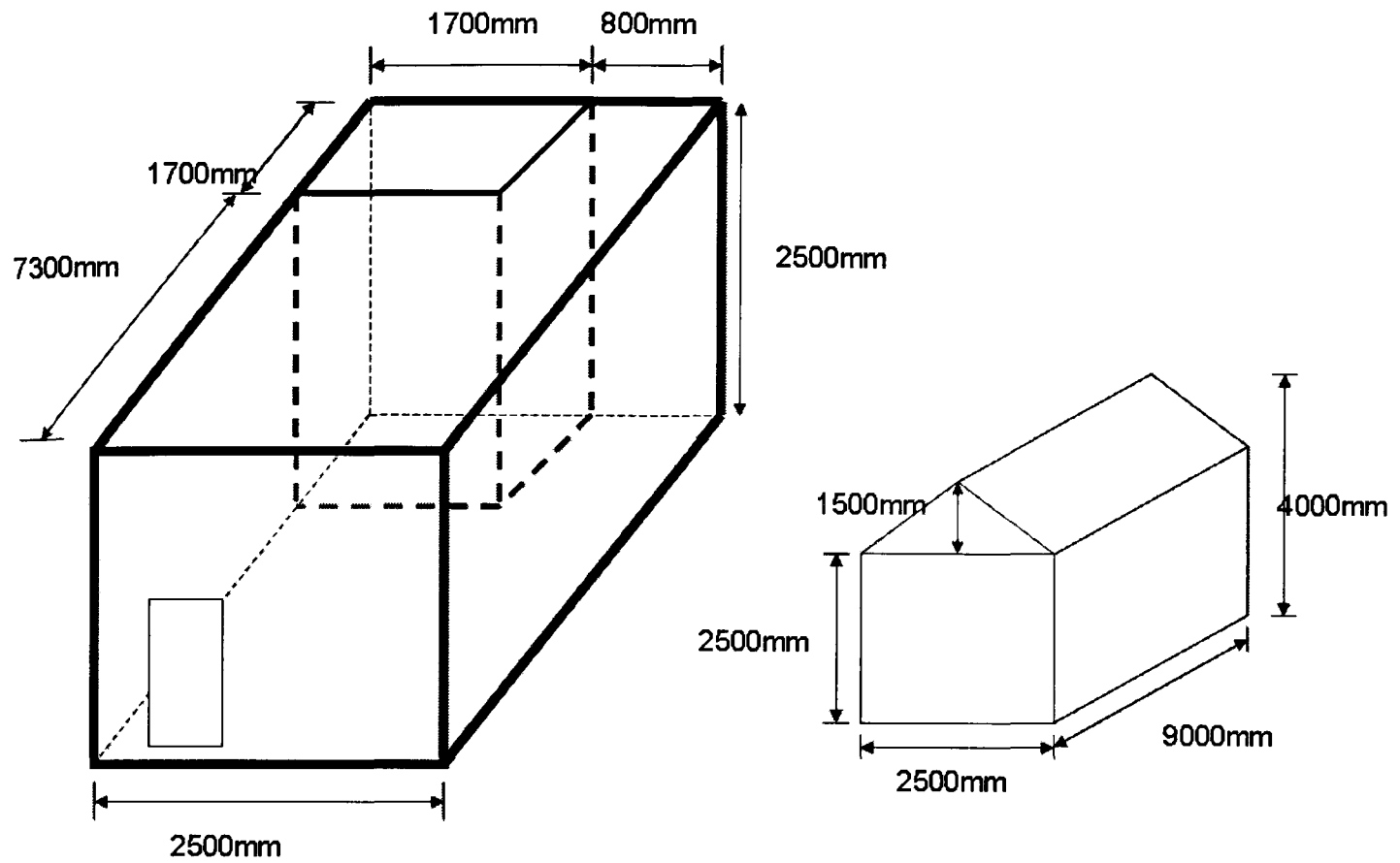


Figure 6.13 Dimensional information of the building studied

6.4.2 Installation of BIHR system on the building

BIHR panel was fitted between the roof trusses over the entire roof space of the building. Figure 6.14 shows the picture of installation and Figure 6.15 shows the schematic diagram of the set up.

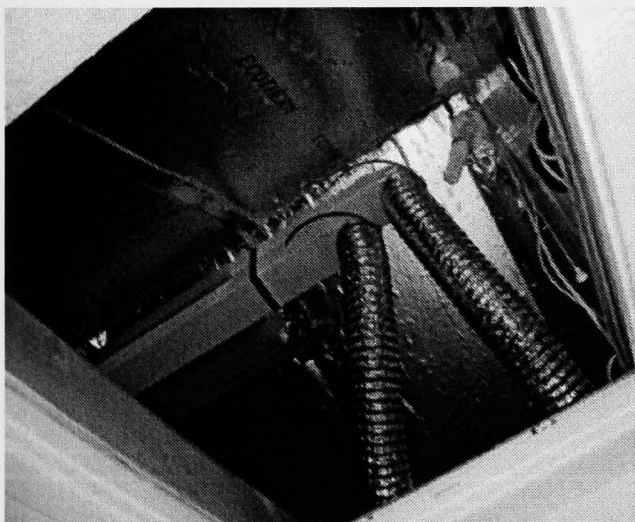
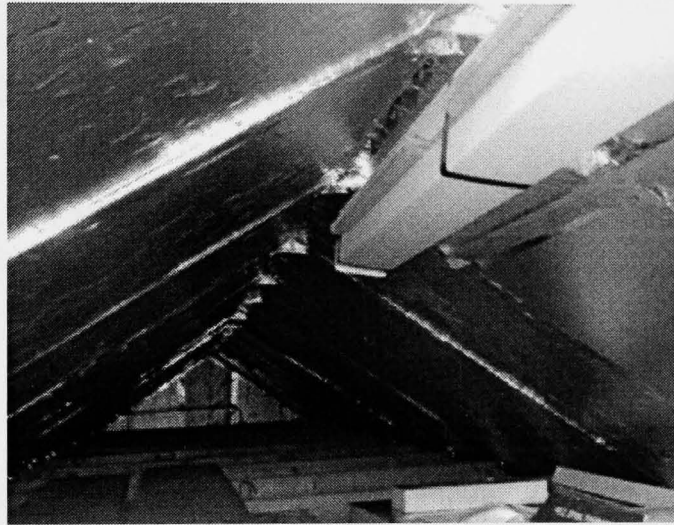
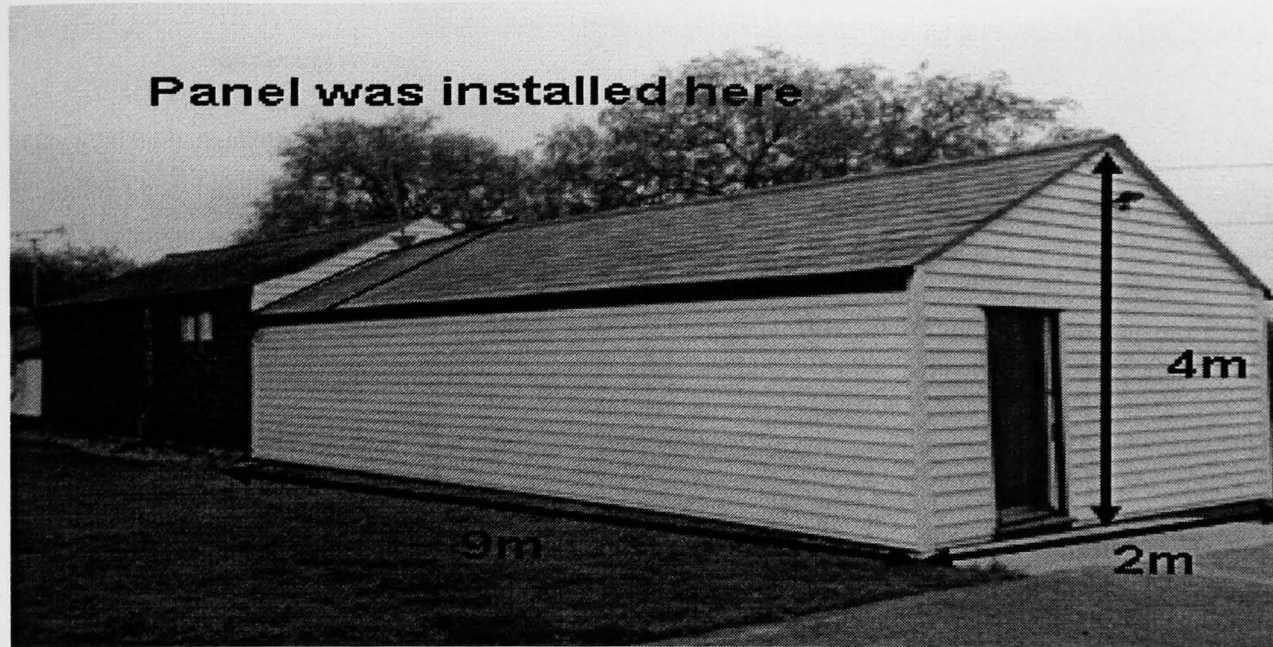


Figure 6.14 Picture of installation

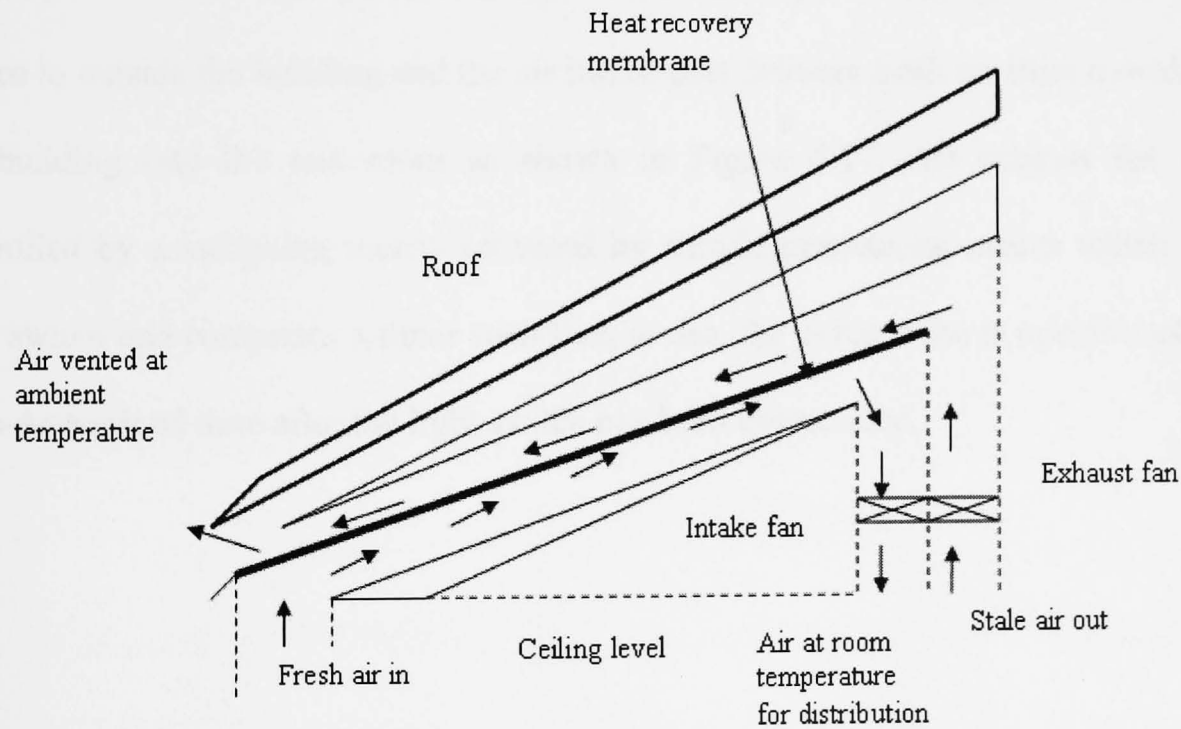
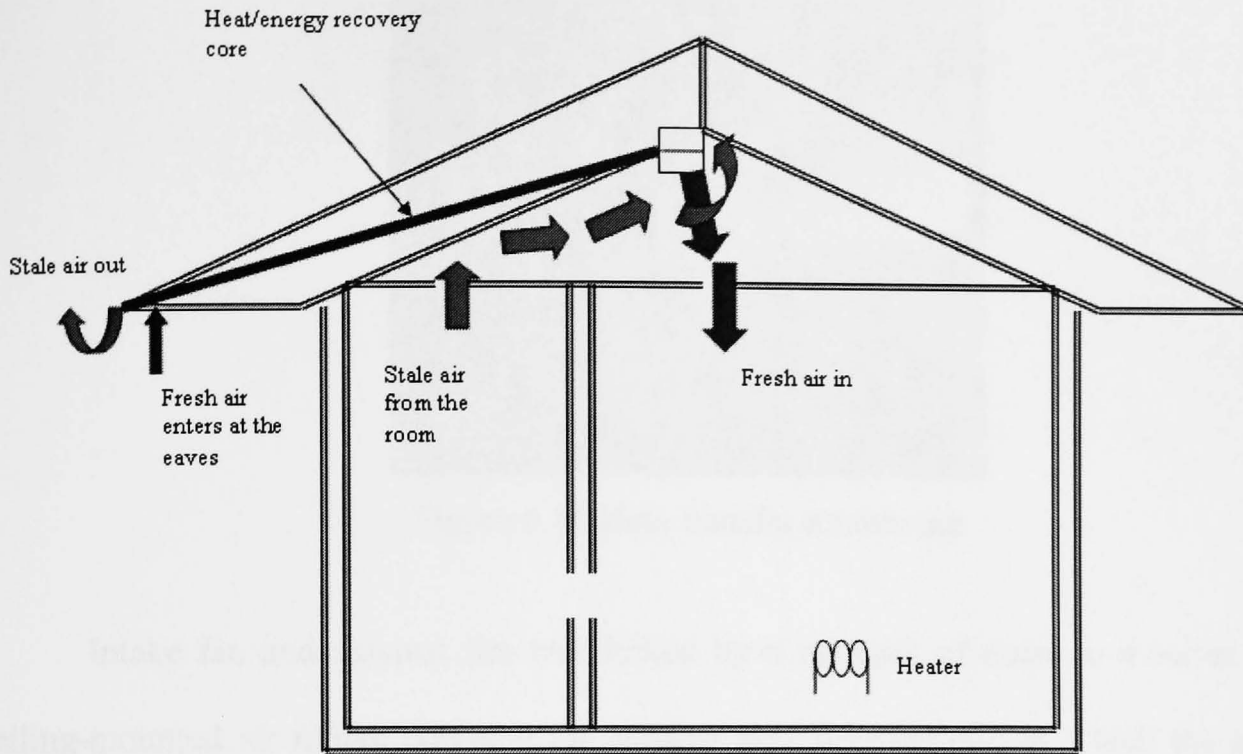


Figure 6.15 Schematic diagram of the set up

The BIHR panel installed on the building has the overall dimensions of 2500mm x 1000mm x 16mm. The supply and exhaust air was separated by a 2mm thick polycarbonate plate. The heat transfer surface has 45 effective internal channels as shown in Figure 6.16.

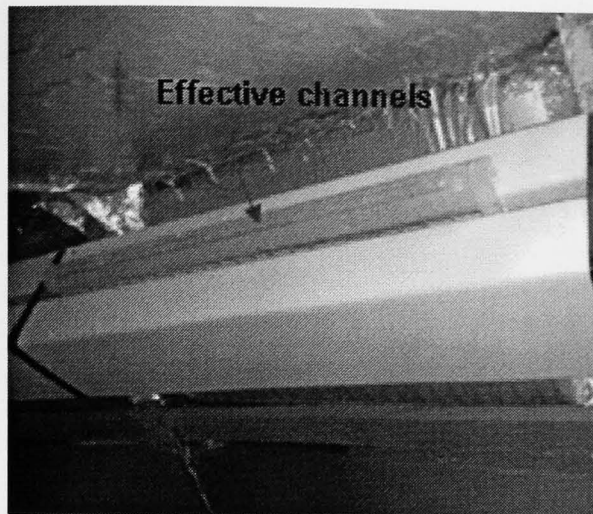


Figure 6.16 Heat transfer membrane

Intake fan and exhaust fan was linked by a network of ducts to a series of ceiling-mounted air intake port and air exhaust port respectively, in which the air-extract port removes stale air from the test room and expel it, through the ventilation device to outside the building and the air intake port delivers fresh air from outside of the building into the test room as shown in Figure 6.17. Air exhaust fan was controlled by a switching means activated by simple mechanical means which is a light switch and comprises a timer such that, in use, the exhaust fan is operational for a pre-determined time after the light switch has been deactivated.

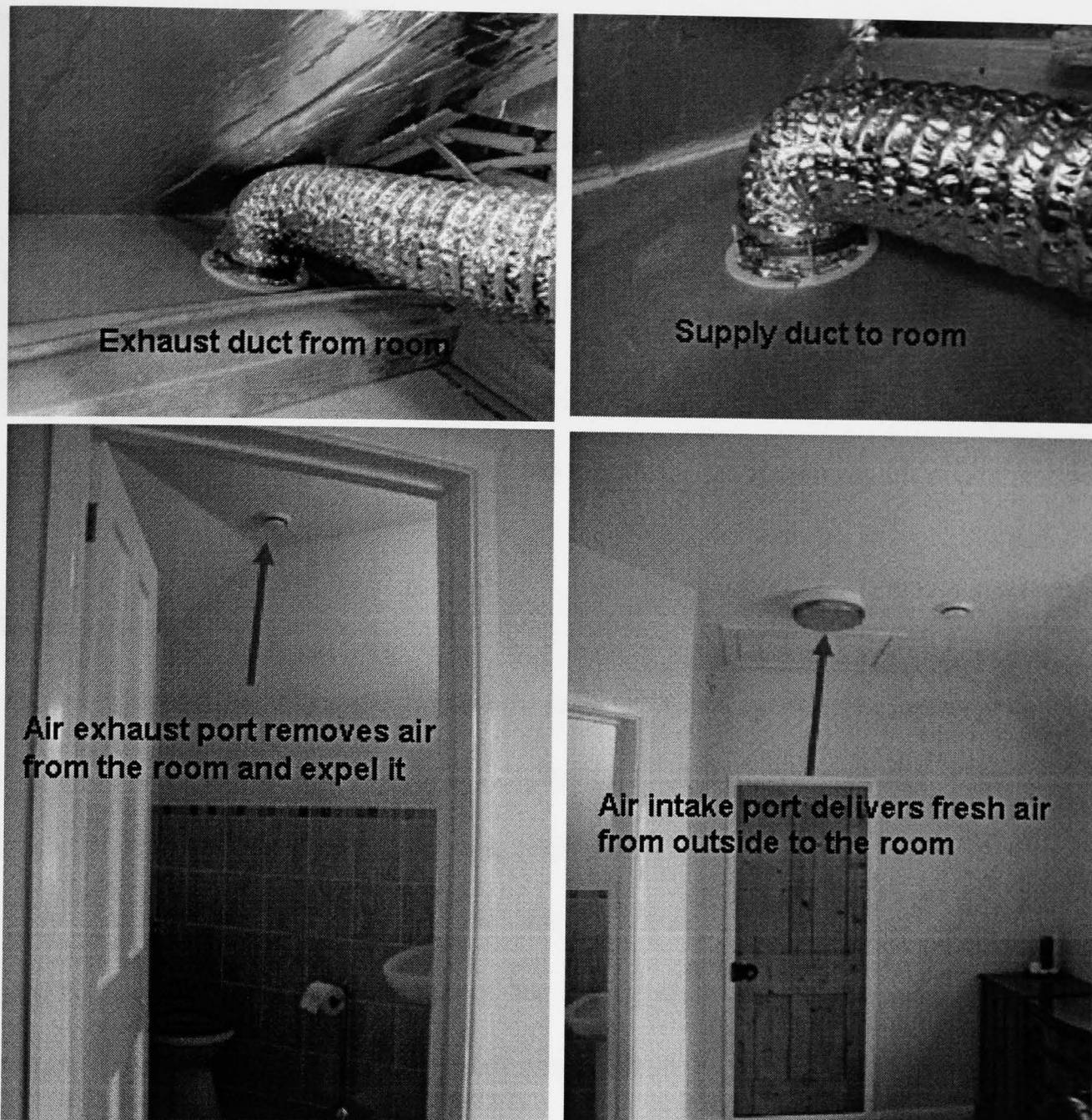


Figure 6.17 Network of ducts

In this system, the lowermost end of the channel was in fluid communication with the eaves and guttering, so that any condensation which develops in the channel could be drained to the guttering and fresh air could be drawn into the system from the eaves (Figure 6.18). In addition, the lowermost end of each channel was provided with a filter to prevent dust, pollen, insects, birds and small mammals from entering the system.

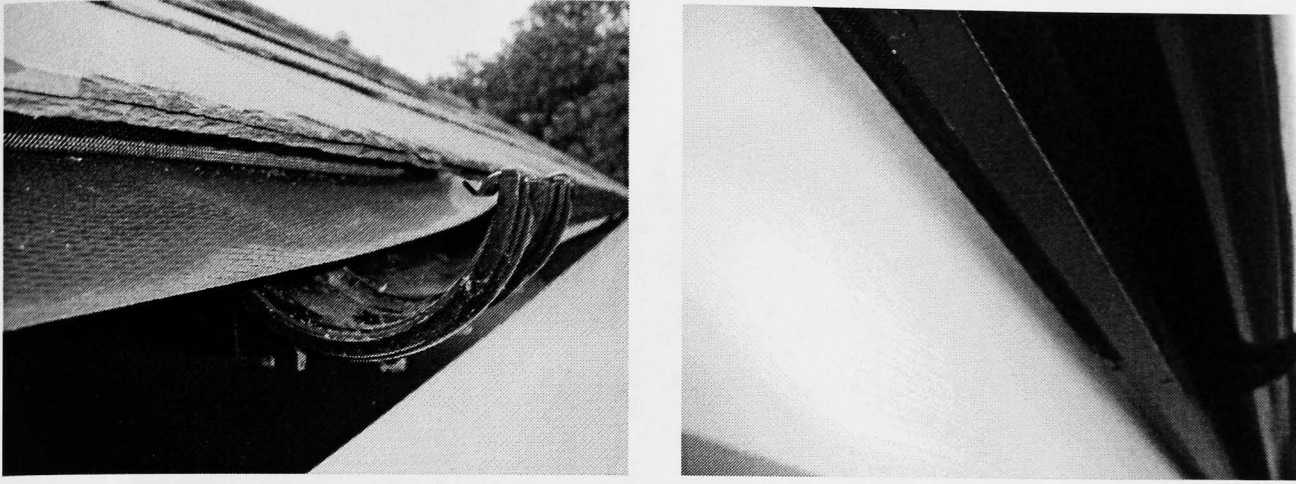


Figure 6.18 Gutter and eaves

6.4.3 Measurements

Investigation of the efficiency of the heat recovery unit requires measurement of air temperatures and flow rates. Thermocouples and hot wire anemometer were used to measure temperatures and airflow rate, respectively on both streams and were recorded by a data logger. Figure 6.19 shows the picture of measurement locations and Figure 6.20 illustrates the schematic of the set up for the measurements. 24 thermocouples have been used across the measurement unit. Before each experiment, the room was heated under appropriate conditions for 1h to reach a steady state.

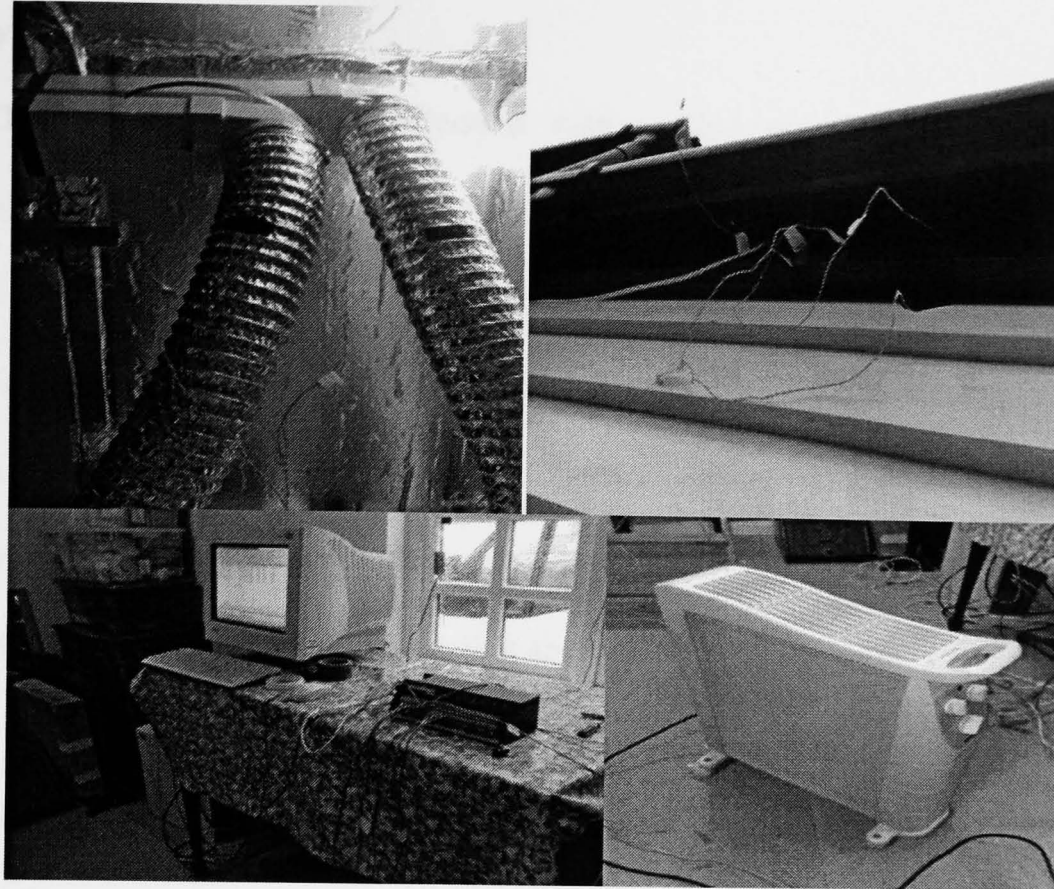
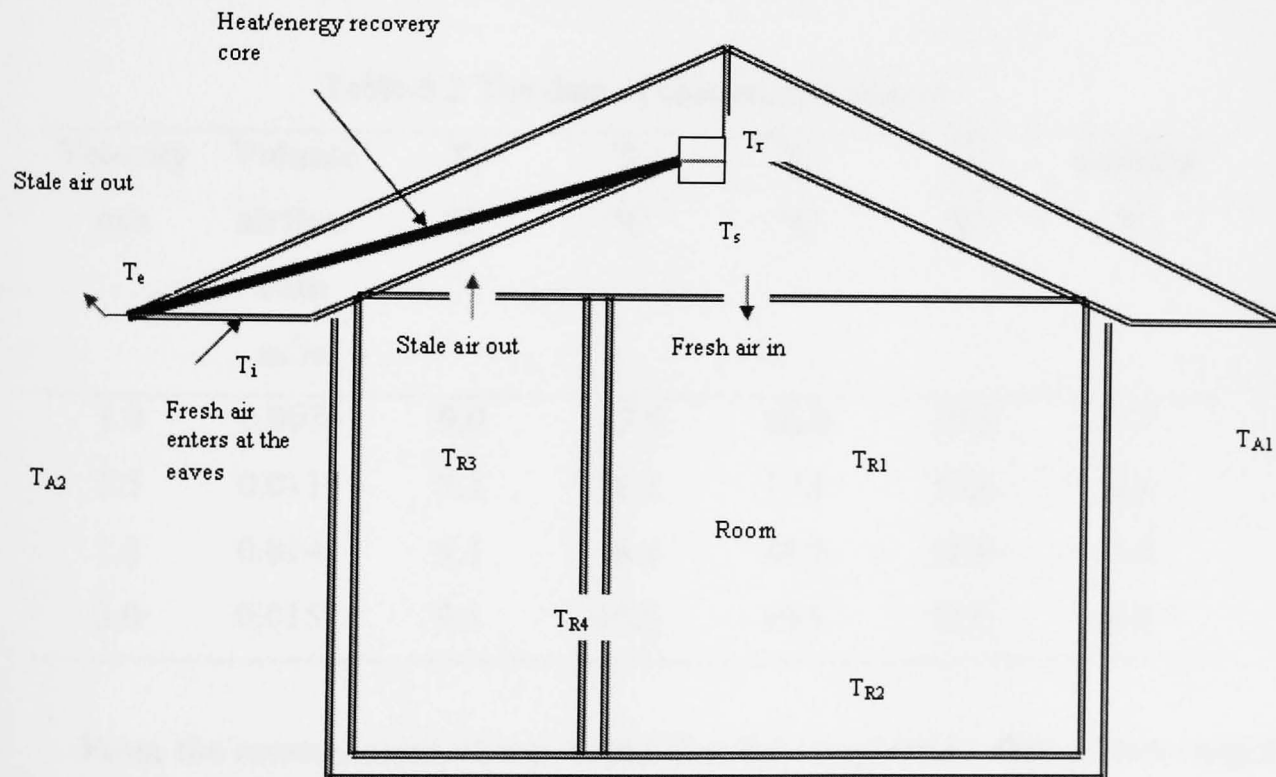


Figure 6.19 Measurement locations



- | | | | |
|---|-------------|---|------------|
| i | Intake air | s | Supply air |
| e | Exhaust air | r | Return air |
| R | Room | A | Ambient |

Figure 6.20 Schematic of the set up for temperature measurements

6.4.4 System performance

The temperature data collection was carried out before conducting the performance test which covered day-time and night-time periods. For both periods, the test mean velocity was 2.0m/s and the mean indoor temperature was at 18°C. From the test, it was found that during day-time test, the fresh intake temperature was about 8.8°C and during night time test the fresh intake temperature was about 5°C. It is also observed that the temperature change of BIHR unit during day-time test and night-time test was approximately similar about 7.7°C.

The tests then were carried out for different air velocities ranged from 1.0 to 2.0m/s. The room temperature was kept at a constant value of 18°C. The measurements data were recorded as shown in Table 6.2.

Table 6.2 The data of case study I (Kent)

Velocity m/s	Volume airflow rate m ³ /s	T _i °C	T _s °C	T _r °C	T _e °C	Ambient °C
1.0	0.0079	9.0	15.5	16.8	10.3	8.7
1.5	0.0118	9.1	16.1	17.8	10.8	8.8
1.8	0.0141	9.1	16.4	18.5	11.0	8.8
2.0	0.0157	9.1	16.9	19.8	12.0	8.8

From the measurement, it was found that the temperature change was ranged from 6.5 to 7.8°C with the highest value corresponding to 2.0m/s or 0.0157m³/s airflow rate.

The calculated results of BIHR efficiency are indicated in Figure 6.21 with respect to airflow rate in the duct. It was found that the BIHR efficiency decreased with increasing airflow rate which ranged from 72.9% at airflow of 0.0157m³/s to 83.3% at airflow rate of 0.0079m³/s.

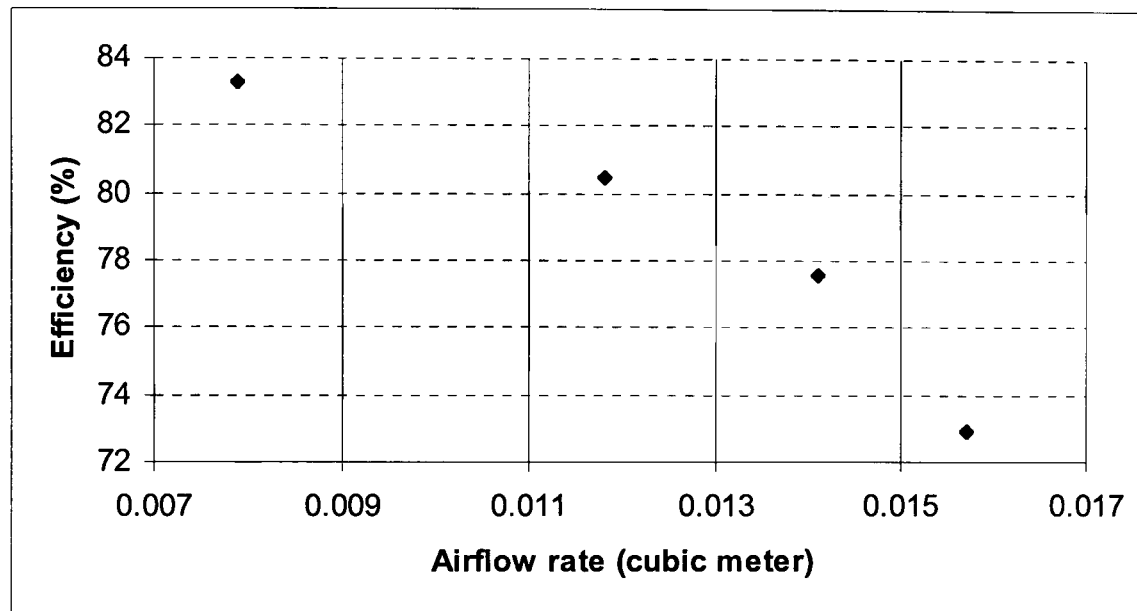


Figure 6.21 Case study I BIHR efficiency

The recovered heat against airflow rate is plotted in Figure 6.22 and it denotes that the highest recovered heat of 147.2W was achieved at 2.0m/s air velocity or 0.0157m³/s airflow rate. The highest recovered heat was achieved at 16.9°C of supply air to indoor space with 7.8°C temperature change.

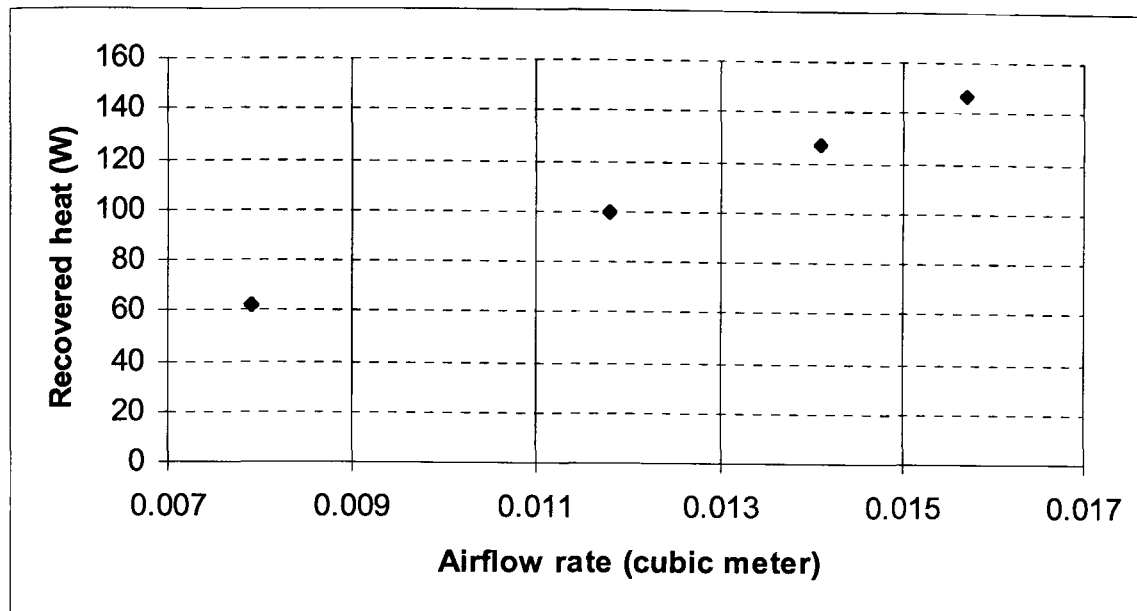


Figure 6.22 Recovered heat against airflow rate

From the pressure difference measurements at the BIHR intake and exhaust streams, Figure 6.23 shows that the pressure difference is proportional to the air velocity. The ASHRAE Systems and Equipment Hand Book (2000) specifies that the operating pressure drop range for fixed plate heat exchanger/recovery used in ventilating system to be between 5 and 450 Pa. It can be seen that the measured pressure difference in this system falls within the above range.

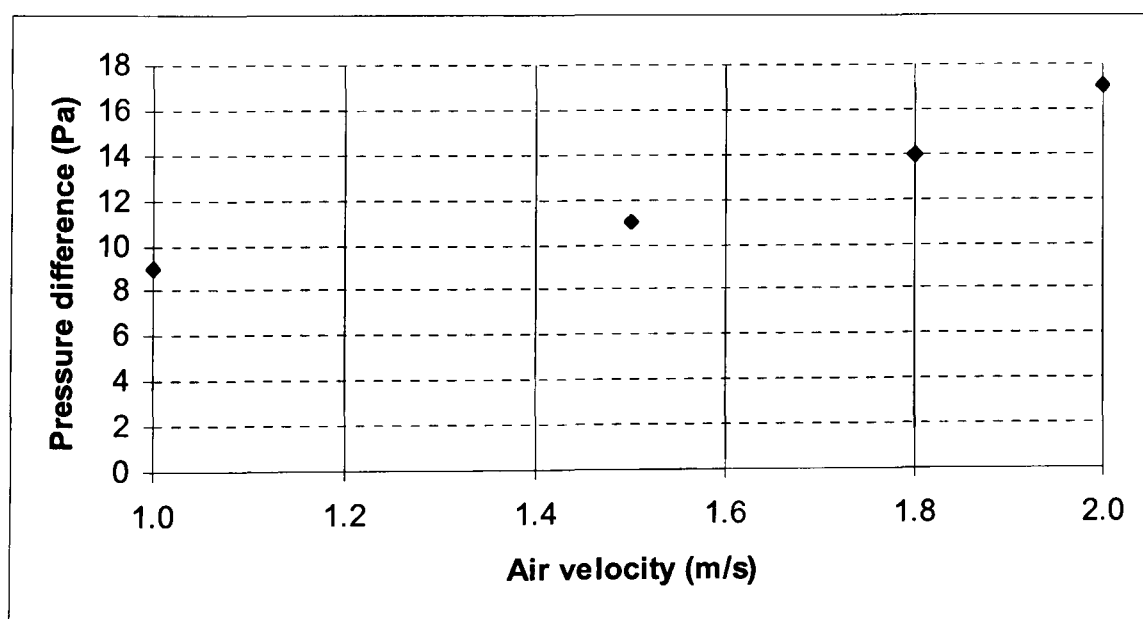


Figure 6.23 Pressure difference at the BIHR intake and exhaust streams

6.4.5 Comparison with prototype panel

A comparison study between prototype and case study I is conducted. From Figure 6.24, it can be seen that heat recovery temperature change of case study I is increasing at more than 50% compared to prototype for different airflow rate. This happens due to the enhancement of BIHR heat transfer surface area. The enhancement of recovered heat was also achieved with increasing heat transfer surface area of similar material as shown in Figure 6.25.

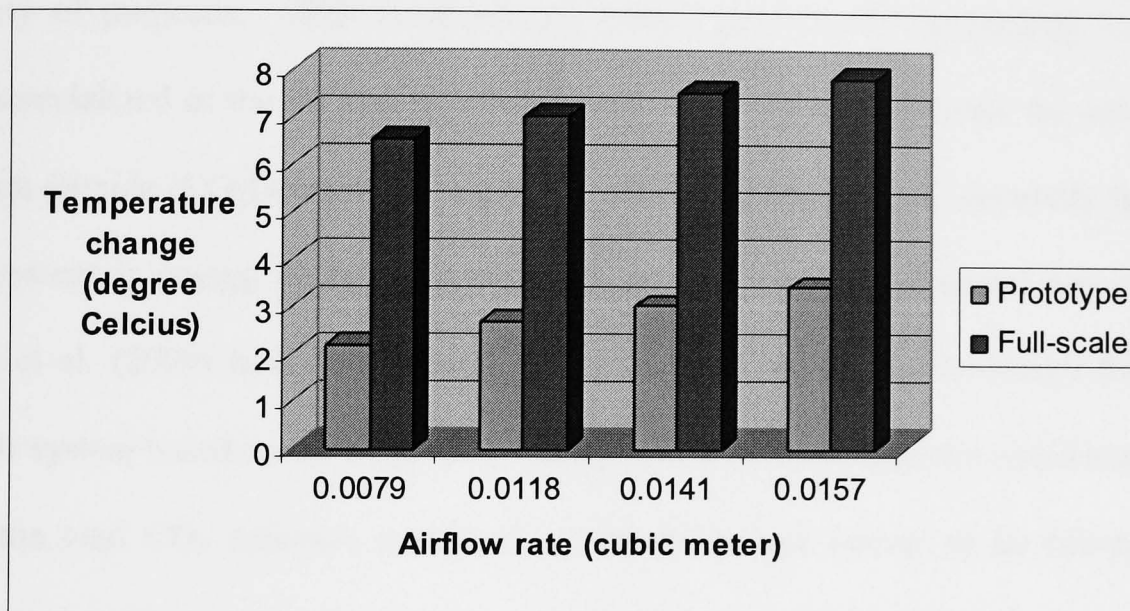


Figure 6.24 Comparison of temperature change between prototype and case study I

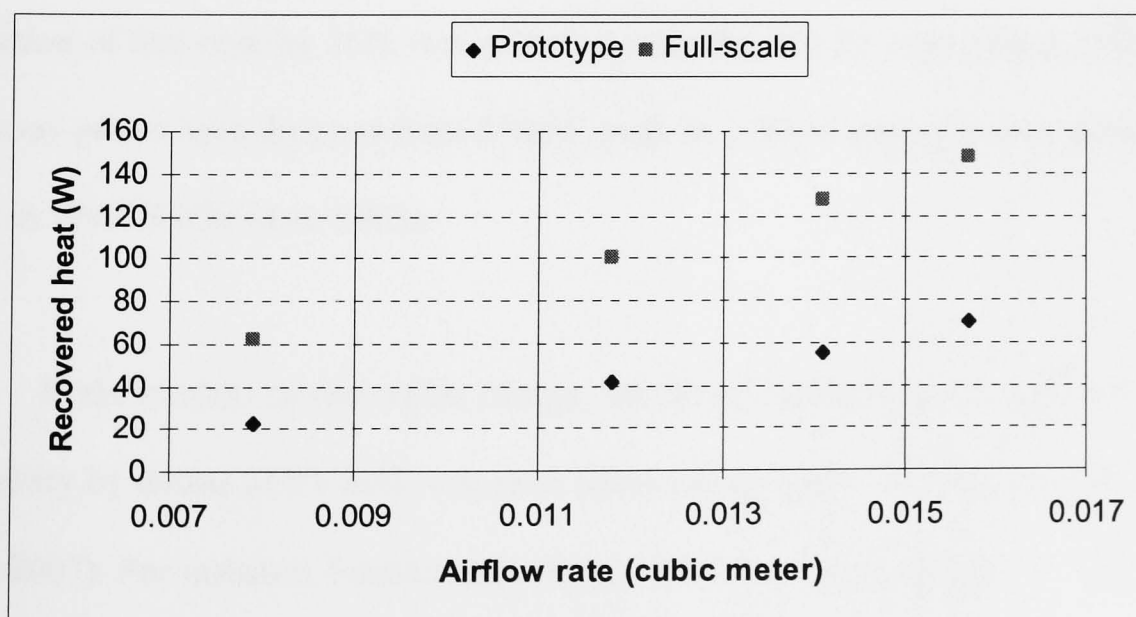


Figure 6.25 The enhancement of recovered heat

6.4.6 Experiments on PV powered fan for BIHR system

In the age of dwindling fossil fuels and the world's deliberation concerning global warming a lot of attention is being focused on renewable energy as an important role in the energy supply of the developing and industrializing countries. The use of photovoltaic (PV) cells is one approach that may assist the reduction of fossil fuels consumption. PV cells have been introduced a few decades ago and used widely for generating power from the sun by converting sunlight to electricity for a variety of purposes. With an escalating market growth, PV technology has been commercialized in the 80's as this technology is eco friendly because the amount of carbon dioxide (CO₂) emissions associated with the production of electricity from the PV system is negligible as compared with conventional coal thermal power plant. Chel et al. (2009) have investigated the sizing and costing methodology for a PV power system based on the number of sunshine hours available in the world and found that the total CO₂ emission mitigated by the PV power system in its lifespan was estimated at 63 tons which correspond to the carbon credits of \$2,048. However PV cells price was too high to be considered as a competitive source of energy until the reduction of this cost by 75% was achieved over the last 20 years (Patel 1999). The PV array prices have dropped from \$500/W peak in 1972 to approximately \$4 to \$5/W peak in 1990 (Kolhe et al. 2002).

In the context of renewable energy, the direct conversion of solar energy into electricity by means of PV cells was then has received much attention in 1990s (Jie Ji et al. 2007). For instance, Sasitharanuwat et al. (2003) have designed a PV cell stand-alone/grid connected system to power the energy for office building and found that each system component and overall system was working effectively. On the other

hand, Tanittererapan and Pan-A (2005) have conducted a study on power supply for photovoltaic powered neon sign for advertising board in remote area. The work presented in this section describes a study on the installation and test of a photovoltaic powered fan for BIHR system in real building at Forstal Farm, Kent, UK.

6.4.6.1 Material and methods

- Electric load estimation

The load consists of two fans with total power 32W at 2.0m/s speed, each fan 16W and 230V AC. In order to size the PV power system for BIHR, the energy needs should be figured out. Thus, at fan consumption of 32W and 230V AC through an inverter would require 2.67 Amps/hour at 12V DC load demand. (32W divided by 12V).

- System configuration

The PV system consisted of two polycrystalline PV cells with high efficiency and durability, one inverter, and one charge controller and battery storage. Figure 6.26 shows the picture of system configuration and Figure 6.27 shows the schematic diagram of PV powered fan for BIHR system.

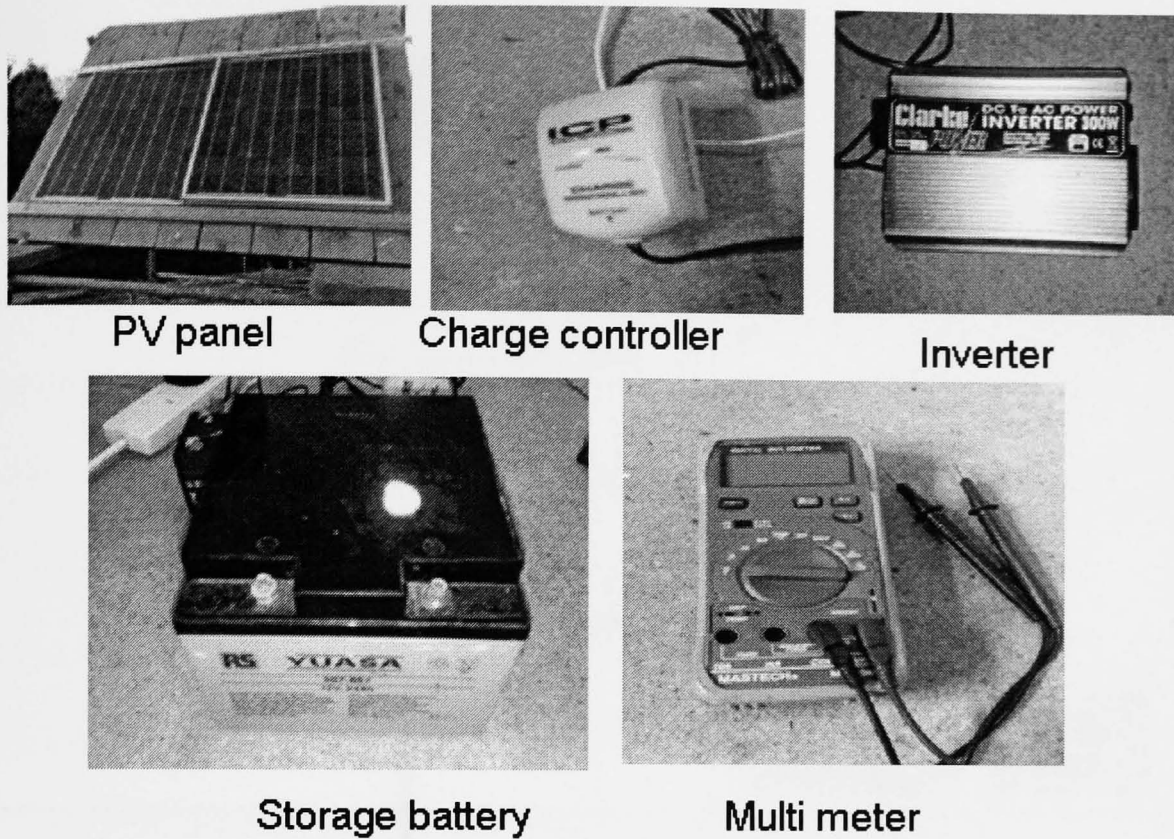


Figure 6.26 The PV system equipments

Each PV panels generates $30W_p$ and 1.78 Amps/hours. Therefore to provide electric power for 2.67 Amps total, two PV modules would be required per system. The total energy generation from two modules is 3.56 Amps. This energy covers the load demand (2.67) consumption and 0.89 Amps to further offset weather and inverter efficiency inherent with PV system.

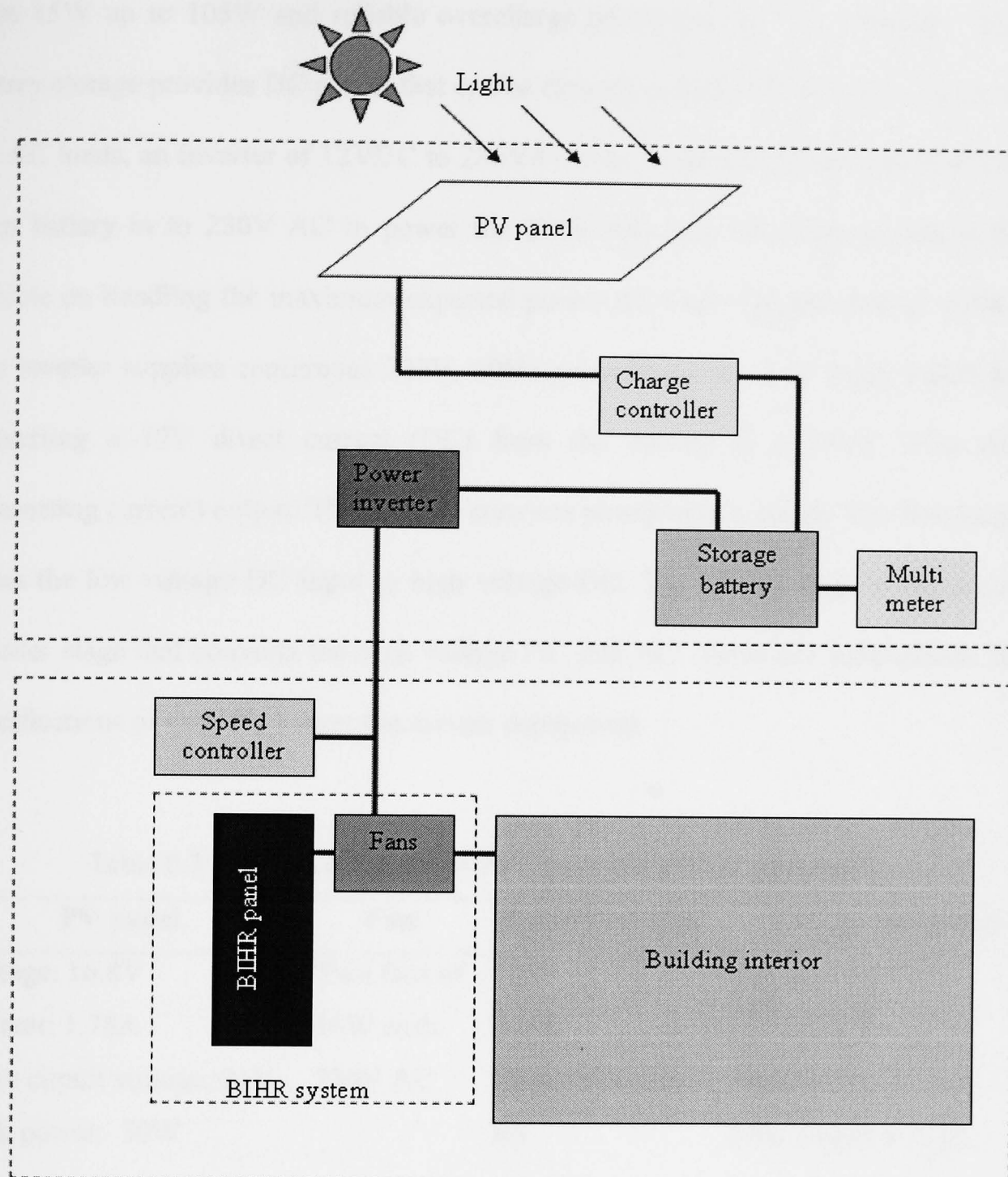


Figure 6.27 The schematic diagram of PV powered fan for BIHR system

The 30W panel each produces sufficient power to charge battery. An ICP 7Amp charge controller connected between the panel and the battery to regulate the charge to the battery and prevents the photovoltaic panel from overcharging the battery. This charge controller is important to ensure the long life of the battery while assuring a complete charge and also to recharge the battery when voltage falls below a predefined value. The ICP 7Amp charge controller is suitable for photovoltaic panels

from 15W up to 105W and reliable overcharge protection for 12V batteries. The battery storage provides DC power that can be directly used for DC loads, but to drive the AC loads, an inverter of 12VDC to 230VAC was connected to convert 12V DC from battery into 230V AC to power the 230V AC fans. The inverter has to be capable of handling the maximum expected power AC loads (Wenham et al. 1994). The inverter supplies continuous 230V, 50Hz power via a standard 3-pin socket by converting a 12V direct current (DC) from the battery to a 230V 50Hz AC (alternating current) output. The inverter converts power in two stages. The first stage raises the low voltage DC input to high voltage DC. The second stage is the actual inverter stage that converts the high voltage DC into AC. Table 6.3 summarizes the specifications of each PV power fan system component.

Table 6.3 The specifications of PV power fan system component

PV panel	Fan	Battery storage	Charge controller
Voltage: 16.8V	Two fans of	12V	Cut out >14.2V
Current: 1.78A	16W each,	24Ah	Cut in 13.0V
Open circuit voltage: 21V	230V AC	Model 597-857	7A load
Peak power: 30W		RS	Stop charge at 1.2A

The system was turned-ON at 12:00 and turned-OFF at 15:00 by means of the timer sensor. The ambient temperature was at 8.7°C during a clear sunshine day and the average wind velocity was within 2.7m/s.

6.4.6.2 Analysis of the PV performance

The test was performed to supply energy for two fans at a maximum speed of 2.0m/s with total power of 32W. The test has been conducted from 12:00 to 15:00.

Figure 6.28 illustrated the PV system output. From the test, the maximum PV array voltage was found to be 12V and 2.65A.

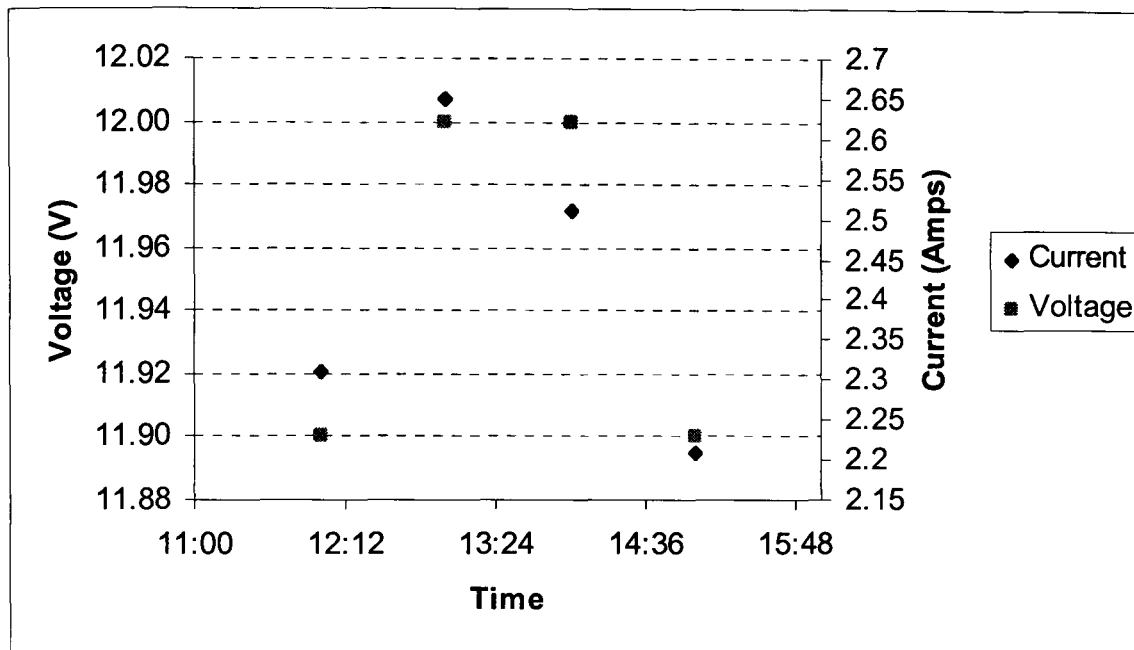


Figure 6.28 PV system output

Figure 6.29 shows the electric power from the PV system. The PV system power was found to be 31.8W at 13:00 and decreased to 26.52W at 15:00pm. The DC output power of the PV cells was transformed into AC by the inverter and consumed by the fan. This results show that PV system would be suitable to supply electricity for BIHR fans system to cover the loads requirement demands without utilizing energy from the electrical grid.

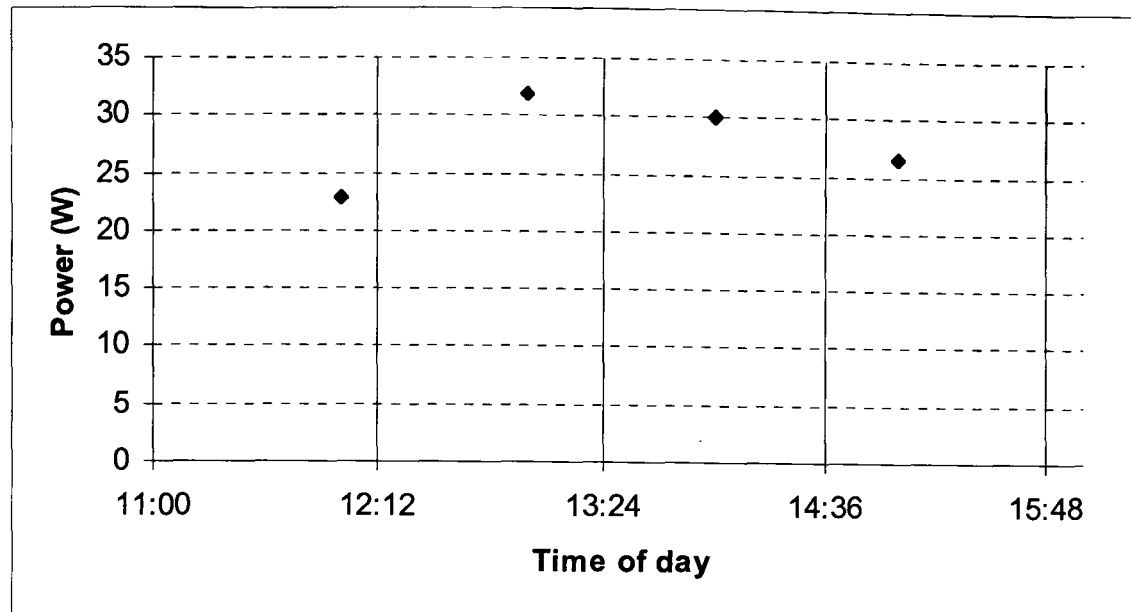


Figure 6.29 Electric power from the PV system

6.5 Case study II: Full-scale measurements of BIHR panel on a real building in Hastings, Sussex

Another full-scale measurement of BIHR panel has been conducted in one of the house in Hastings, Sussex, UK in March 2010. The house has a dimension of 73m² floor area of downstairs and 55m² floor area as shown in Figure 6.30. This house is an old house and fully retrofitted and only been occupied occasionally during weekend by the inhabitant. The living area is composed of a living room, a kitchen, a bathroom downstairs, two bedrooms and a second bathroom upstairs. The thermal envelope characteristics are given below. The ground-floor external walls are made of (from external to the internal face) a 45mm concrete layer, 100mm of insulation material and 50mm of plaster board and sterling board. The pitched-roof wall is insulated with insulation material to avoid heat loss from the house to exterior. All windows are double glazed.

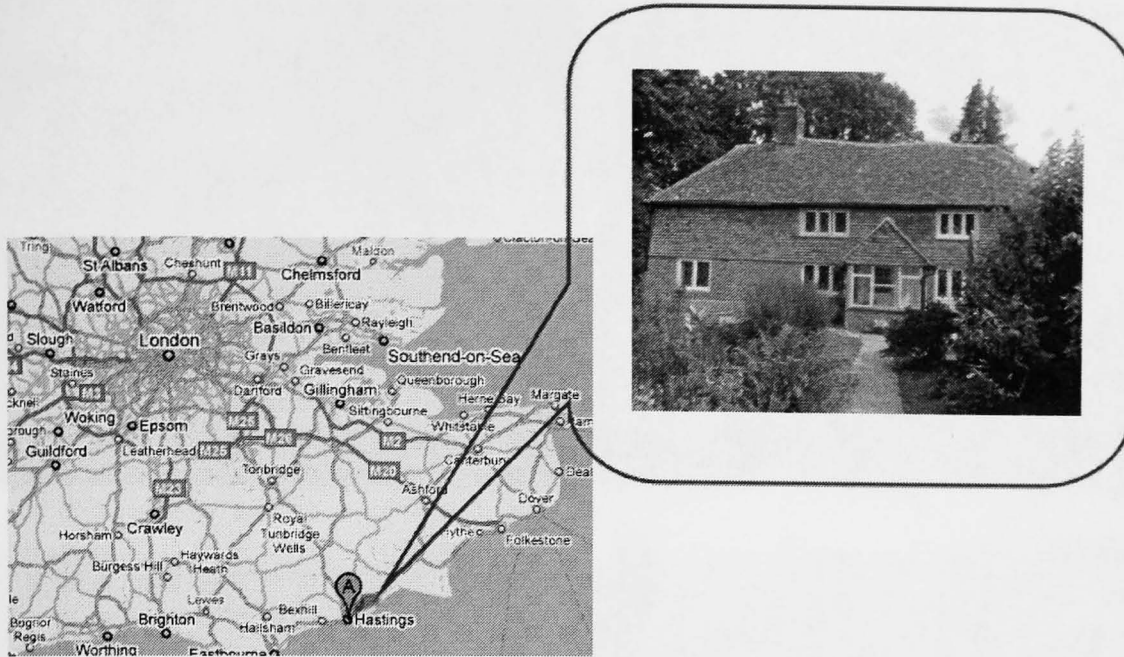


Figure 6.30 House in Sussex, UK

6.5.1 Testing description

BIHR panel which has the overall dimension of 4500mm x1000mm x16mm was fitted over the roof of the house. The supply and exhaust air was separated by 2mm thick polycarbonate plate. Figure 6.31 shows the BIHR panel installed on the building.



Figure 6.31 The installation of BIHR in case study II

Similar to the building in case study I, intake fan and exhaust fan was linked by a network of ducts to a series of ceiling-mounted air intake port and air exhaust port respectively as shown in Figure 6.32.

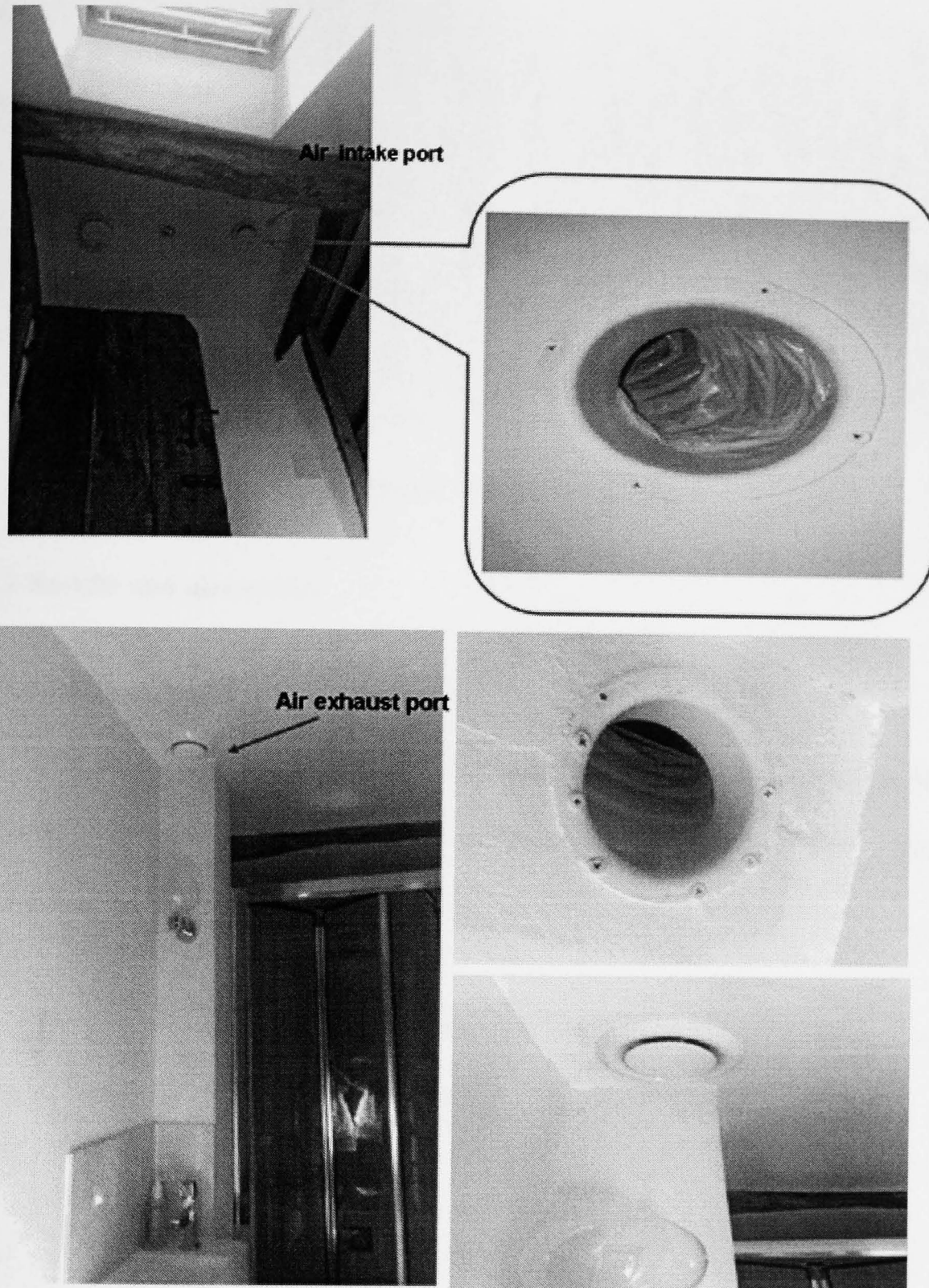


Figure 6.32 Ducting system

Air was extracted from strategic areas in the house, and then ducted to the panel in the loft. The stale air then was expelled under the roof covering with condensate run off to the gutter. The fresh air was drawn from under the eaves through filters and following heat exchange ducted where needed providing a supply of fresh warm or cool air as shown in Figure 6.33.

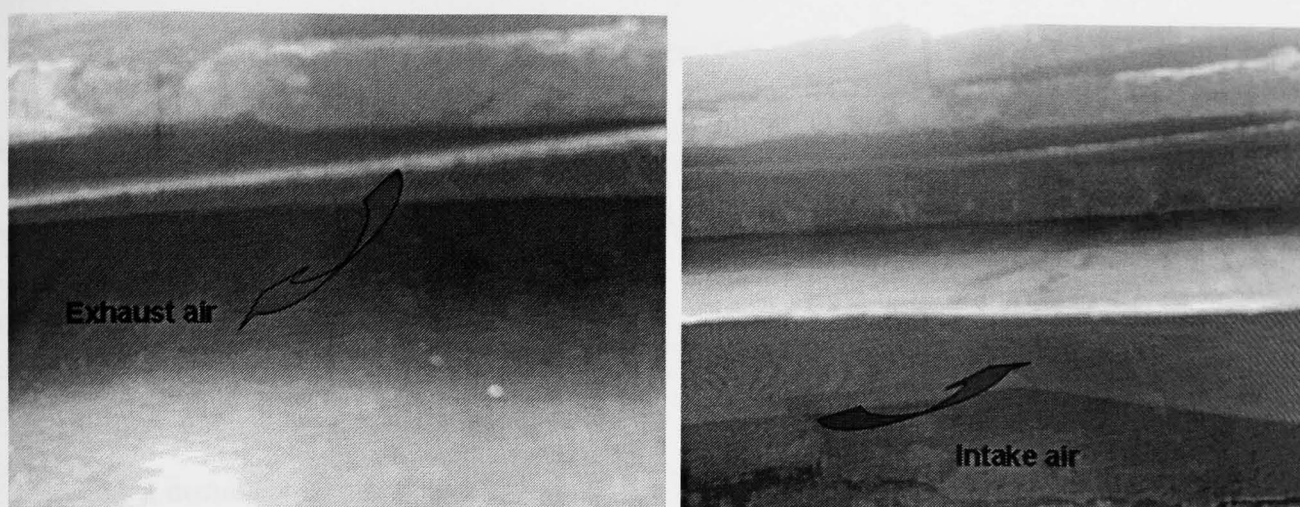


Figure 6.33 The fresh air was drawn from under the eaves and the stale air was expelled under the roof to the gutter

6.5.2 Results and discussion

6.5.2.1 Efficiency and performance

For experiments carried out in this study, the room temperature was fixed at 21°C and air velocities ranged from 1.0 to 3.0m/s. The experiments data is shown in Table 6.4.

Table 6.4 Case study II experiments data (Hastings)

Velocity m/s	Volume airflow rate m ³ /s	T _i °C	T _s °C	T _r °C	T _e °C	Ambient °C	Δt °C	ε _{HR} %
1.0	0.0079	17.5	21.9	21.8	17.4	19.0	4.4	91.7
1.5	0.0118	17.4	22.2	22.3	17.5	18.9	4.8	88.8
2.0	0.0157	17.4	22.4	22.6	17.6	18.9	5.0	86.2
2.5	0.0593	17.5	22.9	23.1	17.7	18.9	5.4	84.7
3.0	0.0237	17.5	23.3	24.2	17.7	19.0	5.8	80.5

From the table, it can be seen that the outlet/return temperatures (T_r) increases as the air velocity increases. Since the heat recovery core under this investigation is the one with counter-flow, the outlet temperature (T_r) after leaving the heat recovery core to the room is higher than that obtained at the exhaust side (T_e).

At a constant room temperature of 21°C, a relationship between efficiency and the airflow rate is illustrated in Figure 6.34. The efficiency increases as the temperature change decreases as a result of rising airflow rate.

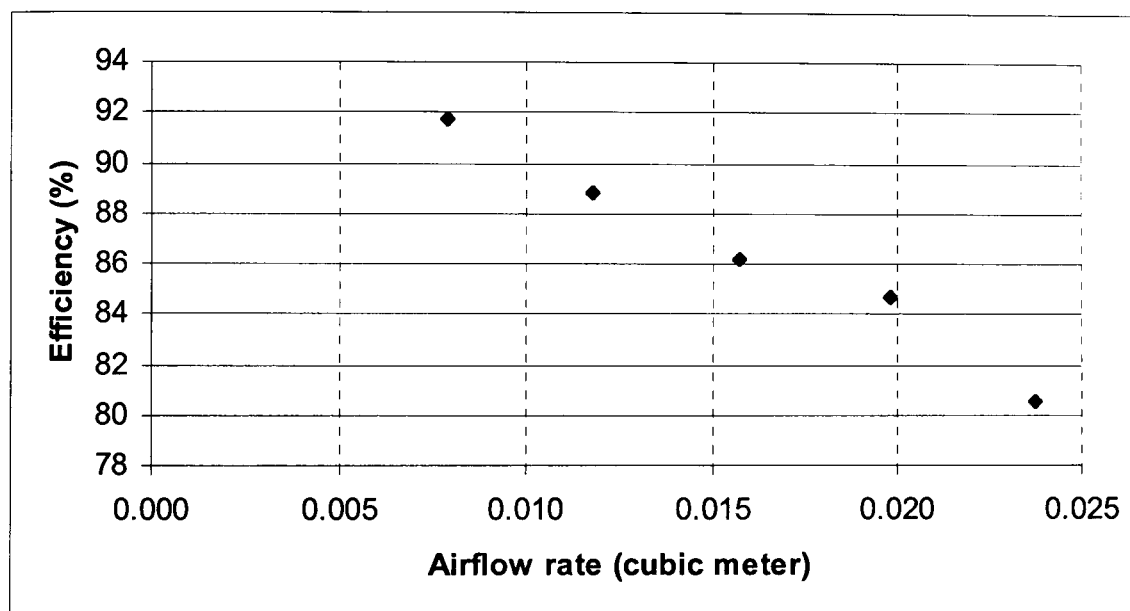


Figure 6.34 Relationship between efficiency and the airflow rate

6.5.2.2 Comparison with prototype and case study I

A comparison study data of prototype, case study I and case study II is shown in Table 6.5. Generally, the enhancement of heat recovery efficiency is achieved by increasing heat transfer surface area of similar material.

Table 6.5 Comparison study data of prototype, case study I and case study II

Airflow rate (m ³ /s)	Prototype (ε %) 1000mm x 1000mm x 16mm	Case study I (ε %) 2500mm x 1000mm x 16mm	Case study II (ε %) 4500mm x 1000mm x16mm
0.0079	61.1	83.3	91.7
0.1180	57.5	80.5	88.8
0.0157	50	72.9	86.2

From Figure 6.35 it can be seen that BIHR in case study II which has 4500mm length of heat transfer surface area has the highest efficiency values compared to prototype and BIHR in case study I with the highest value of 91.7% reflects to 0.0079m³/s or 1.0m/s. This can be explained by the increasing of heat transfer surface area which gives a significant effect to the performance of BIHR system.

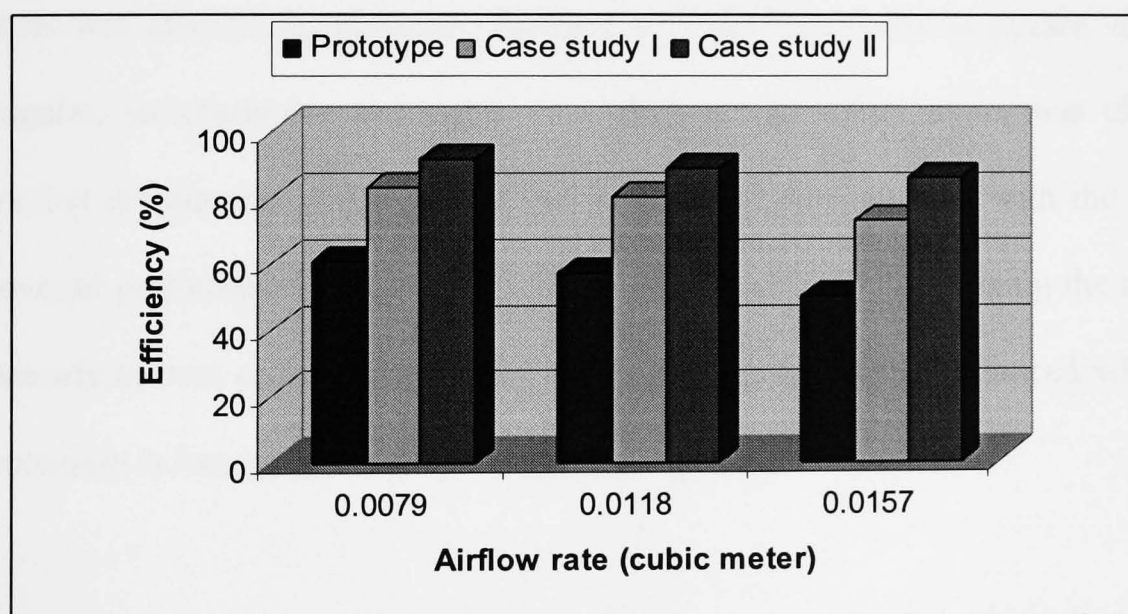


Figure 6.35 Comparison of efficiency of prototype, case study I and case study II

6.6 An improved BIHR system employing corrugated channels with four airstreams

With the rapidly growth of global environmental problems, energy-efficient utilization becomes an ever more important in science and technology. In recent years, due to the increasing demands for heat recovery core or it other word it can be

called heat exchangers that are more efficient, compact and less expensive, heat transfer enhancement has gained great momentum. Many heat exchanger designs involve redistributing the internal flow stream into several passages. This transition can occur anywhere along the flow length and is usually associated with an increase in the heat transfer surface area.

Heat transfer enhancements particularly in heat exchangers have interested many researchers and have been an attractive area of study for the decade. Hasan et al. (2009) evaluated the effect of size and shape of channels of a counter-flow channel of heat/energy core by using numerical simulation. The effect of shapes of the channels was studied for different channels cross-sections such as square, circular, rectangular, iso-triangular and trapezoidal shapes. The effect of various channels shows that the circular channels give the best overall performance, with the second best overall performance achieved by the square channels. By increasing the number of channels in heat exchanger/recovery core, the heat transfer is enhanced while the pressure drop is increased as well.

In addition, for heat transfer enhancement, two techniques have been identified: “passive” and “active” (Webb 1994). Passive technique uses special fluid additives or surface geometries such as corrugated channels to be preferred (Kuppan 2000). In order to achieve enhanced heat transfer, corrugated channels are often employed in the design of plate heat exchangers (Islamoglu 2003). These corrugations force the flow in the channels to experience a continuous change and flow area. Several studies on convection heat transfer for such kinds of configurations were carried out in the past. For instance, Goldstein and Sparrow (1997) were the first to

report local and average convection heat transfer coefficient in a corrugated wall channel using the naphthalene technique.

From the preceded survey, it is obvious that the enhancement of heat transfer using corrugated passages is one of interested subjects to the researchers. Although several studies for corrugated channels have been reported, little knowledge is available on the flow and heat transfer characteristic such as recovered heat and efficiency in such passages for heat recovery purpose. Hence, the present work in this section aimed at developing and experimentally investigated an improvement design of high performance heat recovery (BIHR) employing corrugated channels of polycarbonate with four airstreams.

6.6.1 Development of improved BIHR system

Figure 6.36 shows the new improved BIHR panel. Panel was designed as a counter-flow configuration to recover exhaust heat in order to preheat supply air for buildings with overall dimensions of 1000mm x 1000mm x 50mm.

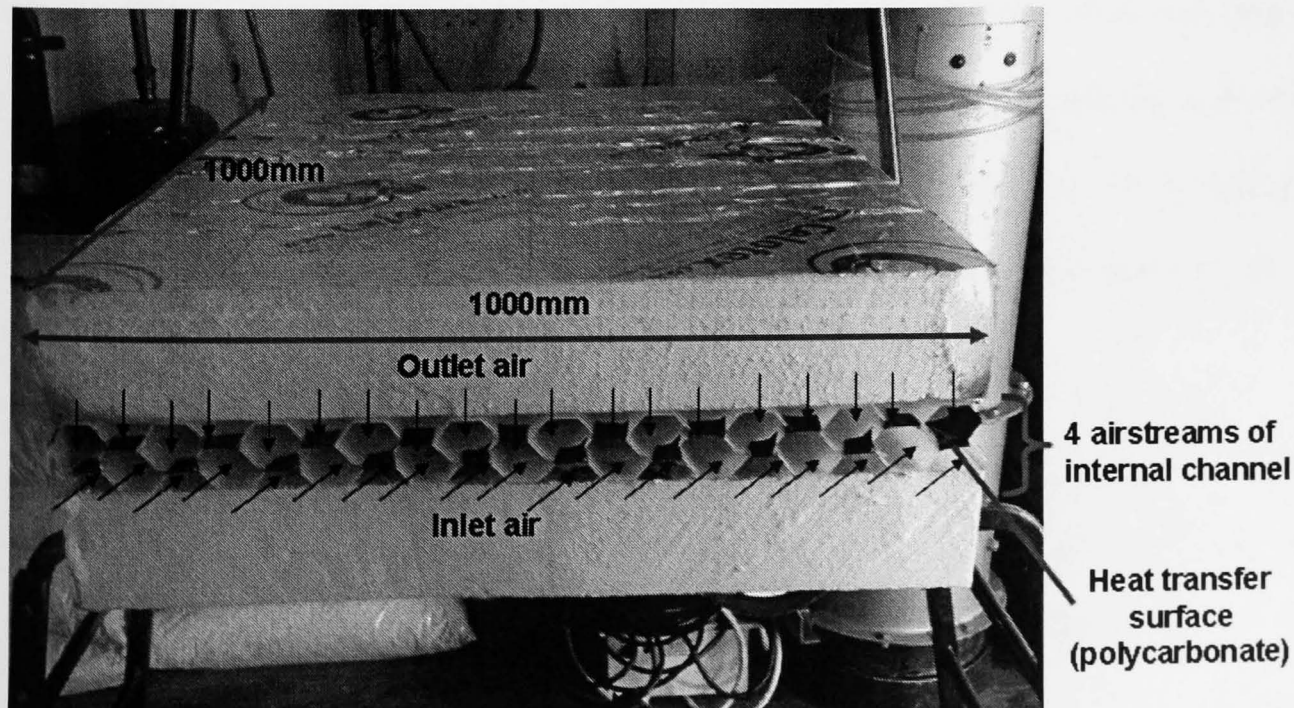


Figure 6.36 New improved BIHR panel

The features and constructions of the improved BIHR are described as follows:

- The layered panel consists of three sheets of corrugated polycarbonate forming the flow channels (50mm) that used for heat transfer surface and insulating panel made of 100mm expanded foam polystyrene.
- Each corrugated polycarbonate sheet has 1000mm length, 1000mm width and 1.0mm thickness and each sheet has 19 crests separated by distance/pitch L of 25mm and A of 18mm as shown in Figure 6.37.

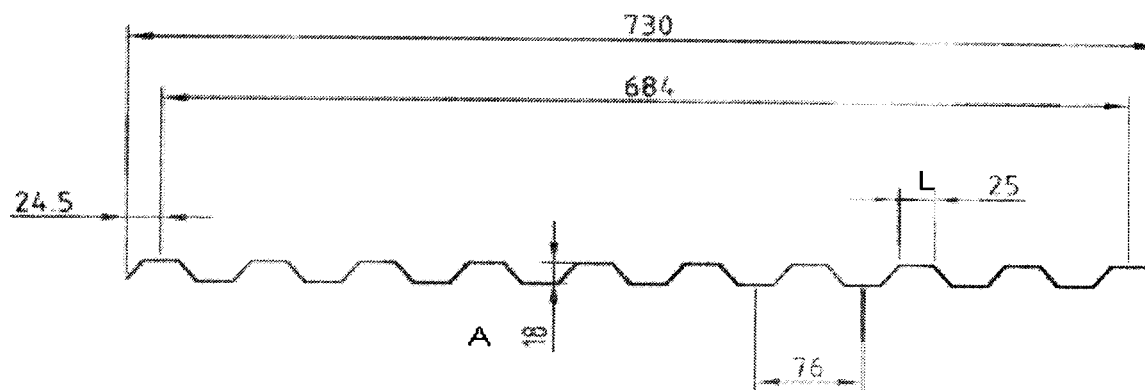


Figure 6.37 Diagram of corrugated polycarbonate

- The corrugated polycarbonate sheets have been properly fixed and sealed through alternate crests into each support using silicon sealant and tape forming four airstreams of 38 effective internal channels and all corrugated walls was symmetrical. The crest of the lower corrugated wall corresponds to the through of the upper corrugated wall of the channel.
- The internal corrugated channels comprised of two air-intake channels (inlet) and two air-exhaust channels (outlet) as shown in Figure 6.38. The internal corrugated channels was divided into inlet and outlet channels by a heat transfer surface which provides a substantially air-tight seal between the inlet

channels and outlet channels and in use permits the transfer of heat energy between airflows within the respective channels.

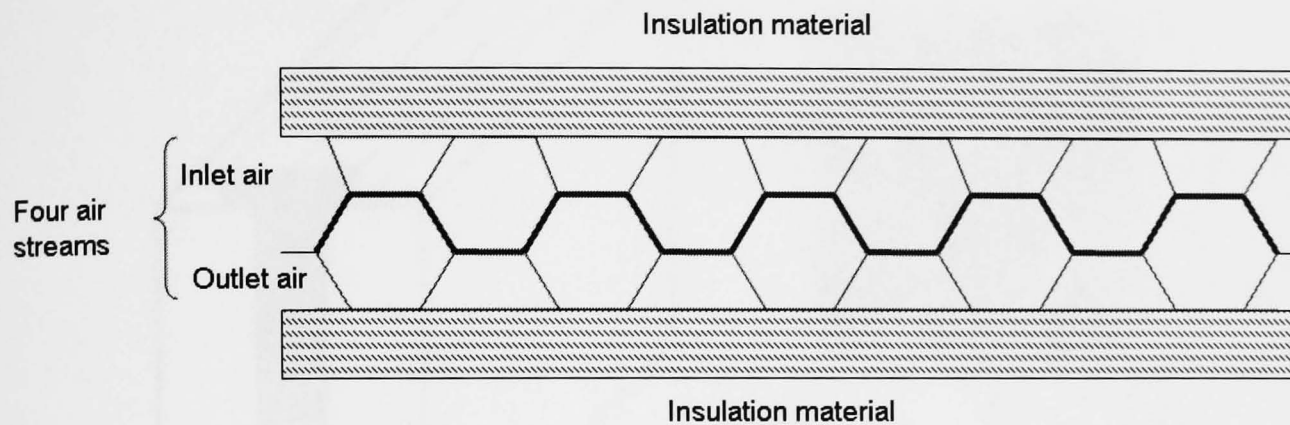


Figure 6.38 Schematic diagram of the design

6.6.2 Performance of the improved system

Experimental investigation has been carried out to evaluate the performance of new improved BIHR employing corrugated channels with four airstreams. Figure 6.39 shows the diagram of new improved system. In order to evaluate the performance of the improved system, similar test room, equipments, measurements and procedures used for prototype BIHR with two airstreams in section 6.3 have been utilised again. Heat transfer in terms of recovered heat, efficiency, effects of temperature and airflow are analysed. Analysed were also conducted to compare the improved system with the previous prototype of BIHR with two airstreams.

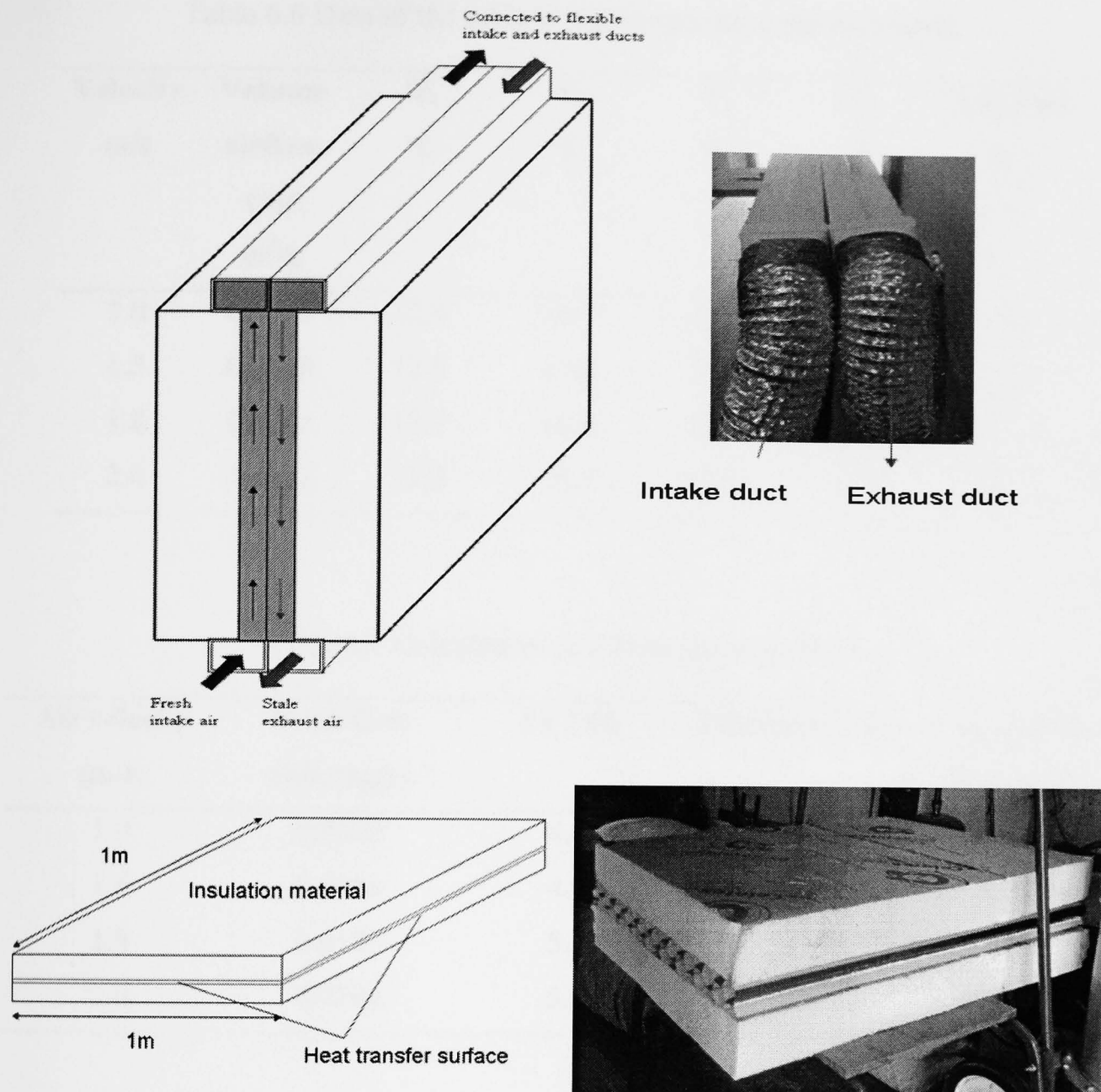


Figure 6.39 Diagram of new improved system

Under the constant room temperature condition about 21°C, experimental data associated with the improvement of internal channels of BIHR were obtained. For this study, tests were performed at mean air velocities ranging from 1.0 to 2.0m/s. The results of the airflow and temperature measurements were summarized in Table 6.6. On the other hand, Table 6.7 shows the calculation data from the experiment.

Table 6.6 Data of the airflow and temperature measurements

Velocity m/s	Volume airflow rate m³/s	T_i °C	T_s °C	T_r °C	T_e °C	Ambient °C
1.0	0.0079	12.4	16.7	19.1	14.7	12.2
1.5	0.0118	12.8	17.6	20.8	15.9	12.1
1.8	0.0141	12.7	18.0	21.9	16.6	12.3
2.0	0.0157	12.5	18.1	23.0	17.4	12.0

Table 6.7 Calculation data from the experiment

Air velocity (m/s)	Mass flow rate (kg/s)	ΔT (°C)	Efficiency (%)	Recovered heat (kW)
1.0	0.0103	4.4	65.7	0.0455
1.5	0.0153	4.9	61.3	0.0753
1.8	0.0183	5.3	57.6	0.0974
2.0	0.0204	5.6	53.3	0.1147

6.6.2.1 Effects of airflow on performance

Again, at the condition stated above, the effects of airflow on the performance of improved BIHR' system was evaluated as shown in Figure 6.40. The figure indicates that the efficiency increases as airflow rate increases. The highest efficiency of 65.7% was achieved at 0.0079m³/s.

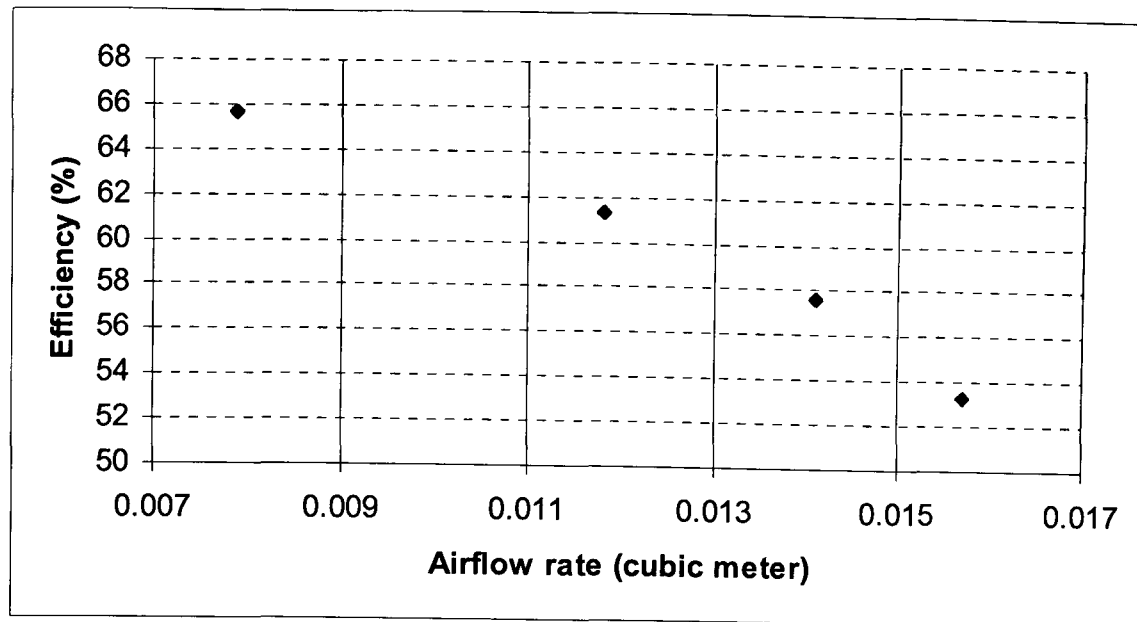


Figure 6.40 Effects of airflow on the performance of improved BIHR' system

Contrary to the above, the trends of recovered heat are observed to be in the opposite directions as shown in Figure 6.41. The maximum recovered heat of 114.7W was achieved at 0.02kg/s mass flow rate or 0.0157m³/s.

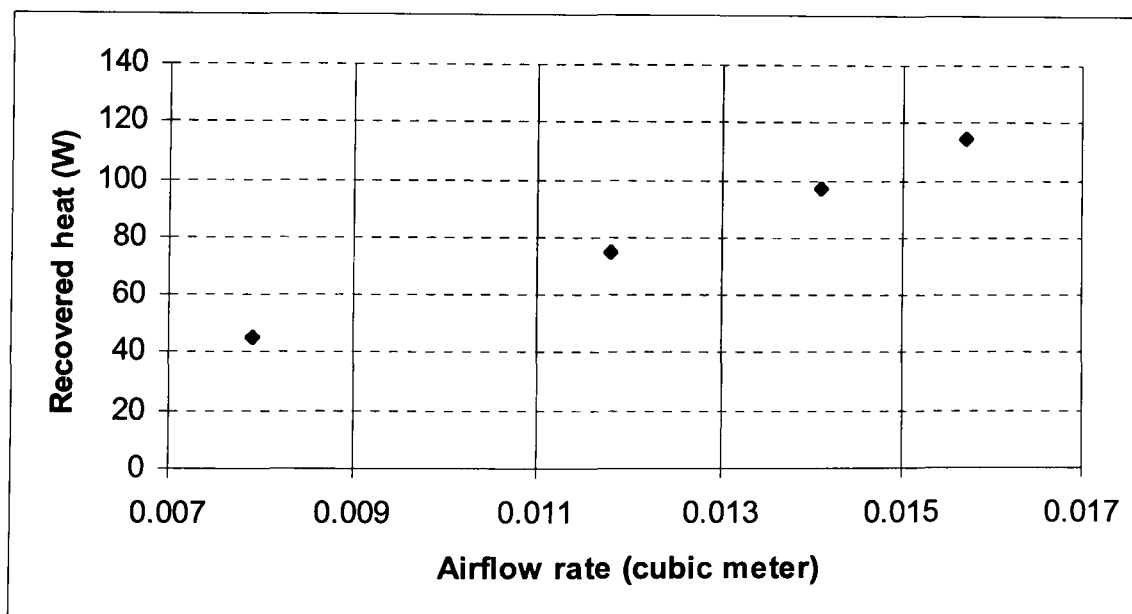


Figure 6.41 Recovered heat against airflow rate

6.6.2.2 Effects of temperature

When the supply air to room temperature increased, the temperature change also increases. As a result, the recovered heat result obtained from these tests increases with rising supply air to room temperature, as shown in Figure 6.42.

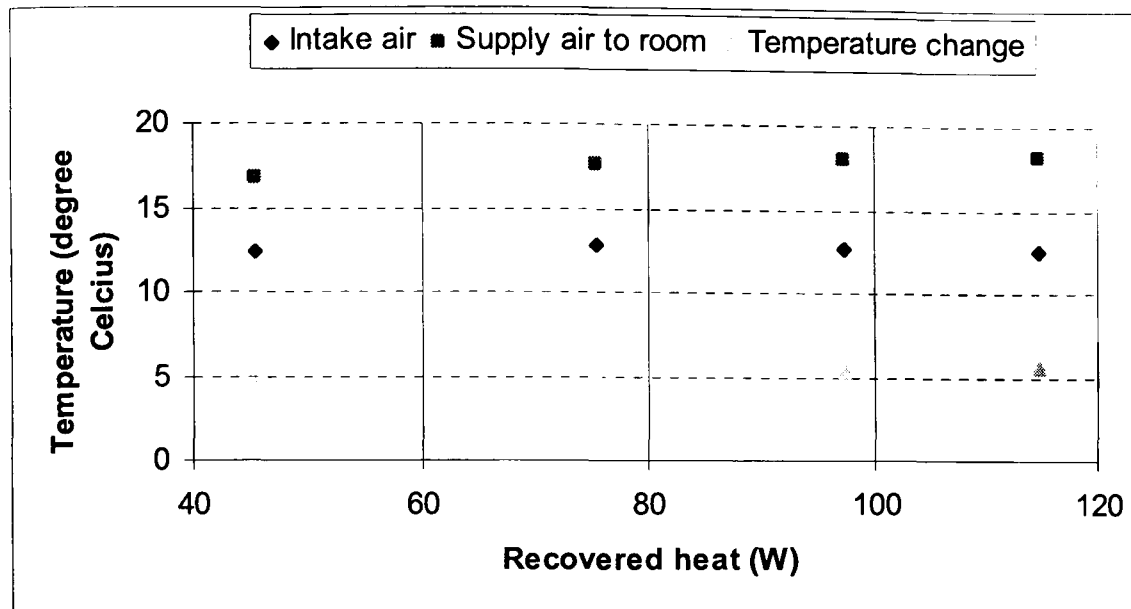


Figure 6.42 Temperature against recovered heat

6.6.3 Comparison with BIHR two airstreams

The comparison of BIHR four airstreams channel which has corrugated channels and BIHR two airstreams channel was conducted for efficiency and temperature change as shown in Figure 6.43 and Figure 6.44 respectively. The efficiency of BIHR corrugated channels with four airstreams is seen to enhance significantly with 65.7% value at $0.079\text{m}^3/\text{s}$ compared to 61.1% for BIHR with two airstreams. This is due to the corrugations geometry forced the flow in the channels to experience a continuous change and flow area and as result turbulence at higher velocities was induced at lower flow. It is evident that the present design has larger efficiency and higher temperature difference than the previous design. Thus, as stated by Han et al. (2010), corrugated plates and fluid flow channels between the plates have high efficiency, small flow resistance, high heat transfer and large bearing pressure capacity.

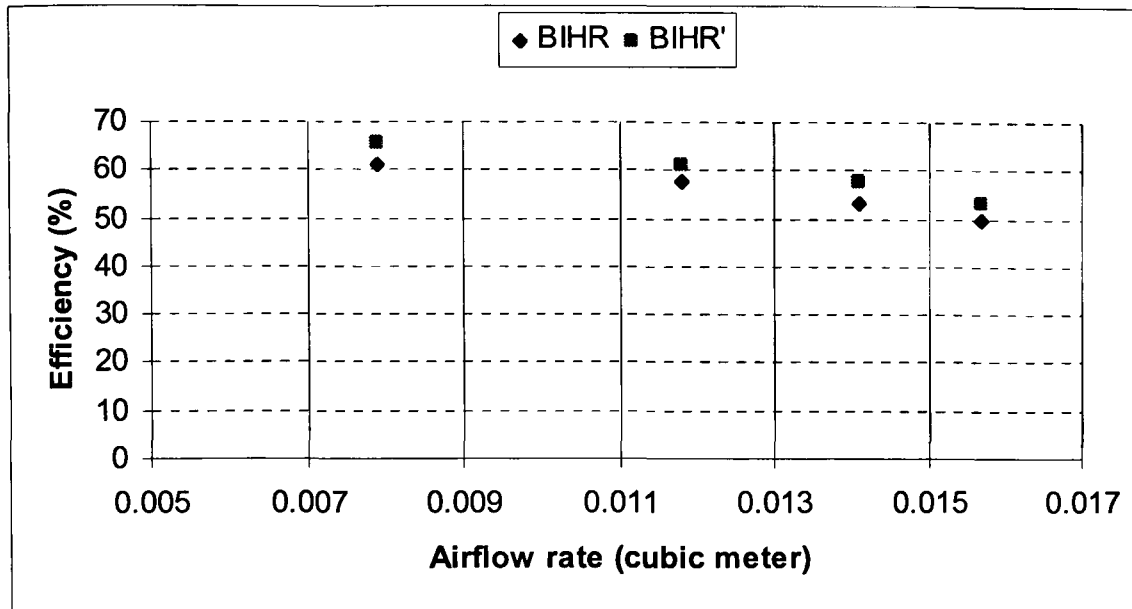


Figure 6.43 Comparison of efficiency between BIHR with two airstreams and new BIHR' corrugated channels with four airstreams

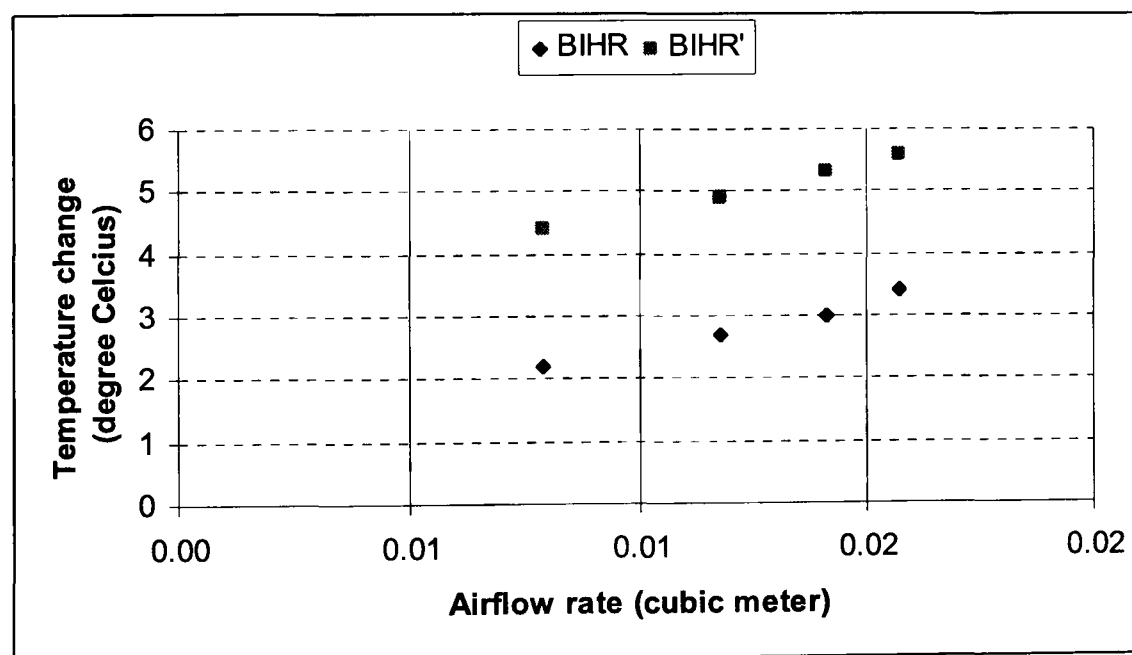


Figure 6.44 Comparison of temperature change between BIHR with two airstreams and new BIHR' corrugated channels with four airstreams

In addition, the comparison of total heat transfer rate for various air velocities is illustrated in Figure 6.45. It is obvious that the corrugated channels in improved design gave higher heat transfer rate by more than 50%. This is because of flow interruption including recirculation and reattachment; the heat transfer characteristics

are quite different than flat plates. The configuration of BIHR corrugated channels with four airstreams with respect to its flow passage shape is important parameters that influence its heat recovery performance.

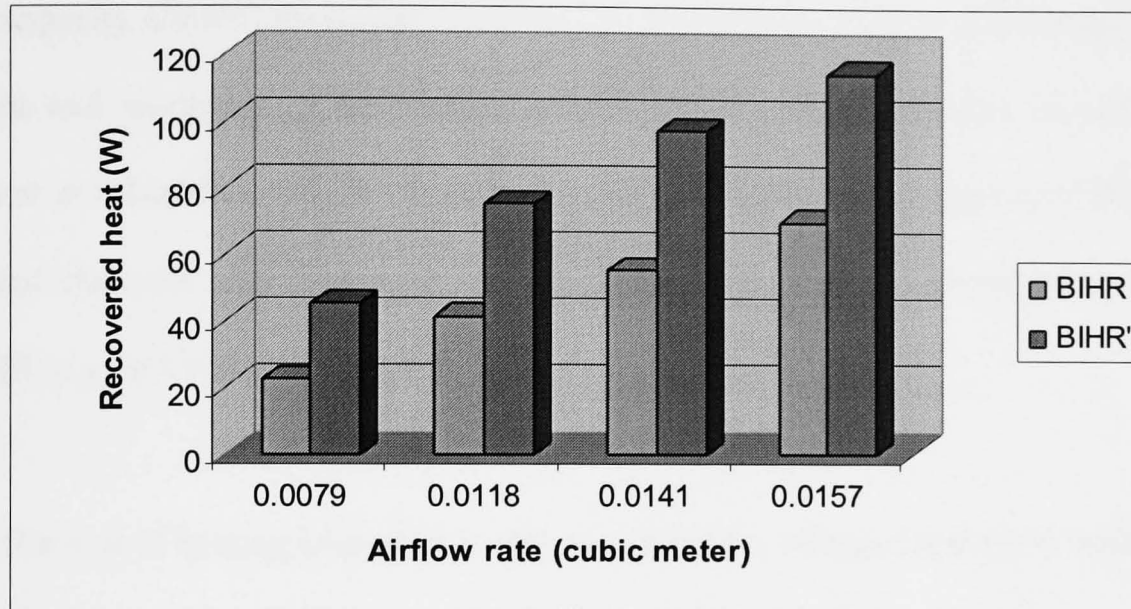


Figure 6.45 Comparison of total heat transfer rate for various air velocities between BIHR with two airstreams and new BIHR' corrugated channels with four airstreams

From the above discussion, it can be said that good enhancement in heat transfer performance was achieved with the improved BIHR employing corrugated channel with four airstreams. As discussed earlier and based on data reported by Islamoglu (2003), the corrugated channels employed in this design would be able to achieve enhanced heat transfer. This is because these types of channels interrupt the thermal boundary layer and thereby increase the convection heat transfer coefficient.

6.7 Economic and environment analysis of BIHR system

It is well known that heat recovery is a promising technology that can reduce energy use and improve profitability. The economic benefits of investing in heat recovery system depend on the volume, duration of ventilation, equipment and cost structure. This structure can be quite different for different users, so that it is difficult

to generalize the results. The main cost items are investment and running costs. In economic analysis, not just the heat recovery system cost must be considered but also the marginal cost saving resulting from the possible reduction of installed heating or cooling capacity allowed by energy recovery in ventilation system. In this section, the economic and environment advantages of this BIHR system installed in heating equipment are described for BIHR prototype with two airstreams, improved BIHR' corrugated channels with four airstreams, BIHR in case study I without PV system and BIHR in case I with PV system.

The cost of heating energy (here the use of electric energy for electric heater is assumed) and the electrical energy for the fans of BIHR system. In this economic analysis, the following conditions are considered.

- Ventilation (heating) without BIHR – The heating capacity (electric heater) necessary for ventilation under design conditions
- Ventilation (heating) with BIHR – BIHR allows lower installed heating capacity, reducing specific costs according to the BIHR efficiency
- Recovery equipment cost – BIHR system must be accounted for
- Equipment cost with BIHR
- Cost without BIHR- electric requirements for heating
- Cost with BIHR – BIHR allows to reduce operational costs according to BIHR efficiency

Using the baseline scenario above, the potential financial (£), energy (kWh) and carbon savings (kg CO₂) have been calculated based for BIHR system. In order to

analyse the economical benefits of the system, several calculations should be done for:

- Annual energy consumption

Annual energy consumption (kWh/y) = Equipment consumption (kW) x number
of operating hours/year

- Annual energy recovered

The annual energy recovered can be calculated by using the formula introduced by Soylemez (2000) at discussed in Equation 3.54 in Chapter 3.

$$Q = \varepsilon_{HR}(MCp)_{\min}\Delta T_{\max}\Delta t$$

- Carbon emissions

Carbon emissions = Annual energy consumption (kW) x Emission factor
(kgCO₂/kWh)

- Annual running cost

Annual running cost = Annual energy consumption (kW) x pence/kWh

- Payback period

Payback period = Investment/ Net annual cash flow

6.7.1 Economic analysis of BIHR prototype with two airstreams and improved BIHR' corrugated channels with four airstreams

An economic analysis of BIHR prototype with two airstreams and improved BIHR' corrugated channels with four airstream with the size of 1.0m length and efficiency of 50% and 53.3%, respectively has been carried out. The capital cost of BIHR prototype with two airstreams is considered at £250, whilst for improved BIHR' corrugated channels with four airstreams is £300. These values are based on airflow rate of $0.0157\text{m}^3/\text{s}$ equivalent to 2.0m/s. It is assumed that both system running 24 hours per day to ventilate the indoor space for 3 months during winter season (October, November and December) each year in the UK and the equipment energy consumption for BIHR fans is 0.032kW. The cost of electric heater is considered at £300 (<http://www.energysaving-shop.co.uk>) with heating capacity of 1.7kW. The unit fuel price for electric is 13p/kWh. The BIHR prototype with two airstream could recover 70kW of waste energy from heating system and improved BIHR' corrugated channels with four airstreams could recover about 0.114kW of waste heat.

The annual energy consumption for heating system without BIHR is found to be 3672kWh and for the both BIHR prototype with two airstreams and improved BIHR' corrugated channels with four airstreams is 69.12kWh used to run the fans. The carbon emissions associated with the energy consumption of heating system without BIHR is found to be 1997.57 kgCO₂e and for the BIHR system is 37.60kgCO₂e. In heating system utilizing BIHR prototype with two airstreams about 41.1kgCO₂e of carbon emission reduction is obtained. While in heating system

utilizing improved BIHR' corrugated channels with four airstreams about 70.72kgCO₂e of carbon emission reduction is gained.

The annual running cost for heating equipment running for 24 hours for three months is £477.36 whilst for BIHR system is £8.99 to run the fans. Considering 50% efficiency of BIHR prototype with two airstreams that could recover the waste energy at from heating system, the annual running cost in recovering the energy is £9.83 and £16.90 for improved BIHR' corrugated channels with four airstreams. The annual saving for BIHR prototype with two airstreams and improved BIHR' corrugated channels with four airstreams is £467.53 and £460.46, respectively. Therefore, the payback period of an investment of about £550 for heating equipment with BIHR prototype with two airstreams is about 1.17 and for investment of £600 for heating equipment with improved BIHR' corrugated channels with four airstreams is 1.3. The results are summarized in Table 6.8.

Table 6.8 Capital and running cost for BIHR prototype with two airstreams and improved BIHR' corrugated channels with four airstreams

	Heating equipment	BIHR prototype (1.0m length)	Heating equipment with BIHR prototype	Improved BIHR corrugated channels (1.0 m length)	Heating equipment with improved BIHR corrugated channels
Capital cost	£300	£250	£550	£300	£600
Energy price	13pence/kWh				
Efficiency	-	0.50		0.53	
Annual running hours	24 hours per day for three months = 2160 hours				
Annual energy recovered	-	75.6kWh		130kWh	
Annual running cost	£477.36 (for heating)	£8.99 (for fans)		£8.99 (for fans)	
Annual energy saving	-	£9.83	£467.53	£16.90	£460.46
Payback period	(Investment required divided by net annual cash flow of heating equipment with BIHR system)				
	1.17			1.30	

6.7.2 Economic analysis of BIHR system in case study I

A BIHR system with the size of 2.5m length and 72.9% efficiency was installed in case study I in at a capital cost of £500. Whilst, capital cost including the PV system to power the fans is £1000. This values are based on airflow rate of $0.0157\text{m}^3/\text{s}$. It is assumed that the BIHR system running 24 hours per day to ventilate the indoor space for 3 months during winter season (October, November and December) each year in the UK and the equipment energy consumption for BIHR fans is assumed to be 0.032kW. The BIHR system could recover 0.147kW of waste

energy from heating system. The cost of electric heater is considered at £300 with heating capacity of 1.7kW. The unit fuel price for electric is 13p/kWh.

The annual energy consumption for heating system without BIHR is found to be 3672kWh and for the BIHR system is 69.12kW. The carbon emissions associated with the energy consumption of heating system without BIHR is found to be 1997.57 kgCO₂e and for the BIHR system is 37.60kgCO₂e. The carbon emission reduction of about 126.09kgCO₂e is gained in this heating equipment utilizing BIHR system. The annual running cost for heating equipment running for 24 hours for three months is £477.36 whilst for BIHR system is £8.99 to run the fans. Considering 72.9% efficiency of BIHR that could recover the waste energy at from heating system, the annual running cost in recovering the energy is £30.31. The resulting saving is £447.05. Therefore, the payback period of an investment of approximately £800 for BIHR without PV system and £1200 for BIHR with PV system is approximately 1.79 and 2.68. The results are summarized in Table 6.9.

Table 6.9 Capital and running cost for BIHR system in case study I

	Heating equipment	BIHR system (2.5m length)	Heating equipment with BIHR system	Heating equipment with BIHR driven by PV system
Capital cost	£300	£500	£800	£1200
Energy price	13pence/kWh			
Efficiency	-	0.73		
Annual running hours	24 hours per day for three months = 2160 hours			
Annual energy recovered	-	231.79kWh		
Annual running cost	£477.36 (for heating)	£8.99 (for fans)		
Annual energy saving	-	£30.13	£447.05	£447.05
Payback period	(Investment required divided by net annual cash flow of heating equipment with BIHR system)			
	1.75		2.63	

6.8 Performance investigation of BIHR system with fibre wick structure for cooling and dehumidification

Hot and dry climate such as Mediterranean areas as well as hot and humid region like South East Asia countries has facing thermal comfort problem in interior space. Excessive heat or humidity is the major problem that causes human thermal discomfort in buildings in these regions. Thermal comfort has been defined by Hensen (1991) as “a state in which there are no driving impulses to correct the environment by the behaviour”. On the other hand, ASHRAE (2004) defined it as “the condition of the mind in which satisfaction is expressed with the thermal environment. In physiological terms, thermal comfort is what we experience when the body functions well. There are many ways of maintaining these body temperatures in a wide range of climates and this has been the case for centuries. Perhaps, air conditioning will be an answer to thermal comfort problem but the process of air

conditioning requires energy which most the people in the developing countries have limited affordability (Zain 2007).

With the issue of thermal comfort in hot region area and problems with conventional air conditioning system, it is significant to propose a new low carbon technology as alternative to the conventional system for the hot condition of incoming air. Considering that, in this chapter, a study of a novel building integrated heat recovery (BIHR) system with fibre wick structure for different hot (summer) air condition using different working fluids was carried out which is the extension of BIHR system. The study has been divided into two different cases as following:

- Summer condition with hot and dry outdoor air. – This system consists of BIHR-fibre wick cooling system using water as working fluid. This system is developed in respond to the limits of BIHR to treat hot summer air in temperate climates and hot and dry region such as Mediterranean areas.
- Summer condition with hot and humid outdoor air. – This system consists of BIHR-fibre wick desiccant dehumidification system using HCOOK solution as working fluid. This system is developed in respond to the limitation and deficiencies of evaporative cooling to be used in hot and humid regions such as Malaysia and South East Asia countries. This system would also overcome the problem faced by conventional air conditioning system.

6.8.1 System description

This system consist of building heat recovery (BIHR) unit and fibre wick structure unit that have been integrated together in one panel to provide a low-cost, energy efficient and environmentally benign method of air cooling or

dehumidification. This is an extension of the research on BIHR system. In this investigation similar unit of BIHR prototype with two air stream described in the previous investigation in section 6.3 was used. As an improvement to the previous BIHR panel, fibrous material has been introduced in the development of internal air channels called fibre wick structure. The performance of this new improved system was then evaluated for two different case studies by using two different working fluids for cooling and dehumidification.

6.8.1.1 Fibre wick structure

The fibre wick structure unit used in this system was made from fibre cloth for making the wet surface which was cut to the required size. It has 1000mm as the length and 15mm as the width for stacking along the each inlet of internal channel of polycarbonate BIHR panel. The thickness of fibre wick structure is 0.5mm. This structure was attached to the interior surface of each inlet channel of BIHR panel (polycarbonate plate) with the help of thermal adhesive as shown in Figure 6.46.

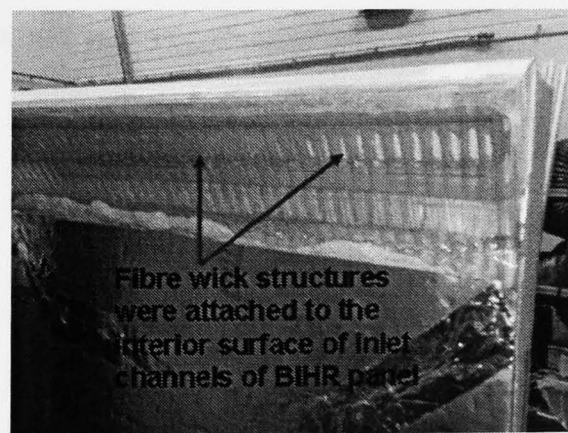


Figure 6.46 Inlet channel of BIHR panel

In developing this system, the fibre wick structure in BIHR internal channels would serve two important functions:

- It provides a cooling or dehumidification mechanism for the hot intake air condition
- It facilitates the evenly distribution of the working fluid over the entire surface of the structures in internal channels.

Figure 6.47 shows the cross sectional view of the internal channel. The working fluid used for cooling or dehumidification would be filled then allowed to flow over the fibre wick structure by gravitation. This mechanism of feeding of working fluid has been chosen to gain good wetting of internal surfaces as good wetting of surfaces were spraying mechanism were found to be critical to achieve a good performance and care should be given to prevent flooding in a study conducted by Saman and Alizadeh (2001). In addition by using fibre wick structure which has been attached to the inner surfaces of the BIHR panel would treat the problem of non-wettability of surfaces while preventing channel flooding.

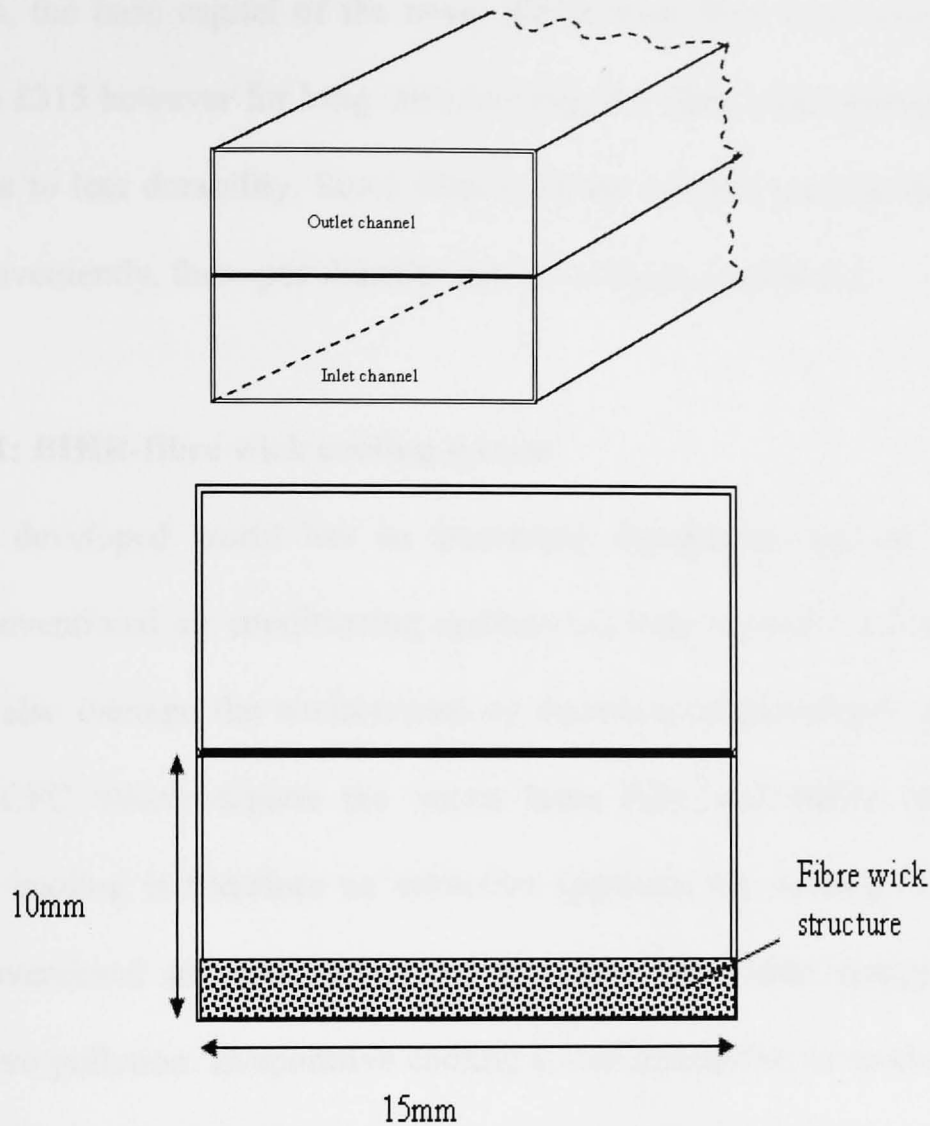


Figure 6.47 Cross sectional view of the internal channel

6.8.1.2 Capital cost

The capital costs incurred on the construction of BIHR with fibre wick structure are details in the following:

BIHR unit (1m x 1m)	= £250
Fibre cloth	= £5.00
Working solution (10kg)	= £10.00
Cooling/Dehumidification tower	= £50.00
Sum	= £315

Thus, the base capital of the novel BIHR with fibre wick structure is quite cheap about £315 however for long term running, the fibre wick structure need to be replaced due to less durability. Since fibre is cheap material and can be shaped and installed conveniently, these peculiarities can cover those conditions.

6.8.2 Case 1: BIHR-fibre wick cooling system

The developed world has an increasing dependence on air conditioning; however conventional air conditioning systems not only consume a large amount of energy but also damage the environment by emission of greenhouse gases and the release of CFC which deplete the ozone layer (Qiu and Riffat 2006). Passive evaporative cooling is therefore an attractive approach for cooling of buildings to replace conventional air conditioning as it uses a renewable energy source and generates zero pollution. Evaporative cooling is one alternative to mechanical vapour compression for air conditioning application (Riangvilaikul and Kumar (2010). These systems usually require only a quarter of the electric power that mechanical vapour compression uses for air conditioning (Cerci 2003). Basically, there are two common types of evaporative cooling system are direct and indirect systems. Direct evaporative cooling system has approximately 70 to 95% effectiveness in terms of temperature depression (Wu et al. 2009). Besides, direct evaporative cooling systems decrease air temperature by direct contact with a water surface or with a wetted solid surface or even with sprays. Solid surfaces such as jute canvas (Ghosal et al. 2003), gunny bags (Nahar et al. 2003) and ceramic jars are more water economical than the water pond (Nahar et al. 2003) or spray (Badran 2003).

Kruger et al. (2010) stated that in hot and dry regions there are also potential benefits of using evaporative cooling, taking advantage of high evaporation rates due to the low air humidity. On the other hand, evaporative cooling systems have a great potential to offer indoor thermal comfort in arid hot climates such as Mediterranean areas (Qiu and Riffat 2006). Thermal comfort in hot and dry climate can also be achieved using space cooling method by improving the performance of roofs since they are the surfaces most exposed to direct solar radiation and can cause excessive heat gain in hot periods (Cheikh and Bouchair 2004). By taking all these into account, in this section BIHR panel which could be fitted in roof is combined together with fibre wick structure in one integrated panel to develop a novel BIHR-fibre wick cooling system that could be used in hot and dry climates to treat the incoming hot air while at the same time recover the heat. In this work, water has been used as working fluid to wet the fibre wick structure in order to give evaporative cooling effects. This section presents the performance investigation of the system with a key objective to reduce the temperature of the incoming hot and dry temperature.

6.8.2.1 Working principle and theoretical psychrometric analysis

This novel system was based on direct evaporative cooling where hot dry air was passed through wetted fibre wick structure, get cooled by evaporation and then be blown to indoor space of building. This method introduces moisture to the unit until the air stream is close to saturation. So the air temperature falls while its moisture contents increases. As a result energy contained in the exit remains unchanged and its wet bulb temperature kept the same. The underlying principle of evaporative cooling is the conversion of sensible to latent heat. When water evaporates into vapour, the water cools both the abutting non-saturated air and the remnant water from which the

necessary sensible is provided. It is obvious that during this process the moisture content of the air is increased and so the process is called direct evaporative cooling.

To evaluate the cooling performance of the fibre wick structure, the system is modelled as shown in Figure 6.48. In this unit, hot and dry air is passed through the wetted fibre wick structure where it is brought into a direct contact with water. The energy needed for the evaporation comes from the hot and dry air and it is cooled. At the same time the air gained increased in moisture content. In steady state condition, the mass balance for hot and dry air is:

$$M_{a1} = M_{a2} = M_a \quad (6.1)$$

For direct evaporative cooling system, the cooling capacity, Q_{fw} can be expressed in terms of mass flow and the enthalpy change across the system as a function of the intake air, T_{ih} and supply air to room, T_{sh} of dry bulb temperature as the followings:

$$Q_{fw} = M_a C_p (T_{sh} - T_{ih}) \quad (6.2)$$

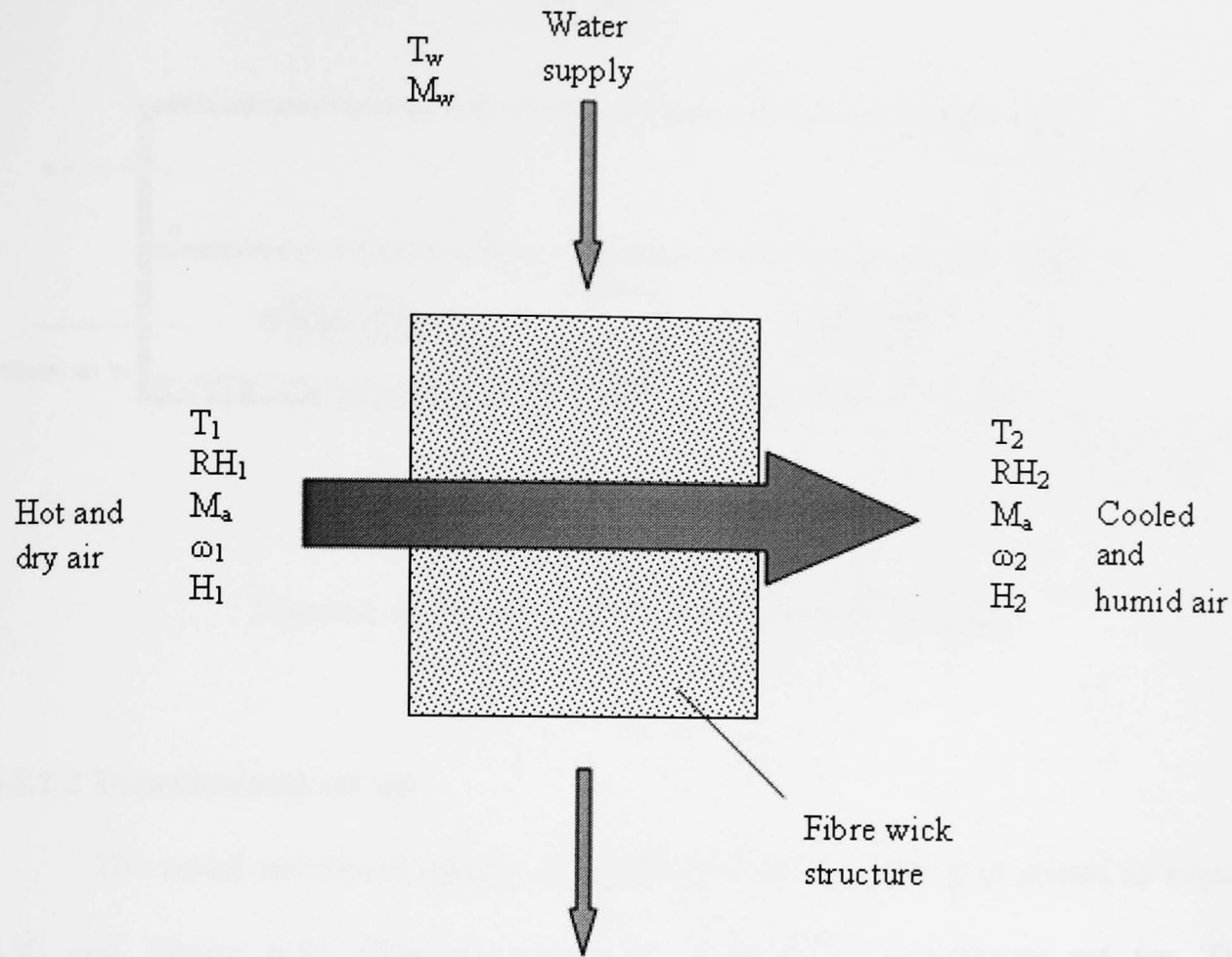


Figure 6.48 Direct evaporative cooling model

For this investigation, fibre wick structure contained in inlet channels of BIHR core made of polycarbonate were used as the water saturated medium. When warm air contains heat entered the channels, the water vaporizes. Warm air contains heat entered and took places in the lower channel by convection through the air and fibre wick structure. The vapour travelled to the end of the channel due to vapour pressure gradient in the channel and then the vapour condenses and release its latent heat vaporization. The release heat is transferred to upper channel by heat transfer surface and rejected to the environment as shown in Figure 6.49.

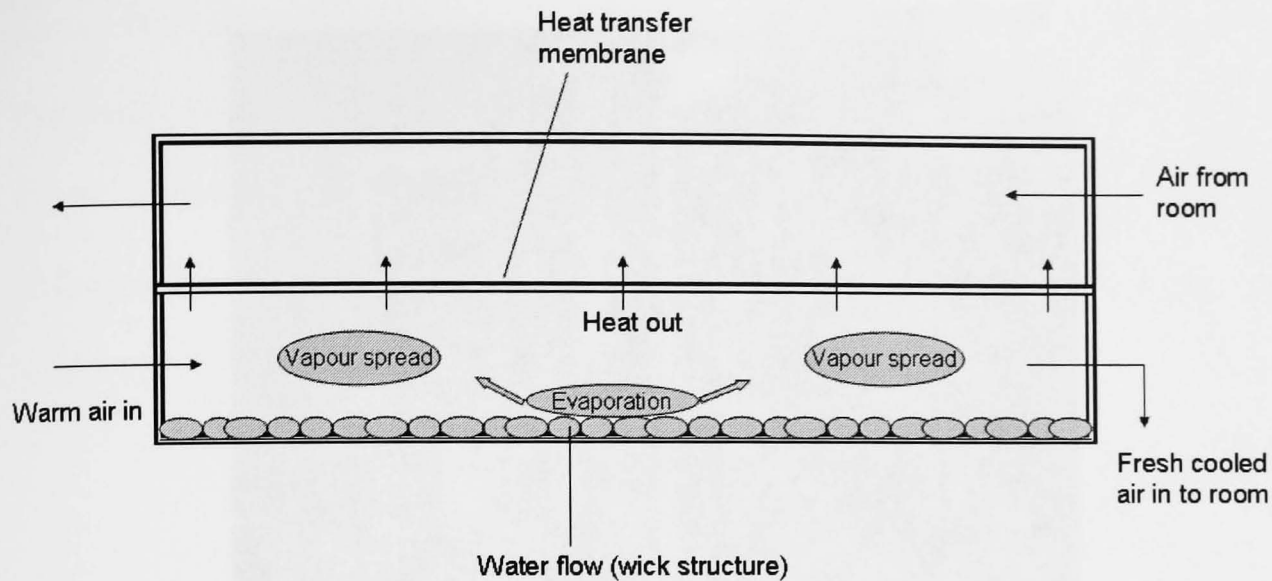


Figure 6.49 Air convection in the internal channel

6.8.2.2 Experimental set up

The novel combined system of BIHR-fibre wick cooling is shown in Figure 6.50 and Figure 6.51 illustrate schematic diagram of experiment set up. The arrangement consists of a chamber containing BIHR unit and fibre wick cooling unit. The system was set up at Energy Learning Laboratory at Department of Architecture and Built Environment, University of Nottingham, UK. An overhead water tank was provided on top of the chamber. In this way water was supplied to the fibre wick structure through a feed line by gravity. Similar test room for BIHR prototype panel in section 6.3 was used in this investigation.

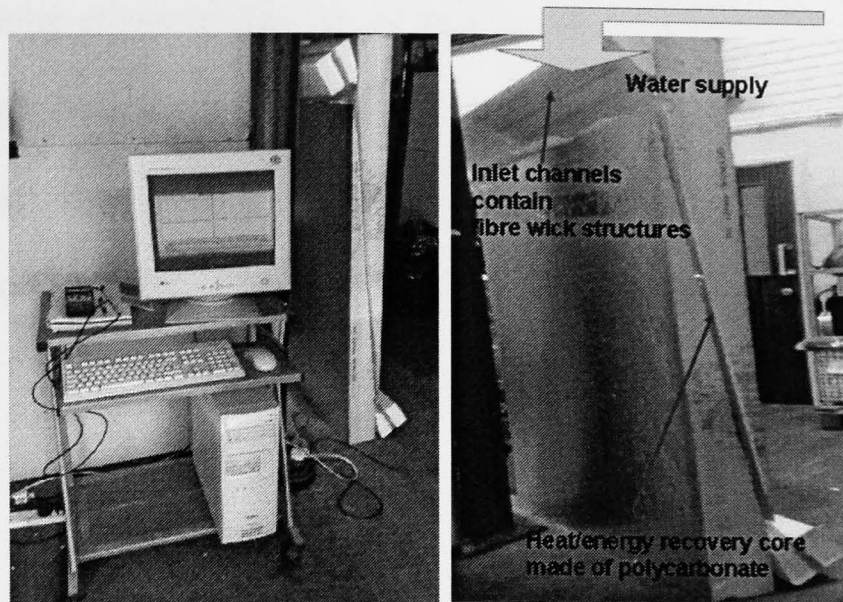


Figure 6.50 The novel combined system of BIHR-fibre wick cooling

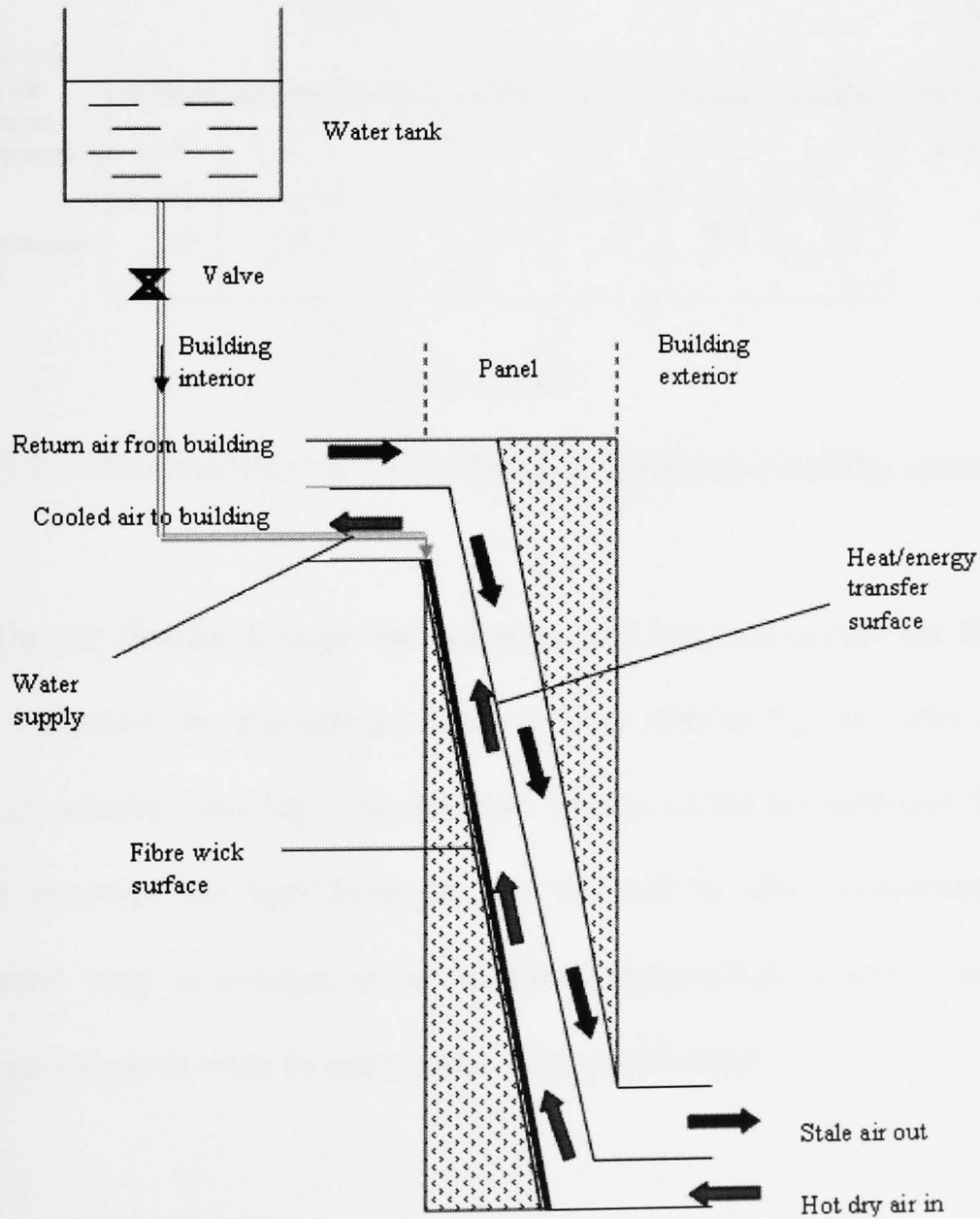


Figure 6.51 Schematic diagram of experiment set up

Each inlet channels consists of fibre wick structure which became wet by absorbing water from the supply water tank as shown in Figure 6.52. The air then passed through the inlet channels containing moistened fibre wick surface. Evaporative cooling takes effect directly and the air was discharged at a high relative humidity.

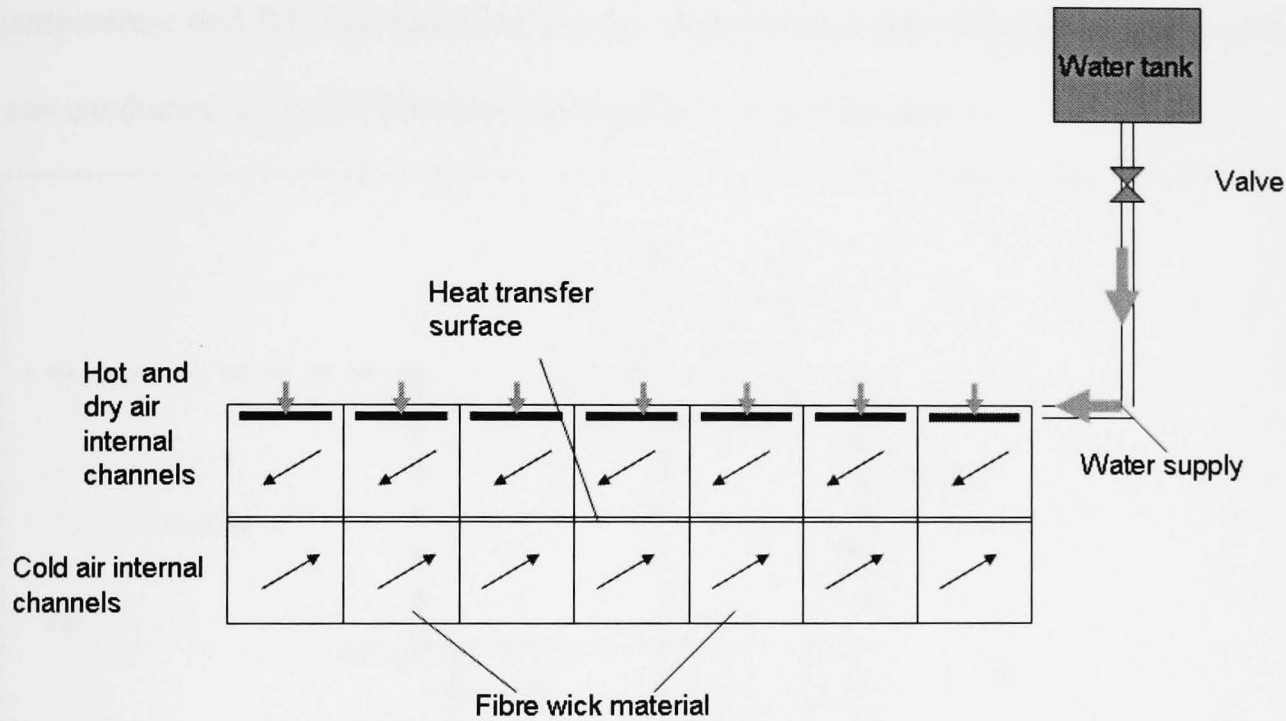


Figure 6.52 Inlet channels consists of fibre wick structure wetted by absorbing water

The air flowed through the channels and lost heat across the heat transfer surface. Therefore its temperature reduced from inlet at T_{ih} to outlet at T_{sh} with increase in relative humidity. The moisture content of the air increased from ω_{ih} to ω_{sh} as it absorbed the heat from the wet channel to effect evaporation process. Experiments were conducted under different temperature, relative humidity and airflow rate values in order to analyse the system performance.

6.8.2.3 Experimental procedure

Similar experiment procedures for the performance investigation were carried out in an environmental control chamber as described in section 6.3. Air temperature and relative humidity (RH) were monitored using thermocouples type K and Vaisala HMPA45A relative humidity probes. Figure 6.53 shows the schematic diagram of temperature and RH measurement points. Experimental data acquisition and logging was conducted using DT500 dataTaker as described in Chapter 4.

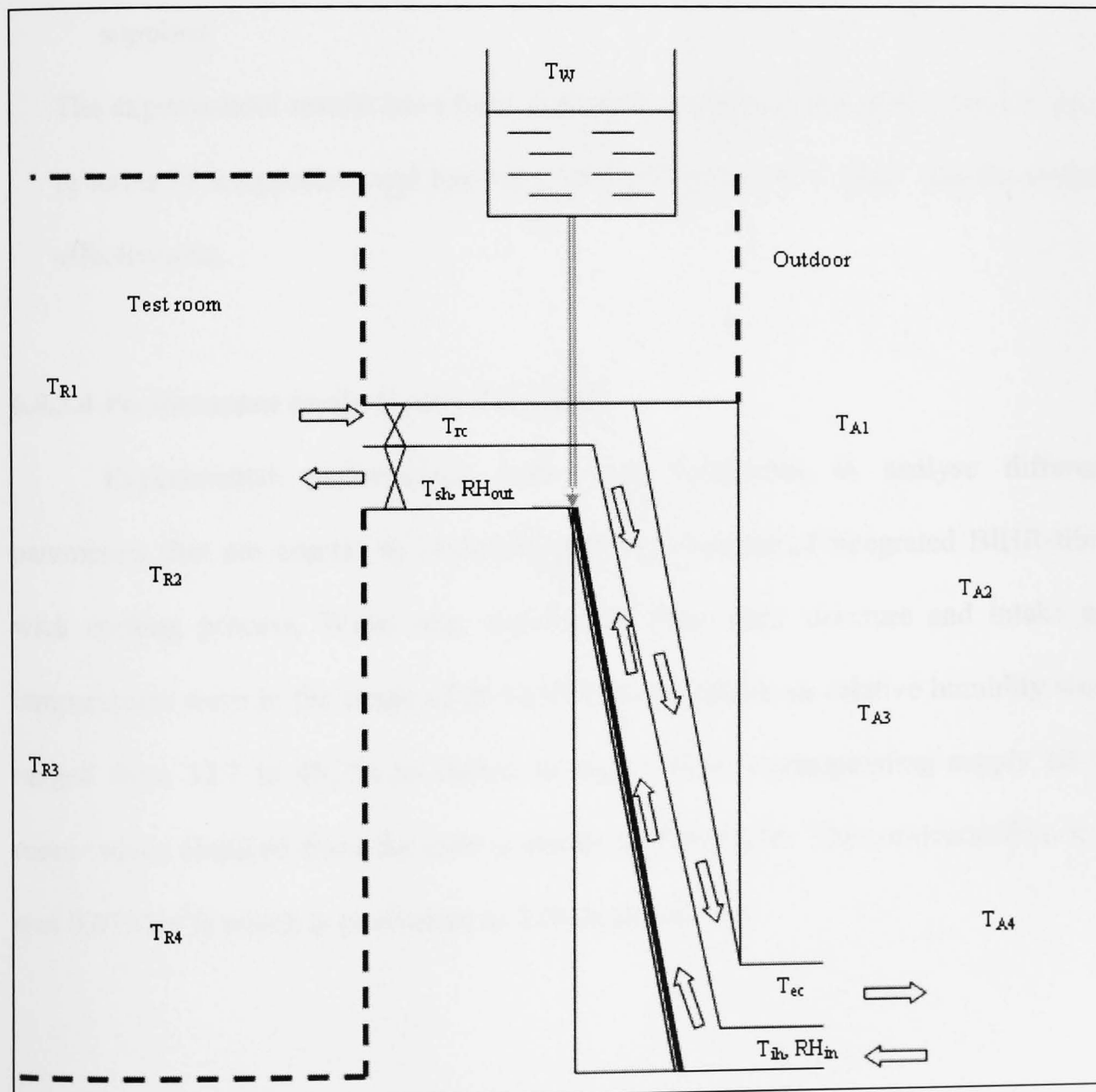


Figure 6.53 Schematic diagram of temperature and RH measurement points

To investigate the performance of the combined BIHR-fibre wick cooling system the following tests were conducted:

- Fibre wick structures were supplied with water at different settings of dry bulb temperature and relative humidity of the intake air at a constant airflow rate (2.0m/s).
- The system was running at different airflow rate, with constant intake air temperature in order to evaluate the efficiency of BIHR unit with water supplied.

The experimental results have been evaluated to quantify the system performance in terms of temperature and humidity level of supply air to room and the system effectiveness.

6.8.2.4 Performance analysis and discussion

Experimental performance tests were conducted to analyse different parameters that are crucial in evaluating the performance of integrated BIHR-fibre wick cooling process. Water was supplied to fibre wick structure and intake air temperatures were in the range of 25 to 38.2°C and intake air relative humidity were ranged from 32.7 to 45.2% as shown in Figure 6.54. Corresponding supply air to room values obtained from the tests is shown in Table 6.10. The volume airflow rate was 0.0157m³/s which is equivalent to 2.0m/s air velocity.

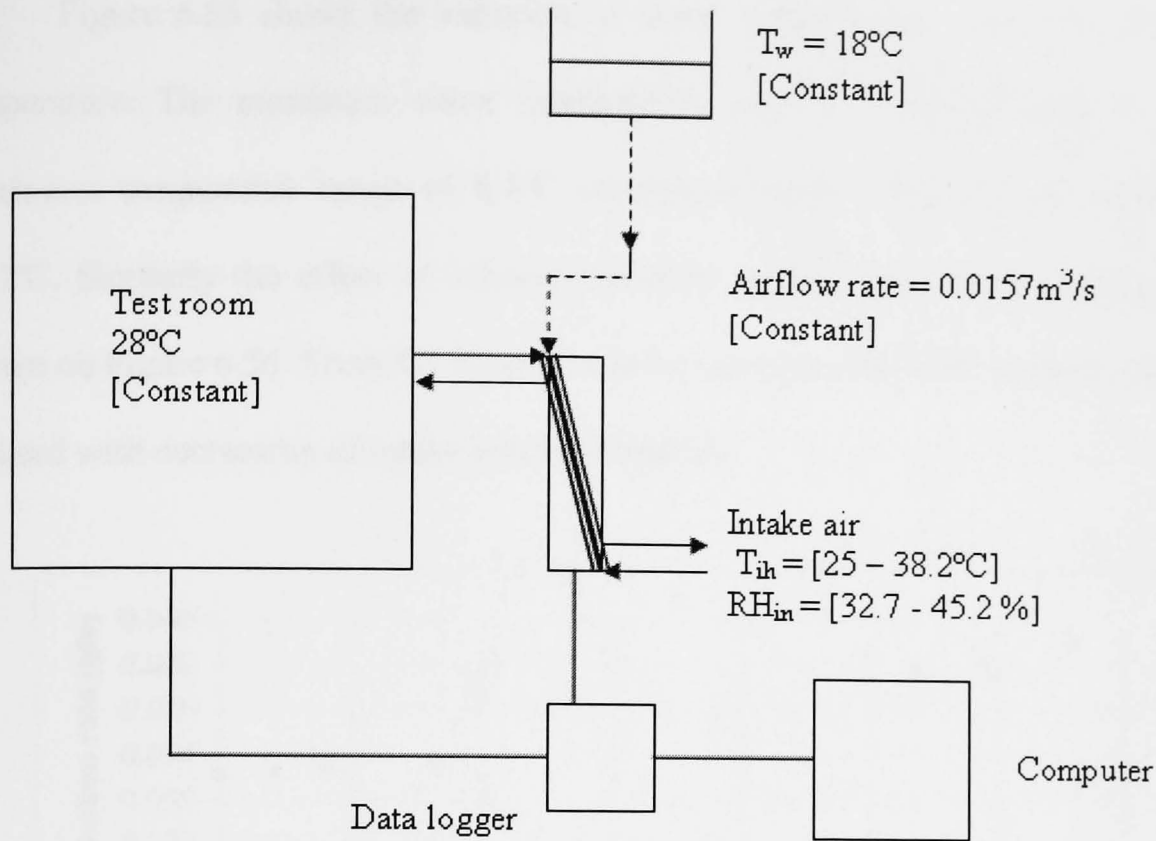


Figure 6.54 Water was supplied to fibre wick structure

Table 6.10 Experimental data

Intake air, T_{ih} $^\circ\text{C}$	Supply air to room, T_{sh} $^\circ\text{C}$	RH in %	RH out %
25.0	23.5	45.2	57.2
25.8	24.1	45.4	57.7
26.6	23.9	44.3	57.4
28.3	25.1	42.1	55.1
30.4	25.5	38.2	52.7
35.7	30.0	36.5	52.3
38.2	31.8	32.7	48.4

From the measurements it was found that the temperature change increased with increasing intake air temperature. For intake air temperature range from 25 to 38.2°C , a change of 1.5 to 6.4°C was recorded. For intake relative humidity range of 32.7 to 45.2%, corresponding increase of 12 to 15.7% was observed at the supply air to room.

Figure 6.55 shows the variation of water consumption rate with intake air temperature. The maximum water consumption rate of 0.042g/s occurred at the maximum temperature range of 6.4°C corresponding to intake air temperature of 38.2°C. Similarly the effect of relative humidity on the water consumption rate is shown on Figure 6.56. From the figure it can be seen that, the water consumption rate reduced with decreasing of intake relative humidity.

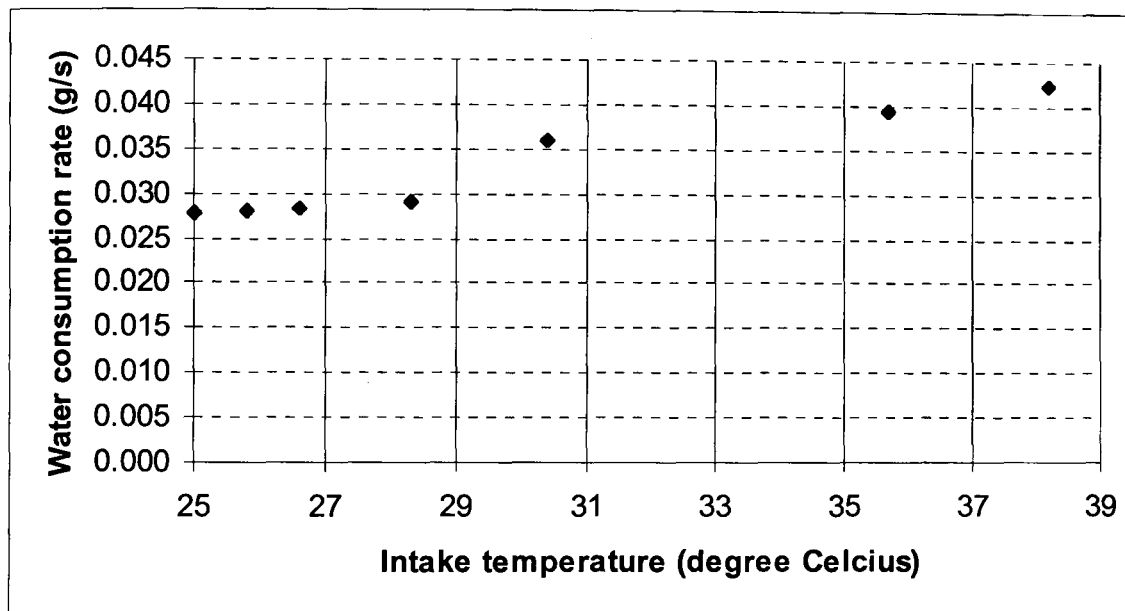


Figure 6.55 Variation of water consumption rate with intake air temperature

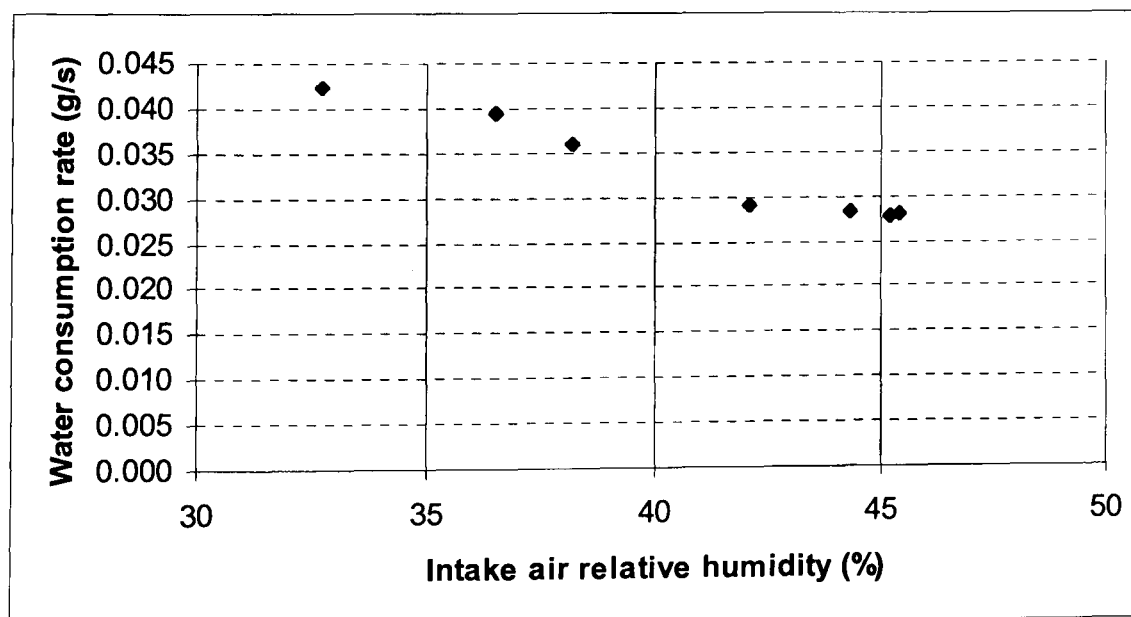


Figure 6.56 Effect of relative humidity on the water consumption rate

Efficiency of the cooling system was calculated by applying wet-bulb efficiency equation described in Chapter 5 on the experimental after obtaining the corresponding wet bulb temperature values by using a psychrometric calculator. Results for instantaneous intake air temperature values are shown in Table 6.11.

Table 6.11 Results for instantaneous intake air temperature values

Intake air, T_{ih} °C	Supply air to room, T_{sh} °C	Wet bulb intake air, T_{wbi} °C	ΔT	ΔTwb	Cooling efficiency
25.0	23.5	17.0	1.5	7.3	0.205
25.8	24.1	17.7	1.7	7.5	0.226
26.6	23.9	18.1	2.1	8.5	0.247
28.3	25.1	19.1	3.2	9.6	0.333
30.4	25.5	19.9	4.9	11.7	0.419
35.7	30.0	23.5	5.7	13.3	0.429
38.2	31.8	24.4	6.4	15.1	0.424

Figure 6.57 shows the variation of BIHR-fibre wick cooling efficiency with respect to intake air temperature. In this test, a value of over 40% was recorded at the maximum temperature change attained. The efficiency increased with increasing intake air temperature and stabilised after 31°C. In this case, the efficiency ranged from 20.5 to 42.4% corresponding to the minimum and maximum of intake air temperature of 25°C and 38.2°C, respectively. Therefore as the temperature change increases as a result of higher dry bulb temperature at the intake air the efficiency also tends to gain higher value.

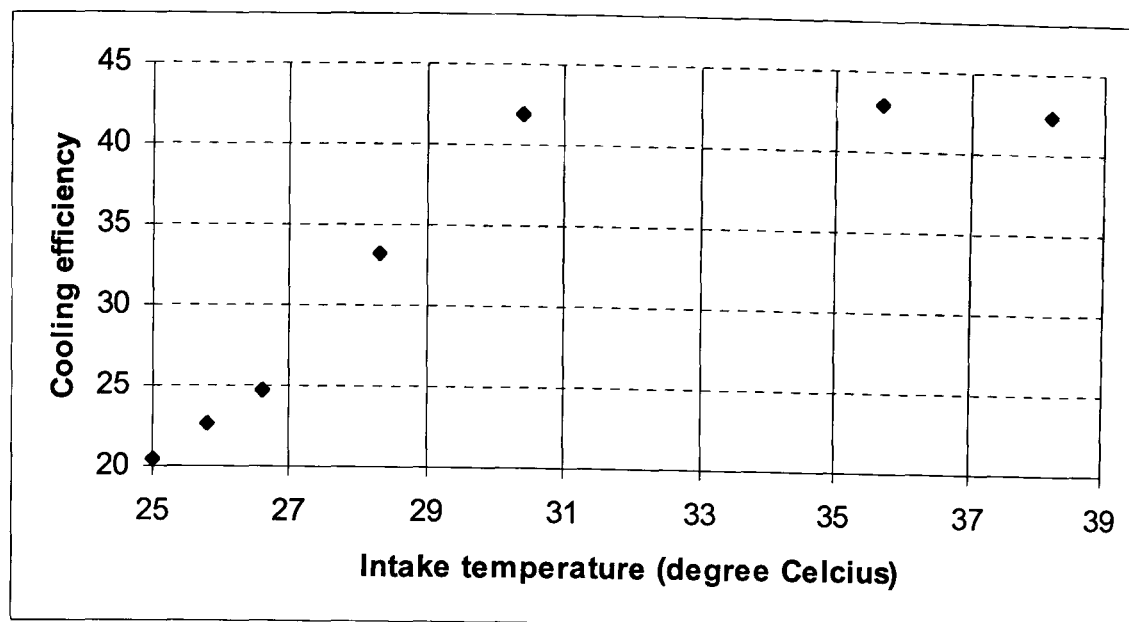


Figure 6.57 Variation of BIHR-fibre wick cooling efficiency with respect to intake air temperature

Tests were also conducted under different air velocities which ranged from 1.0 to 2.0m/s. Under this test, the intake temperature was constant at 30°C. Table 6.12 shows the results of these tests.

Table 6.12 Results of the BIHR fibre wick cooling test

Air velocity m/s	Intake air, T_{ih} °C	Supply air to room, T_{sh} °C	Return air, T_{rc} °C	Exhaust air, T_{ec} °C
1.0	30.0	26.6	24.3	27.6
1.5	30.0	25.9	23.0	27.2
1.8	30.1	25.6	21.9	26.4
2.0	30.0	25.1	20.8	25.7

The BIHR-fibre wick cooling efficiency was calculated using the results in table above. Figure 6.58 shows the variation of BIHR-fibre wick cooling efficiency corresponds to air velocity. From the figure it can be seen that the efficiency ranged from 53.2 to 60.7%. These results were in good agreement as compared to the results for BIHR prototype without the fibre wick structure. This shows that, the utilization

of wetted surface of fibre wick structure in this system helped to cool down the hot and dry of intake temperature and simultaneously increase the humidity of supply air to room.

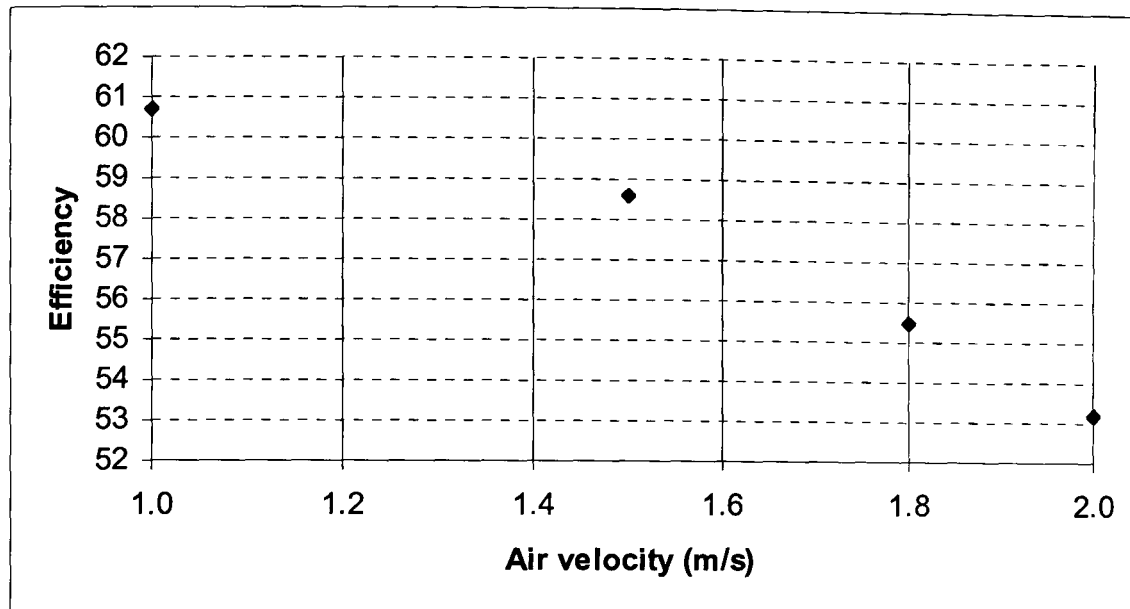


Figure 6.58 Variation of BIHR-fibre wick cooling efficiency corresponds to air velocity

6.8.3 BIHR-fibre wick desiccant dehumidification system

In modern society, people are spending most of their time in indoors. Therefore indoor air qualities in residences, offices and other non-industrial indoor environments have been increasing concerned (Zhang et al. 2005) On the other hand depleting energy resources coupled with increasing environmental pollution have shifted the attention of researchers all over the world to find the alternative air conditioning systems (Jain et al. 1994). As energy shortage emerges as an issue of growing concern in the world, coupled with the threat to environment posed by the conventional HVAC system and thermal comfort issue in hot and humid region, the need to come up with the new energy savings as well as environmental-friendly systems has been more urgent than ever before. Thus, maintaining thermal comfort

for occupants of buildings or other enclosures is one of the important goals in designing the low energy HVAC system.

Since, air temperature and relative humidity are the two major parameters affecting thermal comfort significantly and only sensible load can be handled by an evaporative cooling system (Riangvilaikul and Kumar 2009), conventional evaporative cooling system is suitable for dry and temperate climate where the humidity is low (Heidarinejad et al. 2009). But, for hot and humid climates and even in regions where summers are hot and dry, the rainy season brings in very high relative humidity levels, rendering evaporative cooling ineffective (Jain and Dhar 1995). This is one of the main reasons restricting the widespread acceptance of evaporative cooling in countries like Malaysia and South East Asia countries where the ambient air temperature ranges from 22 to 33°C, while the relative humidity varies from 60 to 90% (<http://www.bbc.co.uk/weather/world>). Occupants in these regions presently use air-conditioning and refrigerant systems in order to reduce the interior moisture levels. This is because the relative humidity in an occupied building must be controlled to within 40-60% for health and comfort (Zhang 2006). However, these systems are expensive to operate and increased global warming as well as environmental impact of CFC. Thus, these deficiencies can be overcome by using air dehumidification technology to remove the bulk of the moisture. There are various techniques for air dehumidification (Zhang 2005, Zhang et al. 2005). Traditionally, latent load and sensible load are treated in a coupled way. Then, there is an increasing trend to separate the treatment of sensible and latent load by using an independent humidity control system.

As well as millennium approaches, innovative efforts are being encouraged to developed efficient and environmentally friendly system (Karthikeyan et al. 1995). Desiccant dehumidification is one of the low carbon technologies that can provide energy-efficient solution. In review to its history, desiccant dehumidification technology has been used in many industry applications for more than 60 years. It has long been adopted for both industrial and agricultural purposes such as humidity control in textile mill and post harvest low-temperature crop-drying in stores and is now taking a more and more prominent role in the air-conditioning field (Mei and Dai 2008). It has also been used for many years in clean rooms, hospitals, museums and other special cases requiring highly controlled humidity level (Pesaran 1994). Mavroudaki and Beggs (2002) reviewed the application of desiccant dehumidification systems in Northern Europe and conclude that there was potential to utilize these technologies in the Southern European countries. Meckler (1993) has discussed various benefits of the desiccant technology, its potential applications and factors that drive its future growth. Desiccant dehumidification systems are especially useful when the latent load is high because they remove moisture more economically than they remove sensible heat (Pesaran 1994). Besides, desiccant dehumidification system can supplement conventional air conditioner (Jain et al. 1994). In response to sick building syndrome and the ASHRAE Standard 62-89 on indoor air quality, desiccant dehumidification system could be use in regions with high humidity as it is cost effective because they use low-grade thermal sources to remove moisture from the air.

In recent years, a novel independent fresh air ventilation system which combines a heat recovery with a mechanical air dehumidification unit has gained much attention (Zhang 2006). In this section a novel BIHR-fibre wick desiccant

dehumidification system was developed and investigated experimentally. The aims of this investigation are to develop, install and investigate the performance of a liquid-desiccant dehumidifier into a prototype BIHR's air channels, which will offer a zero cost ventilation. This work is concerned with the investigation of a novel desiccant dehumidifier integrated with heat recovery system for air conditioning of buildings. The system uses potassium formate (HCOOK) solution as liquid desiccant to reduce the high level of relative humidity in the dehumidifier unit integrated in BIHR prototype panel with two airstreams. This system is developed in respond to the limitation and deficiencies of evaporative cooling to be used in hot and humid regions such as Malaysia and South East Asia countries. This system would also overcome the problem faced by conventional air conditioning system.

6.8.3.1 Theory and development

Desiccants are materials that can directly remove moisture from the air and are basically can be solids or liquids and can hold moisture through adsorption or absorption. Solid desiccant dehumidification system includes desiccant wheel, desiccant pack or desiccant bed, which can adsorb moisture from the airflow. The commonly available solid desiccants include silica gel, zeolite, activated alumina and carbon. Jeong and Mumma (2005) have carried out a study by using silica gel to evaluate the performance for desiccant wheel. Dai et al. (2002) have conducted experiments of solid desiccant dehumidification employing porous and strong hydrophilic materials such as silica gel and activated alumina.

The liquid desiccants are competitive with solid desiccants due to their advantages such as more flexibility, capability of absorbing pollutants and bacteria,

relative lower regeneration temperature and lower air side pressure drop (Daou 2004). Several liquid desiccant are commercially available such as triethylene glycol, diethylene glycol, calcium chloride (CaCl_2), lithium chloride (LiCl), calcium bromide (CaBr_2) which are used singly or in combination (Fumo and Goswami 2001). The earliest liquid-desiccant system was suggested and experimentally tested by Lof (1995) using triethylene glycol as desiccant. In a study of liquid desiccant dehumidification system using aqueous LiCl has been conducted by Fumo and Goswami (2001) and reliable sets of data for air dehumidification were obtained. Gommed and Grossman (2007) experiments found that liquid desiccant system had good cooling performance in the hot and humid climates such as Mediterranean countries to solve the problem of shortage of cooling energy.

The selection of the liquid desiccant is decisive in the overall performance of the dehumidification system and will exert an immediate influence on the mass of dehumidification (Mei and Dai 2008). In 1937, hygroscopic salt solution such as lithium chloride (LiCl), lithium bromide (LiBr) and KCOOH were used as absorbents replacing the commonly solid desiccants to deal with large latent loads. LiBr solution is the most stable desiccant with advantageously low vapour pressure, but its cost is slightly higher compared with others (Liu 2008). In addition, LiBr solutions are that they crystallize at high concentrations and are corrosive to metals (Riffat et al. 1998).

Lazzarin (1999) compared the dehumidifier performance of LiBr and CaCl_2 solutions and deduced that CaCl_2 performed less dehumidification capacity than LiBr solution when their mass concentrations had a similar crystallization temperature. CaCl_2 is the cheapest and most readily available desiccant, but it has the disadvantage

of being unstable at certain air inlet conditions and desiccant concentration (Hassan and Hassan 2008). Glycols perform the dehumidification as absorbents very well and are less corrosive than hygroscopic salt solutions. However, glycols have low evaporative pressure and easily evaporate into the supplying air which will poison the breathing air (Liu 2008).

In this study potassium formate (HCOOK) solution has been used for its many advantages including less corrosion, less expensive manufacture and lower density and viscosity than the conventional absorbents such as LiBr solution (Riffat et al. 1998; Liu et al 2007; Yin et al. 2007)). The physical properties of HCOOK offer many benefits. HCOOK is suitable for high humidity (Shehata 1997). Riffat et al. (1998) have evaluated the performance of HCOOK solution as a new working fluid, a replacement for traditional absorbents and found that HCOOK solution showed very similar absorption and desorption properties to those of LiBr solution. In addition, one of its remarkable advantages is that it is environmentally friendly (Qiu 2007).

Performance study of liquid desiccant dehumidification system has gained a lot of attention amongst researcher recently. Hassan and Hassan (2009) have conducted a performance study of a counter-flow channel type liquid desiccant air dehumidifier and found that higher inlet air temperature and relative humidity shown a better performance index. Li et al. (2005) analysed the operating performance of different mass flow rate ratios between desiccant solution and process air under the theoretical reversible condition of dehumidification process. Ali and Vafai (2004) studied the heat and mass transfer between air and desiccant film for counter-flow configuration. Oliveira et al. (1999) have performed a thermal performance of a novel

air conditioning system using a liquid desiccant. By performing several simulations, it was found that the system performance is sensitive to changes in both indoor and outdoor conditions. In this section, the performance of HCOOK solution to reduce the relative humidity of incoming hot and humid air employed in the novel BIHR-fibre wick desiccant dehumidification system were researched based on experimental investigation and mathematical theory.

6.8.3.2 Principles and features of the liquid-desiccant dehumidification

A liquid-desiccant dehumidifier is a device that employs a liquid desiccant material to produce a dehumidification affect. The process involves exposing the liquid desiccant material to a high relative humidity air stream, allowing it to attract and retain some of the water vapour and then exposing the same desiccants to a lower relative humidity air stream which has the affect of drawing the retained moisture from the desiccant. Typically the low relative humidity air stream is air taken from any available source and heated to reduce its relative humidity. Hence desiccant dehumidifiers consume heat energy to produce a dehumidifying affect.

HCOOK solution was supplied directly along incoming hot and humid air stream of BIHR counter-flow core contain fibre wick structure. In this stage, the solution was supplied from the top of the BIHR panel, in which humid air flowed through the core in the counter-flow direction. The most-used flowing way in the dehumidifier is counter-flow, which is considered as having the highest heat/mass transfer effectiveness (Gommed and Grossman 2004; Liu 2005; Dao et al. 2006; Mesquita 2005). Simultaneously, in the incoming air stream, air was passed and

sensible heat was released via heat transfer surface into the outgoing air stream as shown in Figure 6.59.

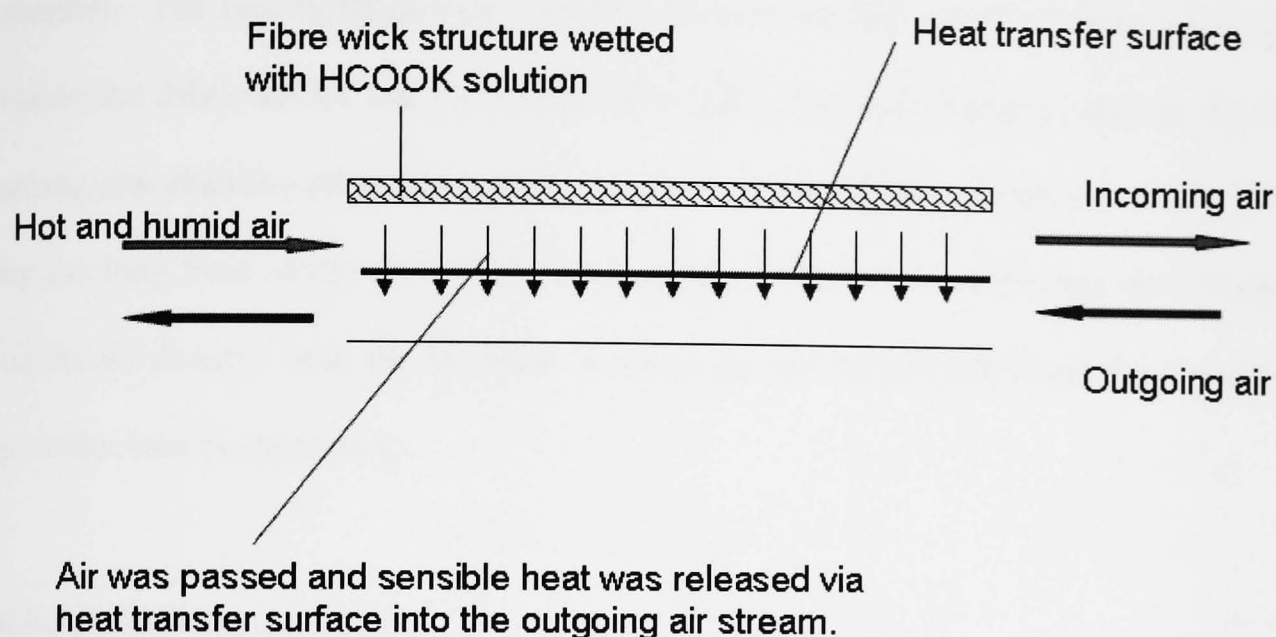


Figure 6.59 BIHR-fibre wick desiccant dehumidification system

In this dehumidifier unit, the HCOOK solution formed an intermittent film, wetter wall dehumidifier which offered a small contacting surface with the air stream and lost particulates to the air stream. HCOOK solution on contacting fibre wick wetted surface would be contacted directly with the humid air and carry out the heat/moisture transfer which can provide enough interfaces between solution and airflow. Wetted wall dehumidifiers have been recommended to enhance the heat and mass transfer during absorption process and usually a vertical tube or plate over which the desiccant solution flows by gravity (Jain and Bansal 2007).

The solution contacted with the air stream through the channels and solution particulates were very well by fibre structure (Dai and Zhang 2004). Hamid et al. (2002) have studied the mass transfer between air and vertical cloth layers after they were soaked in desiccant solution for 24h period. Hassan and Hassan (2009) have

proposed the idea to improve the wettability over the surfaces of desiccant dehumidifier channel by attaching fibrous sheet to the inner surfaces of counter-flow channel. The results found that a good indication for the good wettability of walls inside the dehumidifier and has many advantages over spray feeding. Because of the strong absorbability of the fibre wick structure, the HCOOK solution was firmly hold by the long fibre of the cloth. Therefore, humid airflow flowing through the channel contacted directly with the HCOOK solution as well as did not bring the desiccant particles into the test room.

6.8.3.3 Performance index

The dehumidification effectiveness is a dimensionless humidity ratio or vapour pressure ratio which can give a preliminary prediction of the dehumidification performance (Mei and Dai 2008). The moisture removal rate is one of important parameter in measuring the thermal performance of the dehumidification system. The moisture and removal rate is defined as:

$$\Delta d = d_{ia} - d_{sa} \quad (6.3)$$

where, d_{ia} = humidity ratio of intake air (g/kg dry air)

d_{sa} = humidity ratio of supply air to room (g/kg dry air).

As stated by Dai and Zhang (2004) and Gandhidasan (2004), the dehumidification effectiveness was defined as follows

$$\varepsilon_{de} = \frac{d_{ia} - d_{sa}}{d_{ia} - d_{eq}} \quad (6.4)$$

where ε_{de} =dehumidification effectiveness

d_{eq} = humidity of the air which is in vapour pressure equilibrium with the desiccant solution.

On the other hand, the moisture absorption capacity per litre solution per second is defined as the dehumidification capability of this sort of solution as shown in the following equation (Liu 2008):

$$\varepsilon_{de} = \frac{m_{absorb}^{moist}}{V_{sol}} = \frac{m_a (d_{ia} - d_{sol})}{V_{sol}} \quad (6.5)$$

If the intake air temperature is higher than that of the desiccant solution, Gandhidasan (2004) has defined the dimensionless temperature ratio in his study, which in accordance with previously defined humidity dimensionless ratio in terms of

the form: $\eta = \frac{T_{ia} - T_{sa}}{T_{ia} - T_{sol}}$ (6.6)

6.8.3.4 Laboratory tests

Figure 6.60 shows the laboratory set up of the present system. The system is composed of two parts: a BIHR unit and fibre-wick desiccant dehumidification unit. The experimental test rig mainly consisted of a test room, a liquid desiccant tank and BIHR-fibre wick panel which were set up at Energy Learning Unit Laboratory in University of Nottingham. Similar test room for BIHR prototype panel in section 6.3 was used in this investigation. To obtain the reliable data of testing results, air condition system was set up and controlled to supply hot and humid air with the temperature and relative humidity varying from 30 to 32°C and 70 to 75% respectively in the intake stream. Whilst, the test room which brought the return air to the BIHR core, temperature was kept constant at 20°C. The hot and humid air was forced in to the electrical heater (two 2kW electric heaters) by the two BIHR fans

installed in the ducts which was controlled by the speed controller to supply air at 2.0m/s constantly. Steam was injected in the intake stream to create desired relative humidity level.

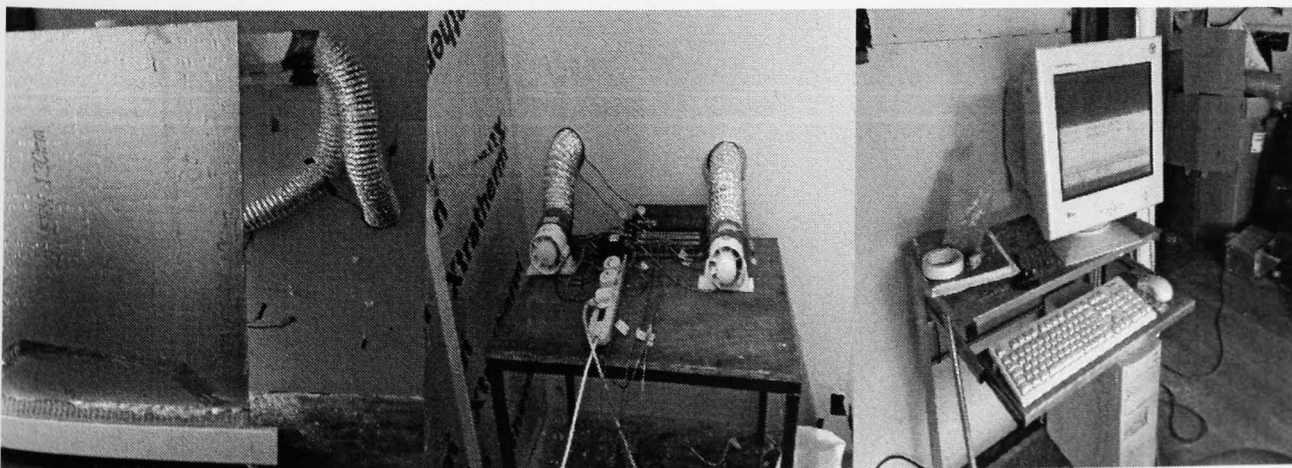
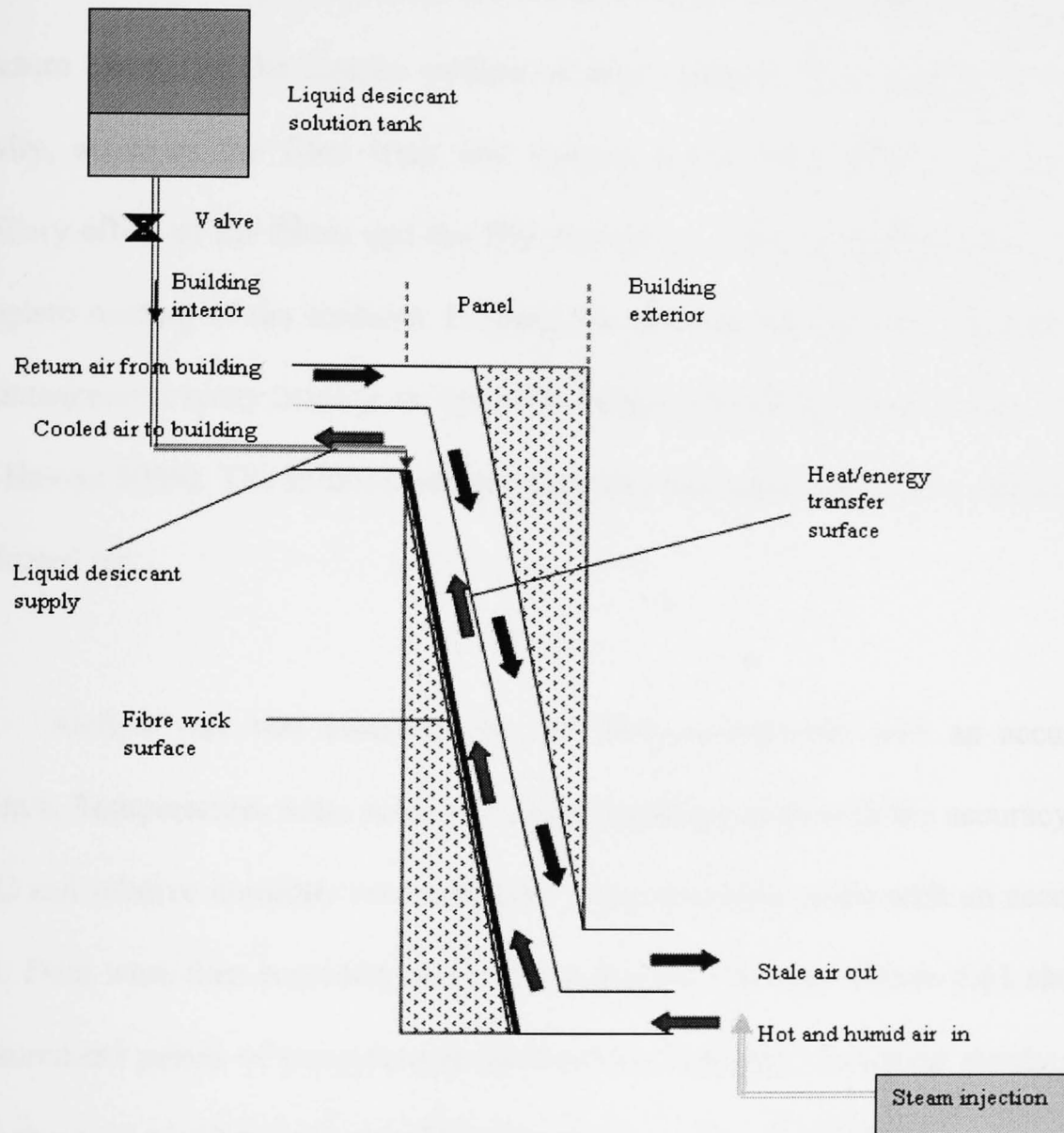


Figure 6.60 Laboratory set up of the present system

In fibre wick desiccant dehumidification or dehumidifier unit, the potassium formate solution (5L) with a concentration of 68.6% at 20°C from its upper tank distributed to each inlet channel by plastic tube which had a hole on it. The solution then flowed out of the hole when the valve was opened and supplied to fibre wick structure located in the interior surface of inlet channels. The solution flowed with gravity, saturates the fibre wick and formed a thin film over the surfaces. The capillary effect of the fibres and the film flowed over the wick structures sustained a complete wetting of the surfaces. Feeding the solution by this mechanism has many advantages over spray feeding as it prevents channel blockage by the solution (Hassan and Hassan 2009). The solution volume flow rate was measured with a stopwatch and graduated jar.

Airflow rate was measured by hot wire anemometer with an accuracy of 0.03m/s. Temperatures were measured using thermocouples with the accuracy within 0.1°C and relative humidity was measured using humidity probe with an accuracy of $\pm 2\%$. Data were then recorded using data acquisition system. Figure 6.61 shows the measurement points of temperatures and relative humidity. To obtain steady state, it took about 30 to 40 minutes to adjust the electrical heater and steam injection in the air control system.

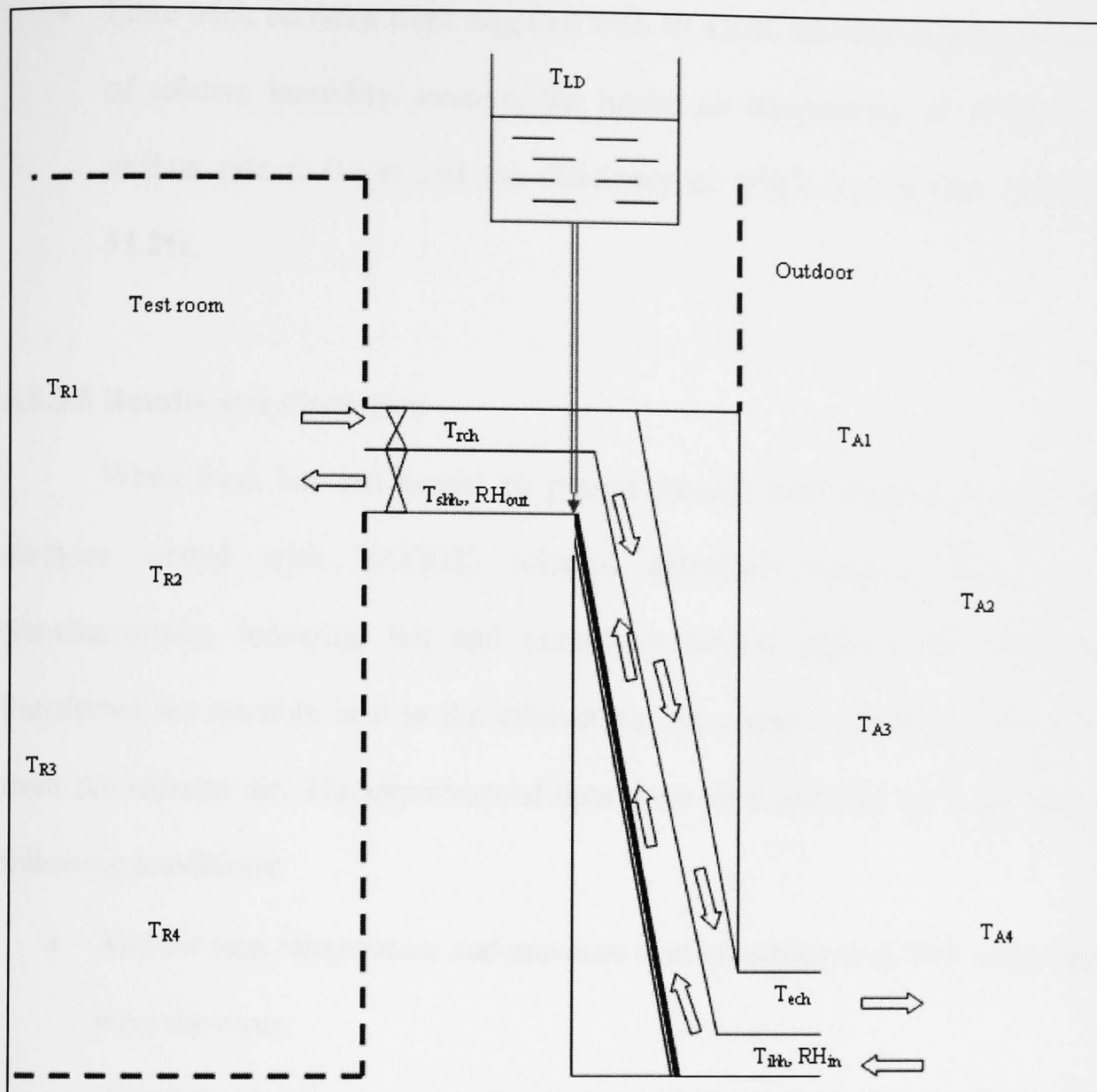


Figure 6.61 Measurement points of temperatures and relative humidity

To investigate the performance of this BIHR-fibre wick dehumidification system, the tests was conducted under following conditions:

- Desiccant (HCOOK solution) temperature and concentration is 20°C and 68.6% respectively.
- Channel length = 1000mm, channel width = 15mm, channel height = 5mm.
- Fibre wick thickness: 0.5mm
- Fibre wick surfaces were supplied with HCOOK solution at different settings of intake air temperature, unvaried relative humidity (70%), constant airflow rate (2.0m/s) and the efficiency of BIHR unit at this airflow was 53.2%.

- Fibre wick surfaces were supplied with HCOOK solution at different settings of relative humidity, keeping the intake air temperature at 30°C, constant airflow rate (2.0m/s) and the efficiency of BIHR unit at this airflow was 53.2%.

6.8.3.5 Results and discussion

When fresh hot and humid air passed through inlet channel, the fibre wick surfaces wetted with HCOOK solution absorbed moisture from the air. Simultaneously, incoming hot and humid air passed through the BIHR panel transferred the sensible heat to the exhaust air. As a result, the heat was recovered from the exhaust air. The experimental data were then analysed by considering the following conditions:

- Airflow rate, temperature and moisture content across each fibre wick channel were the same.
- HCOOK solution temperature and concentration supplied on each fibre wick surface were at similar value and flowed down by gravity effects.
- Fibre wick surfaces were assumed as the desiccant film and had the same temperature with the HCOOK solution and no particulates were carried out by the supplying air.
- Heat or mass transfer occurred vertically between the fibre wick surfaces and air stream.

- **Effect of air temperature on fibre-wick dehumidification performance**

The intake air (outdoor air) temperature for this study was ranged from 30.2 to 35°C corresponding to 20°C of desiccant (HCOOK solution) temperature, keeping the relative humidity in at 75%, desiccant solution concentration at 68.6%, desiccant solution flow rate at 4.05×10^{-3} L/s and airflow rate at $0.0157 \text{ m}^3/\text{s}$. Table 6.13 shows the results of the experiments.

Table 6.13 Results of BIHR fibre wick desiccant dehumidification experiments

Intake air, T_{ia} °C	Supply air to room, T_{sa} °C	Moisture removal rate (Δd)
30.2	25.5	9.04
31.4	26.8	9.88
33.9	28.6	12.15
35.0	30.1	13.07

The HCOOK solution absorbed water vapour from incoming air and this process has released heat and increased the incoming air temperature. However, with the present of BIHR unit in this system which is inherently integrated to simultaneous recovering sensible heat of supply air to room has reduced the dry bulb temperature at range of 25.5 to 30.1°C as shown in Figure 6.62. The drop of temperature ranged from 4.6 to 5.3°C was obtained between the intake air (outdoor air) and the supply air to room.

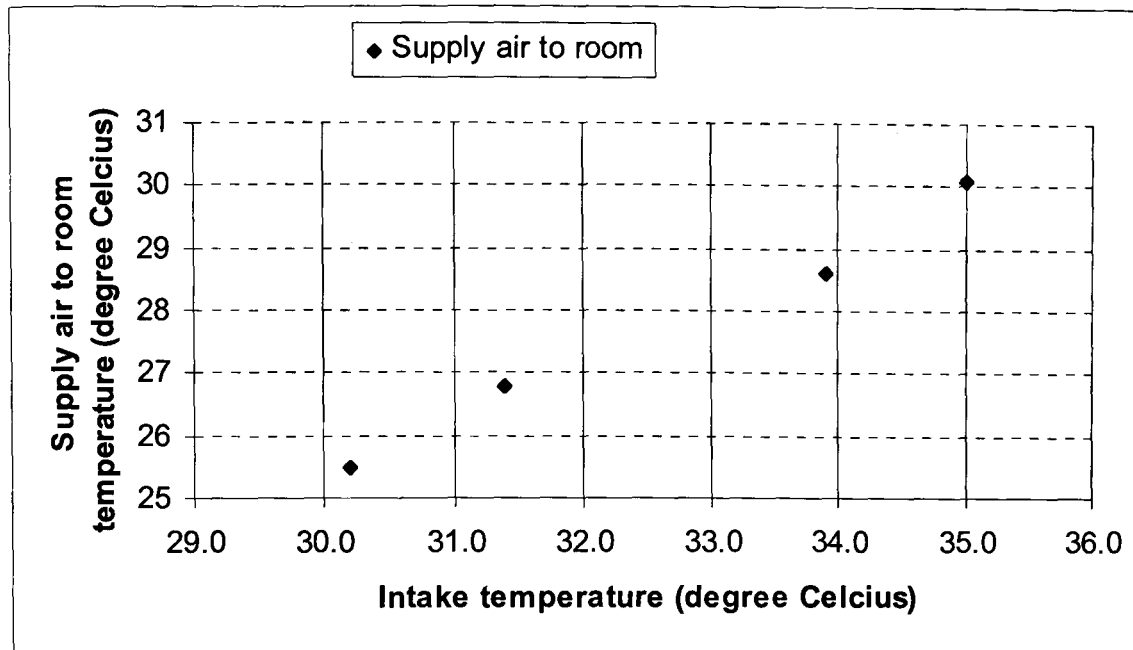


Figure 6.62 Variation of supply air to room temperature with intake air temperature

The effect of air intake temperature on the performance is shown in Figure 6.63. From the figure it can be seen that moisture removal rate increased about 69.1% and 82.9% increase in air temperature change when the intake air temperature increased from 25.5 to 30.1°C.

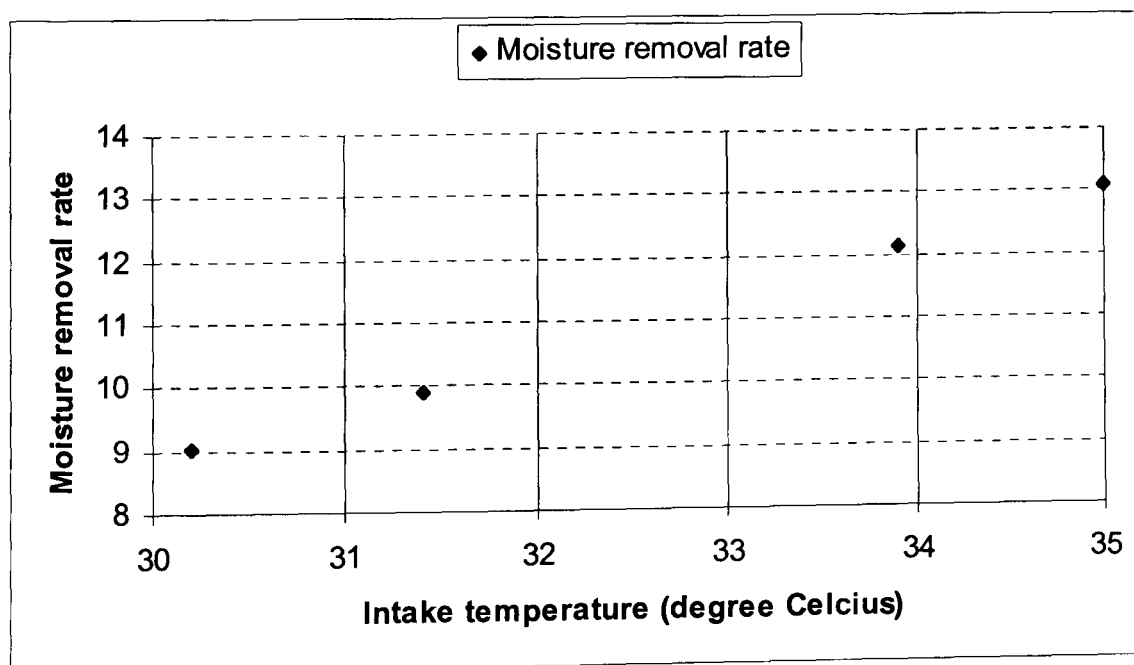


Figure 6.63 Effect of air intake temperature on the performance

As can be seen in Figure 6.64, the moisture absorption capacity increased with increasing intake air temperature which the maximum value of 0.06g/L corresponds to 35°C. In this case, the air entered the fibre wick dehumidification unit at a temperature of 35°C, which is higher than the solution temperature (20°C) it was in contact with, sensibly cooled due to a sensible heat transfer via the BIHR core to outgoing air stream and exits at 25.5°. Table 6.14 summarized the moisture absorption capacity calculated from this experiment.

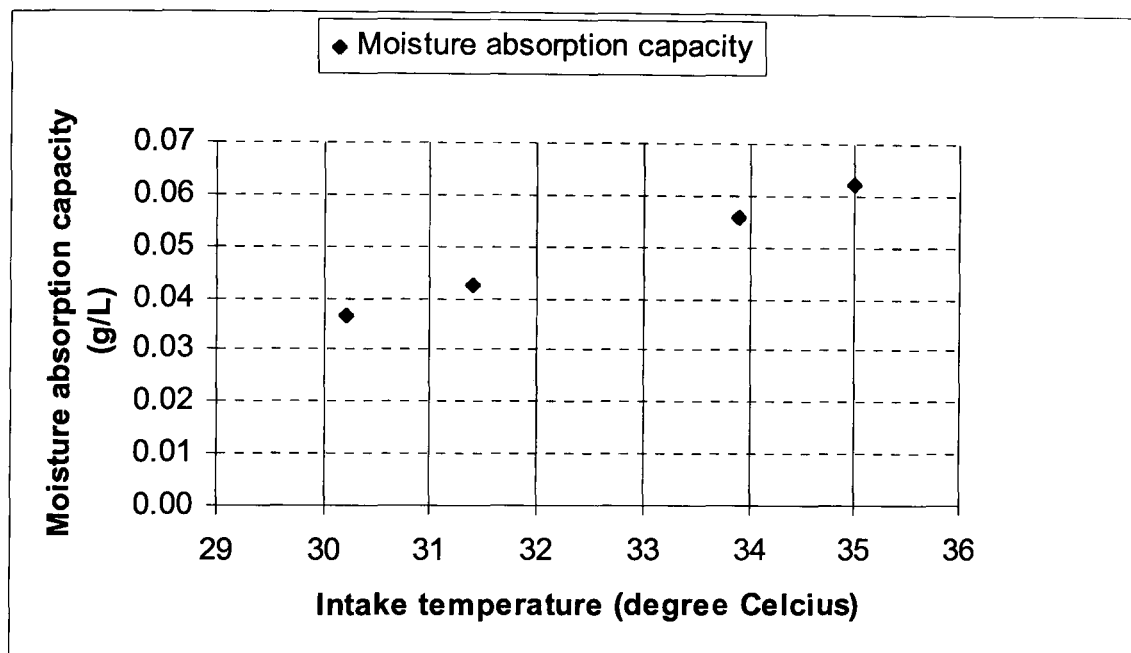


Figure 6.64 Moisture absorption capacity against intake air temperature

Table 6.14 Moisture absorption capacity calculation results

Intake air, T_{ia} °C	Supply air to room, T_{sa} °C	Moisture absorption capacity (g/L)
30.2	25.5	0.037
31.4	26.8	0.043
33.9	28.6	0.056
35.0	30.1	0.062

- **Effect of air relative humidity on fibre-wick dehumidification performance**

Changing intake air relative humidity in the range of 50.7 to 75.0% and keeping the intake air temperature at 30°C, HCOOK solution temperature at 20°C, HCOOK solution concentration at 68.6%, HCOOK solution flow rate at 4.05×10^{-3} L/s and airflow rate at $0.0157 \text{ m}^3/\text{s}$. Table 6.15 shows the results of the experiments.

Table 6.15 Results of the relative humidity experiments

RH in %	RH out %	Supply air to room, T_{sa} °C	Moisture removal rate (Δd)
50.7	30.4	26.8	6.85
60.5	40.5	25.4	8.0
69.8	50.8	24.8	8.82
75.0	55.7	24.1	9.74

The HCOOK solution removed moisture or latent load from the incoming hot and humid which ranged from 50.7 to 75% of RH in and reduced it to 30.4 to 55.7% of RH out as shown in Figure 6.65.

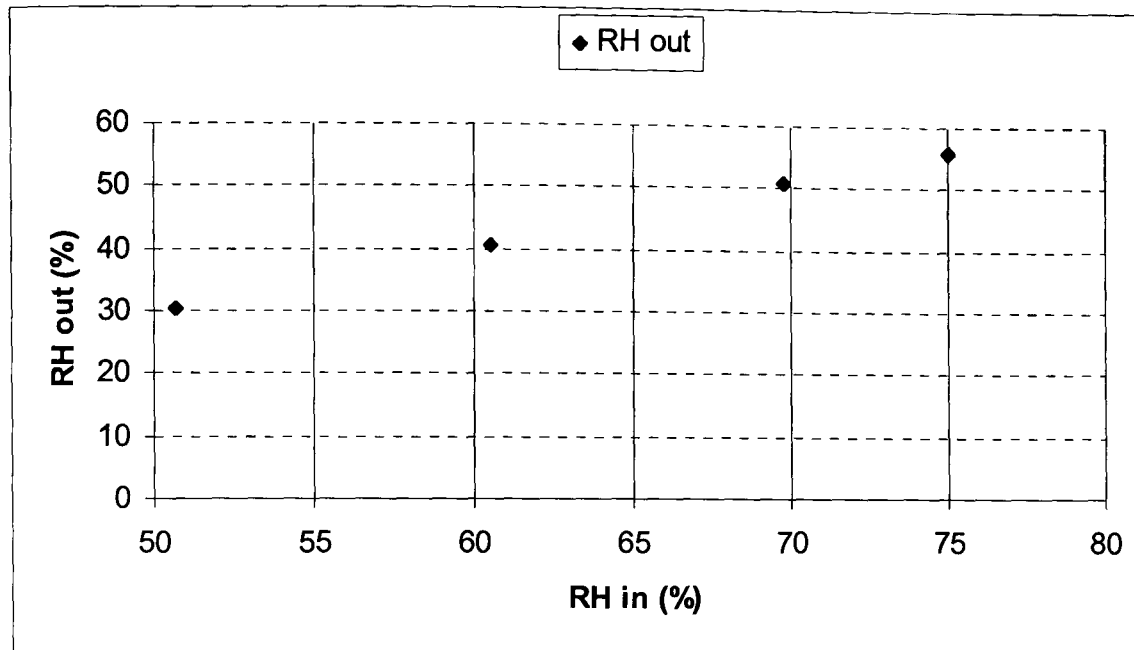


Figure 6.65 Variation of relative humidity

There was about 19 to 20.3% of moisture reduction in relative humidity of air supplied to room which means about 6.65 to 10.44g/kg dry air. Table 6.16 summarizes the results of this data.

Table 6.16 Results of humidity ratio

ΔRH	Humidity ratio of supply air to room (g/kg dry air)
%	
20.3	6.65
20.0	8.17
19.0	9.92
19.3	10.44

Similarly to effect of temperature, an increase from 6.85 to 9.74 in the moisture removal rate occurred when the intake air relative humidity increased from 50.7 to 75% as shown in Figure 6.66.

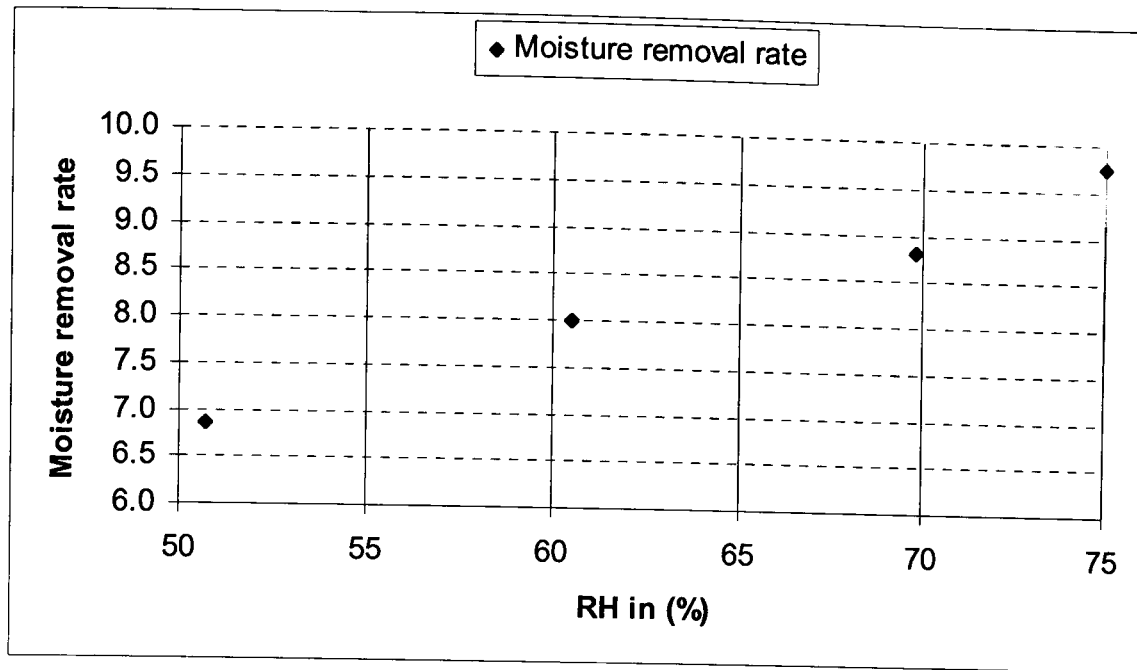


Figure 6.66 Moisture removal rate against RH in

Figure 6.67 illustrates the fibre wick dehumidification performance under constant intake air temperature of 30°C and varied intake relative humidity (RH in). From the figure it can be observed that the moisture absorption capacity increased with increasing RH in. The highest value of 0.04g/L has been obtained at the highest intake relative humidity of 75% in this experiment.

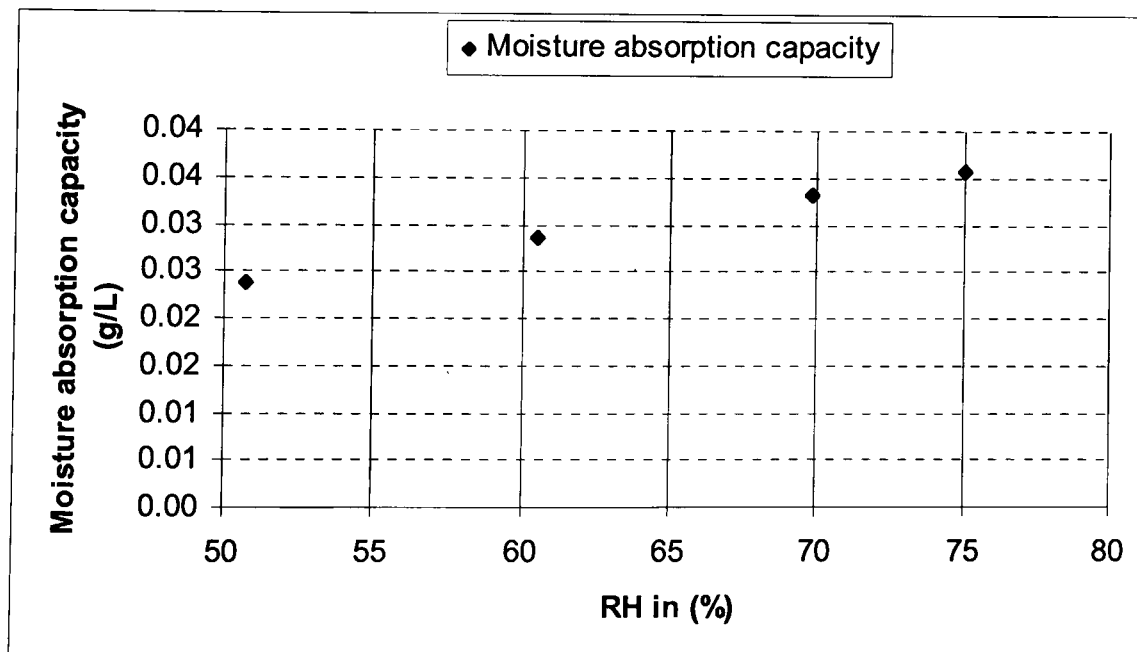


Figure 6.67 Fibre wick dehumidification performance under constant intake air temperature

These results show that HCOOK solution worked well as desiccant dehumidifier to reduce the relative humidity of intake air and these are acceptable as stated by ASHRAE Standard 55 for comfort conditions in summer recommends 50-60% relative humidity (around 10-12g/kg humidity ratio) (ASHRAE 2004).

6.9 Summary

In this chapter, a novel building integrated heat recovery (BIHR) system has been developed and investigated. The work has been done to evaluate the performance of the system including the followings:

- BIHR prototype with two airstreams
- Full-scale measurements of BIHR system on real buildings in UK
- BIHR driven by PV system to supply energy for the fans
- Improved BIHR' corrugated with four airstreams
- BIHR with fibre wick structure for cooling and dehumidification

From the experiments conducted, it was found that through an energy balance on the structure, the efficiency of BIHR prototype was found to be 50 to 61.1% depending on the airflow rate. This efficiency increased to the highest value of 83.3% in a full-scale measurement on a real building in Ashford, Kent as the area of heat transfer surface increases. The increasing of heat surface area again proved a better performance in terms of efficiency as the results on another full-scale measurement on a real house in Hastings, Sussex showed to be 86.2 to 91.7% for air velocities ranged from 1.0 to 2.0m/s.

BIHR driven by PV system to supply power for the fans has also been discussed. The experimental rig was set up in Forstal Farm, Kent, UK. The test was conducted between 12:00 and 15:00 at 8.7°C ambient temperature during a clear sunshine day with average wind velocity of 2.7m/s in October 2009. The BIHR system was operated with energy generated by PV system for the fan speed of 2.0m/s. The study indicated that the PV system was running satisfactorily and the system able to cover the loads requirement demands without utilizing energy from the electrical grid. This study shows that the PV system was running satisfactorily.

The new improvement design of BIHR corrugated channels with four airstreams has significant advantages over the previous BIHR with two airstreams as summarized below:

- With the same equipment, test room, procedure, material, the fan power and velocities, the recovered heat is increased by more than 50%.
- The performance of the present design is confirmed through physical experiments of a prototype.
- Effect of various sizes on heat recovery performance shows that the larger size gives the best performance including both efficiency and recovered heat.
- Effect of number of airstreams channel on heat recovery performance shows that the BIHR with four airstreams channel gives better performance compared to BIHR with two airstreams channel.
- Corrugated channel is one of the very popular channels that are developed to improve heat transfer performance. Because these channels can lengthen the

flow path and cause better mixing, higher heat transfer performance is obtained compared to straight channels.

- A significant heat transfer enhancement was associated for the improved BIHR with four airstreams system as compared to the BIHR with two airstreams.

The economic and environment analysis involve the BIHR system installed in heating equipment for BIHR prototype with two airstreams, improved BIHR' corrugated channels with four airstreams and BIHR in case study I with and without PV system. For the capital cost of £250 of BIHR prototype with two airstreams and £300 of improved BIHR' corrugated channels with four airstream running 24 hours per day to ventilate the indoor space for 3 months during winter season installed in £300 of capital cost of heating equipment, 41.1kgCO₂e and 70.72kgCO₂e of carbon emissions reduction gained, respectively. Whilst in case study I, with capital cost of BIHR at £500 as it has 2.5 bigger in size than the prototype unit, the annual saving of £447.05 with 126.09kgCO₂e carbon emissions reduction as compared to heating equipment without BIHR.

The work of BIHR system with fibre wick structure involved two different case studies for two different working fluids namely water and liquid desiccant to treat the incoming air of hot air. For the first case, water was used to give a direct evaporative cooling effect which is suitable to evaluate the system performance under hot and dry climatic conditions and the second case, potassium formate (HCOOK) solution was used as liquid desiccant for dehumidification under hot and humid climate conditions.

Considering the porosity and pore diameter, fibre wick structure made of cloth used in this system can carry on heat/mass transfer synchronously without air penetration. It is the cheapest materials and can be shaped and installed conveniently, and these peculiarities can cover the shortage of less durability. In this investigation, overall, it can be found that heat, mass and moisture effectiveness decreased with the airflow rate increasing in the experimental testing. Specifically the following results can be found:

- Case 1: BIHR-fibre wick cooling system

Experimental investigation was carried out to evaluate the performance of a novel BIHR-fibre wick cooling system. To evaluate the performance of this system, the water has been used as the working fluid by flowing it over the fibre wick surface with gravity effect. The tests were conducted at different settings of intake air temperature and relative humidity with a constant airflow rate and under constant intake air temperature but varied airflow rate.

With the intake air temperature ranged from 25 to 38.2°C, a difference of 1.5 to 6.4°C has been recorded between intake air temperature and supply air to room temperature. For this condition, supply air to room was ranged from 23.5 to 31.8°C. In terms of humidity, intake air relative humidity was supplied in range of 32.7 to 45.2%. By supplying the water over the fibre wick structure, an increasing of 12 to 15.7 was observed in the supply air to room relative humidity. Maximum water consumption of 0.042g/s has occurred at highest temperature change of 6.4°C. Water consumption rate of this system has shown an increasing value with the increasing intake air temperature however it declined with increasing intake air relative

humidity. With a constant airflow rate of $0.0157\text{m}^3/\text{s}$, the efficiency increased with increasing intake air temperature. The efficiency ranged from 20 to 42.4% corresponding to the minimum and maximum of intake air temperature of 25°C and 38.2°C , respectively.

The test was then conducted for different airflow rate which varied from 1.0 to 2.0m/s with a constant intake temperature of 30°C and relative humidity of 40%. With the variation of airflow rate, the efficiency of the system was found to be 53.2 to 60%. These results were found to be in good agreement with the results of BIHR prototype without the fibre wick structure. By analysing all these results, it can be concluded that the utilization of wetted surface of fibre wick structure contributed to cool down the hot air and simultaneously increased the humidity of supply air to room.

Considering the climatic conditions, the novel BIHR-fibre wick cooling system has the potential as an alternative to replace the conventional air conditioning system and has the ability to reduce the incoming hot air and increase the humidity level in hot and dry region. Simultaneously, with the present of heat recovery core in this system, energy would be recovered from the exhaust air stream. This system may therefore be used to cool and humid the incoming hot and dry air and simultaneously as a heat recovery. In addition, this system would be more compact and cheaper in terms of initial cost, but could only be used in areas where water supply is not a problem. However, since this system is a direct evaporation system, there might be problems related to legionella especially for long term usage. Thus, to overcome this it is important to control the risks of this condition. As we know that legionella is

caused by the bacteria found naturally in water and to prevent this chlorine dioxide can be used to disinfection and kill the bacteria in the water tank.

- BIHR-fibre wick desiccant dehumidification system

Experimental investigation was carried out to evaluate the performance of a novel BIHR-fibre wick desiccant dehumidification. The novelty of this study are the integration of heat recovery unit and desiccant dehumidification in one panel and no experimental work was conducted in the past in integrating desiccant dehumidification and heat recovery unit as one device. To evaluate the performance of this system, the HCOOK solution with concentration of 68.6% has been selected as the desiccant by flowing it over the fibre wick surface with gravity effect. Series of tests were conducted to investigate the influencing factors such as air temperature and relative humidity to dehumidification unit. The system has been tested according to constant intake air relative humidity with different settings of intake air temperature and constant intake air temperature with varied intake air relative humidity.

The supplied air to the room exits with a lower value ranging from 25.5 to 30.1°C with intake air temperature varying from 30.2 to 35°C at a constant intake air relative humidity of 75%. The air temperature decreases to a maximum value inside the fibre wick dehumidifier due to a sensible heat transfer from intake air stream to exhaust air stream via BIHR core. The drop of temperature ranged from 4.6 to 5.3°C was obtained between the incoming air stream and outgoing air stream. The HCOOK solution worked well as liquid desiccant to reduce the moisture content of incoming 30°C of hot and humid air which relative humidity ranged from 50.7 to 75% to 30.4 to 55.7% which equivalent to 6.65 to 10.44g/kg dry air of humidity ratio in supply air to

room. The highest moisture absorption value of 0.04g/L and 9.74 of moisture removal rate has been gained at 75% intake relative humidity. As widely known, in a single liquid desiccant dehumidification system, the desiccant will remove the moisture from the air, which release heat and raises the air temperature. However, in this system the raising air temperature has been sensibly cooled simultaneously by heat recovery unit of BIHR core by transferring heat of the incoming hot air stream to the outgoing air stream via polycarbonate heat transfer surface. The supply air to room temperature of 24.1 to 26.8°C has been observed with 3.2 to 5.9°C temperature range between the incoming air stream and outgoing air stream. Hence, these results show that the integrating of BIHR unit with desiccant dehumidification unit in one panel have an encouraging results however the higher value of supply air to room still need to be cooled by other mean to reduce it to a comfort temperature value of 25°C as recommended by ASHRAE.

For a defined airflow rate of 0.0157m³/s which is also equivalent to 2.0m/s, heat recovery efficiency of about 54%, a lower desiccant (HCOOK solution) temperature of 20°C, concentration of 68.7% with higher intake air temperature and relative humidity produces a better dehumidification performance with a good moisture absorption capacity. Therefore, this system is expected to be used efficiently in hot and humid regions such as Malaysia and Singapore as well as other South East Asia countries. In these regions, this novel BIHR fibre wick desiccant dehumidification system offers reduced electricity demand considerably by providing a drier, more comfortable and cleaner indoor environment with a lower energy bill. In addition it allows more fresh air into buildings, thus improving indoor air quality without using more energy.

The novel BIHR-fibre wick desiccant dehumidification system has the potential to compete with conventional air conditioning systems under conditions involving high temperature and high moisture load. This system may therefore be used as a dehumidifier and simultaneously as a heat recovery. However, several improvements to the system would be possible to make it more compact, efficient and cost-effective. Improvements to the system could include the integrating of this BIHR fibre wick desiccant dehumidification with evaporative cooling system in order to reduce the incoming hot and humid air at higher temperature of more than 30°C. In addition, the integration of this system with the building integrated PV/solar panel should also be considered to be improved whereas the solar panel could be used as the building façade and at the same time it can be used to regenerate the desiccant.

Overall, the use of BIHR system in, above all, air tight buildings, weather in the roof of walls, will help in maintaining energy efficiency, improve interior air quality, will take up less space within the building than a standard MVHR unit and the modular aspect allows for adaptation to individual building requirements and future changes. As a conclusion, with the encouraging performance results, further improvement and wider use of BIHR could be made with attention to the following areas:

- Extreme climates

Considering the use of roof panels in cold climates where long periods of freezing may occur, the formation of ice dams could impair the extract airflow. A suggested way of dealing with this that would need to be tested is to use short blasts of ventilation that would intermittently raise the extract rate, reducing heat

recovery efficiency, so expelling air above freezing whilst maintaining the air change rate

- Combination with other technologies

Alternatively floor panels could also be combined with earth to air heat exchanger (EAHX) used to moderate air temperature in both cold and hot climates. Considering their use in cooled buildings the panels could combine with solar panels, as effectiveness increases and cost reduces, that could power low wattage fans providing ventilation. Heat pump technology could also be used between the two airflows to supplement heating or cooling.

- Optimization of channel dimensions

The rate of heat transfer is inversely proportional to the size of the channels (smaller size increases the heat transfer coefficient but reduces the residence time and creates a higher pressure drop). The size of channel needs to be optimised for economic use of material, thermal performance and fan power.

- Passive ventilation

To reduce the energy used by fans for air movement passive solutions need investigating. For example a flexible heat conducting membrane, combined with sensitive back draught shutters, that uses air pressure changes to bring about a breathing effect could provide sufficient air change during the right conditions.

CHAPTER 7

Conclusions

7.1 Introduction

This research has been carried out to obtain a better understanding of heat recovery system with particular focus in integrated energy-efficient system for building application. The investigation initially carried out a review on heat recovery system, the performance of independent heat recovery system and the integration with other energy-efficient technologies such as wind-catcher, evaporative cooling, photovoltaic and desiccant dehumidification.

7.2 Main conclusions

7.2.1 Literature review

A thorough review of the related knowledge regarding the heat recovery systems was then carried out. Findings from literature review shown that there are different of heat recovery types in the market nowadays such as fixed plate, heat pipe, and rotary wheel and run-around units utilized to recover energy loss. Throughout the literatures, it was found many works have been done since 1980s' related to heat recovery systems. In the past, the works had emphasized more on heat/mass transfer in heat exchanger until the buildings standards are introduced then the efficiency and performance of heat recovery in building applications such as ventilation, air conditioning and dehumidification systems come into concerns. For natural/passive ventilation, heat pipe recovery has been used since no moving part is required in this system. For mechanical ventilation, researchers tend to integrate heat pump so-called

mechanical ventilation heat pump recovery (MVHR) whilst rotary wheel recovery has widely been used in desiccant dehumidification to recover heat and moisture.

On the other hand, many theoretical and experimental works in literature has been conducted for integration heat recovery system with mechanical ventilation, natural ventilation, air conditioning and dehumidification systems. However, combination of heat recovery with low carbon technologies such as evaporative cooling, photovoltaic panel and desiccant dehumidification is just a handful amount and very limited studies have been done to integrate them in one system. In addition there is no practical study for integration of heat recovery with low energy technologies to become one device with multifunction (heat recovery/cooling/air dehumidifier) in one system and no work has been found on building integration of heat recovery system.

7.2.2 Review on theoretical studies of heat recovery system

To study the performance of heat recovery system either sensible or enthalpy, important parameters that should be emphasized are:

- Size, structure and material of heat exchanger,
- Size of ducts and fans
- Flow arrangement
- Heat and mass transfer
- Flow and pressure drop in the ducts
- Temperature and humidity
- Airflow rates

It was proven that the efficiency of heat recovery increased as the area increased. Besides, the selection of fans should be considered since depending on the size of the fan, the size of duct in terms of diameter can be determined needed for this system for the case when the installation of the fans is in the ductwork. Usually, the air flowing in the ducts is turbulent. Besides, the duct structure and material will influence the flow distribution and are also substantial in order to minimize the heat loss from the duct system. Otherwise, the heat loss can reduce the total efficiency of the system significantly. In addition, material and structure of heat exchanger are the predominant factor the heat and mass transfer. Capillary forces or porosity and pore diameter of the materials play significant role in moisture transfer. Recently, membrane-based material is a new approach to heat/mass transfer in heat recovery whereas this material has the capability as an enthalpy recovery. It is believed that flow arrangements have direct impact on heat exchanger effectiveness. In addition, heat transfer efficiency is maximized if the two airstreams have opposite direction in airflow arrangement. The effectiveness of these three flow arrangement, a counter-flow arrangement is the best.

Heat recovery efficiency can be determined by application of three suggested method as following:

- ASHRAE Standard method which can be defined in terms of sensible/temperature efficiency, latent efficiency and enthalpy (total) efficiency.
- Effectiveness-NTU method by which defined by the calculation of NTU and heat capacity ratio, C when flow arrangement is known.

- Global efficiency which takes into account the exfiltration and infiltration rate in ventilation system

In any heat recovery system, reducing airflow rates always increases efficiency. On the other hand, airflows have significant effects on the all types of heat recovery efficiency, pressure loss and transferred (recovered) heat/mass. For both sensible and total efficiency, the temperature of the inlet air appears to have minor influence in heat recovery system. However, the efficiency of heat recovery system in real situation varies with the temperature of supply and return air (temperature difference). In addition, the temperature change increases with increasing the inlet fresh air temperature. On the other hand, the economics of the heat recovery application in terms of energy savings can be calculated by several methods such as degree day method, net saving combination of P_1 - P_2 method, specific net energy saving (SNES) and heating/cooling load reduction method.

Thus, as a conclusion, the energy saving performance of the heat recovery is related to the ambient climatic condition in terms of temperature and relative humidity, effects of airflows, pressure drop and fan power. The larger the indoor-outdoor enthalpy (temperature and humidity) difference, or the higher efficiency, or the lower fan power, or the lower the airflow, or the larger the surface area, the more energy can be saved. However, it will also cost more in high level heat recovery type and high performance of fan. Thus, to improve saving performance, more efficient heat transfer materials and more efficient fans must be explored.

7.2.3 Performance investigation of an individual heat recovery unit

In this chapter, triggered by good numerical results by various past researchers and the intention, a fixed-plate heat recovery unit has been experimentally investigated. The heat performance has been analysed based on the calculation analysis provided by literatures. The experimental tests were conducted on a cross-flow configuration heat recovery unit that utilises cellulose fibre papers (pads) as the heat transfer surface. An overview of the experimental techniques used to investigate the performance of heat recovery including the details of experimental set up, procedures and instrumentations used in a laboratory are presented and experimental results are outlined and discussed.

This chapter discussed experimental work on heat performance of a cross-flow MHM3C that utilises cellulose fibre papers (pads) as the heat transfer surface which was investigated experimentally to understand the performance of various parameters of individual heat recovery unit in recovering heat. The heat performance has been analysed based on the calculation analysis provided by literatures. The experimental tests were conducted on a cross-flow configuration heat recovery unit. The unit was tested in an environmental control chamber under varying airflow rate. As the airflow rate and temperature change increase, the sensible efficiency decreases, and recovered energy increases. At air velocities ranged from 1.0 to 3.0m/s, the sensible efficiency ranged from 66 to 48%. By increasing the airflow rate from 0.010 to 0.031kg/s, a decrease of 18.1% of sensible efficiency observed. Maximum recovered energy of 134W was calculated at 3.0m/s air velocity, respectively. Temperature change ranged from 2.9 to 4.3°C was observed for the air velocities tested.

7.2.4 Integrated heat recovery system associated with wind-catcher and evaporative cooling

This chapter explored development and experimental work of an integrated system of three major working units; heat recovery, wind-catcher and evaporative cooling which have been combined together. The system was investigated in a large-scale model under laboratory condition. The main conclusions that can be drawn from the results obtained during this investigation are that the integrated heat recovery system associated with wind-catcher and evaporative cooling, allow part of the energy from the return airflow to be recovered, thus improving energy efficiency and reducing environmental impact. At air velocities ranged from 1.2 to 3.1m/s, heat recovery efficiency ranged from 70 to 50% for cold air condition and 69 to 49% for warm air condition. The maximum recovered energy of 772.9W was obtained at 5.2°C temperature range of heat recovery unit. From this investigation it can be concluded that the maximum cooling load of 1512.5W was calculated at 4.2°C temperature change and 18.3% has increased in relative humidity across the indirect evaporative cooler at 3.1m.s of air velocity and 30.5°C supply air temperature. The dew point cooling efficiency ranged from 47% at air velocity of 1.5 to 29% at 3.1m/s. Whilst, the wet bulb cooling efficiency ranged from 54% at air velocity of 1.5m/s to 31% at 3.1m/s. In addition, it is observed that the temperature change for heat recovery unit ranged from 4.0 to 4.7°C. Whilst, the temperature change between supply air and outlet air of indirect evaporative cooler under dry condition ranged from 2.0 to 2.5 °C. This results show that when cooling is not requiring in winter season for instance, the system can be run with dry pads. This brings cool air into the buildings and circulates it without using water.

7.2.5 Development and performance investigation of novel building integrated heat recovery (BIHR) system

In this chapter, a novel building integrated heat recovery system has been developed and investigated. The work has been done to evaluate the performance of the system. It presents the design, development, description, and experimental work of prototype unit, full-scale measurements on real buildings, investigation of the system with photovoltaic power, construction and investigation of improved system, economic analysis and the development of the system with fibrous material in the internal channels adaptable for cooling and dehumidification. The work in this chapter aims to integrate heat recovery with building envelope (roof/wall/floor) to become one device with multifunction (building integrated heat recovery/cooling/air dehumidifier).

From the experiments conducted, it was found that through an energy balance on the structure, the efficiency of BIHR prototype was found to be 50 to 61.1% depending on the airflow rate. This efficiency increases to the highest value of 83.3% in a full-scale measurement on a real building in Ashford, Kent as the area of heat transfer surface increases. The increasing of heat surface area again proved a better performance in terms of efficiency as the results on another full-scale measurement on a real house in Hastings, Sussex showed to be 86.2 to 91.7% for air velocities ranged from 1.0 to 2.0m/s. The PV system to supply energy for BIHR fans has also been discussed. The experimental rig was set up in Forstal Farm, Kent, UK. The test was conducted between 12:00 and 15:00 at 8.7°C ambient temperature during a clear sunshine day with average wind velocity of 2.7m/s in October 2009. The BIHR system was operated with energy generated by PV system for the fan speed of 2.0m/s.

The study indicated that the PV system was running satisfactorily and the system able to cover the loads requirement demands without utilizing energy from the electrical grid. The new improvement design of BIHR corrugated channels with four airstreams has significant advantages over the previous BIHR with two airstreams. With the same equipment, test room, procedure, material, the fan power and velocities, the recovered heat is increased by more than 50%.

The economic and environment analysis involve the BIHR system installed in heating equipment for BIHR prototype with two airstreams, improved BIHR' corrugated channels with four airstreams and BIHR in case study I with and without PV system. For the capital cost of £250 of BIHR prototype with two airstreams and £300 of improved BIHR' corrugated channels with four airstream running 24 hours per day to ventilate the indoor space for 3 months during winter season installed in £300 of capital cost of heating equipment, 41.1kgCO₂e and 70.72kgCO₂e of carbon emissions reduction gained, respectively. Whilst in case study I, with capital cost of BIHR at £500 as it has 2.5 bigger in size than the prototype unit, the annual saving of £447.05 with 126.09kgCO₂e carbon emissions reduction as compared to heating equipment without BIHR.

The work of BIHR system with fibre wick structure involved two different case studies for two different working fluids namely water and liquid desiccant to treat the incoming air of hot air. For the first case, water was used to give a direct evaporative cooling effect which is suitable to evaluate the system performance under hot and dry climatic conditions and the second case, potassium formate (HCOOK)

solution was used as liquid desiccant for dehumidification under hot and humid climate conditions.

In the first case, the tests were conducted at different settings of intake air temperature and relative humidity with a constant airflow rate and under constant intake air temperature but varied airflow rate. With the intake air temperature ranged from 25 to 38.2°C, a difference of 1.5 to 6.4°C has been recorded between intake air temperature and supply air to room temperature. For this condition, supply air to room was ranged from 23.5 to 31.8°C. In terms of humidity, intake air relative humidity was supplied in range of 32.7 to 45.2%. By supplying the water over the fibre wick structure, an increasing of 12 to 15.7 was observed in the supply air to room relative humidity. Maximum water consumption of 0.042g/s has occurred at highest temperature change of 6.4°C. With a constant airflow rate of 0.0157m³/s, the efficiency increased with increasing intake air temperature. The efficiency ranged from 20 to 42.4% corresponding to the minimum and maximum of intake air temperature of 25°C and 38.2°C, respectively. With the variation of airflow rate, the efficiency of the system was found to be 53.2 to 60%. These results were found to be in good agreement with the results of BIHR prototype without the fibre wick structure. Considering the climatic conditions, the novel BIHR-fibre wick cooling system has the potential as an alternative to replace the conventional air conditioning system and has the ability to reduce the incoming hot air and increase the humidity level in hot and dry region.

In second case, to evaluate the performance of BIHR fibre wick desiccant dehumidification system the HCOOK solution with concentration of 68.6% has been

selected as the desiccant by flowing it over the fibre wick surface with gravity effect. The system has been tested according to constant intake air relative humidity with different settings of intake air temperature and constant intake air temperature with varied intake air relative humidity. For a defined airflow rate of $0.0157\text{m}^3/\text{s}$ which is also equivalent to $2.0\text{m}/\text{s}$, heat recovery efficiency of about 54%, a lower desiccant (HCOOK solution) temperature of 20°C , concentration of 68.7% with higher intake air temperature and relative humidity produces a better dehumidification performance with a good moisture absorption capacity. Therefore, this system is expected to be used efficiently in hot and humid regions such as Malaysia and Singapore as well as other South East Asia countries.

7.3 Summary of contributions and novel features

Using the reliable data of measurements collected from experiments, the results of this thesis make a novel contribution to the knowledge of heat recovery for building applications by means of the followings:

- On a broader perspective, this thesis has provided a greater insight into the coupling of the heat recovery in a mix-integrated energy-efficient system for building applications in order to achieve good indoor air quality and energy conservation.
- Used an advanced materials for heat/mass transfer made of cellulose fibre to save sensible and latent heat from the exhaust air stream.
- The integrated heat recovery system associated with wind-catcher and evaporative cooling could provide the roof ventilation to negate heat and moisture problem especially in high building and allow part of the energy

from the return airflow to be recovered, thus improving energy efficiency and reducing environmental impact.

- The design and development of BIHR is an advanced technology of building thermal insulation and heat recovery.
- Used the cheap fibre cloth for the construction of wick structures in internal channels of BIHR for cooling or dehumidification.
- BIHR panel that has been developed has the potential to be integrated with photovoltaic panel for power supply.
- The novel BIHR-fibre wick cooling/desiccant dehumidification system has the potential to compete with conventional air conditioning systems under conditions involving high temperature and high moisture load.
- The development of multifunction device in one system; heat recovery, cooling, desiccant dehumidification.

7.4 Future work

The thesis has explored the construction and the performance of novel heat recovery systems for building applications in integration systems of energy-efficient. The conclusions of this research were discussed in the previous section. Due to time constraints, this research lack of data in several areas. Here the ideas for developments and further work are outlined.

- Some improvements can be done for further work by carried out computational or numerical study to look the trends of pressure drop in each internal channels, the effect of membrane spacing, membrane thickness,

temperature distribution, flow distribution, effects of geometry and shape of heat transfer surface or study the optimal design for heat recovery core.

- The study of effects of exfiltration and infiltration to the heat recovery efficiency.
- The study of continuous moisture problems and inlet air below freezing point for BIHR especially for the case where the region has long winter season or arctic climate with attention to frost formation and to means of getting rid the frost.
- The study of full-scale BIHR desiccant dehumidification in real building in hot and humid region.
- BIHR-PVT

BIHR-PVT is an advanced energy-efficient system based on existing photovoltaic technology with the addition of heat recovery unit. This technology can be developed in accordance to the weakness of solar panel when exposed to high temperature which resulting low efficiency. Heat recovery unit in this system would works to cool the photovoltaic panels while providing a heat source for the occupants. The definition of BIHR-PVT system here is a combination of heat recovery components and PVT which produces both electricity and heat from one integrated system from the same surface area exposed to the sun and ambient air as shown in Figure 7.1. This concept allows for heat removal from PV modules and at the same time heat could be recovered. This system would feed the heat recovery ventilation

fans with electricity and to preheat ventilation air while serves to cool the PV cells and hence reduces solar conversion efficiency losses caused by increased cell operating temperatures.

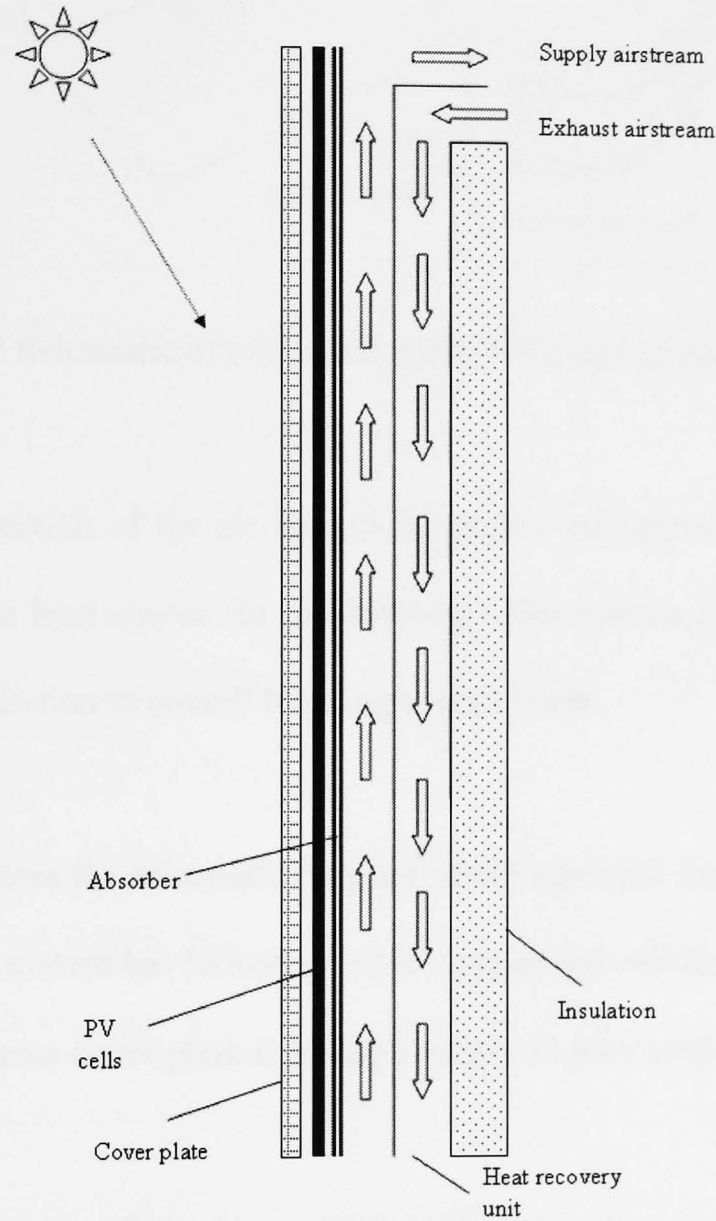


Figure 7.1 Integrated BIHR-PVT concept

This system is considered as a roof integrated system based on existing PVT technology with the addition of a BIHR unit that can be used in new ventilation system for sustainable building (Figure 7.2).

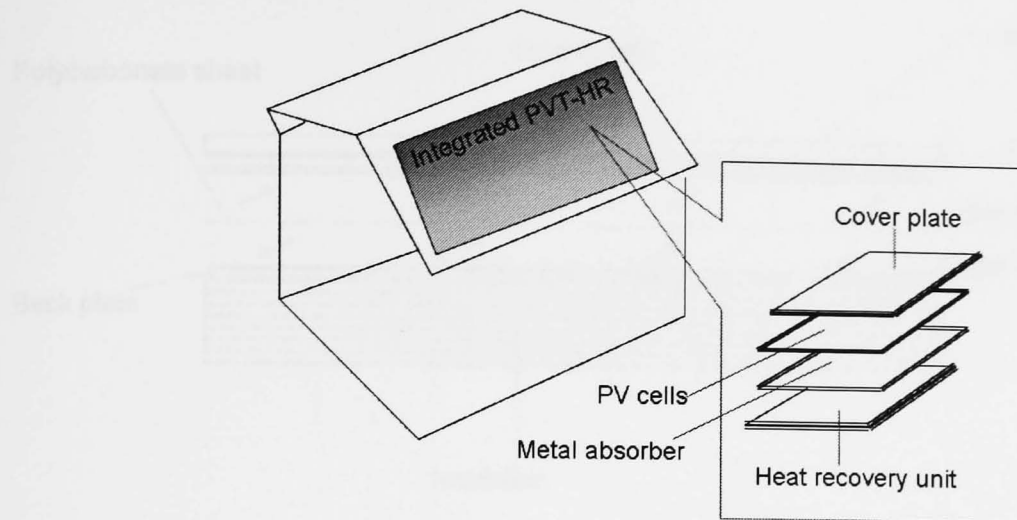


Figure 7.2 Schematic of integrated BIHR-PVT system mounted on roof

The convection of the air behind the panels will serve to cool the PV cells while providing a heat source for the building. This system can make a significant percentage contribution to overall building energy loads.

Figure 7.3 shows the schematic diagram of cut sectional front view of the BIHR-PVT design. The system has following static components which are:

- A transparent cover plate allowing sunlight to pass towards PV cells made of a glass
- A photovoltaic cell for the production of electricity
- A metal absorber plate painted black
- A heat recovery unit called BIHR made of polycarbonate plate for the heat exchanger core which has two air-streams (supply and exhaust)
- A back plate
- A heat insulator to limit the losses by conduction through the walls back and side

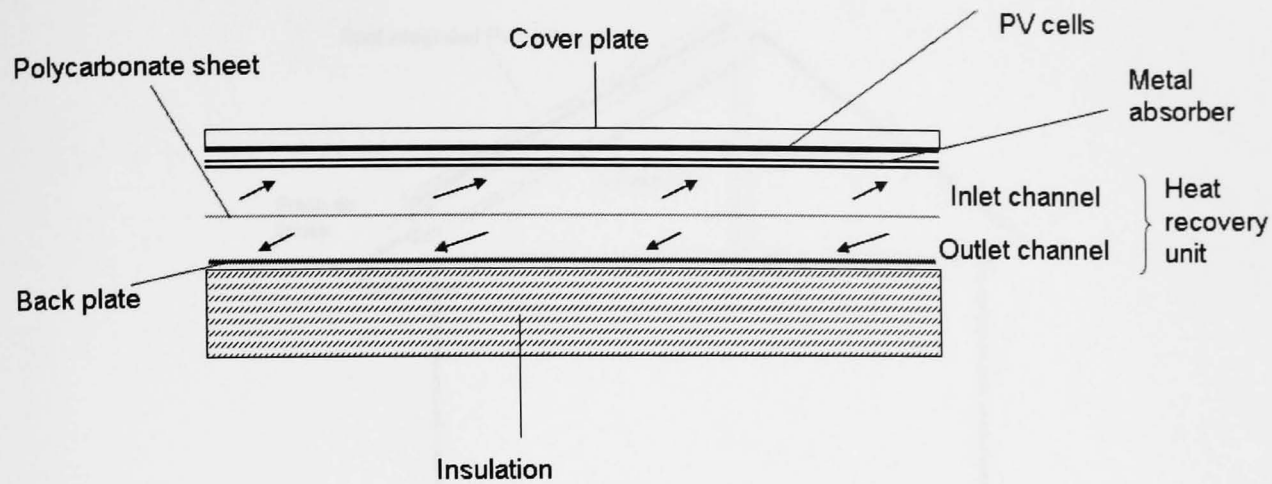


Figure 7.3 Cut sectional front view of BIHR-PVT integrated system

The PV cells are pasted to a metal absorbing plate. In this structure, PV cells are in thermal contact with the absorber. A fraction of the solar energy incident on the collector surface is transformed to electricity while the remaining part of the solar energy is transformed into thermal energy in the same manner as for a conventional PV thermal collector. In order to protect the PV cells from the contact with the airflow and to improve the thermal performance of the system, the cells are covered with protective transparent layer made of glass. The heat recovery unit is placed on the bottom of metal absorber that is connected to air ducts. The heat recovery unit is made of polycarbonate sheets to allow heat exchange between two air airstreams which are inlet and air outlet streams. Each inlet and outlet streams has several internal channels in order to improve the effectiveness of heat recovery. The fundamental benefit of the heat recovery unit in this system is its role as a cooling duct for the PV cells and at the same time as a medium for heat exchange to the incoming fresh air to the buildings. Finally, two fans connected to network of ducts are combined with this system to circulate fresh air to the buildings and bring out stale air to outside. (Figure 7.4).

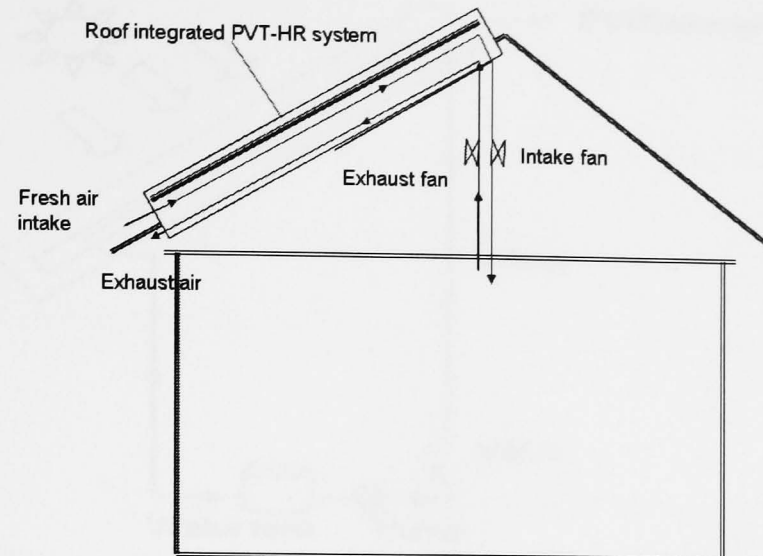
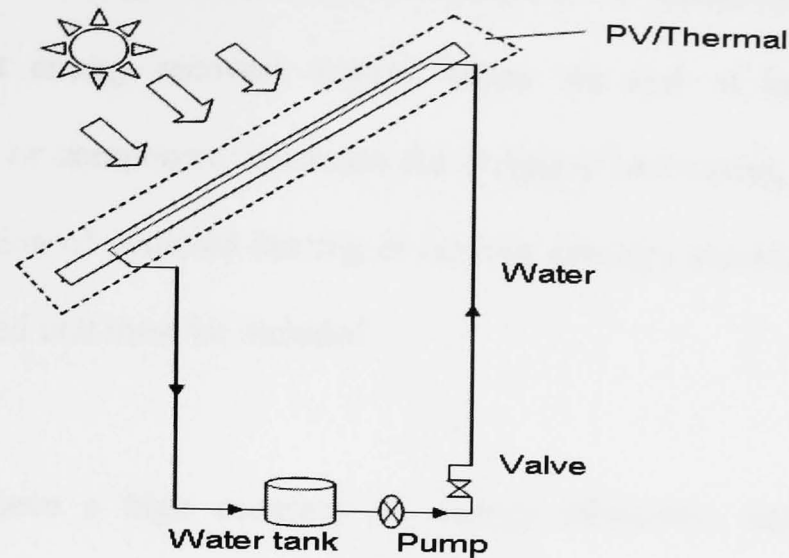
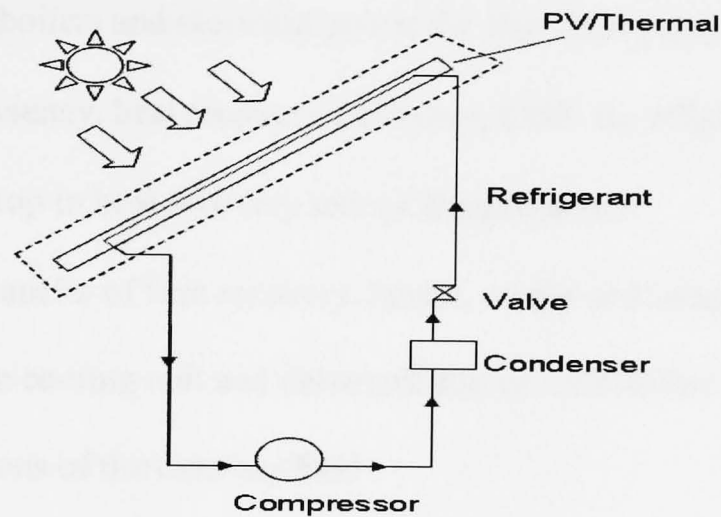


Figure 7.4 Schematic diagram of BIHR-PVT on roof integrated system with fans installed

In this configuration, fresh air enters through the inlet channels of heat recovery unit formed by the absorber plate and polycarbonate sheets. The PV panel becomes a back pass solar air collector with the PC cells acting as the solar heat absorber with ambient air passing around and behind PV panel, removing heat and then the heated air enters the intake duct of heat recovery unit and pass to the interior part of the building. In consequence, this flow arrangement effects greater heat removal from the absorber plate and reduce the heat loss from the PVT collector and simultaneously supplied to the building for ventilation. The air is allowed to pass behind the PV module. Heat generate by the PV module and the metal absorber will be transferred to the air and thereby cooling the PV module causing a higher electrical efficiency for the PV module. BIHR-PVT also could be used for power supply or drive a heat pump unit. Figure 7.6(a) shows a schematic diagram of BIHR-PVT system using water as working fluid and Figure 7.6(b) using refrigerant as working fluid.



(a)



(b)

Figure 7.6 BIHR-PVT could be used for power supply or drive a heat pump unit

In this system, a small portion of the solar energy received will be converted to electricity and the rest was converted as heat.

- Economic analysis

A complete economic analysis of integrated heat recovery system could be conducted for further work. This could be done by several established methods such as degree day method, life cycle cost, payback period and annual net cost. The

investment and running costs should be considered in analysing the economics of integrated heat energy recovery system where the cost of heat recovery, each integrated unit or component must and the marginal cost saving resulting from the possible reduction of installed heating or cooling capacity allowed by heat recovery unit or integrated unit must be included.

To achieve a high accuracy on energy calculation and running cost of integrated heat recovery system, the following factors must be considered:

- The cost of heating energy and cooling energy for HVAC system used in buildings, boilers and electrical power for fans, heat pump etc
- Boiler efficiency, heat recovery efficiency, COP, fan efficiency
- Pressure drop in heat recovery unit or integrated unit
- The heat transfer of heat recovery, heater, cooler and integrated unit such as evaporative cooling unit and dehumidification unit differs a lot depending on the conditions of the entering fluid
- The running hours

REFERENCES

A

O.O. **Abe**, C.J. Simonson, R.W. Besant, W. Shang, Effectiveness of energy wheels from transient measurements: Part II-Results and verification, *International Journal of Heat and Mass Transfer*, 2006 (49), 63-77.

O.O. **Abe**, C.J. Simonson, R.W. Besant, W. Shang, Effectiveness of energy wheels from transient measurements. Part I: Prediction of effectiveness and uncertainty, *International Journal of Heat and Mass Transfer*, January 2006 (49), 52-62.

M. S. **Ahmadi**, E. Blake, C. J. Simonson, R.W. Besant, Transient behaviour of run-around heat and moisture exchanger system. Part I: Model formulation and verification, *International Journal of Heat and Mass Transfer*, 2009(52), 6000-6011.

M. S. **Ahmadi**, E. Blake, C. J. Simonson, R.W. Besant, Transient behaviour of run-around heat and moisture exchanger system. Part II: Sensitivity studies for a range of initial conditions, *International Journal of Heat and Mass Transfer*, 2009 (52), 6012-6020.

ASHRAE, *ASHRAE Handbook of Fundamentals*, American Society of Heating, Refrigerating and Air-Conditioning Engineers, Inc., Atlanta, GA (2005).

ASHRAE, *ASHRAE Standard 55, Thermal Environment Conditions for Human Occupancy*, 2004.

ASHRAE, *ASHRAE Systems and Equipment Hand Book*, 2000.

A. **Ali**, K. Vafai, An investigation of heat and mass transfer between air and desiccant film in an inclined parallel and counter flow channels Original Research Article *International Journal of Heat and Mass Transfer*, 2004 (47), 1745-1760.

B

Ali A. **Badran**, Performance of cool towers under various climates in Jordan, *Energy and Buildings*, 35, Issue 10, November 2003(35),1031-1035.

Morgan D. **Bazilian**, Deo Prasad, Modelling of a photovoltaic heat recovery system and its role in a design decision support tool for building professionals, *Renewable Energy*, 2002(27), 57-68.

R.W **Besant**, C.J. Simonson, Air-to-air energy recovery, *ASHRAE J*, 2000, 31-42.

R. **Brown** et al., Design of the SHARE II monogroov heat pipe in: *Proceedings of the AIAA 26th Thermophysics Conference*, 1999, Paper No. AIAA 91-1359.

M.V. **Brummelen**, *Policies and measures on energy saving in the domestic sector in the Netherlands*, 2006.

C

Y. **Cerci**, A new ideal evaporative freezing cycle, *International Journal of Heat and Mass Transfer*, 2003(46), 2967-2974.

H. B. **Cheikh**, A. Bouchair, Passive cooling by evapo-reflective roof for hot dry climates, *Renewable Energy*, September 2004(29), 1877-1886.

A. **Chel**, G.N. Tiwari, A. Chandra, Sizing and cost estimation methodology for stand-alone residential PV power system, *Int. J. Agile System and Management*, 2009(4), 21-40.

H. **Chen**, L. Thomas, R. W. Besant, Fan supplied heat exchanger fin performance under frosting conditions, *International Journal of Refrigeration*, 2003(26), 140-149.

S. **Chen**, T.L Chan, C.W. Leung, Numerical prediction of laminar forced convection in triangular ducts with unstructured triangular grid method, *Numer. Heat Trans.*, 2000 (38), 209-224.

M. **Ciofalo**, J. Stasiek, M.W. Collins, Investigation of flow and heat transfer in corrugated passages-2, Numerical simulations, *Int. J. Heat Mass Transfer*, 1996(39), 165-192.

R.H. **Crawford**, G.J. Treloar, R.J. Fuller, M. Bazilian, Life-cycle energy analysis of building integrated photovoltaic systems (BiPVs) with heat recovery unit, *Renewable and Sustainable Energy Reviews*, 2006(10), 559-575.

D

Y. J. **Dai**, H. F. Zhang, Numerical simulation and theoretical analysis of heat and mass transfer in a cross flow liquid desiccant air dehumidifier packed with honeycomb paper, *Energy Conversion and Management*, June 2004(45), 1343-1356.

J. **Dallaire**, L.Gosselin, A.K. da Silva, Conceptual optimization of a rotary heat exchanger with a porous core, *International Journal of Thermal Sciences*, February 2010(49), 454-462.

K. **Daou**, R.Z. Wang, Z.Z. Xia, Desiccant cooling air conditioning: a review, *Renewable and Sustainable Energy Reviews*, April 2006(10), 55-77.

P. **Dhital**, R.W. Besant, G.J. Schoenau, Integrating run-around heat exchanger systems into the design of large office buildings, *ASHRAE Trans.* 1995(101), 979-991.

J. **Dieckmann**, K.W. Roth, J. Brodrick, Air-to-air energy recovery heat exchangers, *ASHRAE Journal*, 2003(45), 57-58.

N. **Djongyang**, R.Tchinda, D.Njomo, Thermal comfort: A review paper, *Renewable and Sustainable Energy Reviews*, December 2010(14), 2626-2640.

DTI, Energy Trends 2005, Department of Trade and Industry, the Stationary Office, London, 2005.

E

P. Ekins, E. Lees, The impact of EU policies on energy use in and the evolution of the UK built environment, Energy Policy, December 2008(36), 4580-4583.

M.A. El-Baky, M. M. Mohamed, Heat pipe heat exchanger for heat recovery in air conditioning, Applied Thermal Engineering, 2007(27), 795-801.

A.A. Elmualim, Effect of damper and heat source on wind catcher natural ventilation performance, Energy and Buildings, August 2006(38), 939-948.

E.A.M. Elshafei, M.M. Awad, E. El-Negiry, A.G. Ali, Heat transfer and pressure drop in corrugated channels, Energy, January 2010(35), 101-110

W.H. Emerson, Making the most of run-around coil systems, Journal of Heat Recovery Systems, 1984(4), 265-270.

W. H. Emerson, Designing run-around coil systems Original Research Article Journal of Heat Recovery Systems, Volume 3, Issue 4, 1983, Pages 305-309.

Energy Information Administration (EIA), Residential Energy Consumption Survey, US Department of Energy, 2001.

F

M. Fehrm, W. Reiners, M. Ungemach, Exhaust air heat recovery in buildings, International Journal of Refrigeration, 2002(25), Pages 439-449.

T. Fend, B. Hoffschmidt, R. Pitz-Paal, O.Reutter, P.Rietbrock, Porous materials as open volumetric solar receivers: Experimental determination of thermophysical and heat transfer properties, Energy, 2004(29), 823-833.

W.W Focke, J. Zachariades, I. Olivier, The effects of the corrugation inclination angle on the thermo hydraulic performance of plate heat exchangers, Int.J. heat Mass Transfer, 1985(28), 1469-1479.

B.I. Forsyth, R.W. Besant, The performance of a run-around heat recovery system using aqueous glycol as a coupling liquid, ASHRAE Trans., 1988(94), 532-545.

N. Fumo, D. Y. Goswami, Study of an aqueous lithium chloride desiccant system: air dehumidification and desiccant regeneration, Solar Energy, 2002(72), 351-361.

M. Francisco, P. Mario, G. Eloy, D. Fernando, M. Ruth, Design and experimental study of a mixed energy recovery system heat pipe and indirect evaporative equipment for air conditioning, Energy and Buildings, 2003(35), 1021-1030.

G

G. **Gan**, S. B. Riffat, Naturally ventilated buildings with heat recovery: CFD simulation of thermal environment, *Building Serv Eng Res Technol*, 1997(18), 67-75.

G. **Gan**, S. B. Riffat, A numerical study of solar chimney for natural ventilation of buildings with heat recovery, *Applied Thermal Engineering*, 1998(18), 1171-1187.

P. **Ghandidhasan**, A Simplified model for air dehumidification with liquid desiccant, *Sol Energy*, 2004 (76), 409-416.

M. K. **Ghosal**, G. N. Tiwari, N. S. L. Srivastava, Modeling and experimental validation of a greenhouse with evaporative cooling by moving water film over external shade cloth, *Energy and Buildings*, 2003(35), 843-850.

L. C, **Gómez**, H. A. Navarro, S. M. de Godoy, A. Campo, J.M.S. Jabardo, Thermal characterization of a cross-flow heat exchanger with a new flow arrangement, *International Journal of Thermal Sciences*, November 2009(48), 2165-2170.

K. **Gommed**, G. Grossman, Experimental investigation of a liquid desiccant system for solar cooling and dehumidification, *Solar Energy*, 2007(81), 131-138.

G. **Gong**, W. Zeng, L. Wang, C. Wu, A new heat recovery technique for air-conditioning/heat-pump system, *Applied Thermal Engineering*, December 2008(28), 2360-2370.

Z. **Gu**, H. Liu, Y. Li, Thermal energy recovery of air conditioning system-heat recovery system calculation and phase change materials development, *Applied Thermal Engineering*, December 2004(24), 2511-2526.

X.C. **Guo**, T. S. Zhao, A parametric study of an indirect evaporative air cooler, *International Communications in Heat and Mass Transfer*, 1998(25), 217-226.

H

A.M. **Hamed**, A. A. Sultan, Mass transfer in vertical cloth layers impregnated with calcium chloride for recovery of water from air, *Renewable Energy*, 2002(27), 13-25.

H. **Han**, Y.B. Choo, Y.I. Kwon, An experimental study on the effect of outdoor temperature and humidity conditions on the performance of a heat recovery ventilator, *Proceedings of Clima, Well Being Indoors*, 2007.

X.H. **Han**, L.Q. Cui, S.J. Chen, G.M. Chen, Q. Wang, A numerical and experimental study of chevron, corrugated-plate heat exchangers, *International Communications in Heat and Mass Transfer*, 2010(37), 1008-1014.

A.A.M. **Hassan**, M. Salah Hassan, Dehumidification of air with a newly suggested liquid desiccant, *Renewable Energy*, 2008(33), 1989-1997.

M. S. Hassan, A.A.M. Hassan, Performance of a proposed complete wetting surface counter flow channel type liquid desiccant air dehumidifier, *Renewable Energy*, October 2009(34), 2107-2116.

G. Heidarinejad, M. Bozorgmehr, S. Delfani and J. Esmaeelian, Experimental investigation of two-stage indirect/direct evaporative cooling system in various climatic conditions, *Building and Environment*, 2009(44).

K. Hemzal, Rotary heat exchanger efficiency influenced by air tightness, *Ventilation Conference Praha*, 2006.

J.L.M. Hensen, On the thermal interaction of building structure and heating and ventilating system. PhD thesis, Technische Universiteit Eindhoven, 1991.

H.D. M. Hettiarachchi, M. Golubovic, W.M. Worek, The effect of longitudinal heat conduction in cross flow indirect evaporative air coolers, *Applied Thermal Engineering*, 2007(27), 1841-1848.

Hong Kong Energy Efficiency Award, EMSD.n.d <http://www.eeawards.emsd.gov.hk>.

C. A. Hviid, S. Svendsen, Analytical and experimental analysis of a low-pressure heat exchanger suitable for passive ventilation, *Energy and Buildings*, In Press, Corrected Proof, 2010.

G.S. Hwang, M. Kaviany, W.G. Anderson, J. Zuo, Modulated wick heat pipe, *International Journal of Heat and Mass Transfer*, 2007(50), 1420-1434.

I

M. Idicula et al. Thermophysical properties of natural fibre reinforced polyester composites, *Composites Science and Technology*, 2006 (66) 2719-2725.

IEA, Renewables for heating and cooling: untapped potential. France:OECD/IEA, 2007.

F. P Incropera, D. P. Dewitt, in: *Introduction to Heat Transfer 3rd Edition*, John Wiley & Son, New York, 1996.

F.P Incropera, D. P. Dewitt, *Fundamentals of Heat and Mass Transfer, 3rd Edition*, John Wiley & Son, New York, 1990.

IPCC, *Climate Change 2007*, In: S. Solomon, D. Qin, M. Manning, Z. Chen, M. Marquis, K.B. Averyt, M. Tignor, H.L. Miller, editors. The physical science basis. Contribution of the working group I to the fourth assessment report of the intergovernmental panel on climate change. Cambridge: Cambridge University press, 2007.

Y. Islamoglu, Cem Parmaksizoglu, The effect of channel height on the enhanced heat transfer characteristics in a corrugated heat exchanger channel, *Applied Thermal Engineering*, 2003(23), 1979-1987.

Y. **Islamoglu**, C. Parmaksizoglu, Numerical investigation of convective heat transfer and pressure drop in a corrugated heat exchanger channel Applied Thermal Engineering, 2004(24), Pages 141-147.

J

S. **Jain**, P.L. Dhar, S.C. Kaushik, Evaluation of liquid desiccant based evaporative cooling cycles for typical hot and humid climates, Heat Recovery Systems and CHP, 1994(14), 621-632.

S. **Jain**, P. L. Dhar, S. C. Kaushik, Evaluation of solid-desiccant-based evaporative cooling cycles for typical hot and humid climates, International Journal of Refrigeration, 1995(18), 287-296.

S. **Jain**, P.K. Bansal, Performance analysis of liquid desiccant dehumidification systems, International Journal of Refrigeration, 2007(30), 861-872.

J. **Ji**, G. Pei, T.T Chow, K. Liu, H. He, J. Lu, C. Han, Experimental study of photovoltaic solar assisted heat pump system, Solar Energy, 2008(82), 43-52.

J. **Jokisalo**, J. Kurnitski, M. Vuolle, A.Torkki, Performance of balanced ventilation with heat recovery in residential buildings in a cold climate, The International Journal of Ventilation, 2003(2).

B.M. **Jones**, R.Kirby, Quantifying the performance of a top-down natural ventilation Windcatcher™, Building and Environment, 2009(44), 1925-1934.

K. A. **Joudi**, S. M. Mehdi, Application of indirect evaporative cooling to variable domestic cooling load, Energy Conversion and Management, 2000(41), 1931-1951.

E. **Juodis**, Extracted ventilation air heat recovery efficiency as a function of a building's thermal properties, Energy and Buildings, 2006(38), 568-573.

C. **T'Joen**, Y. Park, Q. Wang, A. Sommers, X. Han, A. Jacobi, A review on polymer heat exchangers for HVAC&R applications, International Journal of Refrigeration, 2009(32), 763-779.

K

G. **Karthikeyan**, A. Mani, S. S. Murthy, Performance of different working fluids in transfer-tank operated vapour absorption refrigeration systems, Renewable Energy, 1995(6), 835-842.

W.M. **Kays**, A.L. London, Compact Heat Exchangers, 3rd edition, McGraw-Hill Book Co. New York, 1984.

N. **Khan**, Y. Su, S.B. Riffat, A review on wind driven ventilation techniques, Energy and Buildings, 2008(40), 1586-1604.

T. **Kho**, H.U. Zettler, H. Müller-Steinhagen, D. Hughes, Effect of Flow Distribution on Scale Formation in Plate and Frame Heat Exchangers, *Chemical Engineering Research and Design*, 1997(75), 635-640.

T. **Kho**, H. Müller-Steinhagen, An Experimental and Numerical Investigation of Heat Transfer Fouling and Fluid Flow in Flat Plate Heat Exchangers, *Chemical Engineering Research and Design*, 1999(77), 124-130.

Y. Y. **Kim**, K.S. Kim, G.H. Jeong, S. Jeong, An experimental study on the quantitative interpretation of local convective heat transfer for a plate fin and tube heat exchanger using the lumped capacitance method, *International Journal of Heat and Mass Transfer*, January 2006(49), 230-239.

M. **Kolhe**, S. Kolhe, J.C Joshi, Economic viability of stand-alone solar photovoltaic system in comparison with diesel-powered system for India, *Energy Economics*, 2002 (24), 155-165.

J. **Korsgaard**, Mechanical ventilation and house dust mites: a controlled investigation, in: Van Moerbeke, editor. *Dust mite allergens and asthma*, Brussel: UCB Institute of Allergy, 1991, 87-90.

J. **Kragh**, J. Rose, T.R. Nielsen and, S. Svendsen, New counter flow heat exchanger designed for ventilation systems in cold climates, *Energy and Buildings*, 2007(39), 1151-1158.

E. **Krüger**, E. G. Cruz, B. Givoni, Effectiveness of indirect evaporative cooling and thermal mass in a hot arid climate, *Building and Environment*, 2010(45), 1422-1433.

T. **Kuppan**, *Heat exchanger design handbook*, New York:Marcel Dekker Inc, 2000.

A. G. **Kwok**, N. B. Rajkovich, Addressing climate change in comfort standards, *Building and Environment*, 2010(45), 18-22.

L

B.R. **Lamb**, Plate heat exchangers-a low cost route to heat recovery, *Journal of Heat Recovery Systems*, 1982(2), 247-255.

R. **Lambert**, Heat transfer through roofs of low cost Brazilian houses, PhD thesis, UK: University of Leeds, 1988.

R. M. **Lazzarin**, A. Gasparella, Technical and economical analysis of heat recovery in building ventilation systems, *Applied Thermal Engineering*, 1998(18), 47-67.

Z. **Li**, Y. Jiang. X.L. Chen, X.H. Liu, Matching conditions for flow rate and heat in the heat and mass transfer process between humid air and liquid desiccant, *Heat Ventil Air Condition*, 2005 (35), 103-110.

C.H. **Liang**, L.Z. Zhang, L.-X. Pei, Performance analysis of a direct expansion air dehumidification system combined with membrane-based total heat recovery *Energy*, 2010(35), 3891-3901.

C.H. **Liang**, L.Z. Zhang, L.X. Pei, Independent air dehumidification with membrane-based total heat recovery: Modeling and experimental validation, *International Journal of Refrigeration*, 2010(33), 398-408.

M.W. **Liddament**, *A Guide to Energy Efficient Ventilation*, 1996.

S. **Lin**, J. Broadbent, R. McGlen, Numerical study of heat pipe application in heat recovery systems, *Applied Thermal Engineering*, 2005(25), 127-133.

D. **Lindley**, K.S. O'Rourke, Future building packages: Is domestic heat recovery really necessary? *Journal of Heat Recovery Systems*, 1981(1), 167-179.

D. **Liu**, F.Y. Zhao, G.F. Tang, Active low-grade energy recovery potential for building energy conservation, *Renewable and Sustainable Energy Reviews*, 2010(14), 2736-2747.

S. **Liu**, S. Riffat, X. Zhao, Y. Yuan, Impact of adsorbent finishing and absorbent filming on energy exchange efficiency of an air-to-air cellulose fibre heat & mass exchanger, *Building and Environment*, 2009(44), 1803-1809.

X. **Liu**, Y. Jiang, J. Xia, X. Chang, Analytical solutions of coupled heat and mass transfer processes in liquid desiccant air dehumidifier/regenerator, *Energy Conversion and Management*, July 2007(48), 2221-2232.

X.H. **Liu**, K.Y. Qu, Y. Jiang, Empirical correlations to predict the performance of the dehumidifier using liquid desiccant in heat and mass transfer *Renewable Energy*, 2006(31), 1627-1639.

X.H. **Liu**, X.M. Chang, J.J. Xia, Y. Jiang, Performance analysis on the internally cooled dehumidifier using liquid desiccant, *Building and Environment*, 2009(44), 299-308.

X.H. **Liu**, Y. Zhang, K.Y. Qu, Y. Jiang, Experimental study on mass transfer performances of cross flow dehumidifier using liquid desiccant, *Energy Conversion and Management*, 2006(47), 2682-2692.

A.L. **London**, W.M. Kays, The liquid-coupled indirect transfer regenerator for gas-turbine plants, *ASME Trans.*, 1951(73), 529-542.

M

K. **Mahmud**, G I. Mahmood, C. Simonson, R. W. Besant, Performance testing of a counter-cross-flow run-around membrane energy exchanger (RAMEE) system for HVAC applications, *Energy and Buildings*, July 2010(42), 1139-1147.

Z.A. **Manan**, L.J. Shiun, S.R.W. Alwi, H. Hashim, K.S. Kannan, N. Mokhtar, A.Z. Ismail, Energy Efficiency Award system in Malaysia for energy sustainability, *Renewable and Sustainable Energy Reviews*, 2010(14), 2279-2289.

H. **Manz**, H. Huber, A. Schälín, A. Weber, M. Ferrazzini, M. Studer, Performance of single room ventilation units with recuperative or regenerative heat recovery, *Energy and Buildings*, 2000(31), 37-47.

H. **Manz**, H. Huber, Experimental and numerical study of a duct/heat exchanger unit for building ventilation, *Energy and Buildings*, 2000(32), 189-196.

H. **Manz**, H. Huber, D. Helfenfinger, Impact of air leakages and short circuits in ventilation units with heat recovery on ventilation efficiency and energy requirements for heating, *Energy and Buildings*, 2001(33), 133-139.

F. J. R. **Martínez**, M.A.Á.G. Plasencia, E. V. Gómez, F. V. Díez, R. H. Martín, Design and experimental study of a mixed energy recovery system, heat pipes and indirect evaporative equipment for air conditioning, *Energy and Buildings*, 2003(35), 1021-1030.

P. **Mavroudaki**, C. B. Beggs, P. A. Sleight, S. P. Halliday, The potential for solar powered single-stage desiccant cooling in southern Europe, *Applied Thermal Engineering*, 2002(22), 1129-1140.

L. **Mei**, Y.J. Dai, A technical review on use of liquid-desiccant dehumidification for air-conditioning application, *Renewable and Sustainable Energy Reviews*, 2008(12), 662-689.

L.C.S. **Mesquita**, S.J. Harrison, D. Thomey, Modeling of heat and mass transfer in parallel plate liquid-desiccant dehumidifiers, *Solar Energy*, 2006(80), 1475-1482.

J. **Min**, M. Su, Performance analysis of a membrane-based energy recovery ventilator: Effects of membrane spacing and thickness on the ventilator performance, *Applied Thermal Engineering*, June 2010(30), 991-997.

J. **Min**, M. Su, Performance analysis of a membrane-based enthalpy exchanger: Effects of the membrane properties on the exchanger performance, *Journal of Membrane Science*, 2010(348), 376-382.

H. **Montazeri**, R. Azizian, Experimental study on natural ventilation performance of one-sided wind catcher, *Building and Environment*, December 2008(43), 2193-2202.

H. **Montazeri**, F. Montazeri, R. Azizian, S. Mostafavi, Two-sided wind catcher performance evaluation using experimental, numerical and analytical modeling, *Renewable Energy*, 2010(35), 1424-1435.

A. **Muley**, R. M. Manglik, Enhanced heat transfer characteristics of single-phase flows in a plate heat exchanger with mixed chevron plates, *J. Enhanc. Heat Transfer* 4 1997, 187-201.

N

N. M. **Nahar**, P. Sharma, M. M. Purohit, Performance of different passive techniques for cooling of buildings in arid regions, *Building and Environment*, 2003(38),109-116.

M. **Nasif**, R. AL-Waked, G. Morrison, M. Behnia, Membrane heat exchanger in HVAC energy recovery systems, systems energy analysis, *Energy and Buildings*, 2010(42), 1833-1840.

H.A.**Navarro**, L. C.-Gómez, A new approach for thermal performance calculation of cross-flow heat exchangers, *International Journal of Heat and Mass Transfer*, 2005(48), 3880-3888.

W.W. **Nazaroff**, M.L. Boegel, C.D. Hollowell, G.D. Roseme, The use of mechanical ventilation with heat recovery for controlling radon and radondaughter concentrations in houses, *Atmospheric Environment* (1967), 1981(15), 263-270.

G.F. **Nellis**, S.A. Klein, Regenerative heat exchangers with significant entrained fluid heat capacity, *International Journal of Heat and Mass Transfer*, 2006(49), 329-340.

G.F. **Nellis**, J.M Pfotenhauer, Effectiveness-NTU Relationship for a counterflow heat exchanger subjected to an external heat transfer, *Journal of Heat Transfer*, 2005(127), 1071-1073.

A. **Nguyen**, Y.Kim, Y. Shin, Experimental study of sensible heat recovery of heat pump during heating and ventilation, *International Journal of Refrigeration*, 2005(28), 242-252.

J. L. **Niu**, L. Z. Zhang, Membrane-based Enthalpy Exchanger: material considerations and clarification of moisture resistance, *Journal of Membrane Science*, 2001(189), 179-191.

C.E.L. **Nóbrega**, N.C.L. Brum, Modeling and simulation of heat and enthalpy recovery wheels, *Energy*, 2009(34), 2063-2068.

O

K. **Okada**, M. Ono, T. Tomimara, T. Okuma, H. Konno, S. Ohtani, Design and heat transfer characteristics of new plate heat exchanger, *Heat Transfer-Jap.*, 1972, 90-95.

A. C. **Oliveira**, C.F. Afonso, S. B. Riffat, P.S. Doherty, Thermal performance of a novel air conditioning system using a liquid desiccant, *Applied Thermal Engineering*, 2000(20), 1213-1223.

P

M. **Patel**, *Wind and solar power systems*, New York, Crc Press, 1999.

C.S.P. **Peng**, J.R. Howell, Analysis and design of efficient absorbers for low temperature desiccant air conditioners, *ASME J Sol Energy Eng* 1981(103), 67-74.

L. Pérez-Lombard, J. Ortiz, C. Pout, A review on buildings energy consumption information, *Energy and Buildings*, 2008(40), 394-398.

L. Pérez-Lombard, J. Ortiz, J. F. Coronel, I. R. Maestre, A review of HVAC systems requirements in building energy regulations, *Energy and Buildings*, In Press, Corrected Proof, 2010.

A.A. Pesaran, A review of desiccant dehumidification technology, Proceedings of EPRI's Electric Dehumidification: Energy Efficient humidity Control for Commercial and Institutional Buildings Conference, 1994.

D. Pietruschka, U. Eicker, M. Huber, J. Schumacer, Experimental performance analysis and modelling of liquid desiccant cooling systems for air conditioning in residential buildings, *International Journal of Refrigeration*, 2006 (26), 110-124.

Promotion of Energy Efficiency and Conservation (PROMEEC) report by Energy Conservation Centre of Japan (ECCJ), 2008.

Q

G.Q. Qiu, S.B. Riffat, Novel design and modelling of an evaporative cooling system for buildings, *International Journal of Energy Research*, 2006 (30), 985-999.

G.Q. Qiu, A Novel evaporative/desiccant cooling system. PhD thesis, University of Nottingham, UK, 2007.

G.Q. Qiu, S.B. Riffat, Experimental investigation on a novel air dehumidifier using liquid desiccant, *International Journal of Green Energy*, 2010 (7), 174-180.

R

M. Rasouli, C.J. Simonson, R. W. Besant, Applicability and optimum control strategy of energy recovery ventilators in different climatic conditions, *Energy and Buildings*, 2010(42) 1376-1385.

Recognising Excellence in Energy Conservation and Efficiency, National Energy Efficiency Award. n.d <http://www.energyawards.org.uk>.

B. Riangvilaikul, S. Kumar, An experimental study of a novel dew point evaporative cooling system, *Energy and Buildings*, 2010(42), 637-644.

B. Riangvilaikul, S. Kumar, Numerical study of a novel dew point evaporative cooling system, *Energy and Buildings*, November 2010(42), 2241-2250.

S. B. Riffat, N. J. Shankland, Rotary storage heat pump, *Heat Recovery Systems and CHP*, 1994(14), 421-426.

S. B. Riffat, A. P. Warren, R. A. Webb, Rotary heat pump driven by natural gas, *Heat Recovery Systems and CHP*, 1995(15), 545-554.

S. B. **Riffat**, G. Gan, Determination of effectiveness of heat-pipe heat recovery for naturally-ventilated buildings, *Applied Thermal Engineering*, 1998(18), 121-130.

S.B **Riffat**, S.E. James, C.W. Wong, Experimental analysis of the absorption and desorption rates of HCOOK/H₂O and LiBr/H₂O, *International Journal of Energy Research*, 1998(22), 1099-1103.

S. B. **Riffat**, M. C. Gillott, Performance of a novel mechanical ventilation heat recovery heat pump system, *Applied Thermal Engineering*, 2002(22), 839-845.

C. -A. **Roulet**, F. D. Heidt, F. Foradini, M. -C. Pibiri, Real heat recovery with air handling units, *Energy and Buildings*, 2001(33), 495-502.

R. **Ruotsalainen**, Ventilation, indoor air quality and human health and comfort in dwellings and day-care centers, Helsinki University of Technology, HVAC laboratory. Report A1, Espoo, 1995, 57-58.

S

W.Y **Saman**, S Alizadeh, Modelling and performance analysis of a cross-flow type plate heat exchanger for dehumidification/cooling, *Solar Energy*, 2001(70), 361-372.

W. Y. **Saman**, S. Alizadeh, An experimental study of a cross-flow type plate heat exchanger for dehumidification/cooling, *Solar Energy*, 2002(73), 59-71.

J.Y. **San**, S.C. Hsiau, Effect of axial solid heat conduction and mass diffusion in a rotary heat and mass regenerator, *International Journal of Heat and Mass Transfer*, 1993(36), 2051-2059.

A. **Sasitharanuwat**, W. Rakwichian, N. Ketjoy, S. Yammen, Performance evaluation of a 10 kW_p PV power system prototype for isolated building in Thailand *Renewable Energy*, 2007(32) 1288-1300.

J. M. **Schultz**, B. Saxhof, Natural ventilation with heat recovery, *Air Infiltration Rev.*, 1994(15), 9-12.

L. **Shao**, S.B. Riffat, G. Gan, Heat recovery with low pressure loss for natural ventilation, *Energy and Buildings*, 1998(28), 179-184.

L. **Shao**, S. B. Riffat, Flow loss caused by heat pipes in natural ventilation stacks, *Applied Thermal Engineering*, 1997(17), 393-399.

R.K. **Shah**, D.P. Sekulic, *Fundamentals of Heat Exchanger Design*, John Wiley & Son, Inc, New York, 2003.

R.K **Shah**, A.L. London, in: *Laminar Flow Forced Convection in Ducts*, Academic Press Inc, New York, 1978.

H.A Shehata, S.B Riffat, L. Shao, The desic-air air conditioning system, Institute of Building Technology, School of the Built Environment, University of Nottingham, UK, 1997.

W, **Shurcliff**, Air-to-air heat exchangers for houses, Annual Review Energy, 1988(13), 1-22.

C. J. **Simonson**, R. W. Besant, Energy wheel effectiveness: part I-development of dimensionless groups, International Journal of Heat and Mass Transfer, 1999(42), 2161-2170.

C. J. **Simonson**, R. W. Besant, Energy wheel effectiveness: part II-correlations International Journal of Heat and Mass Transfer, 1999(42), 2171-2185.

M. S. **Söylemez**, On the optimum heat exchanger sizing for heat recovery, Energy Conversion and Management, 2000(41), 1419-1427.

J. **Stasiek**, M Ciofalo, I.K. Smith, M.W Collins, Investigation of flow and heat transfer in corrugated passages-1: Experimental results, Int. J. Heat Mass Transfer, 1996(39), 149-192.

Y. **Su**, S.B. Riffat, Y.L.Lin, Naghman Khan, Experimental and CFD study of ventilation flow rate of a Monodraught™ windcatcher, Energy and Buildings, 2008(40), 1110-1116.

Y. **Sukamongkol**, S. Chungpaibulpatana, B. Limmeechokchai, P. Sripadungtham, Condenser heat recovery with a PV/T air heating collector to regenerate desiccant for reducing energy use of an air conditioning room, Energy and Buildings, 2010(42), 315-325.

T

L. **Tadrist**, M. Miscevic, O. Rahli, F. Topin, About the use of fibrous materials in compact heat exchangers, Experimental Thermal and Fluid Science 2004 (28), 193-199.

R. **Tauscher**, U. Dinglreiter, B. Durst, F. Mayinger, Transport processes in narrow channels with application to rotary exchangers, Heat and Mass Transfer, 1999(35), 123-131.

R. **Taylor**, R. Krishna, Multi-component Mass Transfer, Wiley, New York, 1993.

M. **Thirugnanasambandam**, S. Iniyar, R. Goic, A review of solar thermal technologies, Renewable and Sustainable Energy Reviews, 2010(14), 312-322.

P. **Tiwari**, Energy efficiency and building construction in India, Building and Environment, 2001(36), 1127-1135.

V

A. **Vali**, C.J. Simonson, R.W. Besant, G. Mahmood, Numerical model and effectiveness correlations for a run-around heat recovery system with combined counter and cross flow exchangers, *International Journal of Heat and Mass Transfer*, 2009(52), 5827-5840.

W

K. K.W. **Wan**, H.W.D. Li, D. Liu, J.C. Lam, Future trends of building heating and cooling loads and energy consumption in different climates, *Building and Environment*, 2011(46), 223-234.

J. C.Y. **Wang**, Practical thermal design of run-around air-to-air heat recovery system, *Journal of Heat Recovery Systems*, 1985(5), 493-501.

L. **Wang**, J. Gwilliam, P. Jones, Case study of zero energy house design in UK, *Energy and Buildings*, 2009(41), 1215-1222.

N. **Wang**, Y.C. Chang, V. Dauber, Carbon print studies for the energy conservation regulations of the UK and China, *Energy and Buildings*, May 2010(42), 695-698.

Y. **Wang**, R. W. Besant, C. J. Simonson, W. Shang, Application of humidity sensors and an interactive device, *Sensors and Actuators B: Chemical*, 2006(115), 93-101.

P. **Wargocki**, D.P. Wyon, J. Sundell, G. Clausen, P.O. Fanger, The effects of outdoor air supply rate in an office on perceived air quality, sick building syndrome (SBS) symptoms and productivity, *Journal of Indoor Air*, 2000, 222-236.

F.G. **Waugaman**, A. Kini, C.G.Kettleborough, A review of desiccant cooling systems. *Journal of Energy Resources Technology*, 1993(115), 1-8.

R.L. **Webb**, *Principals of enhanced heat transfer*. New York: John Wiley & Sons Inc, 1994.

J. **Wen**, Y. Li, A. Zhou, K. Zhang, An experimental and numerical investigation of flow patterns in the entrance of plate-fin heat exchanger, *International Journal of Heat and Mass Transfer*, 2006(49), 1667-1678.

S.R. **Wenham**, M.A. Green, M.E. Watt, *Applied photovoltaics*, Australia: Center for Photovoltaic Devices and System, 1994.

M. **Wetter**, Simulation model air-to-air plate heat exchanger, Simulation Research Group, Building Technologies Department, Lawrence Berkeley National Laboratory, 1999.

J.M. **Wu**, X. Huang, H. Zhang, Theoretical analysis on heat and mass transfer in a direct evaporative cooler, *Applied Thermal Engineering*, 2009(29), 980-984.

J.M. **Wu**, X. Huang, H. Zhang, Numerical investigation on the heat and mass transfer in a direct evaporative cooler, *Applied Thermal Engineering*, 2009(29), 195-201.

Y. Wu, Chinese building energy conservation: existing situation, problems and policy, presentation, in: International Conference on Sustainable Development in Building and Environment, China, 2003.

Y

R. Yao, B. Li, K. Steemers, Energy policy and standard for built environment in China, *Renewable Energy*, 2005(30), 1973-1988.

Y.H. Yau, Experimental thermal performance study of an inclined heat pipe heat exchanger operating in high humid tropical HVAC systems, *International Journal of Refrigeration*, 2007(30), 1143-1152.

Y.H. Yau, Application of a heat pipe heat exchanger to dehumidification enhancement in a HVAC system for tropical climates-a baseline performance characteristics study, *International Journal of Thermal Sciences*, 2007(46), 164-171

Y.H. Yau, Theoretical determination of effectiveness for heat pipe heat exchangers operating in naturally ventilated tropical buildings, Technical Note, *IMEchE*, 2001(215) Part A.

Y.H. Yau, M. Ahmadzadehtalatapeh, A review on the application of horizontal heat pipe heat exchangers in air conditioning systems in the tropics, *Applied Thermal Engineering*, 2010(30), 77-84.

C.C. Yeh, C.N.Chen, Y.M.Chen, Heat transfer analysis of a loop heat pipe with biporous wicks, *International Journal of Heat and Mass Transfer*, 2009(52), 4426-4434.

Y.Yin, X. Zhang, Z. Chen, Experimental study on dehumidifier and regenerator of liquid desiccant cooling air conditioning system, *Building and Environment*, 2007(42), 2505-2511.

Z

Z.M. Zain, M. N.Taib, Shahrizam M.S. Baki, Hot and humid climate: prospect for thermal comfort in residential building, *Desalination*, 2007(209), 261-268.

L. Z. Zhang, Y. Jiang, Heat and mass transfer in a membrane-based energy recovery ventilator, *Journal of Membrane Science*, 1999(163), 29-38.

L.Z. Zhang, Thermally developing forced convection and heat transfer in rectangular plate-fin passages under uniform plate temperature, *Numer. Heat Trans. A. Appl.*, 2007(52), 549-564.

L. Z. Zhang, J. L. Niu, Energy requirements for conditioning fresh air and the long-term savings with a membrane-based energy recovery ventilator in Hong Kong, *Energy*, 2001(26), 119-135.

L. Z. **Zhang**, J. L. Niu, Performance comparisons of desiccant wheels for air dehumidification and enthalpy recovery, *Applied Thermal Engineering*, 2002(22), 1347-1367.

L.Z. **Zhang**, J.L. Niu, Effectiveness correlations for heat and mass transfer process in an enthalpy exchanger with membrane cores, *ASME Journal of Heat Transfer* 2002(122), 922-929.

L.Z. **Zhang**, *Air dehumidification*, Beijing: China Chemical Industry Press, 2005.

L.Z. **Zhang**, Convective mass transport in cross-corrugated membrane exchangers, *Journal of Membrane Science*, 2005(206), 75-83.

L.Z. **Zhang**, Energy performance of independent air dehumidification systems with energy recovery measures, *Energy*, 2006(31), 1228-1242.

L.Z. **Zhang**, D.S. Zhu, X.H. Deng and B. Hua, Thermodynamic modelling of a novel air dehumidification system, *Energy and Buildings*, 2005(37), 279-286.

L.Z. **Zhang**, Heat and mass transfer in a cross-flow membrane-based enthalpy exchanger under naturally formed boundary conditions, *International Journal of Heat and Mass Transfer*, 2007(50), 151-162.

L.Z. **Zhang**, Flow maldistribution and thermal performance deterioration in a cross-flow air to air heat exchanger with plate-fin cores, *International Journal of Heat and Mass Transfer*, 2009(52), 4500-4509.

L.Z. **Zhang**, Heat and mass transfer in plate-fin enthalpy exchangers with different plate and fin materials, *International Journal of Heat and Mass Transfer*, 2009(52), 2704-2713.

L.Z. **Zhang**, An analytical solution for heat mass transfer in a hollow fibre membrane based air-to-air heat mass exchanger, *Journal of Membrane Science*, 2010(360), 217-225.

L.Z. **Zhang**, Heat and mass transfer in a quasi-counter flow membrane-based total heat exchanger, *International Journal of Heat and Mass Transfer*, 2010(53), 5478-5486.

Y. **Zhang**, Y.Jiang, L.Z. Zhang, Y. Deng, Z. Jin, Analysis of thermal performance and energy savings of membrane based heat recovery ventilator *Energy*, 2000(25), 515-527.

X. **Zhao**, J.M. Li, S.B. Riffat, Numerical study of a novel counter-flow heat and mass exchanger for dew point evaporative cooling, *Applied Thermal Engineering*, 2008(28), 1942-1951.

X. **Zhao**, S. Liu, S.B. Riffat, Comparative study of heat and mass exchanging materials for indirect evaporative cooling systems, *Building and Environment*, 2008(43), 1902-1911.

X. **Zhao**, S. Yang, Z. Duan, S. B. Riffat, Feasibility study of a novel dew point air conditioning system for China building application, *Building and Environment*, 2009(44), 1990-1999.

Y.P. **Zhou**, J.Y. Wu, R.Z. Wang, Performance of energy recovery ventilator with various weathers and temperature set-points, *Energy and Buildings*, 2007(39), 1202-1210.

W. **Zheng**, W.M Worek, D. Novolsel, Effect of operating conditions on optimal performance of rotary dehumidifiers, *ASME Journal of Energy Resouces Technology*, (117), 62-66.

Website

<http://www.bbc.co.uk/weather/world>)

<http://www.aseanenergy.org>.

<http://www.bee-india.nic.in>

<http://www.truetex.com>

APPENDIX

Calculation of airflow rate

Air velocity 1.0 m/s

$$\begin{aligned}
 A &= 7.855 \times 10^{-3} \text{ m}^2 \\
 Q &= VA \\
 &= 1.0 \text{ m/s} \times 7.855 \times 10^{-3} \text{ m}^2 \\
 &= 7.9 \times 10^{-3} \text{ m}^3/\text{s} \\
 &= 7.9 \text{ l/s}
 \end{aligned}$$

$$T_i = 16.9 + 273 = 296.5$$

T	Cp	p
275	1.0038	1.284
300	1.0049	1.177

$$\text{Density, } \rho = \frac{x - 1.177}{1.284 - 1.177} = \frac{296.5 - 275}{300 - 275}$$

$$x = 1.284 - 1.177 \times \frac{289.9 - 275}{300 - 275} + 1.177$$

$$\begin{aligned}
 \rho &= 0.107 \times 21.5/25 + 1.177 \\
 &= 1.27 \text{ kg/m}^3 \\
 &= 1.3 \text{ kg/m}^3
 \end{aligned}$$

$$\text{Specific heat, } C_p = \frac{x - 1.0038}{1.0049 - 1.0038} = \frac{289.9 - 275}{300 - 275}$$

$$x = 1.0049 - 1.0038 \times \frac{289.9 - 275}{300 - 275} + 1.0038$$

$$\begin{aligned}
 C_p &= 1.1 \times 10^{-3} \times 21.5/25 + 1.0038 \\
 &= 1.0045 \text{ kJ/kgK} \\
 &= 1.005 \text{ kJ/kgK}
 \end{aligned}$$

$$\begin{aligned}
 \text{Mass flow rate, } M &= \rho \times Q \\
 &= 1.3 \text{ kg/m}^3 \times 7.9 \times 10^{-3} \text{ m}^3/\text{s} \\
 &= 0.0010 \text{ kg/s}
 \end{aligned}$$

Table A.1 summarized the calculation data

Table A.1 Calculation data

V Air velocity m/s	Q Volume airflow rate m³/s	Q Volume airflow rate l/s	M Mass flow rate
1.0	0.0079	7.9	0.01
1.5	0.0118	11.8	0.015
2.0	0.0157	15.7	0.02
2.5	0.0196	19.6	0.026
3.0	0.0236	23.6	0.031

Calculation of pressure drop in ducts

Friction between the fluid flowing through a duct and its inside wall causes losses, which are quantified as pressure drop. The pressure drop over a length of duct can be determined using the following step :

Calculation of Reynolds Number (Re)

$$\begin{aligned}
 \text{Re} &= \frac{1000 \times V \times D}{\nu} \\
 &= \frac{1000 \times 1.0\text{m/s} \times 100\text{mm}}{14 \text{ centiStokes}} \\
 &= 7142.86
 \end{aligned}$$

Calculation of friction factor (f)

The formula used to calculate the friction factor is dependent on the magnitude of the Reynolds Number. The Reynolds Number (Re) calculated at 1.0m/s air velocity is greater than 2300 but less than 100,000 which means the flow is turbulent. Thus the following formula can be used to calculate the friction factor :

$$\begin{aligned}
 f &= 0.3164 \times \text{Re}^{-0.25} \\
 &= 0.3164 \times 7142^{-0.25} \\
 &= 0.03441
 \end{aligned}$$

Calculation of pressure drop

Pressure drop can be calculated using following formula:

$$\begin{aligned}\Delta p &= \frac{V^2 \times f \times L \times \rho}{2D} \\ &= \frac{1^2 \text{m/s} \times 0.03441 \times 2\text{m} \times 1.2\text{kg/m}^3}{2(0.10)\text{m}} \\ &= 0.413 \text{ Pa}\end{aligned}$$

Summary of the calculation results shown in Table A.2

Table A.2

Velocity m/s	Reynolds		Pressure drop (Δp)
	Number (Re)	Friction factor (f)	
1.0	7142.86	0.0344	0.413
1.5	10714.29	0.0311	0.840
2.0	14285.71	0.0294	1.389

Calculation of energy balance

The energy balance ratio (EBR), is defined as energy extracted from the exhaust air stream divided by energy transferred to the supply air stream. It is evident that EBR values, for all cases examined, are ranging from 0.67 to 1.09 as shown in Table A.3.

$$\begin{aligned}\text{EBR} &= \Delta H_s / \Delta H_e \\ &= 0.9 / 1.35 \\ &= 0.67\end{aligned}$$

Table A.3

Average air velocity (m/s)	Energy balance error %
1.0	0.67
1.5	0.80
2.0	0.77
2.5	1.27
3.0	1.09

Technical data of HMP45A Humidity probe

General

Operating temperature range	-40...+60 °C	
Storage temperature range	-40...+80 °C	
Supply voltage	7...35 VDC	
Settling time	500 ms	
Power consumption	<4 mA	
Output load	>10kohm (to ground)	
Weight	350 g (incl. package)	
Cable length	3.5 m	
Housing material	ABS plastic	
Housing classification (electronics)	IP65	
Sensor protection:		
standard:	membrane filter	part no. 2787HM
optional:	sintered filter 37 µm	part no. 6685
	sintered filter 216 µm	part no. 6686
	grid	part no. 6597

Relative Humidity

HMP45A & HMP45D

Measuring range:	0.8 to 100 %RH
Output scale	0...100 %RH equals 0...1 VDC
Accuracy at +20 °C (incl. nonlinearity and hysteresis)	
against factory references	±1 %RH
field calibration against references	
	±2 %RH (0...90 %RH)
	±3 %RH (90...100 %RH)
Typical long-term stability	< 1% RH / year
Temperature dependence	±0.05 %RH/°C
Response time (90% at +20 °C)	10 s with membrane filter
Humidity sensor	HUMICAP® 180

HMP45D

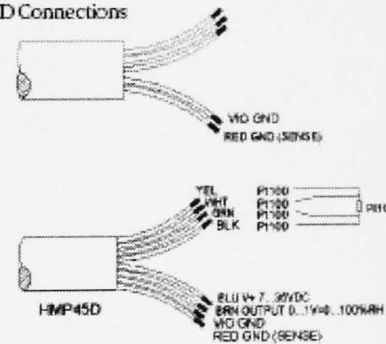
Measurement range	-40...+60 °C
Output signal	resistive four wire connection
Temperature sensor	Pt 100 IEC 751 1/3 Class B

Complies with EMC standard EN61326-1:1997 + Am 1:1998; Generic Environment.

Dimensions

Dimensions in mm.

HMP45A/D Connections



HMP45A/D Probe

